FINAL REPORT

Quantifying the Presence and Activity of Aerobic, Vinyl Chloride-Degrading Microorganisms in Dilute Groundwater Plumes by Using Real-Time PCR

SERDP Project ER-1683

July 2013

Tim Mattes
Yang Oh Jin
Meredith Dobson
Meng-chen Lee
Stephanie Schmidt
Samuel Fogel
Margaret Findlay
Donna Smoler
The University of Iowa

This document has been cleared for public release

SERDP
DOD ▪ EPA ▪ DOE

REPORT DOCUMENTATION PAGE

Form Approved
OMB No. 0704-0188

Public reporting burden for this collection of information is estimated to average 1 hour per response, including the time for reviewing instructions, searching existing data sources, gathering and maintaining the data needed, and completing and reviewing this collection of information. Send comments regarding this burden estimate or any other aspect of this collection of information, including suggestions for reducing this burden to Department of Defense, Washington Headquarters Services, Directorate for Information Operations and Reports (0704-0188), 1215 Jefferson Davis Highway, Suite 1204, Arlington, VA 22202-4302. Respondents should be aware that notwithstanding any other provision of law, no person shall be subject to any penalty for failing to comply with a collection of information if it does not display a currently valid OMB control number. **PLEASE DO NOT RETURN YOUR FORM TO THE ABOVE ADDRESS.**

1. REPORT DATE *(DD-MM-YYYY)*
04-05-2013

2. REPORT TYPE

3. DATES COVERED *(From - To)*
4-20-2009 to 4-5-2013

4. TITLE AND SUBTITLE
Quantifying the Presence and Activity of Aerobic, Vinyl Chloride-Degrading Microorganisms in Dilute Groundwater Plumes by Using Real-Time PCR

5a. CONTRACT NUMBER
W912HQ-09-C-0013

5b. GRANT NUMBER

5c. PROGRAM ELEMENT NUMBER

6. AUTHOR(S)
Timothy E. Mattes, Yang Oh Jin, Meredith Dobson, Meng-chen Lee, Stefanie Schmidt, Samuel Fogel, Margaret Findlay, and Donna Smoler

5d. PROJECT NUMBER
ER-1683 (SERDP)

5e. TASK NUMBER

5f. WORK UNIT NUMBER

7. PERFORMING ORGANIZATION NAME(S) AND ADDRESS(ES)

The University of Iowa
Controller and Asst. VP
Business Office, 4 Jessup Hall, Iowa City, IA 52242

Bioremediation Consulting, Inc.
39 Clarendon St.
Watertown, MA 02472

8. PERFORMING ORGANIZATION REPORT NUMBER

9. SPONSORING / MONITORING AGENCY NAME(S) AND ADDRESS(ES)
Strategic Environmental Research and Development Program
4800 Mark Center Drive
Suite 17D08
Alexandria, VA 22350

10. SPONSOR/MONITOR'S ACRONYM(S)
SERDP

11. SPONSOR/MONITOR'S REPORT NUMBER(S)

12. DISTRIBUTION / AVAILABILITY STATEMENT
Approved for public release; distribution is unlimited

13. SUPPLEMENTARY NOTES

14. ABSTRACT

15. SUBJECT TERMS

16. SECURITY CLASSIFICATION OF:			17. LIMITATION OF ABSTRACT	18. NUMBER OF PAGES	19a. NAME OF RESPONSIBLE PERSON
a. REPORT	b. ABSTRACT	c. THIS PAGE		169	19b. TELEPHONE NUMBER *(include area code)*

Standard Form 298 (Rev. 8-98)
Prescribed by ANSI Std. Z39.18

This report was prepared under contract to the Department of Defense Strategic Environmental Research and Development Program (SERDP). The publication of this report does not indicate endorsement by the Department of Defense, nor should the contents be construed as reflecting the official policy or position of the Department of Defense. Reference herein to any specific commercial product, process, or service by trade name, trademark, manufacturer, or otherwise, does not necessarily constitute or imply its endorsement, recommendation, or favoring by the Department of Defense.

Table of Contents

List of Tables iii
List of Figures viii
List of Acronyms xviii
Keywords xviii
Acknowledgements xviii
Abstract 19
Objective 21
Background 22
Materials and Methods 25
Results and Discussion 47
Task 1 Develop qPCR techniques for etheneotrophs (and methanotrophs) 47
Subtask 1.1 DNA extractions from Sterivex filters 47
Subtask 1.2 qPCR primer development and testing 50
Subtask 1.3 Develop qPCR standard curves 66
Subtask 1.4 Testing qPCR primer sets on environmental samples 74
Task 2 Develop RT-qPCR technique for etheneotrophs 87
Subtask 2.1 Develop a RNA extraction protocol suitable for groundwater samples 87
Subtask 2.2 Develop etheneotroph RT-qPCR method 90
Task 3 Investigate the normalized rate of VC oxidation 97
Subtask 3.1 Preliminary Carver microcosm study (2009) 97
Subtask 3.2 Microcosm study of groundwater from Carver well RB63-I (2010 and 2011) . 98
Subtask 3.3 Methane, ethene, and VC enrichment cultures from Carver site well RB63-I 112
Subtask 3.4 Pure culture experiments with *Mycobacterium* strain JS622 and pMMO-expressing *Methylocystis* sp. ATCC 49242 122
Conclusions and Implications for Future Research/Implementation 148
Development of a qPCR method for etheneotrophs 148
Methanotroph qPCR protocol 149
RT-qPCR method development and applications 149
Microcosm study with VC-contaminated well 63-I groundwater from the Carver, MA site . 150
Literature Cited 155

Appendices 162
Appendix A – Methanotroph qPCR primer selection and optimization experiments 162
Kolb Primer Results 162
pmoA 178 and pmoA 330 PCR Efficiency Variations 162
Methanotroph qPCR Primer Optimization 163
Primer Validation 173
pmoA 472 and mmoX primer set Validation Experiments 176
16S T1, T2 and Universal primer validation 178
Soldotna, AK Environmental Samples – methanotroph qPCR 180
Naval Air Station Oceana, Virginia Environmental Samples 181
Carver, MA Environmental Samples 183
Carver, MA – Task 2 cDNA Experiment 184
Appendix B qPCR standard curve parameters 187
Appendix C - Data from Carver, MA VC-assimilation microcosms 190
List of Scientific/Technical Publications 194

List of Tables

Table 1. Bacterial strains used in this study. 30

Table 2. Oligonucleotides used for qPCR in this study 34

Table 3. Oligonucleotides used to generate qPCR standards. 35

Table 4. Concentrations (mg/L) of macro and micronutrients in well RB-63I native and amended groundwater 44

Table 5. Mass of VOCs added to microcosms containing mineral amended well 63-I groundwater in the 2010 microcosm experiment. 44

Table 6**.** Dilution approach used to prepare experimental bottles. Prior to each experiment 504 ml each of JS622 and ATCC49242 was prepared at initial OD_{600} = 0.1, then different volumes were mixed as shown below to provide different percentages of each microbial group as desired. 46

Table 7. Substrate and culture ratios used in pure culture experiments. 46

Table 8. Results of qPCR primer specificity testing. A "+" indicates that a band of the expected size was observed, while a "-" indicates that a band of the expected size was absent. The number of bands that were not of the expected size (non-specific products) was also noted. Based on the results of this test, the primers RTC9/RTC6 and RTE15/RTE16 were chosen for more detailed analysis. 52

Table 9**.** RTC PCR products sequencing results. Please refer to Table 1 and reference *(38)* for additional information about the pure cultures and clone sequences indicated in this table. 56

Table 10**.** RTE PCR product sequencing results. Please refer to Table 1 and *(38)* for additional information about the pure cultures and clone sequences indicated in this table. 58

Table 11. List of the “mixed real-time” (MRT) primers - a set of non-degenerate primers that account for all available *etnC* or *etnE* primer combinations at the same priming sites as the previously described “real-time” (RT) primers. 64

Table 12. Inter-assay standard curve parameters for *etnC* (with RTC primers) and *etnE* (with RTE primers) using DNA template from *Mycobacterium* strain JS60, *Mycobacterium* strain JS623, and *Nocardioides* strain JS614. Data was collected in quintuplicate. BSA was not used in this experiment. The dynamic range is the range of gene copy numbers used in qPCR standards. The slope, R^2, and y-intercept were derived by a linear regression of log (initial gene copy numbers) vs. Ct data. Amplification efficiencies (AE) were calculated by the equation $10^{(-1/slope)} - 1$. Fluorescence thresholds were defined by manual operator adjustment in the Applied

Biosystems Sequence Detection System software (version 1.2.3). These data represent the average of five replicates. 68

Table 13. Average quantification results for known amounts of methanotrophic DNA amplified with 16S T1, 16S T2, pmoA 178, and pmoA 330 primer sets. The standard curve PCR efficiencies for the pmoA 178, pmoA 330, 16S T1, and 16S T2 primer sets were 95.8%, 94.5%, 95.5%, and 87.3%, respectively. The primer sets were used at 300 nM, 300 nM, 800 nM, and 200 nM, respectively (for more standard curve characteristics for this experiment, see Appendix A). Although the 16S T2 standard curve PCR efficiency is outside of the desirable range (95% to 105%) *(78)*, the most important issue raised by this experiment is the inefficient amplification of pure culture methanotroph template DNA by both pmoA primer sets. Dissociation curves for pmoA 178, pmoA 330, 16S T1, and 16S T2 qPCR assays can be found in Appendix A. 70

Table 14. Average quantification results for known amounts of methanotrophic DNA amplified using 16S T1, 16S T2, pmoA 472, and mmoX primer sets. Standard curves were constructed using the new pmoA 472, mmoX, and the 16S gene (16S U) primers. The primers were used at the same concentrations as stated in the original papers (300 nM for all) and were validated using the same technique as previously described. The standard curve PCR efficiencies for the pmoA 472, mmoX, 16S T1, and 16S T2 primer sets were 98.0%, 94.2%, 103%, and 101%, respectively (for more standard curve characteristics for this experiment, see Appendix A). Dissociation curves for pmoA 472, 16S T1, and 16S T2 qPCR assays can be found in Appendix A. 71

Table 15. Average quantification results for known amounts of methanotrophic DNA amplified using 16S T1, 16S T2, and 16S U primer sets. The standard curve PCR efficiencies for the 16S T1, 16S T2, and 16S U primer sets were 101%, 99.2%, and 102%, respectively. The primer sets were used at 800 nM, 200 nM, and 300 nM, respectively (for all standard curve characteristics for this experiment, see Appendix A). Dissociation curves for the 16S T1, 16S T2, and 16S U primer assays can be found in Appendix A. 72

Table 16. Effect of BSA addition (400 ng/µL) on amplification efficiencies (AE) in six different groundwater DNA extracts. The RTC and RTE primer sets were used. Template DNA was diluted by 5X, 10X, 20X, and 40X for the purpose of estimating standard curve linearity (via R^2 from a linear regression analysis) and amplification efficiencies (via analysis of the slope of the regression line). Amplification efficiencies were calculated by plotting log (dilution) vs. Ct, determining the slope of a linear regression line with the data, and using the equation: $10^{(-1/slope)} - 1$..... 76

Table 17. Abundance of *etnC* and *etnE* in groundwater samples collected from monitoring wells at three VC-contaminated sites. DNA from single Sterivex filter samples was extracted and analyzed from each well. The number of gene copies reported for each sample is the average of three analytical replicates ± the standard deviation. The lowest C_t values in the no template controls (NTCs) were 35.7 (*etnC*) and 35.2 (*etnE*).)). Intra-assay standard PCR efficiencies

were 105.5% when using *etnC* primers (-slope = 3.21, R^2 = 0.999; Y-intercept = 38.55, threshold = 0.21) and 100.0% when using *etnE* primers (-slope = 3.32, R^2 = 0.998; Y-intercept = 38.53, threshold = 0.24). Using these intra-assay standard curves, along with template DNA concentrations (ng/µL), groundwater sample volume (L), and mass (ng) of DNA per L of groundwater, we calculated *etnC* and *etnE* gene copies per liter of groundwater. Additional detail concerning sampling, DNA extraction, and analysis of gene copy abundance is provided in Table 18..... 77

Table 18. Additional information concerning sampling, DNA extraction, and analysis of gene copy abundance in environmental samples. DNA extracted from each filter was eluted with 70 µL buffer as described in the materials and methods..... 78

Table 19. Comparison of estimated abundance of *etnC* and *etnE* in groundwater samples collected from monitoring wells at three VC-contaminated sites using two different degenerate primer sets. PCR efficiencies of the standard curves in this experiment were 105.0% (MRTC) and 108.1% (MRTE) with R^2>0.99. The linear dynamic range of the MRTC and MRTE standards were 100-3×10^7. Primer concentrations used: 800 µM for MRTC_F, 600 µM for MRTC_R, 600 µM for MRTE_F, and 900 µM for MRTE_R..... 79

Table 20. Average methanotroph gene abundance at the Soldotna, Alaska contaminated site. Standard curve PCR efficiencies for each primer set were 101 % and 97.6 %, respectively (for more standard curve characteristics, see Appendix A. Dissociation curves for the pmoA 472 primer assays can also be found in Appendix A..... 81

Table 21. Average methanotroph gene abundance (copies/L groundwater) at NAS Oceana. Primer concentrations were 300 nM, 300 nM, 800 nM, and 200 nM, respectively, and produce standard curve PCR efficiencies of 100 %, 99.4 %, 102 %, and 94.5 %, respectively. The 16S T2 PCR efficiency fell below the desired range (95% to 105%) and implies slightly decreased amplification efficiency for that primer set. This decrease in efficiency will cause the 16S T2 quantifications to appear smaller than they would otherwise in a qPCR reaction amplifying at 100%. For more standard curve characteristics and dissociation curves, see Appendix A..... 85

Table 22. Average methanotroph gene abundance at Carver contaminated site estimated using the 16S universal, 16S T1, and 16S T2 primer sets. Sampling date: 6/23/2009Primer concentrations were 300 nM, 800 nM, 200 nM, and 100 nM, respectively, and produce standard curve PCR efficiencies of 99.4 %, 99.3 %, 99.9 %, and 99.8 %, respectively. For more standard curve characteristics and dissociation curves, see Appendix A..... 86

Table 23. Methanotroph relative abundances as determined by qPCR. 86

Table 24: *pmoA* and *mmoX* transcript per gene ratios. Primer concentrations were 300 nM for both functional genes (pmoA 472 and mmoX) and 100 nM for the Luciferase control gene

Standard curve PCR efficiencies for each primer set were of 98.6 %, 96.7 %, and 100 %, respectively. Percent recoveries for the Luciferase control gene ranged from 9.3 % to 60.1 %. For more standard curve characteristics and detailed Luciferase recovery ratios, see Appendix A. With regard to the mmoX dissociation curve, results mirrored those of Soldotna, with the presence of the standard-curve double peak at 76°C and 86°C. Environmental samples contained two peak temperatures as well. It is suspected that the primer-dimer artifact in environmental samples is due to low target gene abundance. Dissociation curves for the pmoA 472, mmoX, and Luciferase primer assays can be found in Appendix A). 96

Table 25. Functional gene copy abundance for etheneotrophs and methanotrophs in well RB63I, as estimated by qPCR and expressed as Gene copies per liter of groundwater as described previously *(61)*. 98

Table 26. Observed lag periods and times for 50% degradation of VC, methane, and/or ethene in microcosms constructed in 2011. Lag and 50% degradation times are averages of duplicate or triplicate measurements ± the range. 103

Table 27. Observed lag periods and times for 50% degradation of VC, methane, and/or ethene in single microcosms constructed in 2010. 106

Table 28. The effect of epoxyethane concentration on time for 50% ethene use in Carver well 63I derived ethene enrichment cultures that were subjected to ethene starvation. Bottles contained mineral media and 82 µmols ethene/bottle, with 0.3 ml ethenotroph culture added per bottle at the start of the experiment..... 118

Table A29: Average standard curve characteristics for primer set pmoA 178 amplifying template DNA from *Methylocystis* sp. strain Rockwell. 164

Table A30: Average standard curve characteristics for primer set pmoA 178 amplifying template DNA from *Methylococcus capsulatus*. 165

Table A31: Average standard curve characteristics for primer set pmoA 330 amplifying template DNA from *Methylocystis* sp. strain Rockwell. 166

Table A32: Average standard curve characteristics for primer set pmoA 330 amplifying template DNA from *Methylococcus capsulatus*. 167

Table A33: Average standard curve characteristics for 16S T1 primer set amplifying template DNA from *Methylococcus capsulatus*. 168

Table A34: Average standard curve characteristics for 16S T2 primer set amplifying template DNA from *Methylocystis* sp. strain Rockwell. 169

Table A 35. Average standard curve characteristics for pmoA 178 and pmoA 330 primer validation experiments. 173

Table A 36. Average standard curve characteristics for pmoA 472 and mmoX primer validation experiment..... 177

Table A 37. Average standard curve characteristics for 16S T1 and 16S T2 primer validation experiment..... 177

Table A 38. Average standard curve characteristics for pmoA 472 and mmoX in Soldotna, AK environmental sample qPCR assay. 180

Table A 39. No Template Control (NTC) Ct values for Soldotna, AK standard curves. 180

Table A 40. Average standard curve characteristics for pmoA 472, mmoX, 16 T1, and 16S T2 in NAS Oceana, VA environmental sample qPCR assay. 181

Table A 41. No Template Control (NTC) Ct values for NAS Oceana, VA standard curves. 181

Table A 42: Average standard curve characteristics for 16S U, 16 T1, 16S T2 and Luciferase in Carver, MA environmental sample qPCR assay..... 183

Table A 43: No Template Control (NTC) results for Carver, MA standard curves shown in Table A 42..... 183

Table A 44. Luciferase gene recovery ratios for Carver, MA qPCR experiments. 184

Table A 45. Average standard curve characteristics for 16S U, 16 T1, 16S T2 and Luciferase in Carver, MA environmental sample qPCR assay..... 184

Table A 46: No Template Control (NTC) results for Carver, MA standard curves shown in Table A 45..... 184

Table B 48**.** qPCR standard curve parameters using different primer sets and template DNA from pure cultures. ABI 7000 System SDS Software (Applied Biosystems) was used to analyze real-time PCR fluorescence data. The "auto baseline" function was used in all situations. All fluorescence threshold numbers for each set of standards and samples were manually optimized as described previously. PCR efficiency was derived by $E = (1\text{-}10^{(-1/slope)})$. The linear dynamic range for all standards was between 3×10^{2}-3×10^{7} gene copies. 187

List of Figures

Figure 1. Conceptual plan and profile views of the VC-contaminated site in Carver, Massachusetts *(43)*. The location of monitoring wells where groundwater samples were taken for qPCR and microcosm studies is shown..... 26

Figure 2. The north VC plume at NAS Oceana illustrating the location of monitoring wells 18, 19, and 25 *(44)*. The left hand side of the figure illustrates the extent of the VC plume. The purple dots on the right hand side of the figure indicate the oxygen releasing compound (ORC) injection points..... 27

Figure 3. Aerial view of Soldotna, AK site with methane and VC plumes delineated. The location of monitoring wells where groundwater samples were taken is also shown. 28

Figure 4. Flow chart illustrating the separate extraction of DNA and RNA from filtered groundwater samples. 40

Figure 5. Flow chart depicting an approach for simultaneous DNA and RNA extraction from a single Sterivex filter..... 41

Figure 6. Killed control microcosms for both 2010 and 2011 Carver site groundwater experiments..... 43

Figure 7**.** A) Nucleic acid mass recovery following DNA extraction from pure cultures of VC-assimilating *Mycobacterium* JS60 (clear greeen bars) and *Nocardioides* JS614 (hatched blue bars) using a variety of extraction methods and kits. The mass of DNA recovered was normalized to the BB method. The bar height is the average of three replicates and the error bars are the 95% confidence interval. B) Comparison of estimated *etnC* gene abundance by qPCR following DNA extraction. The *etnC* abundance was normalized to the abundance estimated in the PWS DNA extract.Abbreviations: BB: Nucleic acid extraction by bead beating, followed by phenol:chloroform:isoamyl alcohol extraction. PS: Mo Bio Powersoil extraction kit. MPS: Mo Bio Powersoil extraction kit with additional zirconium/silica beads added. PW: Mo Bio PowerWater extraction kit. MPW: Mo Bio PowerWater extraction kit with additional zirconium/silica beads added. PWS: MoBio PowerWater Sterivex extraction kit..... 49

Figure 8**.** Specificity testing of the *etnE* primers RTE15 and RTE16 by standard PCR using DNA from pure cultures (E.coli, Xan. (propene-degrading *Xanthobacter* Py2), VC-assimilating strains JS614, JS60, JS616, JS617, JS621, TM1, TM2, etheneotrophic strains JS622, JS623, JS624, JS625, and 16 environmental samples (GW1-6 = Carver, MA samples; GW7-13 = Soldotna, AK samples; GW14-16 = NAS Oceana samples). In all cases a single band of the expected size was observed, a result which strongly suggested good primer specificity..... 53

Figure 9. Specificity testing of the etnC primers RTC9 and RTC6 by standard PCR using DNA from pure cultures (*E.coli*, Xan. (propene-degrading Xanthobacter Py2), VC-assimilating strains JS614, JS60, JS616, JS617, JS621, TM1, TM2, etheneotrophic strains JS622, JS623, JS624, JS625, and 16 environmental samples (GW1-6 = Carver, MA samples; GW7-13 = Soldotna, AK samples; GW14-16 = NAS Oceana samples). The top gel image shows PCR products generated with a 55°C annealing temperature. At an annealing temperature of 60°C (bottom gel image), the larger incorrectly sized band disappears. However, no bands were observed initially in samples GW7-16, likely due to low target gene concentration. NC, NC2 = negative control (no template or E.coli template). 54

Figure 10**.** Results of a nested PCR experiment with *etnC* primers. The initial PCRs were carried out with environmental DNA and the primers NVC105 and NVC106 *(72)*. Then, 2 µl of each PCR was used as template in a second PCR with the RTC9 and RTC6 primer set. In all cases, a band of the expected size was noted, supporting the hypothesis that *etnC* concentrations were low in samples GW7-GW16. Note that GW1-6 = Carver, MA samples; GW7-13 = Soldotna, AK samples; GW14-16 = NAS Oceana samples. NC = negative control (no template). 55

Figure 11. Melt-curve analysis (temperature vs. change in fluorescence intensity) of PCR products generated during qPCR analysis of DNA from Carver site well RB46D. 59

Figure 12. Melt-curve analysis (temperature vs. change in fluorescence intensity) of PCR products generated during qPCR analysis of DNA from NAS Oceana well MW25. 60

Figure 13. Melt-curve analysis (temperature vs. change in fluorescence intensity) of PCR products generated during qPCR analysis of DNA from Soldotna, AK well MW40. 61

Figure 14**.** Comparison of *etnC* and *etnE* abundance (per ng of genomic DNA) in four different cultures (JS60, JS614, JS617, and JS623) estimated with non-degenerate GSPs and degenerate primer sets. Bar heights are the average of three analytical replicates and the error bars are the 95% confidence interval. 65

Figure 15. Comparison of average quantifications between pmoA 472, mmoX, 16S T1, and 16S T2 primer sets amplifying known amounts of genomic DNA. Type I DNA was extracted from *Methylococcus capsulatus* pure culture. Type II DNA was extracted from *Methylocystis* sp. strain Rockwell. The bar heights for each sample are the average of replicate measurements and error bars represent the range of data. 72

Figure 16. Dissociation curve for *mmoX* primer set amplifying *Methylococcus* sp. (Type I) and *Methylocystis* sp. (Type II). Multiple peaks were observed, implying primer-dimer artifacts or non-specific amplification. 73

Figure 17. Comparison of average quantifications between 16S T1, 16S T2 and 16S U primer sets amplifying known amounts of genomic DNA. Type I DNA was extracted from *Methylococcus capsulatus* pure culture. Type II DNA was extracted from *Methylocystis* sp. strain Rockwell. The bar heights for each sample are the average of replicate measurements and error bars represent the range of data. 73

Figure 18. Change in average *pmoA* gene abundance in contaminated groundwater from MW 40 in Soldotna, AK. The bar heights for each sample are the average of replicate measurements and error bars represent the range of data. 81

Figure 19. Change in average *pmoA* gene abundance in contaminated groundwater from MW 6 in Soldotna, AK. The bar heights for each sample are the average of replicate measurements and error bars represent the range of data. 82

Figure 20. Change in average *mmoX* gene abundance in contaminated groundwater from MW 6 in Soldotna, AK. The bar heights for each sample are the average of replicate measurements and error bars represent the range of data. 82

Figure 21. Change in average *mmoX* gene abundance in contaminated groundwater from MW 40 in Soldotna, AK. The bar heights for each sample are the average of replicate measurements and error bars represent the range of data. 83

Figure 22. Dissociation curve for *mmoX* primer set standard curve. Multiple peaks were observed and appear to be primer-dimer artifacts since the no-template control contains only one peak quantification. The environmental sample melt curve contained a single peak at the 86°C (Figure 23). 83

Figure 23. Dissociation curve for *mmoX* primer set amplifying environmental samples from the Soldotna, AK site. The single dissociation peak demonstrates absence of primer-dimer artifacts. 84

Figure 24. Top graph: Nucleic acid mass recovery following RNA extraction from pure cultures of VC-assimilating *Mycobacterium* JS60 (clear greeen bars) and *Nocardioides* JS614 (hatched blue bars) using a variety of extraction methods and kits. The mass of RNA recovered was normalized to the BB method. The bar height is the average of three replicates and the error bars are the 95% confidence interval. Bottom graph: Comparison of estimated *etnC* transcript abundance by RT-qPCR following RNA extraction. The *etnC* abundance was normalized to the abundance estimated in the PWS RNA extract. Abbreviations: BB: Nucleic acid extraction by bead beating, followed by phenol:chloroform:isoamyl alcohol extraction. PS: Mo Bio Powersoil extraction kit. MPS: Mo Bio Powersoil extraction kit with additional zirconium/silica beads added. PW: Mo Bio PowerWater extraction kit. MPW: Mo Bio PowerWater extraction kit with additional zirconium/silica beads added. PWS: MoBio PowerWater Sterivex extraction kit. 89

Figure 25**.** These experiments, conducted with ethene- and VC-grown cultures of the VC-assimilating *Nocardioides* sp. strain JS614, illustrate the relationship between growth on VC, ethene, and acetate (as well as VC and ethene starvation) and the transcript/gene ratio for both functional genes (*etnC* and *etnE*). Liquid samples were taken periodically, DNA and RNA were extracted simultaneously from liquid samples, and extracts were subjected to RT-qPCR analysis with internal controls. (A) This graph shows accumulative ethene consumption and resulting microbial growth (measured indirectly by the optical density at 600 nm wavelength (OD_{600}) with time. Liquid samples were taken at the times where data points are shown. (B) This graph shows accumulative VC consumption and resulting microbial growth with time. Liquid samples were taken at the times where data points are shown. (C) The transcripts per gene ratio for functional genes (*etnC* and *etnE*) vs. sampling time and condition when JS614 was grown on ethene or acetate, (D) The transcripts per gene ratio for functional genes (*etnC* and *etnE*) vs. sampling time and condition when JS614 was grown on VC. 92

Figure 26. These graphs illustrate the application of our RT-qPCR method to groundwater samples from a VC-contaminated site (Carver, MA). Biomass was collected on Sterivex filters. Filters from RNA analysis were preserved with RNA later. DNA and RNA were extracted separately from a total of 6 filters per well (3 each for DNA and RNA) using the Mo Bio PowerWater DNA and PowerWater RNA kits, respectively, using slightly modified protocols. Internal controls were added, RT-qPCR was performed for both functional genes (*etnC* and *etnE*), and the transcript/gene ratio calculated. This analysis was performed with samples from three different monitoring wells: RB46D (A), RB63I (B), and RB64I (C). The error bars represent the 95% CI. The calculated gene copies were 1.7×10^4 *etnC* and 9.5×10^3 *etnE* per L of groundwater (RB46D), 2.4×10^4 *etnC* and 1.6×10^4 *etnE* per L of groundwater (RB63I), and 1.3×10^3 *etnC* and 2.5×10^3 *etnE* per L of groundwater (RB64I). The calculated transcripts were 6.5×10^3 *etnC* and 3.5×10^3 *etnE* per L of groundwater (RB46D), 1.6×10^4 *etnC* and 1.3×10^4 *etnE* per L of groundwater (RB63I), and 7.6×10^3 *etnC* and 5.7×10^3 *etnE* per L of groundwater (RB64I). For the DNA plate, standard curve amplification efficiencies were 100.8% (MRTC), 104.3% (MRTE), and 96.6% (ref) with a good linear fit and $R^2>0.99$ in all cases. The linear dynamic range for DNA were $10\text{-}3\times10^5$ copies for both *etnC* and *etnE* standard and $30\text{-}3\times10^7$ copies for reference gene standard. Reference DNA(2.3×10^8 copies) was added and the fractional recoveries were 32.7% (RB46D), 67.6% (RB63I) and 15.9% (RB64I). For the cDNA plate, standard curve amplification efficiencies were 102.2% (MRTC), 112.7% (MRTE), and 102.4% (ref) with a good linear fit and $R^2>0.99$ in all cases. The linear dynamic ranges for cDNA were $10\text{-}3\times10^5$ copies for both *etnC* and *etnE* standard and $30\text{-}3\times10^7$ copies for reference gene standard. Reference mRNA(4.1×10^9 copies) was added and the fractional recoveries were 4.4% (RB46D), 1.2% (RB63I) and 2.3% (RB64I)..... 95

Figure 27. Aerobic biodegradation of VC, methane, and/or ethene added to microcosms constructed with groundwater from the Carver site containing methanotrophs, ethenotrophs, and vinyl chloride-assimilating bacteria. Single substrate bottles were constructed in duplicate.

Multiple substrate bottles were conducted in triplicate. The results from duplicate or triplicate bottles are shown separately for clarity. (a) VC added, (b) Methane added (c) Ethene added, (d) Methane and VC added, (e) Ethene and VC added, (f) Methane and ethene added, (g) Methane, ethene, and VC added. The symbol legend in panel (g) applies to all panels. Comparison of substrate utilization under different conditions was based on lag time and days for 50% utilization. VC was degraded faster in the presence of both methane and ethene (g), than in the presence of either methane alone (d) or ethene alone (e). Abbreviations: meth: methane, ethe: ethene 104

Figure 28. Aerobic biodegradation of A) methane (red circles), B) ethene (blue squares), and C) VC (green triangles) added singly to microcosms constructed with groundwater from the Carver site containing methanotrophs, etheneotrophs, and vinyl chloride-assimilating bacteria. Comparison of substrate utilization under different conditions was based on lag time and days for 50% utilization. 107

Figure 29. Aerobic biodegradation of 0.08 umol VC in the presence of a range of methane concentrations in microcosms constructed with groundwater from the Carver site containing methanotrophs, etheneotrophs, and vinyl chloride-assimilating bacteria. Comparison of substrate utilization under different conditions was based on lag time and days for 50% utilization. 108

Figure 30. Aerobic biodegradation of 0.08 umol VC in the presence of a range of ethene concentrations in microcosms constructed with groundwater from the Carver site containing methanotrophs, etheneotrophs, and vinyl chloride-assimilating bacteria. Comparison of substrate utilization under different conditions was based on lag time and days for 50% utilization. 109

Figure 31. Aerobic biodegradation of 2 µmol methane and 2 µmol ethene in a microcosm constructed with groundwater from the Carver site containing methanotrophs, etheneotrophs, and vinyl chloride-assimilating bacteria. Comparison of substrate utilization under different conditions was based on lag time and days for 50% utilization. 110

Figure 32. Aerobic biodegradation of 0.08 µmol VC in the presence of a range of methane and ethene concentrations in microcosms constructed with groundwater from the Carver site containing methanotrophs, etheneotrophs, and vinyl chloride-assimilating bacteria. Comparison of substrate utilization under different conditions was based on lag time and days for 50% utilization. 111

Figure 33. Biodegradation of methane, VC and a methane+VC mixture by methane enrichment cultures derived from Carver well RB63I. These results indicate that the methanotrophs in this culture cannot degrade VC in the absence of methane, and slowly cometabolize VC in the presence of methane. 114

Figure 34. Biodegradation of methane, VC and a methane+VC mixture by methane enrichment cultures derived from Carver well RB63I. These results are a repeat of the experiment depicted in Figure 33 and confirm that the methanotrophs in this culture cannot degrade VC in the absence of methane, and slowly cometabolize VC in the presence of methane. 115

Figure 35. Biodegradation of ethene and formation of epoxyethane by methane enrichments cultures from the Carver site. This indicates that methanotrophs can produce epoxyethane, a molecule known to stimulate etheneotroph gene expression. 117

Figure 36. The effect of epoxyethane concentration on time for 50% ethene use in Carver well 63I derived ethene enrichment cultures that were subjected to ethene starvation. 119

Figure 37. The effect of epoxyethane concentration on time for 50% ethene use in Carver well 63I derived ethene enrichment cultures that were subjected to ethene starvation. Three bottles received no epoxyethane (green lines) , and 3 bottles received 6 μmole/bottle epoxyethane (purple lines). 120

Figure 38. Degradation of methane (a) ethene (b) and VC (c) as single substrates for ethene-grown JS622 cells in separate bottles. All values shown are in μM. The slopes of the regression lines shown represent the degradation rates (initial OD_{600} = 0.1). 124

Figure 39. Aerobic biodegradation of methane+VC (d), ethene+VC (e), methane+ethene (f), methane+ethene+VC (g) by ethene-grown JS622. The slopes represent the degradation rates. 125

Figure 40. Degradation of a) methane, b) ethene, and c) VC as single substrates for methane-grown *Methylocystis* sp. ATCC49242 in separate bottles. The slopes of the regression lines shown represent the degradation rates. 127

Figure 41. Aerobic biodegradation of methane+VC(d), ethene+VC (e), methane+ethene (f), methane+ethene+VC (g) by *Methylocystis* ATCC49242. The slopes of the regression lines shown represent substrate degradation rates. 128

Figure 42. Degradation of methane (a), ethene (b), VC (c) as a sole substrate for a 1:1 JS622 and ATCC49242 mixture (initial OD_{600} = 0.1). The slopes of the regression lines represent the degradation rates. 131

Figure 43. Aerobic biodegradation of methane+VC (d), ethene +VC (e), methane+ethene (f), methane+ethene+VC (g) by a JS622 and ATCC49242 (1:1) mixture. The slopes represent the degradation rates. 132

Figure 44. The degradation patterns of methane, ethene, VC as single substrate by different JS622/ATCC49242 ratios. The slopes represent the degradation rates. 136

Figure 45. The degradation patterns of methane+VC and ethene+VC by different JS622/ATCC49242 ratios. The slopes represent the degradation rates. 137

Figure 46. The degradation patterns of methane+ ethene and methane+ ethene+ VC by different JS622/ATCC49242 ratios. The slopes represent the degradation rates. 138

Figure 47. The degradation patterns of methane, ethene, VC as single substrate by different JS622/ATCC49242 ratios. The slopes represent the degradation rates 141

Figure 48. The degradation patterns of methane+VC by different JS622/ATCC49242 ratios where the mass of methane fed is 20 times that of VC. The slopes of the regression lines represent the degradation rates discussed in the text. 143

Figure 49. The degradation patterns of ethene+VC by different JS622/ATCC49242 ratios in the gas ratio of 2:1. The slopes represent the degradation rates. 145

Figure 50. The degradation patterns of methane+ethene by different JS622/ATCC49242 ratios in the gas ratio of 10:1. The slopes represent the degradation rates. 146

Figure 51. The degradation patterns of methane+VC and ethene+VC by different JS622/ATCC49242 ratios in the gas ratio of 20:2:1. The slopes of the regression lines represent the initial degradation rates. 147

Figure A52: End point PCR products of Kolb primers and *Methylococcus* (lane 7) and *Methylocystis* (lane 8) template DNA. 162

Figure A 53: Comparison of pmoA 178 PCR efficiencies as related to varying primer concentrations. Template DNA was from *Methylocystis* sp. strain Rockwell. Bolded borders indicate optimal primer concentration, and light grey bars represent chosen template species for the indicated primer set. The bar heights at each concentration are the average of triplicate measurements and error bars represent standard deviations. 165

Figure A54: Comparison of pmoA 178 PCR efficiencies as related to varying primer concentrations. Template DNA was from *Methylococcus capsulatus*. Bolded borders indicate optimal primer concentration. The bar heights are the average of triplicate measurements and the error bars represent standard deviations. 166

Figure A55: Comparison of pmoA 330 PCR efficiencies as related to varying primer concentrations. Template DNA was from *Methylocystis* sp. strain Rockwell. Bolded borders indicate optimal primer concentration, and light grey bars represent chosen template species for the indicated primer set. The bar heights at each concentration are the average of triplicate measurements and error bars represent standard deviations. 167

Figure A56: Comparison of pmoA 330 PCR efficiencies as related to varying primer concentrations. Template DNA was from *Methylococcus capsulatus*. Bolded borders indicate optimal primer concentration. The bar heights at each concentration are the average of triplicate measurements and error bars represent standard deviations. 168

Figure A57: Comparison of 16S T1 PCR efficiencies as related to varying primer concentrations. Template DNA was from *Methylococcus capsulatus*. Light grey bars indicate optimal primer concentration. The bar heights at each concentration are the average of triplicate measurements and error bars represent standard deviations. 169

Figure A58: Comparison of 16S T2 PCR efficiencies as related to varying primer concentrations. Template DNA was from *Methylocystis* sp. strain Rockwell. Light grey bars indicate optimal primer concentration. The bar heights at each concentration are the average of triplicate measurements and error bars represent standard deviations. 170

Figure A 59: Dissociation curve for primer set pmoA 178 amplifying template DNA from *Methylocystis* sp. strain Rockwell at a primer concentration of 300 nM. Double peaks are seen in samples containing little (10^2) to no (no-template control) template DNA, indicating probable primer-dimer artifacts. 170

Figure A 60: Dissociation curve for primer set pmoA 178 amplifying template DNA from *Methylococcus capsulatus* at a primer concentration of 300 nM. Double peaks are seen in samples containing little (10^2) to no (no-template control) template DNA, indicating probable primer-dimer artifacts. 171

Figure A 61: Dissociation curve for primer set pmoA 330 amplifying template DNA from *Methylocystis* sp. strain Rockwell at a primer concentration of 300 nM. Double peaks are seen in no-template control samples indicating probable primer-dimer artifacts. 171

Figure A62: Dissociation curve for primer set pmoA 330 amplifying template DNA from *Methylococcus capsulatus* at a primer concentration of 300 nM. Double peaks are seen in all samples. PCR products were purified and sequence results indicated that both peaks represented the *pmoA* gene. 172

Figure A 63: Dissociation curve for primer set 16S T1 amplifying template DNA from *Methylococcus capsulatus* at a primer concentration of 800 nM. 172

Figure A64: Dissociation curve for primer set 16S T2 amplifying template DNA from *Methylocystis* sp. strain Rockwell at a primer concentration of 200 nM. 173

Figure A 65: Dissociation curve for primer set pmoA 178. The ~89°C peak represents standard curve melting temperatures, while the ~84°C peak represents melting temperature of the Type I/Type II sample mixtures. 174

Figure A 66: Dissociation curve for primer set pmoA 330 amplifying standard curve template DNA and Type I/Type II sample mixtures at a primer concentration of 300 nM. 174

Figure A67: Dissociation curve for primer set pmoA 16S T1 amplifying standard curve template DNA and Type I/Type II sample mixtures at a primer concentration of 800 nM. 175

Figure A 68: Dissociation curve for primer set pmoA 16S T2 amplifying standard curve template DNA and Type I/Type II sample mixtures at a primer concentration of 200 nM. 175

Figure A69: Dissociation curve for primer set pmoA 472 amplifying standard curve template DNA and Type I/Type II sample mixtures at a primer concentration of 300 nM. This curve is associated with the data presented in Table 20. 176

Figure A70: Dissociation curve for primer set 16S T1 amplifying standard curve template DNA and Type I/Type II sample mixtures at a primer concentration of 800 nM. 176

Figure A 71: Dissociation curve for primer set primer set 16S T2 amplifying standard curve template DNA and Type I/Type II sample mixtures at a primer concentration of 200 nM. 177

Figure A 72: Dissociation curve for primer set 16S T1 amplifying standard curve template DNA and Type I/Type II sample mixtures at a primer concentration of 800 nM. 178

Figure A 73: Dissociation curve for primer set 16S T2 amplifying standard curve template DNA and Type I/Type II sample mixtures at a primer concentration of 200 nM. 178

Figure A 74: Dissociation curve for primer set 16S U amplifying template DNA from *Methylocystis* sp. strain Rockwell at a primer concentration of 300 nM. 179

Figure A 75: Dissociation curve for primer set pmoA 472 amplifying standard curve template DNA and environmental samples from VC contaminated groundwater in Soldotna, AK. 180

Figure A 76: Dissociation curve for primer set pmoA 472 amplifying standard curve template DNA and environmental samples from VC contaminated groundwater in NAS Oceana, VA. . 181

Figure A 77: Dissociation curve for primer set mmoX amplifying standard curve template DNA and environmental samples from VC contaminated groundwater in NAS Oceana, VA. 182

Figure A 78: Dissociation curve for pmoA 472 primer set amplifying standard curve template DNA and environmental samples from VC contaminated groundwater in Carver, MA..... 183

Figure A 79: Dissociation curve for *mmoX* primer set standard curve Carver, MA cDNA experiment. Multiple peaks were observed and appear to be primer-dimer artifacts since the no-template control contains only one peak. 185

Figure A 80: Dissociation curve for *mmoX* primer set amplifying environmental samples from Carver, MA cDNA experiment. Multiple peaks were observed and appear to be primer-dimer artifacts caused by low target gene abundances. Sample 63I showed high quantities of the target gene, which could explain why it did not have a melting temperature associated with the primer- 185

Figure A 81: Dissociation curve for Luciferase primer set amplifying standard curve template DNA and environmental samples from VC contaminated groundwater in Carver, MA..... 186

List of Acronyms

ABI	Applied Biosystems Inc.
AkMO	Alkene monooxygenase
ATCC	American Type Culture Collection
bps	base pairs
BCI	Bioremediation Consulting, Inc.
cDNA	Complementary Deoxyribonucleic acid
CoM	Coenzyme M
DNA	Deoxyribonucleic acid
DoD	Department of Defense
EaCoMT	Epoxyalkane Coenzyme M Transferase
etnC	alkene monooxygenase alpha subunit gene
etnE	Epoxyalkane Coenzyme M Transferase gene
GSP	Gene Specific Primer
MCL	Mass Contaminant Level
MBT	Molecular Biology Tool
mRNA	messenger Ribonucleic Acid
NAS	Naval Air Station
ORC	Oxygen Release Compound™
ORP	Oxidation Reduction Potential
P	Phosphorus
PCE	Tetrachloroethene
PCR	Polymerase Chain Reaction
ppb	parts per billion
qPCR	real-time quantitative Polymerase Chain Reaction
RNA	Ribonucleic Acid
rRNA	Ribosomal Ribonucleic Acid
RT-qPCR	real-time, reverse-transcription quantitative Polymerase Chain Reaction
RT-PCR	reverse-transcription Polymerase Chain Reaction
TCE	Trichloroethene
SWMU	Solid Waste Management Unit
STE	Salt-Tris-EDTA buffer
VC	Vinyl Chloride

Keywords

Quantitative PCR, aerobic vinyl chloride biodegradation, etheneotroph, methanotroph, cometabolism, natural attenuation, dilute VC plumes

Acknowledgements

We would like to thank Bill Richard (EST Associates, Inc.), Tim McDougall (OASIS Environmental), and Angela Petree (CH2M Hill) for directing groundwater sampling and Sam Fogel (Bioremediation Consulting, Inc.), Jim Begley (MT Environmental Restoration), Laura Cook (CH2M Hill) and Sharon Richmond (Alaska DEC) for sharing geochemical data and coordinating sampling efforts. We also thank Michelle Stolzoff and Stefanie Schmidt for technical assistance. This research was supported by the Strategic Environmental Research and Development Program (SERDP) under project ER-1683.

Abstract

Objectives: Vinyl chloride (VC), a known human carcinogen with a USEPA maximum contaminant level of 2 ppb, is a significant contaminant of concern present as dilute groundwater plumes at many DoD sites. The objective of this project is to develop quantitative real-time PCR (qPCR) and reverse-transcription qPCR (RT-qPCR) techniques to estimate the abundance and activity of aerobic, VC-oxidizing bacteria (including methanotrophs and etheneotrophs/VC-assimilating bacteria) in groundwater. Two functional genes known to participate in VC oxidation in aerobic, ethene- and VC-assimilating bacteria (the alkene monooxygenase subunit gene *etnC* and the epoxyalkane:CoM transferase gene *etnE*) were targeted for quantification.

Technical approach: Using known etnC and etnE sequences from isolates, enrichment cultures and environmental samples, two sets of degenerate qPCR primers were developed for each functional gene. After extensive testing of primer specificity, we developed a SYBR green-based qPCR method for quantification of etnC and etnE.

The qPCR method for etheneotrophs was extended to incorporate mRNA analysis (i.e. RT-qPCR), which entailed selecting appropriate reference nucleic acids (ref mRNA or ref DNA) and adding known amounts of these reference material into samples following the RNA and DNA extraction steps, respectively. Following conversion of RNA to cDNA by reverse-transcription (RT), the abundance of ref nucleic acids was quantified alongside the etnC and etnE genes (on the same qPCR plate). This facilitated calculation of the percent ref nucleic acid recovery The ref nucleic acid recovery allows assessment of RNA (and DNA) losses in the sample during several steps in the protocol (e.g. during the RT step).

Results: The qPCR method for etheneotrophs was successfully applied to 9 different samples from three different VC-contaminated sites, in some cases over a 3 year period. The abundance of *etnC* ranged from $1.3\times10^3 – 1.0\times10^5$ genes per liter of groundwater (LGW). The abundance of *etnE* ranged from $1.9\times10^3 – 6.3\times10^5$ genes per LGW. Because field application of this method is limited, conclusions regarding these gene abundances cannot be made other than etheneotrophs were found to be present at all three sites.

Methanotroph qPCR for methane monooxygenase functional genes *pmoA* and *mmoX* was also performed on many of the same samples. This revealed that *pmoA* abundance ranged from $1.6\times10^4 – 4.1\times10^7$ genes/LGW and that *mmoX* abundance ranged from $2.5\times10^2 – 6.5\times10^6$ genes/LGW. The *pmoA* qPCR data suggest that methanotrophs are relatively more abundant at VC-contaminated sites than etheneotrophs. This is expected since methane concentrations are typically much higher than ethene and VC concentrations at the sites examined.

RT-qPCR was applied to *Nocardioides* sp. strain JS614 cultures grown on acetate, ethene, and VC as well as to starved JS614 cultures. Both transcript and gene abundances were measured and the gene expression results reported as “transcripts per gene”. These experiments indicated that when JS614 was starved, transcript per gene ratios were low (0.1-0.2). Acetate-grown JS614 cultures displayed transcript per gene ratios of 0.5-0.6. In contrast ethene- and VC-grown JS614 cultures featured transcript per gene ratios of 2-12, suggesting that when the transcript per gene ratio is greater than 1, then the bacteria expressing *etnC* and/or *etnE* are active.

RT-qPCR was successfully applied to 4 different groundwater samples from a VC-contaminated site in Carver, MA. Transcript/gene ratios were estimated as follows: 0.4 for both *etnC* and *etnE* in RB46D, 0.7 for *etnC* and 0.8 for *etnE* in RB63I, 5.7 for *etnC* and 2.2 for *etnE* in

RB64I, and 9.3 for *etnC* and 12.6 for *etnE* in RB73. These promising results suggest that RT-qPCR could be useful for interrogating the physiological status of etheneotrophs within the zone of influence of monitoring wells.

RT-qPCR for methanotrophs was also performed on the same samples from Carver wells RB46D, RB63I, and RB64I. Transcript/gene ratios were estimated as follows: 0.02 for *pmoA* and 0.24 for *mmoX* in RB46D, 0.02 for *pmoA* and 0.00 for *mmoX* in RB63I, and 0.11 for *pmoA* and 0.2 for *mmoX* in RB64I. These values are substantially lower than the etheneotroph transcript per gene ratios estimated in the same samples. This suggests that although methanotrophs were more abundant in these wells, they were not necessarily more active than the less abundant etheneotrophs. We recommend that additional studies be conducted to better delineate the differences in methanotroph/etheneotroph abundance and gene expression in environmental samples.

Effective RNA extraction was not always possible from Sterivex filters that had been preserved with RNAlater and stored at -80C for a period of time prior to analysis. This is currently a drawback to our RT-qPCR method. Based on anecdotal reports it is possible that freezing filters preserved with RNAlater at -80C could lead to rapid RNA degradation. Ideally, nucleic acids are to be extracted from filters as soon as possible after sampling and freezing should be avoided. We recommend more research to determine the appropriate sample preservation and handling procedures for filtered groundwater samples in combination with our RT-qPCR method.

In addition to the qPCR and RT-qPCR aspect of this project, groundwater, enrichment culture, and pure culture microcosm experiments were conducted to gain a better understanding of the factors that affect the rate of VC oxidation in groundwater. More specifically, microcosms were designed to address substrate interactions during VC cometabolism in groundwater scenarios with relatively low concentrations of ethene, methane and VC (all less than 100 µg/L) which are typical for groundwater down gradient of sites having previously undergone reductive dechlorination of chlorinated ethenes.

These experiments suggest that in general when both methane and ethene are present, there is a mixture of positive and negative substrate interactions that lead to an overall enhanced potential for VC to be completely degraded by cometabolism. Methanotrophs can produce epoxyethane, a compound known to stimulate ethene and VC degradation by etheneotrophs, in methane enrichment cultures fed ethene. Conversely, ethene appears to be inhibit methane and VC oxidation by methanotrophs. Substrate interactions during VC cometabolism in groundwater systems will be site-specific and depend highly on the abundance of methanotrophs and etheneotrophs as well as the concentrations of VC, ethene, and methane present (assuming oxygen is not limiting the process. These factors should be considered in the design of future VC bioremediation strategies involving cometabolism by applying the tools described here.

<u>Benefits</u>: These experiments will help us better understand the normalized rate of VC oxidation in dilute plumes. Molecular biology tools (MBTs) represent an innovative approach for providing direct lines of evidence for aerobic natural attenuation of VC and will thus support existing anaerobic bioremediation technologies that generate VC as a metabolic intermediate and facilitate improved decision-making in ongoing and future bioremediation studies. We have several strategies for technology transition, including presenting this work at national conferences, publishing peer-reviewed journal articles, applying for ESTCP support for technology demonstration, and eventually commercializing our qPCR technology.

Objective

The primary objective of this project is to develop and perform preliminary validation of real-time PCR techniques to estimate the abundance and activity of aerobic, VC-degrading bacteria (including methanotrophs, etheneotrophs, and VC-assimilating bacteria) in environmental samples from dilute groundwater VC plumes. Another objective of this project is to investigate the normalized rate of VC oxidation in groundwater samples. Initially, we aim to investigate the factors that contribute to and possibly work against cometabolic VC oxidation in groundwater. This includes the interactions among methanotrophs and etheneotrophs in the presence of VC, ethene, and methane in groundwater microcosms, enrichment cultures and pure cultures, and pure culture mixtures. *These techniques will improve the ability evaluate, demonstrate and measure natural and enhanced attenuation of dilute VC plumes, and is therefore directly relevant to SERDP ERSON-09-01.* The resulting improved VC bioremediation approach would thereby improve decision making, save time, and ultimately, reduce the life cycle costs for remediation of dilute VC plumes.

Background

Vinyl chloride (VC), a known human carcinogen *(1)* and common groundwater contaminant *(2)*, is often generated in groundwater by incomplete reductive dechlorination of the widely used chlorinated solvents tetrachloroethene (PCE) and trichloroethene (TCE), also common groundwater contaminants *(2)*. PCE and TCE, as well as their daughter products cDCE and VC are key contaminants of concern to the Department of Defense (DoD). Anaerobic reductive dechlorination is a promising biotechnology for remediation of PCE- and TCE-contaminated groundwater, but the potential for production of a mobile VC plume by this process represents a threat to public health if the VC plume migrates or could migrate into drinking water source zones. At some sites, VC will escape the anaerobic zone and enter aerobic groundwater, forming dilute plumes. Aerobic groundwater zones are typically low in organic carbon content, which limits the use of natural attenuation strategies that rely on the generation of reducing conditions in the aquifer. However, VC is often observed to readily degrade in aerobic groundwater *(3-5)*. It seems likely that microorganisms are responsible for the observed aerobic attenuation of VC. The formation of methane and ethene under anaerobic conditions that may comigrate into aerobic zones along with VC can potentially contribute to cometabolic VC oxidation by methanotrophic *(6, 7)* and etheneotrophic bacteria *(8)*. Bacteria (e.g. *Mycobacterium, Nocardioides, Pseudomonas* and *Ochrobactrum* strains) that grow on VC as a carbon and energy source (i.e. VC-assimilating bacteria) also appear to be widespread, and have been isolated from soil *(9)*, groundwater *(9, 10)*, sediment *(11)*, and sewage sludge samples *(9, 11, 12)*. This suggests that aerobic natural attenuation of VC may also proceed at VC-contaminated sites in the absence of cometabolic substrates.

Active remedial strategies involving cometabolism of VC by ethene-degrading bacteria (both methanotrophs and ethenotrophs) are currently being developed. One strategy involves injection of methane or ethene and oxygen into a dilute VC plume to stimulate growth of the ethenotrophs and subsequent cometabolic oxidation of VC. In addition, the process of VC-assimilation *in situ* seems particularly suited to more passive natural attenuation strategies at PCE/TCE-contaminated sites experiencing incomplete reductive dechlorination or at sites where dilute VC plumes have developed and entered aerobic groundwater zones, because it would be self-sustaining and predictable in comparison to cometabolic strategies. However, to effectively implement these remedial strategies it is important to know if methanotrophs, etheneotrophs and VC-assimilators are present in the aquifer. The presence or absence of methanotrophs and etheneotrophs is currently measured with enrichment culture techniques that involve taking a groundwater sample and mixing it with a nutrient containing synthetic groundwater. The sample is then amended with methane (for methanotrophs) or ethene (for etheneotrophs) and oxygen, and monitored for methane/ethene degradation with a concomitant increase in turbidity indicating microbial growth. This analysis can provide fairly clear evidence of microbial presence, but typically requires 50-60 days to complete.

Fundamental scientific advances concerning reductive dechlorination of chlorinated ethenes has led to the development of a variety of molecular biology tools (e.g. real-time PCR) for quantifying the abundance of *Dehalococcoides* spp. in environmental samples *(13)*. The development of similar MBTs for aerobic VC-assimilating bacteria has lagged due to a general lack of scientific knowledge. Recent progress has led to the sequencing of VC/ethene biodegradation functional genes from several VC- and ethene-assimilating bacteria *(9, 14-18)*.

There are also relatively recent reports of real-time PCR methods for methanotrophs *(19, 20)*, which can degrade VC cometabolically. As a result, there is now the opportunity to apply this knowledge to site cleanup. The scientific and technical merit of this project will be to develop quantitative molecular biology techniques for assessing the presence and activity of VC-degrading microbes that would be rapid, convincing, and more cost effective than current practices.

Mycobacterium aurum strain L1, isolated from VC-contaminated soil, was the first organism reported to grow aerobically on VC *(11, 21)*. Strain L1 grew on ethene, and ethene-grown strain L1 also degraded VC, suggesting that the same enzymes were responsible for both VC and ethene biodegradation *(21)*. The enzyme initiating the attack on VC by strain L1 was shown to be AkMO, which transformed VC into chlorooxirane *(11)*. It was also noted that over a one year period the doubling time of strain L1 on VC decreased from 40 to 12 hr *(21)* suggesting that VC adaptation was an ongoing process in strain L1. VC-assimilating *Pseudomonas aeruginosa* strain MF1 was isolated from an enrichment culture that began degrading VC after an 80 day lag period *(12)*. As observed with strain L1, strain MF1 could also grow on ethene and appeared to use a monooxygenase to convert VC to chlorooxirane. Furthermore, strain MF1 readily switched from growth on ethene to growth on VC without a lag period, suggesting that the same enzyme system was used to assimilate both compounds.

Verce et al. advanced the field by demonstrating that a pure culture of *Pseudomonas* strain DL1, isolated from activated sludge using ethene as the sole carbon and energy source, could adapt to VC as a growth substrate *(22)*. Ethene-grown DL1 cultures degraded VC, but several lines of evidence indicated that strain DL1 was not deriving carbon or energy from VC. Extended incubation of ethene-grown strain DL1 with VC as sole carbon and energy source resulted in a gradual transition from cometabolic VC degradation to growth-coupled VC oxidation, which was supported by the observation that the optical density of these VC-acclimated cultures was increasing as each VC spike was consumed *(22)*. This evidence supports the hypothesis that ethene-assimilating bacteria alter their existing ethene biodegradation enzyme system in some way such that they evolve into VC-assimilating bacteria.

In 2002, the isolation of 12 different VC-assimilating bacteria (11 *Mycobacterium* strains and 1 *Nocardioides* strain) was reported *(9)*. Initial characterization of these microbes confirmed that they grew on ethene, and that ethene monooxygenase activity was induced by VC. These results further support the hypothesis that ethene biodegradation enzymes are used for VC metabolism. Because of the recent report of VC adaptation by strain DL1, ethene-assimilating *Mycobacterium* strain K1 and *Corynebacterium* strain K3 were tested for their ability to adapt to VC. Surprisingly, strain K1 immediately grew on VC, while strain K3 did not degrade VC after a 12 day incubation time. However, the results of these experiments with respect to VC adaptation are inconclusive as strain K1 was already adapted to VC and longer incubation times could have resulted in adaptation of strain K3 to VC.

The biochemistry and kinetics of aerobic cometabolism of chlorinated ethenes is well understood. Methane *(6, 23)*, ethene and ethane *(8, 24)*, propane *(25-27)*, propene *(28, 29)*, and ammonia *(30)* induce broad substrate range monooxygenases that fortuitously oxidize chloroethenes such as VC. Much of the relevant literature has been reviewed previously *(31)*.

Technologies employing aerobic TCE cometabolism have been implemented at the field scale *(32)*, but the process has many disadvantages. For example, the growth substrate must be present to fuel cell growth, sustain oxygenase expression, and maintain oxygenase activity by regeneration of reducing power. The growth substrate and the chloroethene cosubstrate will compete for the active site of the oxygenase resulting in inhibition of cometabolism over a range of growth substrate concentrations. Cometabolism of chloroethenes by oxygenases also produces reactive, electrophilic, and unstable epoxides *(7, 33, 34)*. Chlorooxirane (VC epoxide) forms covalent DNA adducts in certain mediating organisms *(35)*. There are no published reports of field-scale cometabolic biodegradation of VC by etheneotrophs. However, it is known that ethene-assimilators produce epoxyethane (oxirane), which is structurally similar to chlorooxirane, as a metabolic intermediate. This suggests that oxirane degradation enzymes could readily detoxify VC epoxide and that field-scale cometabolic VC degradation strategies are plausible.

Continued characterization of *Mycobacterium* strain JS60 revealed that a multi-subunit AkMO catalyzes the initial oxidation of ethene to epoxyethane and VC to chlorooxirane *(15)*. The strain JS60 AkMO genes (*etnABCD)* were sequenced. In a breakthrough, it was also revealed that EaCoMT was involved in the VC/ethene biodegradation pathways in strain JS60. The gene encoding EaCoMT, *etnE*, was found immediately upstream of, and shown to be co-transcribed with, *etnA*, the AkMO β subunit. Heterologous expression of EaCoMT in *Mycobacterium smegmatis* strain mc^2-155 showed that EaCoMT converted epoxyethane to 2-hydroxyethyl CoM in a CoM-dependant fashion. CoM-dependent chlorooxirane degradation was also observed, but the expected CoM conjugate was not observed *(15)*. Investigation of VC biodegradation enzymes in *Nocardioides* strain JS614 confirmed that the initial steps in the VC and ethene oxidation pathway in this strain are the same those in *Mycobacterium* strain JS60 and resulted in the sequencing of a large region of genes in the vicinity of *etnEABCD (17)*.

Collectively, this body of information provides strong evidence that VC-assimilating bacteria are specialized ethene-degraders that have made the transition from cometabolic VC biodegradation to growth-coupled VC biodegradation. *Therefore dilute VC plume bioremediation strategies involving the stimulation of etheneotrophs have the potential for success not only as a result of VC cometabolism, by via adaptation of etheneotrophs to VC as a growth substrate*. The important initial enzymes in the VC and ethene biodegradation pathways (AkMO and EaCoMT) were identified and the genes encoding these enzymes were sequenced in strains JS60 and JS614. Subsequent studies of other VC and ethene-assimilating bacteria revealed the presence of AkMO *(14)* and EaCoMT genes *(16, 18)*. We have recently sequenced complete AkMO and EaCoMT genes from *Mycobacterium* strain JS623 *(16, 36)*, plus partial *etnC* sequences from *Mycobacterium* strains JS622, JS624, and JS625 *(16, 36)*. We have also isolated *etnE*-containing fosmid clones from VC-assimilating *Mycobacterium* strains JS616 and JS621. These recent results add significantly to the growing database of catabolic genes from VC- and ethene-assimilating bacteria. Therefore, we are poised to begin development of molecular biology tools (MBTs) aimed at enumeration of the presence and activity of AkMO and EaCoMT genes in environmental samples. In conclusion, the body of work reviewed in this section makes it clear that our scientific knowledge of VC- and ethene-assimilating bacteria has increased in recent years, *but that there still remains a technology gap in that there are no MBTs available for detecting the presence and activity of these microbes in the environment.*

Materials and Methods

Site information. Samples from three different VC-contaminated sites that displayed geochemical conditions favorable for VC oxidation were acquired and investigated during this project. Initially, DNA extracted from these groundwater samples was used to test the specificity of qPCR primer sets. After the primers were developed, qPCR was used to estimate the abundance of functional genes from both etheneotrophs and methanotrophs at these site.

The main study site in Carver, MA (Figure 1) is located down gradient from a landfill in which PCE, along with other organic compounds, was disposed in 1986 *(37, 38)*. These chemicals generated anaerobic conditions and served as electron donors for reductive dechlorination of PCE to its daughter products, creating a VC plume extending 4600' downgradient from the landfill into an aquifer of silt and fine sand. By 2002, a detached VC plume 3000' long, 40' wide and 30' thick, was located 50' below the water table, having VC concentrations ranging from 2 - 27 µg/L, migrating at about 0.5 feet/day. In 2003, a full-scale bioremediation project was initiated to stimulate aerobic VC oxidation, by transecting the plume with a line of gas infusion points screened over the full depth of contamination. Over the next two years, additional gas infusion lines were installed down gradient along the plume. The system was operated to alternately inject O_2 and ethene *(39)*. In 2005, a laboratory microcosm test verified that site groundwater contained both methanotrophs and etheneotrophs able to aerobically degrade VC *(40)*. By 2008, VC in groundwater from wells down gradient from the second and third treatment lines was below the treatment goal of 2 µg/L, and by 2009, although VC was still migrating into the treatment area, wells down gradient from the first treatment line showed significantly lower VC concentrations *(37)*.

Environmental samples were also collected from two additional VC-contaminated sites. Adilute VC plume, originating from a TCE source at NAS Oceana, VA SWMU 2C has been undergoing bioremediation treatment under both aerobic and anaerobic conditions (Figure 2). Groundwater samples were collected from several monitoring wells in the North plume (MW18, MW19, and MW25) over a period of a few years. This portion of the plume had been treated with an oxygen-releasing substrate in an effort to stimulate aerobic VC degradation. VC concentrations in affected monitoring wells have trended downward over time *(41)*.

At the Soldotna, AK site ongoing efforts to anaerobically remediate a tetrachloroethene (PCE) spill has generated a VC plume that is migrating into the adjacent Kenai River *(42)*. Consistent decreases in VC concentrations in Kenai River sediments and pore water suggest that VC oxidation is occurring *(42)*. Groundwater samples from this site were collected from monitoring wells that are most likely to be aerobic (Figure 3).

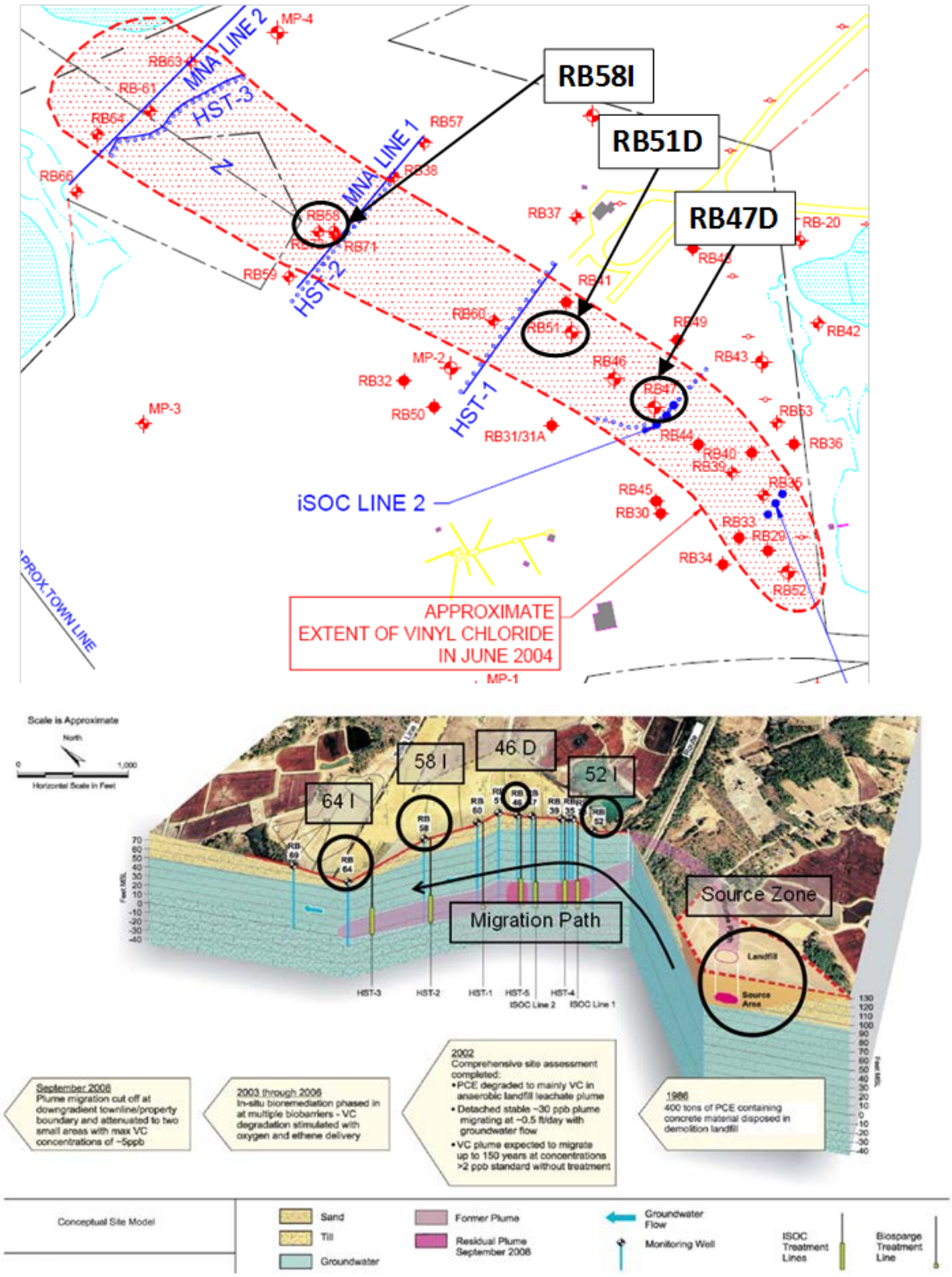

Figure 1. Conceptual plan and profile views of the VC-contaminated site in Carver, Massachusetts *(43)*. The location of monitoring wells where groundwater samples were taken for qPCR and microcosm studies is shown.

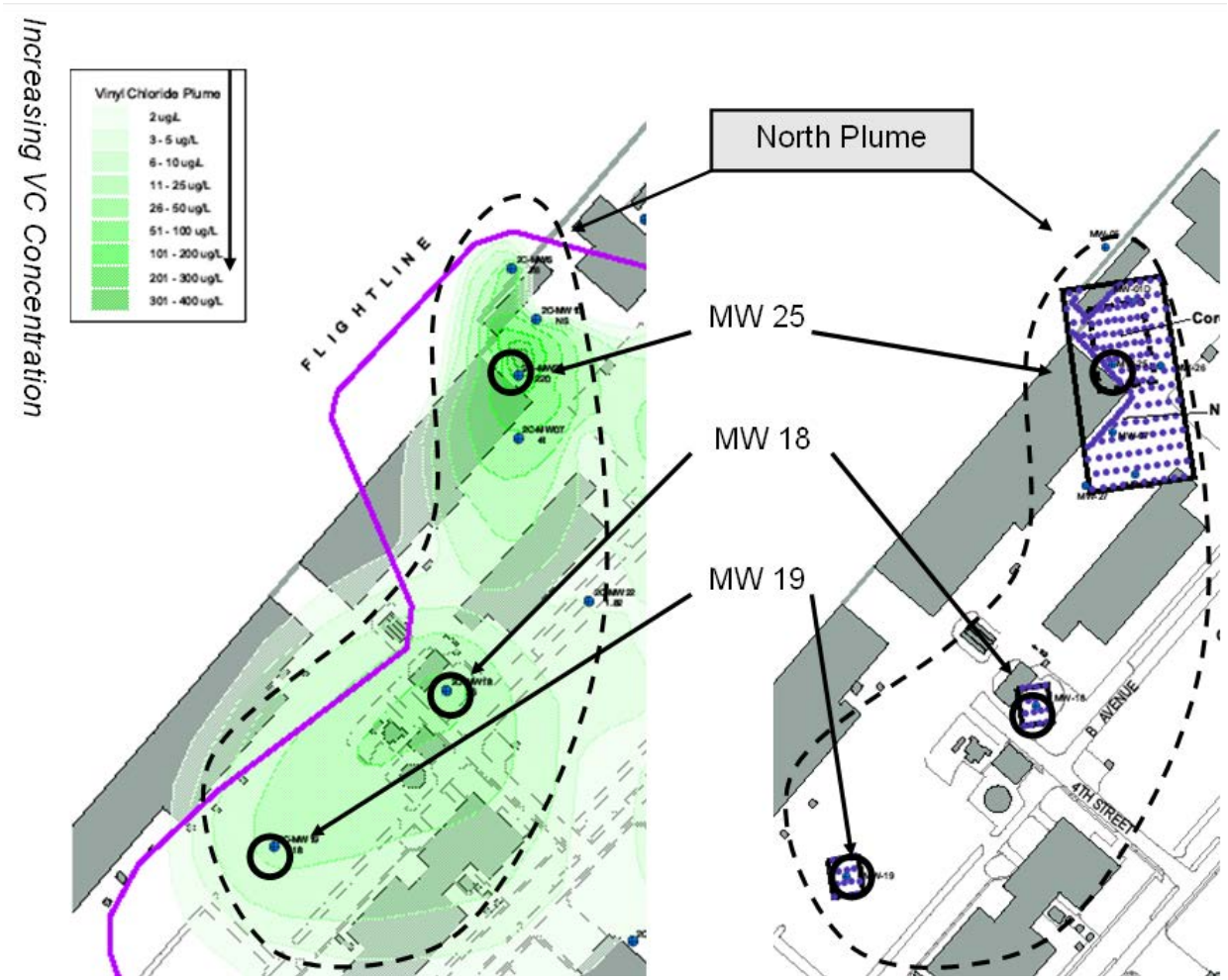

Figure 2. The north VC plume at NAS Oceana illustrating the location of monitoring wells 18, 19, and 25 *(44)*. The left hand side of the figure illustrates the extent of the VC plume. The purple dots on the right hand side of the figure indicate the oxygen releasing compound (ORC) injection points.

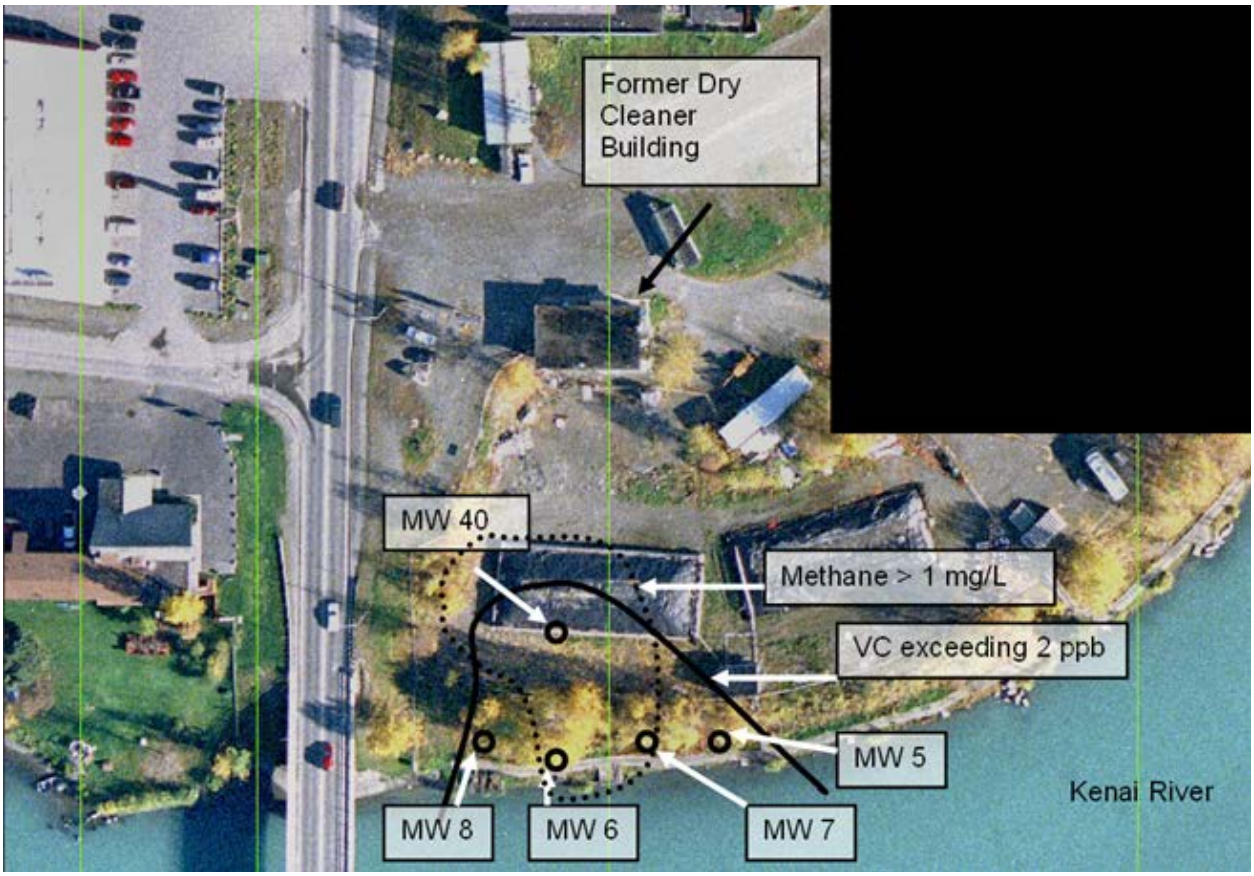

Figure 3. Aerial view of Soldotna, AK site with methane and VC plumes delineated. The location of monitoring wells where groundwater samples were taken is also shown.

Groundwater sample collection. Groundwater was collected according to USEPA/540/S-95/504 procedures from two monitoring wells at each of the three sites investigated. For MBT analysis, groundwater was passed through Sterivex-GP 0.22 µm membrane filter cartridges (Millipore) until the filter clogged (or a maximum of 3L was filtered). The volume of filtered water was recorded and Sterivex filters were immediately placed on ice and shipped overnight to the University of Iowa, where they were stored at -20°C prior to DNA extraction. Groundwater for microcosms from the Carver site was collected in 1-L glass bottles, delivered on the same day to Bioremediation Consulting Inc. (BCI), and refrigerated until use (no later than one month after collection). In September 2009, groundwater was collected from 14 wells at the Carver, MA site to screen for the presence of methanotrophs, etheneotrophs, and VC-assimilating bacteria, and to select a well having all three microbial types for the 2010 study. The wells represented increasing distances along the plume within the treatment area. Based on the 2009 screening test, well 63-I, located 100 feet down gradient from the fourth cross-plume line of air infusion points, was selected for further testing. In March 2010, groundwater was collected from Carver well 63-I into 1-L glass bottles for a more detailed microcosm test. Well water from 63-I (which contained methane, ethene and VC at 195, 0.35 and <2 µg/L respectively was analyzed in 2010 for Cl^-, NO_3^-, and SO_4^{2-} by capillary ion electrophoresis according to EPA Method 6500, for PO_4^{3-} by Hach Method 8048, and for other elements by EPA Method 200.8. In 2011, the dissolved gas concentrations in the groundwater were similar (157, 0.43 and < 2 µg/L, respectively).

Chemicals, bacterial strains, and growth conditions. Methane (99.995%) was obtained from Scott Specialty Gases, Ethene (99%) was from Airgas or Scott Specialty Gases, VC (and VC in methanol) was from Restek, propene (>99%) was from Aldrich, and all other chemicals were reagent grade or better.

In groundwater microcosm experiments, Dilute VC gas stock was prepared by injecting 0.5 ml of VC in methanol (67.8 mg/ml) into a sealed 160 ml serum bottle containing 77.5 ml deionized water. After equilibration, the headspace of this solution was the source of dilute VC stock for feeding microcosms.

One liter of minimal salts medium (MSM) was prepared as follows: 0.95 g KH_2PO_4, 2.27 g K_2HPO_4, 0.67 g $(NH_4)SO_4$ per liter of deionized water. MSM was autoclave sterilized at 121 degrees Celsius (°C) for 30 minutes. One liter of trace metals solution (TMS) was prepared as follows: 60 g $MgSO_4{\bullet}7H_2O$, 6.37 g EDTA ($Na_2(H_2O)_2$), 1 g $ZnSO_4{\bullet}7H_2O$, 0.5 g $CaCl_2{\bullet}2H_2O$, 2.5 g $FeSO_4{\bullet}7H_2O$, 0.1 g $NaMoO_4{\bullet}2H_2O$, 0.1 g $CuSO_4{\bullet}6H_2O$, 0.2 g $CoCl_2{\bullet}6H_2O$, 0.52 g $MnSO_4{\bullet}H_2O$ per liter of deionized water. TMS was not autoclaved but instead filter sterilized with a 0.22µm, GP Express membrane from Steritop, and was stored at 4°C in a foil wrapped container to prevent photodegradation.

One liter of 1/10th strength trypticase soy agar plus 1% glucose (TSAG) plates was prepared as follows: 3g Tryptic Soy Broth (TSB), 15g Bacto agar, 10g glucose(1%) per liter of deionized water. One liter of TSAG broth was autoclave sterilized at 121 degrees Celsius (°C) for 30 minutes, after cooling at room temperature for about 1 hour, the broth was poured in 2 sleeves of petri dish in the laminar flow hood and stored at 4 °C.

Eleven different strains VC- and ethene-assimilating bacteria (Table 1) were grown on ethene in minimum salts medium (MSM-ethene) and harvested for DNA extraction as described in *(36)*. *Xanthobacter autotrophicus* Py2 was grown on MSM-propene as described previously *(45)* and *E. coli* DH5α was grown in Luria Bertani (LB) medium according to New England Biolabs protocols.

Table 1. Bacterial strains used in this study.

Bacterial strains	Relevant characteristics	Substrate	Reference
Nocardioides sp. strain JS614	ATCC BAA-499	VC	*(9)*
Mycobacterium sp. strain JS60	ATCC BAA-494	VC	*(9)*
Mycobacterium sp. strain JS616	ATCC BAA-496	VC	*(9)*
Mycobacterium sp. strain JS617	ATCC BAA-497	VC	*(9)*
Mycobacterium sp. strain JS621	ATCC BAA-498	VC	*(9)*
Mycobacterium sp. strain TM1	Not available in the ATCC	VC	*(9)*
Mycobacterium sp. strain TM2	Not available in the ATCC	VC	*(9)*
Mycobacterium sp. strain JS622	Not available in the ATCC	Ethene	*(16)*
Mycobacterium sp. strain JS623	Not available in the ATCC	Ethene	*(16)*
Mycobacterium sp. strain JS624	Not available in the ATCC	Ethene	*(16)*
Mycobacterium sp. strain JS625	Not available in the ATCC	Ethene	*(16)*
Methylococcus capsulatus	ATCC 33009	Methane (Type I)	
Methylocystis sp. strain Rockwell	ATCC 49242	Methane (Type II)	
Xanthobacter autotrophicus Py2	ATCC BAA-1158	propene	*(16)*
E. coli strain DH5α F'I^q	F' *proA*$^+$B$^+$ *lacI*^{q} Δ(*lacZ*)M15 zzf::Tn10 (Tet^R)/fhuA2Δ(*argF-lacZ*)U169 *phoA* glnV44 Ø80 Δ(*lacZ*)M15*gyrA*96 *recA1* *endA1* thi-1 hsdR17	Luria broth	New England BioLabs

When growing cultures, culture purity was periodically tested by streaking the cultures on agar plates. Etheneotrophs and VC-assimilators were plated onto 1/10th strength TSAG plates, which if pure, should reveal only one colony type after incubating at 30°C within 1-2 weeks, depending on the strain. Methanotrophs streak plates onto 1/10th strength TSAG plates should reveal no colonies after incubating at 30°C within 2 weeks. Methanotrophs cannot metabolize C_6 compounds like glucose as carbon and energy source, therefore the absence of colonies on TSAG plates indirectly indicates the purity of the culture.

Two species of methane oxidizing bacteria, *Methylococcus capsulatus* (ATCC 33009, Type I methanotroph) and *Methylocystis* sp. strain Rockwell (ATCC 49242, Type II methanotroph), were used in this study. Methanotroph cultures were grown in modified 1 liter Erlenmeyer flasks containing MSM (250 mL), filter-sterilized TMS (500 µL), and filter-sterilized methane (60 mLs). Polyvinylidene fluoride (PVDF) filters from Millpore (Millex, 0.22 µm) were used for filter sterilizations. M. *capsulatus* cultures were incubated at 37 °C while *Methylocystis* sp.

cultures were grown at room temperature (RT, ~25°C). Both cultures were agitated on a circular shaker operating at 200 revolutions per minute (rpm). M. *capsulatus* required the added glycerol while *Methylocystis* sp. strain Rockwell did not. To revive the *Methylocystis* cell line, thawed frozen-stock was added directly to fresh media. Due to the presence of glycerol in the M. *capsulatus* frozen stocks, it was necessary to wash them twice in sterile MSM before cells could be added to growth media. A single wash step consisted of the following: (1) resuspending frozen stock in 25 mLs sterile MSM, (2) pelleting cells in centrifuge (5 min, 5000 rpm), (3) removing supernatant.

Periodically, frozen stocks were made of each bacterial strain for cell line maintenance. When cultures reached mid-exponential growth phase, they were pelleted via centrifugation, resuspended in 10 mL of either MSM or MSM/glycerol (50% MSM, 50% glycerol), and distributed per ml in 1.5 ml cryovials and stored at -80°C

DNA extraction from pure cultures and environmental samples. To prepare pure cultures for DNA extraction experiments, *Mycobacterium* strain JS60 and *Nocardioides* strain JS614 were grown on ethene and harvested at mid-exponential phase (OD_{600} = 0.33 for JS60 and 0.52 for JS614).

When the previously reported beadbeating DNA extraction method was used *(36)*, 10 mL of the liquid samples were centrifuged at 6,150×g with 0.1% Tween80 and then resuspended with 600 µL STE buffer. When testing DNA extraction from Sterivex filters, each culture was kept well-mixed, and 10 mL of each culture was passed through separate Sterivex filters. All DNA extractions were performed in triplicate.

Prior to DNA extraction from Sterivex filters, the filters were removed from the freezer, thawed and any remaining liquid in the filter housing was eliminated by syringe. Filter housings were opened with a tubing cutter. When using the MoBio PowerSoil DNA kit (PS), the filter membrane was aseptically removed, excised into 64 pieces and DNA was extracted from filter pieces according to the manufacturer's protocol or with the following modifications: approximately 300 µL (660 mg) of 0.1 mm zirconia/silica beads were added to the beadbeating tube prior to beadbeating with a Bio-Spec MiniBeadbeater-8 (2 minutes, high speed). Cell lysate (450 µL) was transferred into a clean microcentrifuge tube for the next step in the protocol. Finally, a second elution step (using 20 µL of elution buffer) was used to further increase DNA yield (by 19-20%). These modifications increased DNA yield by 43% in comparison to our previously reported beadbeating method *(36)*. At times in this document, "modified" in the contect of DNA or RNA extraction indicates the addition of 0.1 mm zirconia/silica beads to certain kits (300 µL and 1,500 µL for the Modifed PowerSoil kit (MPS) and Modified PowerWater kit (MPW), respectively).

When using the MoBio PowerWater DNA kit (PW/MPW), the filter membrane was aseptically removed, placed into 5 ml vortexing tube with cell lysis buffer provided in the PowerWater DNA/RNA kit and vortexing was performed for 5 min. When using the MoBio PowerWater Sterivex kit (PWS), the protocol did not require the filter membrane was not removed from the housing. The manufacturer's suggested protocol was followed. DNA concentrations were

routinely measured on a Qubit™ fluorometer (Invitrogen) using the Quant-iT dsDNA HS assays (Invitrogen).

DNA was extracted from methanotroph pure cultures using the MoBio PowerSoil DNA kit (#12800-50) according to the manufacturer's protocol or using a previously reported bead-beating extraction method with the cells grown on MSM and methane (0.44 mg/mL) instead of trypticase soy agar and glucose (TSAG). DNA extracted from pure cultures was used as a template in endpoint PCR procedures.

To monitor DNA losses during the extraction process, a Luciferase gene control was used. Luciferase is used as an external gene control because it is a very rare gene only found in fireflies, therefore, it would not be mistaken for any other gene in the methanotroph genome. After genomic DNA or RNA is removed from the Sterivex filter, 7.5×10^7 copies of the Luciferase gene were added to each environmental sample. At the end of the extraction process, the copies of Luciferase gene were measured using a qPCR standard curve, and a percent recovery was calculated. That percent recovery was then used to adjust gene abundance calculations from environmental samples *(46)*.

qPCR primer design and analysis. Primer Express 2.0 (Applied Biosystems) was used to design qPCR primers. Default parameters were used, except that the amplicon length was allowed to vary between 100 and 150 bp. Nucleic acid and protein sequence alignments used in primer design were generated with ClustalX *(47)* and visualized in Bioedit (www.mbio.ncsu.edu/BioEdit/bioedit.html). Specificity of selected primer combinations with respect to the NCBI non-redundant nucleotide collection was tested with Primer BLAST (www.ncbi.nlm.nih.gov/tools/primer-blast). Default program parameters were used except that the misprimed product size deviation was reduced to 500 bp. The primer specificity stringency was set to 4 total mismatches, and 4 mismatches within the last 7 bps at the 3' end.

Endpoint PCR procedures. PCR mixtures (25-50 µL) contained 12.5-25 µL of Qiagen HotStart PCR Master Mix, 2 µM of each primer, and 2 ng of template DNA. The thermocycling protocol was 95°C for 5 min, then 35 cycles of 95°C (20 s), 55 or 60°C (20 s) and 72°C (30 s), followed by a final extension cycle (72°C, 4 min). PCR products were visualized by agarose gel electrophoresis, then purified with the Qiagen PCR Purification Kit (#28104). DNA concentrations were measured on a Qubit™ fluorometer (Invitrogen) using the Quant-iT dsDNA HS assays (Invitrogen). Selected PCR products were cloned and sequenced as described previously *(48)* and were also used as the template for qPCR standard curves.

Real-time PCR procedures. Real-time PCR was performed with an ABI 7000 Sequence Detection System (Applied Biosystems). Assays proceeded through 3 stages. Stage 1: 1 cycle of 95°C for 10 min (DNA denaturing), stage 2: 40 cycles of 95°C (15 sec) and 60°C for 60 sec (denaturing, annealing, elongation, and data collection), and stage 3: a PCR product dissociation protocol. For construction of the dissociation curve, the temperature inside each reaction was increased in small intervals (0.3 – 0.4°C) from 65-95°C. After each temperature increase, fluorescence in each reaction well was measured and plotted. PCR mixtures were prepared in 25 µL volumes using 12.5 µL of Power SYBR Green PCR Master Mix (Applied Biosystems), 750 nM of each primer for etheneotrophs and 100 nM to 800 nM of each primer for methanotrophs

(as determined in preliminary qPCR experiments), and 2 µL of DNA template (DNA concentration varied 0.16 - 38.4 ng/µL). In addition, 400 ng/µL Bovine Serum Albumin (BSA; New England Biolabs) was added to qPCR mixtures containing DNA template from environmental samples as these may contain humic substances that can interfere with the PCR process *(49, 50)*.

The number of gene copies per µl of PCR product was calculated by:

$$\frac{\text{DNA concentration}\left(\frac{\text{ng}}{\mu\text{L}}\right) * 6.022 \times 10^{23}\ \frac{\text{bp}}{\text{mole bp}}}{\text{PCR product size}\left(\frac{\text{bp}}{\text{gene copy}}\right) * 1 \times 10^{9}\ \frac{\text{ng}}{\text{g}} * 660\ \frac{\text{g}}{\text{mole bp}}}$$

Avogadro's number is 6.023 x 10^{23} molecules per 1 mole, and the average molecular weight of double stranded DNA is 660 g/mole. ABI 7000 System SDS Software (Applied Biosystems) was used to analyze real-time PCR fluorescence data. Data analysis was performed using the proprietary software provided for the Applied Biosystems 7000 System. The "auto" function was used to determine the threshold fluorescence values (used for determining the threshold cycle Ct) for each set of standards and samples analyzed. The "auto baseline" function was used in all situations. However, the threshold fluorescence value (used for determining the threshold cycle C_t) for each set of standards and samples that were analyzed was optimized manually in certain instances.

Real-time PCR Primer Sets. A list of all qPCR primers used in this study can be found in Table 2. To develop standard curves, we designed new primer sets to amplify the *etnC* from strains JS60 (JS60 EtnCF, JS60 EtnCR; 1043 bp product), JS614 (JS614 EtnCF, JS614 EtnCR; 1138 bp product), and JS623 (JS623 EtnCF, JS623 EtnCR; 1163 bp product) (Table 3). We used the CoMF1L and CoMR2E primer set to produce 891 bp *etnE* PCR products from JS60, JS614 and JS623 template DNA (Table 3).

Eight primer sets from the literature were compiled and evaluated to determine which pairs most accurately detected methanotroph populations in groundwater qPCR assays. Four primer sets targeted the *pmoA* gene encoding β-subunit of the particulate methane monooxygenase enzyme (pMMO), three targeted the 16S rRNA gene, and one targeted the *mmoX* gene encoding a subunit of the soluble MMO enzyme (sMMO). The specific pmoA primer sets were as follows: A189 F (GGN GAC TGG GAC TTC TGG) and Mb661 R (GGT AAR GAC GTT GCN CCG) *(51)*, pmof1 (GGG GGA ACT TCT GGG GIT GGA C) and pmor (GGG GGR CIA CGT CIT TAC CGA A) *(52)*, pmof2 (TTC TAY CCD RRC AAC TGG CC) and pmor *(52)*, and A189 F and mb661r (CCG GMG CAA CGT CYT TAC C) *(53, 54)*. Hereafter, these primer sets will be referred to as Kolb, pmoA 330, pmoA 178 and pmoA 472, respectively.

Table 2. Oligonucleotides used for qPCR in this study

qPCR oligonucleotides (target gene)	**Sequence (5′-3′)**	**Product size (bp)**	**Reference**
RTC (*etnC*)			
RTC_F	ACCCTGGTCGGTGTKSTYTC	106	This study
RTC_R	TCATGTAMGAGCCGACGAAGTC		
RTE (*etnE*)			
RTE_F	CAGAAYGGCTGYGACATYATCCA	151	This study
RTE_R	CSGGYGTRCCCGAGTAGTTWCC		
Kolb (pmoA)			
A189 F	GGNGACTGGGACTTCTGG	472	*(51)*
Mb661 R	GGTAARGACGTTGCNCCG		
pmoA 330			
pmof1	GGGGGAACTTCTGGGGITGGAC	330	*(52)*
pmor	GGGGGRCIACGTCITTACCGAA		
pmoA 178			
pmof1	GGGGGAACTTCTGGGGITGGAC	178	*(52)*
pmof2	TTCTAYCCDRRCAACTGGCC		
pmoA 472			
A189 F	GGNGACTGGGACTTCTGG	472	*(53, 54)*
mb661r	CCGGMGCAACGTCYTTACC		
16S U (16S rRNA)			
16SU f	TCCTACGGGAGGCAGCAGT	466	*(55)*
16SU r	GGACTACCAGGGTATCTAATCCTGTT		
16S Type 1 Methanotroph			
U785F	GGATTAGATACCCTGGTAG	221	*(56, 57)*
MethT1bR	GATTCYMTGSATGTCAAGG		
16S Type 2 Methanotroph			
U785F	GGA TTA GAT ACC CTG GTA G	232	*(56, 57)*
MethT2R	CAT CTC TGR CSA YCA TAC CGG		
***mmoX* (sMMO)**			
536f	CGCTGTGGAAGGGCATGAAGCG	362	*(54, 58)*
898r	GCTCGACCTTGAACTTGGAGCC		

Table 3. Oligonucleotides used to generate qPCR standards.

Oligonucleotides used to generate qPCR standard products	**Sequence (5′-3′)**	**Product size (bp)**	**Ref.**
JS60 EtnCF	GATCCATTTCGTTCGATGCT	1043	This study
JS60 EtnCR	GGCAATTCCTGCAACAAGAT		
JS614 EtnCF	GCGATGGAGAATGAGAAGGA	1138	This study
JS614 EtnCR	TCCAGTCACAACCCTCACTG		
JS623 EtnCF	GAACTCAGACAGGGCTACGC	1163	This study
JS623 EtnCR	TACTTCAGCGGGTCCTTCAC		
NVC105 (*etnC*)	CAGGAGTCSCTKGACCGTCA	360	*(14)*
NVC106 (*etnC*)	CARACCGCCGTAKGACTTTGT		
CoM-F1L (*etnE*)	AACTACCCSAAYCCSCGCTGGTACGAC	891	*(16, 17)*
CoM-R2E (*etnE*)	GTCGGCAGTTTCGGTGATCGTGCTCTTGAC		
RefSTF	CCAGGGATTTCAGTCGATGT	1014	This study
RefSTR	TTTTCCGTCATCGTCTTTCC		
JS60 GSPEtnCF	ACGCTGGTCGGTGTTCTTTC	106	
JS60 GSPEtnCR	TCATGTAAGAGCCGACGAAGTC		
JS614 GSPEtnCF	ACACTCGTCGGCGTTGTTTC		
JS614 GSPEtnCR	TCATGTACGAGCCGACGAAGTC		
JS617 GSPEtnCF	ACCCTGGTCGGTGTGCTCTC		
JS617 GSPEtnCR	TCATGTACGAGCCGACGAAGTC		
JS623 GSPEtnCF	ACCCTGGTCGGTGTGCTCTC		
JS623 GSPEtnCR	TCATGTACGAGCCGACGAAGTC		
JS60 GSPEtnEF	CAGAATGGCTGTGACATTATCCA	151	
JS60 GSPEtnER	CCGGTGTACCCGAGTAGTTACC		
JS614 GSPEtnEF	GACAACGGCTGCGACATCATTCA		
JS614 GSPEtnER	CGGGTGTGCCGGAGTAGTTGCC		
JS617 GSPEtnEF	CAGAACGGCTGCGACATCATCCA		
JS617 GSPEtnER	CCGGCGTGCCGGAGTAGTTTCC		
JS623 GSPEtnEF	CAGAACGGCTGCGACATCATCCA		
JS623 GSPEtnER	CTGGTGTACCCGAGTAGTTTCC		

The 16S primer sets each targeted a separate conserved region of the rRNA gene which allowed for identification of distinct bacterial populations. One primer set detected bacteria universally, while the other two sets amplified the rRNA gene of either type 1 or type 2 methanotrophs. The specific 16S primer sets were as follows: 16S universal primers – 16SU f (TCC TAC GGG AGG CAG CAG T) and 16SU r (GGA CTA CCA GGG TAT CTA ATC CTG TT) *(55)*, 16S type 1 methanotroph primers – U785F (GGA TTA GAT ACC CTG GTA G) *(56)* and MethT1bR (GAT TCY MTG SAT GTC AAG G) *(57)*, 16S type 2 methanotroph primers – U785F and MethT2R (CAT CTC TGR CSA YCA TAC CGG) *(57)*. Hereafter, these primer sets will be referred to as 16S U, 16S T1 and 16S T2, respectively. The mmoX primer set was as follows: 536f (CGC TGT GGA AGG GCA TGA AGC G) and 898r (GCT CGA CCT TGA ACT TGG AGC C) *(54, 58)*, and hereafter will be referred to as mmoX.

It should be noted that based on the phylogenetic trees in the literature review, these primer sets will likely be biased against the recently discovered *Methylacidophilium* and *Crenothrix* methanotrophs because their sequences are generally far removed from the "classical" methanotrophs. Primer bias occurs when primers do not efficiency bind to certain species sequence and therefore do not always provide a complete picture of the microbial population based on those primers.

Optimization of qPCR primer concentrations (Methanotrophs). The pmoA 178, pmoA 330, 16S T1, and 16S T2 primer sets were assayed to find their optimal working concentrations. For pmoA 178 and pmoA 330, approximately 15 qPCR plates were run amplifying template NDA with primer concentrations ranging from 200 nM to 1000 nM. Both pmoA primer sets (pmoA 178 and pmoA 330) were used to amplify both our isolated methanotroph DNA templates (*Methylococcus* sp. and *Methylocystis* sp.). The goal of this experiment was to determine the optimal standard templates, primer set, and primer concentration for these specific primer sets.

For 16S T1 and 16S T2, approximately 5 qPCR plates were run amplifying template DNA with primer concentrations ranging from 200 nM to 1000 nM. The 16S T1 primer set amplified from the Type I methanotroph DNA (*Methylococcus* sp.); while the 16S T2 primers amplified form the Type II methanotroph DNA (*Methylocystis* sp.). The goal of this experiment was to determine the optimal primer concentration for these specific primer sets.

Methanotroph qPCR Primer Validation and Comparison. In order to validate each primer set, known amounts of methanotroph DNA were quantified using the pmoA 178, 330, 16S T1, and T2 primer sets and subsequently compared. Assuming there is one copy of each gene per organism genome, then this technique would be expected to validate the qPCR primers because the gene abundance derived from them would be with in the same order of magnitude. Genomic DNA was extracted from *Methylococcus capsulatus* (Type I) and *Methylocystis* sp. strain Rockwell (Type II) and used to assemble 5 different mixtures of Type I and Type II methanotroph DNA. The mixtures were as follows: 100% (T1); 75:25 (T1:T2); 50:50 (T1:T2); 25:75 (T1:T2); 100% (T2). The concentration of each mixture was 5 ng/uL, with a total of 15 ng used per reaction. The mixtures were as follows: 100% (T1); 75:25 (T1:T2); 50:50 (T1:T2); 25:75 (T1:T2); 100% (T2). The concentration of each mixture was 5 ng/uL and 3 uL were used per reaction for a total of 15 ng/rxn.

RNA extraction from pure cultures and environmental samples. Pure cultures of VC-assimilating *Mycobacterium* strains JS60 and *Nocardioides* strain JS614 were used to test various approaches to RNA extraction directly from the cultures or after passing the cultures through a Sterivex filter. The cultures were prepared as described previously *(36)* – they were grown and harvested at mid-exponential phase (OD_{600} 0.3306 for JS60 and 0.5202 for JS614), then 10 mL of culture sample was filtered through Sterivex units (0.22 µm) in triplicate, RNAlater (3 mL) was added, and all samples were stored in -80 ^{0}C. For beadbeating of liquid cultures, the 10 mL samples were centrifuged at 6,150×g in the presence of 0.1% Tween 80 and resuspended with 600 µL STE (100 mM NaCl,10 mM Tris-Cl, 50 mM EDTA).

The beadbeating (BB) protocol for DNA extraction from pure cultures was modified for RNA extraction as follows: 100 µL RNAlater and 500 µL STE were used for sampling, 10 µL of beta-mercaptoethanol (BME) was added right before running the beadbeater, and 100 µL RNase/DNase free water was used for RNA elution. For modification of PS/MPS DNA Isolation Kit and PW/MPW RNA Isolation Kit for RNA extraction, 10 µL BME was added right before running beadbeater or vortex. To increase cell lysis, 300 µL and 1,500 µL of zirconia/silica beads were added to MPS DNA/RNA Kit and MPW DNA/RNA Kit, respectively.

When working with the PWS kit, which is performed inside the Sterivex filter housing, we continually experienced problems with filter clogging. This was attributed to the high total dissolved solids content of RNAlater, the RNA preservative used following cell capture onto the filter. To counteract this problem, Phosphate Buffer Saline (PBS, 20 mL) was passed through the filter sample to wash away the RNAlater when the extractions were performed.

Following RNA extraction, DNase treatment is required to digest any contaminating DNA. Since on-column DNase treatment was not present when using the and PS/MPS, , DNase I treatment was performed with modifications (10-times higher DNase I stock and 20 mins incubation at 37 ^{0}C) followed by RNA clean-up step by RNeasy Kit (Qiagen). The concentration of all DNA and RNA samples was measured by Quanti-iT^{TM} dsDNA HS and RNA Assay Kits (Invitrogen). RNA samples were reverse transcribed by SuperScript II Kit (Invitrogen) with random primers. In PWS RNA method, two optional steps (70 ^{0}C incubation for 5 mins and vortexing with glass beads for 5 mins) are present. Based on our preliminary experiments, a 70^{0}C incubation was eliminated from the RNA extraction protocol (data not shown). Following beadbeating, known copies of reference RNA (~2×10^9 copies) *(59)* were added into each 5 ml vortexing tube. All other procedures were followed by manufacture's protocol: PCR inhibitor removal, on-column DNA/RNA capturing, on-column DNase treatment for RNA isolation, and DNA/RNA elution.

When RNA extraction was performed, it was typically in tandem with a DNA extraction. DNA and RNA extractions were sometimes performed separately (using separate Sterivex filters), but we also investigated simultaneous DNA and RNA extraction from a single Sterivex filter in both pure cultures and environmental samples. Flow charts illustrating these different extraction procedures are shown in Figure 4 and Figure 5. When performing a simultaneous DNA and RNA extraction, samples were thawed, centrifuged, resuspended with PWR1 buffer, and then injected into 5 mL vortexing tube. All other procedures were exactly same as separate DNA/RNA extraction method, except that DNA and RNA were extracted from same sample by PowerWater RNA Isolation kit without on-column DNase treatment. After isolating DNA and RNA together,

half of the extracts were treated by in-solution DNase treatment (Invitrogen) followed by RNA purification with RNeasy Kit (Qiagen). RNA concentrations were measured by Qubit™ fluorometer (Invitrogen) with the Quanti-iT RNA assay.

Groundwater samples were collected in 2010 on Sterivex filters from three monitoring wells (RB46D, RB63I, and RB64I) at the Carver, MA site using previously described sampling and subsequent handling procedures *(60)*. The entire membrane was inserted with cell lysis buffer into 5 ml vortexing tube provided in the PowerWater DNA/RNA kits and vortexing was performed for 5 min. Internal nucleic acids were added as described below. RNA was also reverse transcribed to cDNA as described below. The results of this RT-qPCR experiment are described in the results under Task 2.

Internal reference technique for reverse-transcription qPCR (RT-qPCR). Luciferase control RNA (Promega) was used as an internal control nucleic acid *(59)*. It was reverse transcribed to Luciferase cDNA by SuperScript II Reverse Transcriptase (Invitrogen) with Random Hexamer (Invitrogen). Luciferase cDNA was subsequently used as PCR template for amplification of "reference DNA". The *Taq* PCR Master Mix (Qiagen), primers for reference DNA standards described below, and previously described 16S rRNA PCR thermocycler parameters *(36)* were used in this reaction. The PCR product was visualized through gel electrophoresis (1.5% w/v agarose gel in 0.5× Tris/Borate/EDTA (TBE) buffer and 150 W for 30 min), purified by PCR Purification Kit (Qiagen), and used for reference DNA. The concentration of reference DNA and RNA was measured with fluorometer and calculated as transcript and gene copies as described previously *(61)*. Known copies of reference RNA were injected in RNA isolation procedure and reference DNA was used for qPCR standard.

Primers and qPCR Standard. To develop standard curves, we designed new primer sets for amplification of reference DNA from reference mRNA (Luciferase, accession number X65316; refSTF forward primer CCAGGGATTTCAGTCGATGT, refSTR reverse primer TTTTCCGTCATCGTCTTTCC; 1014 bp product) and used previously designed primer sets for amplification of the *etnC* and *etnE* standard from JS614 (JS614EtnCF, JS614EtnCR; 1138 bp product and CoMF1L, CoMR2E; 881 bp product) (Table 5). The refSTR also was used in preliminary reverse transcription and RT efficiency comparison experiments. Preparation of qPCR standards was same as previously described *(61)*. Then, we converted ref mRNA into ref cDNA using the SuperScript II Reverse Transcriptase Kit and the refSTR primer. The final product was used in 100 µL PCRs containing 50 µL of Hotstart PCR Master Mix, 50 pmol (each) of refSTF and refSTR primers, 1 µL of RT product, and water to bring the column up to 100 µL. The thermocycling parameters were as follows: initial 94^0C for 5 min (hot start), then 30 cycles of 94^0C (30 sec), 55^0C (30 sec), and 72^0C (1 min), followed by a 72^0C, 5 min final extension. The PCR product was subsequently purified and used to develop qPCR standards over a range of 3 - 30×10^7 copies of double strand ref cDNA template. These standards were used to develop five replicate qPCR standard curves. We used the refF and refR primers described in *(62)* for use in ref mRNA quantification experiments. The linear dynamic range of these standard curves was 5 - 3×10^7, the R^2 was 0.9972, the fluorescence threshold was 0.11, and the PCR efficiency was 100.4% (linear regression slope = -3.3127 and Y-intercept = 37.417). These are acceptable qPCR standard curve parameters.

For the functional genes, MRTCF&R and MRTEF&R were developed in a previous study *(63)*. All oligonucleotides used are summarized in Table 2 and Table 3.

Reverse Transcriptase Efficiency. To estimate reverse transcriptase (RT) efficiencies, Luciferase control RNA was diluted to ~20ng/µL and used as template. Random Hexamer or refSTR were used as a primer for comparison the RT efficiencies from two different reverse transcriptase primers. The initial control RNA concentration was measured, RT reactions were done with refSTR or Random Hexamer, and qPCR was done for quantification of reference cDNA gene copies. The standard curve was developed by the purified PCR product with refSTF and refSTR. By comparing cDNA copies produced by qPCR to initial reference RNA copies, the RT efficiencies were produced. All RT reaction conditions were conducted according to the manufacturer's protocol.

DNA contamination in RNA isolation and ref. mRNA stock. DNA contamination could be caused by incomplete DNase treatment during isolation step and affect transcript quantification sensitivity. Whenever possible RNA extracts were used for qPCR template to quantify *etnC*, *etnE*, and reference genes (luciferase) – which could be potential DNA contaminants in RNA extracts.

RT-qPCR Procedures. RT-qPCR was performed with an intra-assay (i.e. same plate) standard. Its conditions and Software for data analysis were same as described previously *(61)* except that qPCR primer concentration was 100 nM per single primer sequence *(63)*. Three sets of qPCR standards (*etnC*, *etnE*, and reference gene) were prepared as described previously *(63)*. Quantification of gene or transcript copies were performed with correction of reference DNA or RNA

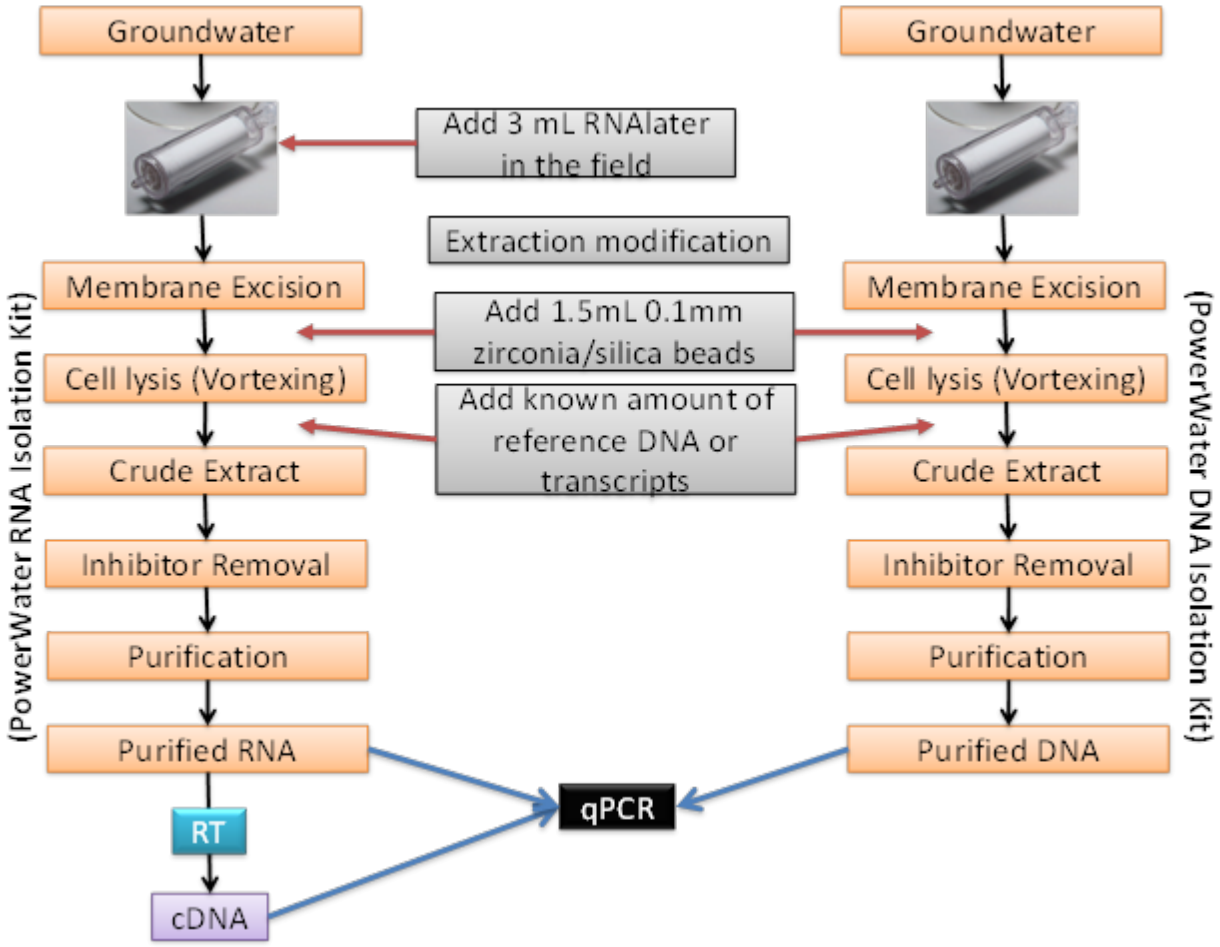

Figure 4. Flow chart illustrating the separate extraction of DNA and RNA from filtered groundwater samples.

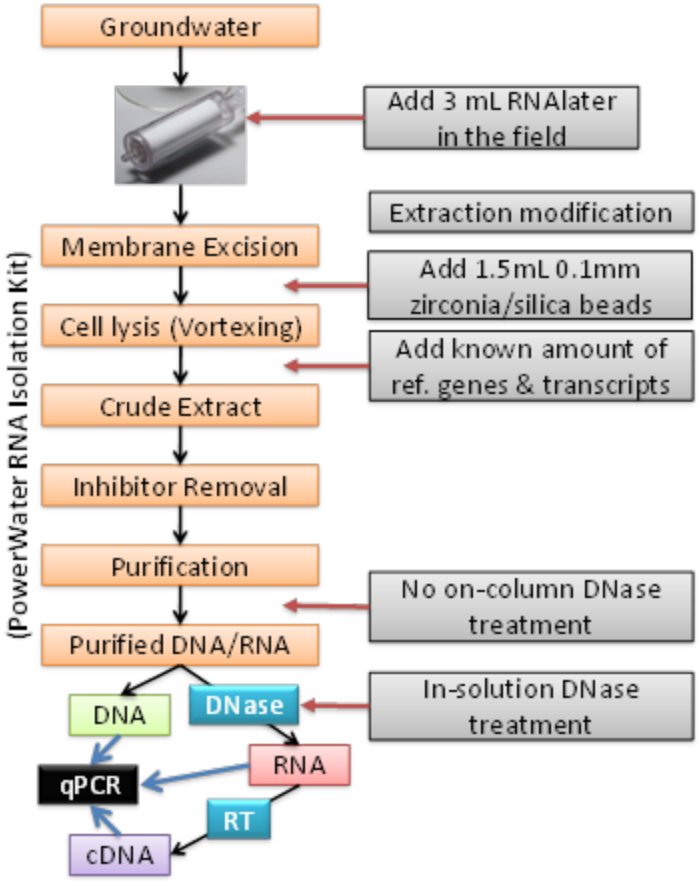

Figure 5. Flow chart depicting an approach for simultaneous DNA and RNA extraction from a single Sterivex filter.

To normalize gene copy quantifications to the amount of groundwater tested, the following equations were used:

Reference DNA Recovery Ratio

$$RDRR = \frac{[Quantified\ Gene\ Copies/PCR\ Rxn)] \times [DNA\ Elution\ Volume\ (uL)]}{[Total\ Gene\ Copies\ Added\ before\ Extraction] \times [Template\ DNA\ (uL)]}$$

RNA Transcript Copies per Liter Groundwater

$$\frac{RNA\ TC}{L\ GW} = \frac{[Transcript\ Copies/PCR\ Rxn] \times 4 \times [RNA\ Elution\ Volume\ (uL)]}{[RDRR] \times [Template\ cDNA\ (uL)] \times [GW\ Sample\ Volume\ (L)]}$$

DNA Gene Copies per Liter Groundwater

$$\frac{DNA\ GC}{L\ GW} = \frac{[Quantified\ Gene\ Copies/PCR\ Rxn] \times [DNA\ Elution\ Volume\ (uL)]}{[RDRR] \times [Template\ DNA\ (uL)] \times [GW\ Sample\ Volume\ (L)]}$$

PCR efficiency was calculated using the following equation. An ideal slope of -3.32 cycle #/ Log [concentration] would yield an efficiency of 100%.

$$PCR\ Efficiency = \left[\left(10^{-1/slope}\right) - 1\right] \times 100$$

Microcosm Construction and Analysis

Carver, MA site screening tests for microbial types in fourteen wells. For each well sample, three microcosms were constructed in 160 ml serum bottles, having 40 ml groundwater and 60 ml mineral salts media *(6)*, and sealed with a Teflon-coated butyl rubber septum through which small samples could be transferred by syringe. Each bottle received a full mineral supplement, pH control via a mineral salts buffer, and excess O_2. Each contained 40 mL groundwater and 60 mL sterile mineral salts media (MSM) in 160 mL serum bottles, having 60 mL air headspace, which provided 12.5 mL of O_2. Each bottle was sealed with a Teflon-coated butyl rubber septum through which small samples could be removed by syringe for monitoring. For two of the well samples, a second microcosm was set up as a killed control by lowering the pH to 2 with HCl. The MSM contained appropriate concentrations of the minerals needed by aerobic bacteria, and was buffered at pH 6.8. Bottles were given either 330 µmol methane, 250 µmol ethene, or 1 µmol VC as substrate. Prior to adding VC, newly-constructed microcosms (except those for 64-I and 78) were sparged with air at 100 ml/min for 2 to 7 minutes to remove native methane and ethene. Then 0.25 ml of a dilute VC gaseous stock was injected into each microcosm and the gases were allowed to equilibrate. Based on day-1 analysis of 8 of the 14 microcosms, the concentrations of methane ranged from 0.01 to 1.2 µmol/bottle, those of ethene ranged from <0.004 to 0.01 mmol/bottle, and the VC was 1.0 ± 0.1 µmol/bottle. Microcosms were incubated at 22°C, on their sides, in darkness, and shaken by hand three times per week. Bottles for methanotrophs, etheneotrophs, and VC-assimilators were incubated for 28, 70 and 133 days.

Data collection was terminated at day 133 for most samples. Additional data were collected for three microcosms showing partial VC removal on day 133.

Well 63-I groundwater microcosms containing methane, ethene and VC. Based on the screening test described above, well 63-I, located 100 feet down gradient from the fourth cross-plume line of air infusion points, was selected for further testing. To remove native methane and ethene, the groundwater was bubbled with air until the native methane had been removed to < 0.02 µmol/bottle. The groundwater was amended by addition of stock solutions of KNO_3, KH_2PO_4, Na_2HPO_4, and trace element mix *(6)*, giving a pH of 6.8. Microcosms were constructed by transferring 100 ml of mineral-amended groundwater to each of fifteen 160 ml serum bottles, which were sealed with septa as described above. The native and amended concentrations in the amended groundwater are given in Table 4. The low Cu concentration (4 µg/L) was expected to allow expression of sMMO by the native methanotrophs *(64)*. In 2010 experiments, thirteen microcosms and a killed control were constructed with 100 ml of mineral-amended groundwater as described above. The microcosms were injected with dilute VC gas stock by syringe through the septa to give 0.08 µmol/bottle. Methane and/or ethene were injected to give 0, 0.7, 2.0, or 6.0 µmol/bottle (Table 5). In 2011 experiments, a total of 19 microcosms were constructed, including four sets of triplicates and three sets of duplicates, representing seven conditions. Only conditions with 1.6 µmol/bottle methane and ethene were tested. Killed controls containing representative concentrations of methane, ethene and VC were prepared by lowering the pH to 2. Concentrations of the analytes in the killed controls did not change during the test periods, confirming that there was no abiotic loss of compounds (Figure 6).

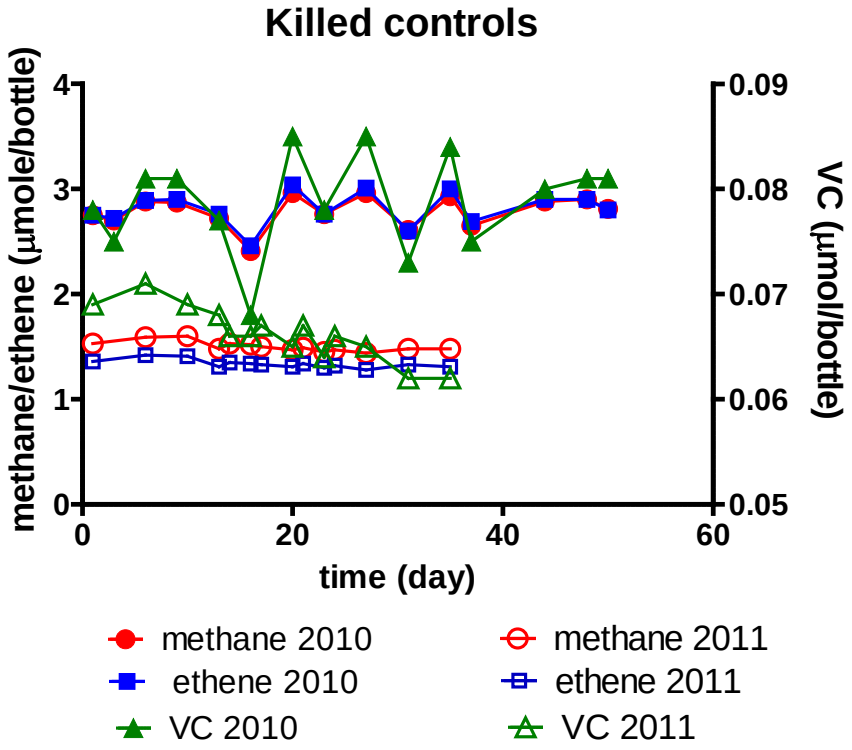

Figure 6. Killed control microcosms for both 2010 and 2011 Carver site groundwater experiments.

Table 4. Concentrations (mg/L) of macro and micronutrients in well RB-63I native and amended groundwater

	native	amended
NO_3	< 0.4	44
PO_4	0.03	61
SO_4	74	74
Cl	37	37
K	1.8	39
Na	22	40
Ca	27	27
Fe	6.6	6.6
Mg	7.9	7.9
B	0.24	0.24
Cu	<0.001	0.004
Co	0.009	0.034
Mn	1.50	1.51
Mo	<0.001	0.012
Se	0.001	0.001
Zn	0.031	0.047
Ni	0.006	0.011

Table 5. Mass of VOCs added to microcosms containing mineral amended well 63-I groundwater in the 2010 microcosm experiment.

Bottle #		Initial VOC mass added µmol /bottle		
		VC	methane	ethene
1	Killed Control	0.08	2.8	2.8
2	VC only	0.08	0	0
3	M, no VC	0	0.7	0
4	VC, low M	0.08	0.7	0
5	VC, med M	0.08	2.0	0
6	VC, high M	0.08	5.6	0
7	E, no VC	0	0	0.7
8	VC, low E	0.08	0	0.7
9	VC, med E	0.08	0	2.0
10	VC, high E	0.08	0	5.6
11	M, E, no VC		2.0	2.0
12	VC, high M /high E	0.08	2.0	2.0
13	VC, low M /high E	0.08	0.7	2.0
14	VC, high M /low E	0.08	2.0	0.7
15	Methanol control	0	0.7	0

Groundwater microcosm analytical methods. Groundwater sampled from Carver well RB-63I was analyzed for Cl^-, NO_3^- and SO_4^{2-} by capillary ion electrophoresis according to EPA Method 6500, for PO_4 by Hach Method 8048, and for other elements by EPA Method 200.8. Bottles were monitored by removing a 100 µL headspace samples and injecting directly into a HP 5890 gas chromatograph according to EPA method 5021A. Standards were prepared similarly, and analyzed in the same manner as samples. ChemStation software was used to calculate response factors and quantitate results. Ethene, methane and VC were detected by flame ionization, and O_2 and CO_2 were detected by thermal conductivity. Initial aqueous concentrations of the substrates were calculated with the following dimensionless Henry's Law constants: methane (24.4), ethene (7.15) and VC (1.0) *(65-67)*. Using graphs of substrate utilization with time, the lag times before *initiation* of substrate utilization, and the times for 50% utilization were estimated. These parameters are used in describing the results, and in interpreting the interactions of the three substrates and the three microbial processes, cometabolism by ethene- and methane-utilizers, and utilization by VC-assimilators. For the 2011 results, the averages of the lag times and 50% degradation times for duplicate and triplicate microcosms were used.

Experiments with mixtures of pure ethene-assimilating and methanotroph mixtures. Pure culture mixtures of ethene-oxidizing *Mycobacterium* strain JS622 and methane-oxidizing Alphaproteobacterium, *Methylocystis sp.* strain Rockwell (ATCC 49242) were used to investigate the degradation activity of ethene, methane, and vinyl chloride mixtures in serum bottles during Task 3. *Mycobacterium* strain JS622 stock (1 ml) was thawed and added to a modified 2-liter Erlenmeyer flasks containing 500 mL of MSM, 1 ml of filter-sterilized trace metal solution (TMS), and 100 ml of ethene filter-sterilized by 0.22 µm PVDF membrane from MILLEX. *Methylocystis sp.* strain Rockwell (ATCC 49242) stock (1 ml) was thawed and added to a modified 2-liter Erlenmeyer flasks containing 500 ml of MSM, 1 ml of filter-sterilized TMS, and 120 ml of filter-sterilized methane. Both cultures were incubated aerobically on a circular shaker at 200 revolutions per minute (rpm) at room temperature (RT, ~22°C).

It took about 5 days for JS622 to reach mid-exponential phase (OD_{600}= 0.3-0.35), and about 3 days for ATCC49242. When both cultures both reach their mid-exponential phase at the same time, they were pelleted separately via centrifugation for 5 min at 6438 x*g*. The cultures were resuspended into 10 mL MSM (OD_{600} ~16.5-17.5). These dense cultures were used to prepare mixed liquid cultures at an initial OD_{600} of 0.1 for experiments, as described below.

In each experiment seven 160-ml serum bottles were prepared, to which 72 ml of liquid culture (initial OD_{600} = 0.1) was added, leaving with 88 ml of headspace. The bottles were then capped with slotted Wheaton gray butyl rubber septa and aluminum crimp caps. Autoclaved controls were also prepared in parallel to test for abiotic losses. For any particular experiment involving seven bottles, a total of 504 ml of culture volume with an initial OD_{600} of 0.1 was required. To achieve the initial OD_{600} in any particular bottle required dilution of dense cultures described previously (Table 6). Five different methanotroph and etheneotroph cell concentration ratios were also investigated: (1) 100% JS622; (2)100% ATCC49242;(3) JS622: ATCC 49242=1:1;(4) JS622: ATCC49242=3:1; (5) JS622:ATCC49242=1:3.

Table 6**.** Dilution approach used to prepare experimental bottles. Prior to each experiment 504 ml each of JS622 and ATCC49242 was prepared at initial OD_{600} = 0.1, then different volumes were mixed as shown below to provide different percentages of each microbial group as desired.

	The volume constitution for each culture ratio (ml)						
JS622	504	378	252	126	50.4	25.02	0
ATCC49242	0	126	252	378	453.6	478.8	504
Culture ratios	100%	75%	50%	25%	10%	5%	0%

Once capped and crimped, gases were added to the bottles as follows: (1) methane alone; (2) ethene alone; (3) methane+VC; (4) ethene +VC ; (5) VC alone; (6) methane+ethene; (7) methane+ethene+VC; (8) culture medium control containing methane+ethene+VC. The amount of gas added to each bottle for each set of experiments is described in Table 7. The control bottle that contained 72 ml of MSM and methane+ethene+VC was also prepared in each experiment.

Table 7. Substrate and culture ratios used in pure culture experiments

	Culture ratios tested (expressed in terms of JS622 percentage)						
MTH:ETH:VC (µmol)	100% JS622	75% JS622	50% JS622	25% JS622	10% JS622	5% JS622	0% JS622
40:40:40	X		X				X
400:400:20	X	X	X	X			X
400:40:20	X	X	X	X	X	X	X

Analytical methods. To test the optical density of liquid cultures, the modified 2-liter Erlenmeyer flask containing the growing culture was inverted couple of times, then 1 ml of the liquid sample was taken by 1-ml plastic syringe with a needle (22G 1.5), and added into a disposable cuvette. UV absorption spectra of the liquid culture were performed on a *Cary 50 Bio* UV-Visible spectrophotometer at 600 nm.

The bottles were incubated on a circular shaker at 200 revolutions per minute (rpm) at room temperature throughout the observation period. A 0.25-ml Pressure-Lok gas-tight syringe with a side-ported needle was used to take 0.1 ml headspace samples during each measurement. Three measurements were taken in the first day of incubation, during which the gases were consumed rapidly by the bacteria. Two measurements were taken on the next two days, and one measurement was taken each day approximately after day 4.

Gases were analyzed on a Hewlett-Packard 5890 series II gas chromatograph using a stainless steel column (8.0 ft x 1/8 in. x 2.1mm) packed with 1% SP-1000 phase on 60/80 Carbopack B. A flame ionization detector was used with a nitrogen carrier gas flow rate of 30 ml/min and an oven temperature of 90 °C. Each compound forms a peak at its specific retention time (minutes): methane at 1.4; ethene at 1.8; VC at 4.4. Peak areas for each compound determined by GC analysis were calibrated to external standards to give the total mass in the bottle. Standard curves for methane and ethene ranged from 0 µmol to 800 µmol, and ranging from 0 µmol to 50 µmol for VC.

Results and Discussion

Task 1 Develop qPCR techniques for etheneotrophs (and methanotrophs)

Subtask 1.1 DNA extractions from Sterivex filters

Because groundwater is much easier to sample from existing monitoring wells our technology was developed with the intent that gene abundance measurement could be routinely measured from groundwater samples. In accordance with other established protocols groundwater for qPCR analysis is sampled and biomass is collected from the groundwater by passing it through sterile, Sterivex membrane filter cartridges, while measuring the flow through in a graduated cylinder. Once the target sample volume is reached or the filter clogs, the sample volume is noted so that accurate estimates of gene and transcript abundance can be made *(68)*. For filters intended for RNA analysis, 3 ml of RNAlater is passed through the filter following sampling. Filters are placed in sterile Falcon tubes, immediately stored on ice and shipped back to the laboratory by express courier, where they are stored at -80°C until analysis.

An important task in this project was to develop an effective protocol for extracting DNA from the Sterviex filters. As this project progressed, it became apparent that once qPCR primers are designed and working, that the main obstacle to quantifying genes in environmental samples lies in the DNA extraction step. VC-contaminated groundwater samples from three different sites (Carver, MA; Soldotna, AK, and NAS Oceana, VA) were periodically available during the course of the study. We used a portion of these samples to evaluate several DNA extraction kits produced by MoBio. Initially, we utilized the MoBio PowerSoil DNA kit primarily because this kit was already adopted by Microbial Insights, Inc. for qPCR analysis of DNA extracted from Sterivex filters. Although Sterivex units were beneficial for easier sampling and shipping, the trade-off appeared to be decreased DNA extraction efficiency when compared to conventional laboratory methods such as beadbeating suspended cells.

The initial DNA extraction protocol with the MoBio Powersoil kit entailed aseptically removing the filter from its housing, slicing it into approximately 30 pieces with a sterile razor blade, and mixing the filter pieces into tubes containing beads provided by the kit. Following these steps, the DNA extraction protocol was carried out as recommended by MoBio. Additional experimentation led us to further refine the Sterivex filters DNA extraction procedure using the PowerSoil kit. These small modifications were: after thawing the filter, push any remaining liquid through the filter with a sterile syringe. Cut the Sterivex filter into 64 pieces (instead of 30 as described above). After beadbeating and centrifugation (per the kit instructions), precisely transfer 450 µL of the supernatant. Finally, complete the procedure with two DNA elution steps. This is because in a beadbeating protocol only a portion of the supernatant is typically removed – some of it remains trapped within the bead matrix. We determined that following removal of the supernatant after beadbeating, by washing the beads with buffer and subjecting the buffer to the remainder of the DNA extraction protocol, we could recover additional DNA from an environmental sample. However, as described below, we found that addition of 0.1 mm zirconia/silica beads to the beads provided by the MoBio kits resulted in higher DNA yields.

Our DNA extraction method evolved during this project primarily by changing the sampling method and modifying commercial kit (i.e. MoBio) protocols. As described above, our initial qPCR development study employed the PowerSoil DNA kit *(61)*. In a subsequent study of these qPCR primers we employed the MoBio PowerWater kit *(69)*. In late 2011, MoBio introduced a new extraction kit optimized for Sterivex filters, called the PowerWater Sterivex DNA kit. This led us to conduct a brief study of several MoBio DNA extraction kits and modified protocols with pure VC- and ethene-assimilating cultures cultures (*Mycobacterium* JS60 and *Nocardioides* JS614) to compare their yield of DNA and determine if a particular kit and/or modified protocol was preferred over the others.

An earlier preliminary study of DNA extraction efficiency suggested that the type of bacteria affected DNA extraction and recovery efficiency. In particular we observed that the degree of cell lysis and subsequent DNA extraction was different when *Mycobacterium* JS60 or *Nocardioides* JS614 cultures were used. In our most recent study we compared DNA yields from *Mycobacterium* JS60 and *Nocardioides* JS614 cultures when using Beadbeating DNA purification (Phenol/chloroform/Isoamyl alcohol purification)(BB), PowerSoil DNA Isolation (PS), Modified PowerSoil DNA Isolation (MPS), PowerWater DNA Isolation (PW), Modified PowerWater DNA Isolation (MPW), and PowerWater Sterivex DNA Isolation (PWS). All kits were produced by MoBio. In general, original protocols were applied to (PS), (PW), and (PWS). "Modified" indicated that addition of 0.1 mm zirconia/silica beads (300 µL and 1,500 µL for (MPS) and (MPW), respectively).

The data from this experiment is presented and summarized in Figure 7A. The total mass of JS60 DNA extracted from beadbeating method (BB) was 14,900 ± 300 ng (95% confidence interval, CI) and it was used as a reference for all the other extraction since the highest mass of DNA was obtained. Extracted DNAs were 880 ± 160 ng (PS), 8,780 ± 1,580 ng (MPS), 2,180 ± 810 ng PW), 9,070 ± 1,850 ng (MPW), and 8,350 ± 820 ng (PWS). Based on these results, the efficiency of JS60 DNA extraction with (MPS), (MPW), and (PWS) was not significantly different at the 95% CI. The mass of JS614 DNA extracted from (BB) was 36,670 ± 3,500 ng. The mass of extracted DNA was 1,490 ± 300 ng (PS), 12,700 ± 470 ng (MPS), 2,240 ± 910 ng (PW), 16,330 ± 4,970 ng (MPW), and 21,120 ± 4,210 ng (PWS). In the case of JS614, (MPW) and (PWS) had the highest DNA yield among commercial kits and there was no significant difference between them at the 95% CI. Based on this comparison of DNA yield with various MoBio kits, the Modified PowerWater DNA Isolation Kit or the (new) PowerWater Sterivex DNA Isolation Kit are most favorable.

We have improved the recovery of DNA from Sterivex filters and revealed potential variability in DNA extraction from mycobacterial VC/ethene-oxidizers. However, yield is not the only important aspect of a good DNA extraction protocol. The DNA must be of high quality and relatively free of compounds that could inhibit the qPCR experiments. PCR inhibition experiments are discussed in Subtask 1.4. To better assess the quality of the DNA we estimated gene abundance in each of the extracts as described in *(70)* and later in this document, except that JS60 gene specific primers (GSP) and JS614 GSP were used for standards (Table 5). The results of this experiment are shown in Figure 7B. This shows that the quality of the DNA extracted from the PowerSoil kit is the best, in terms of gene abundance estimates, but that there

is low yield of DNA when using this kit. The best balance between DNA yield and DNA quality was achieved with the MPS and new PWS kits.

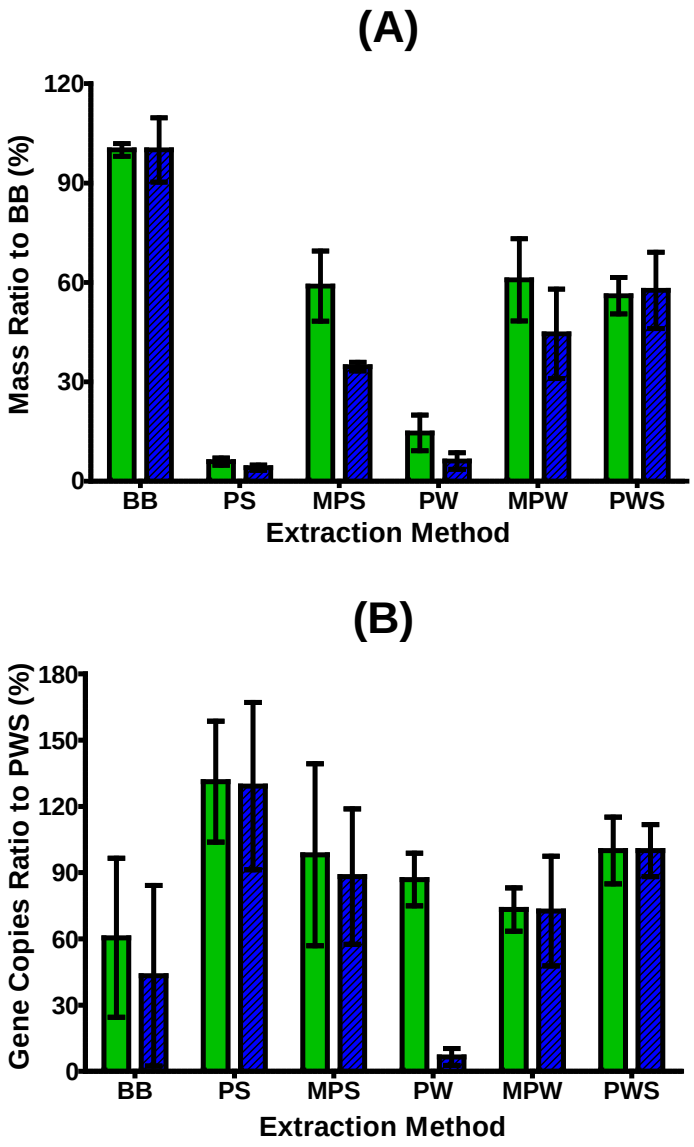

Figure 7**.** A) Nucleic acid mass recovery following DNA extraction from pure cultures of VC-assimilating *Mycobacterium* JS60 (clear greeen bars) and *Nocardioides* JS614 (hatched blue bars) using a variety of extraction methods and kits. The mass of DNA recovered was normalized to the BB method. The bar height is the average of three replicates and the error bars are the 95% confidence interval. B) Comparison of estimated *etnC* gene abundance by qPCR following DNA extraction. The *etnC* abundance was normalized to the abundance estimated in the PWS DNA extract.Abbreviations: BB: Nucleic acid extraction by bead beating, followed by phenol:chloroform:isoamyl alcohol extraction. PS: Mo Bio Powersoil extraction kit. MPS: Mo Bio Powersoil extraction kit with additional zirconium/silica beads added. PW: Mo Bio PowerWater extraction kit. MPW: Mo Bio PowerWater extraction kit with additional zirconium/silica beads added. PWS: MoBio PowerWater Sterivex extraction kit.

Subtask 1.2 qPCR primer development and testing

The main goal of this subtask was to generate real-time PCR primer sets that would effectively quantify functional genes from both etheneotrophic and VC-assimilating bacteria. We targeted two different functional genes known to be involved in VC and ethene biodegradation by these bacteria: the alkene monooxygenase (AkMO) alpha subunit (encoded by the gene *etnC*) and epoxyalkane:coenzyme M transferase (EaCoMT) (encoded by the gene *etnE*)*(15, 17, 71)*. In July 2009 only three complete *etnC* and *etnE* sequences were known. However, this has since changed because several etheneotrophs and VC-assimilators have recently had their genomes sequenced. These sequences, from VC-assimilating *Mycobacterium* strain JS60, *Mycobacterium* strain JS623 and *Nocardioides* strain JS614, were entered into Primer Express 2.0 and used to develop over 200 candidate qPCR primer sets. Candidate primer sequences were then manually compared with nucleotide and protein sequence alignments of 25 partial *etnC* and 13 partial *etnE* sequences found either in GenBank or sequenced in our laboratory. This comparison procedure allowed us to design 8 *etnC* and 11 *etnE* degenerate primer sets that account for variability among the sequences that were available. Our goal was to design primers that amplify the extant diversity of *etnC* and *etnE* sequences in environmental samples while minimizing (and ideally eliminating) the amplification of non-specific products.

1.2.1 PCR specificity testing

A battery of PCR tests was conducted to evaluate the specificity of the candidate primer sets and determine the best *etnC* and *etnE* primer set for subsequent experiments with groundwater DNA. The PCRs included two different negative controls. DI water was used as a negative DNA control for the presence of DNA template contamination. We also included *E. coli* DNA, which does not contain *etnC* and *etnE* template, as a control for non-specific PCR products from DNA templates. We also tested DNA from *Xanthobacter autotrophicus* Py2, a propene-oxidizing strain that contains an EtnE gene distantly related to the EtnE genes found in etheneotrophic and VC-assimilating strains. Amplification of *etnE* sequences from microbes such as Py2 would be considered a false positive as they are not expected to participate in VC biodegradation in environments that are lacking propene.

The specificity of candidate primers was also tested with DNA from VC-assimilating *Nocardioides* JS614, and VC-assimilating *Mycobacterium* strain JS60, JS616, JS617, JS621, JS622, JS623, JS624, JS625, TM1, and TM2. Each of these strains can be considered positive controls as they all possess *etnC* and *etnE*. We selected the best *etnC* and *etnE* primer sets that produced the expected product size (106 bp for *etnC*; 151 bp for *etnE*) in all positive control DNA templates, but that did not produce any non-specific products or any PCR products in the *E.coli*, Py2, and DI water controls (Table 8). These primer sets (RTC9, RTC6 and RTE15, RTE16) were subsequently tested in PCRs with DNA from 16 groundwater samples among three different VC-contaminated sites (Carver, MA, Soldotna, AK, and NAS Oceana, VA). Interestingly, *etnE* bands of the expected size were readily amplified directly from all samples and all sites (Figure 8). Conversely, *etnC* bands of the expected size were initially amplified only from the pure cultures and Carver, MA site DNA (Figure 9). Nested PCR experiments were designed that involved an initial amplification with a previously published degenerate *etnC* primer set (NVC 105 and NVC106; *(72)*). After the initial amplification, 2 µl of the PCR mixture was used in a subsequent amplification with our selected *etnC* qPCR primer set. This

procedure resulted in a band of the expected size in all Soldotna and NAS Oceana samples (Figure 10).

These results were valuable in determining whether SYBR green or TaqMan real-time PCR chemistry would be used in subsequent experiments (one of our early go/no-go decisions). A disadvantage of SYBR Green chemistry is that any non-specific products produced during PCR are detected and will affect quantitation. However, we have found that our qPCR primers are highly specific in both pure cultures and environmental samples. In addition, degenerate qPCR primers are compatible with SYBR green real-time PCR chemistry. Degenerate PCR primers are desirable for interrogation of environmental samples because the extant diversity of *etnC* and *etnE* is not known *a priori*. TaqMan chemistry, on the other hand, requires the design of an additional probe specific to the target gene. To capture extent gene diversity in a sample, this would require the design of a separate TaqMan probe for every new *etnC* or *etnE* sequence we encounter in an environmental sample, which is impractical. Therefore, our results support the use of SYBR Green real-time PCR chemistry in subsequent experiments. However, the results depicted in Figure 8 and Figure 9 do not provide conclusive evidence of primer specificity. Thus, we continued to rigorously test the specificity of our primers with cloning, sequencing, and bioinformatic approaches, as discussed in the following sections.

We examined the specificity and diversity of *etnC* sequences amplified from VC-contaminated groundwater with our recently developed qPCR primers (Table 9). The main rationale for these experiments was to determine if variation in sequence existed among the PCR products. This information helped us decide whether to proceed with SYBR Green chemistry or to consider switching to TaqMan probe chemistry. We tested one groundwater sample from each geographically different site (e.g. well RB46D at the Carver, MA site, well MW20 at Soldotna, AK site, and well MW19-08C at NAS Oceana, VA site). DNA was extracted from the Sterivex filters using the modified MoBio kit protocol and subjected to PCR with NVC105 and NVC106 primers *(14)* and with RTC primers *(61)* using a nested PCR protocol. After purifying PCR products, clone libraries were constructed, plasmids (pCR2.1-TOPO vectors) containing the sequences were isolated and the inserts sequenced. We obtained 39 partial sequences ranging in size from 18-104 bp in length. The expected size of the PCR product was 106 bp. The reason for the differences in size of retrieved sequences is currently unknown, but poor signal at the beginning of the sequencing reaction is thought to be partially responsible.

These sequences were subjected to BLAST analysis using default search parameters. Of the 39 sequences obtained, 29 sequences showed top BLAST hits that were 93-100% identical to *etnC* sequences from VC-assimilating strains JS60 and JS623, and ethene-assimilating strains NBB1 and NBB2. Ten sequences (ranging in size from 23-62 bp) returned a BLAST error message and required altered search parameters to receive a BLAST result. The short length of these sequences along with the fact that we could not locate both ends of the vector sequence in 8 of them indicates that they are of questionable quality. However, BLAST hits to *etnC* sequences were found in 6 of the 10 sequences that required altered BLAST search parameters. It is possible that 4 of the sequences (incidentally, all from the NAS Oceana site) were non-specific amplicons, but conclusive evidence was not obtained.

Table 8. Results of qPCR primer specificity testing. A "+" indicates that a band of the expected size was observed, while a "-" indicates that a band of the expected size was absent. The number of bands that were not of the expected size (non-specific products) was also noted. Based on the results of this test, the primers RTC9/RTC6 and RTE15/RTE16 were chosen for more detailed analysis.

Template		**Primer set**																		
		***etnC* (RTC)**								***etnE* (RTE)**										
		1-2	3-4	5-6	7-6	**9-6**	11-12	13-14	15-16	1-2	3-4	5-6	7-8	9-10	11-12	13-14	**15-16**	17-18	19-20	21-22
NC	DI	-	-	-	-	-	-	-	-	-	-	-	-	-	-	-	-	-	-	-
	E. coli	-	-	-	-	-	+	-	-	-	+	-	-	-	+	-	-	-	-	-
Nocar.	JS614	+	+	+	-	+	+	-	+	-	-	+	-	-	-	-	+	-	+	-
Xan.	Py2	-	+	-	-	-	+	+	-	-	+	+	-	-	-	-	+	+	+	-
Myco.	JS60	+	+	+	+	+	+	+	+	+	+	+	+	+	+	+	+	+	+	+
	JS616	+	+	+	+	+	+	+	+	+	+	+	+	+	+	+	+	+	+	+
	JS617	+	+	+	+	+	+	+	+	+	+	+	+	+	+	+	+	+	+	+
	JS621	+	+	+	+	+	+	+	+	+	+	+	+	+	+	+	+	+	+	+
	JS622	+	+	+	+	+	+	+	+	+	+	+	+	+	+	+	+	+	+	+
	JS623	+	+	+	+	+	+	+	+	+	+	+	+	-	+	+	+	+	+	+
	JS624	+	+	+	+	+	+	+	+	+	+	+	+	+	+	+	+	+	+	+
	JS625	+	+	+	+	+	+	+	+	+	+	+	+	+	+	+	+	+	+	+
	TM1	+	+	+	+	+	+	+	+	+	+	+	+	+	+	+	+	+	+	+
	TM2	+	+	+	+	+	+	+	+	+	+	+	+	+	+	+	+	+	+	+
Environ. Samples (Carver, MA)	I-L	+	+	+	+	+	+	+	+	+	+	+	+	-	+	+	+	+	+	-
	RB35I	+	+	+	+	+	+	+	+	+	+	+	+	-	+	+	+	+	+	-
	RB39I	+	+	+	+	+	+	+	+	+	+	+	+	-	+	+	+	+	+	-
	RB46D	+	+	+	+	+	+	+	+	+	+	+	+	-	+	+	+	+	+	-
	RB61	+	+	+	+	+	+	+	+	+	+	+	+	-	+	+	+	+	+	-
	RB64I	+	+	+	+	+	+	+	+	+	+	+	+	-	+	+	+	+	+	-
# of non-specific products		12	5	0	7	**0**	16	0	7	3	10	0	0	0	0	0	**0**	0	4	1

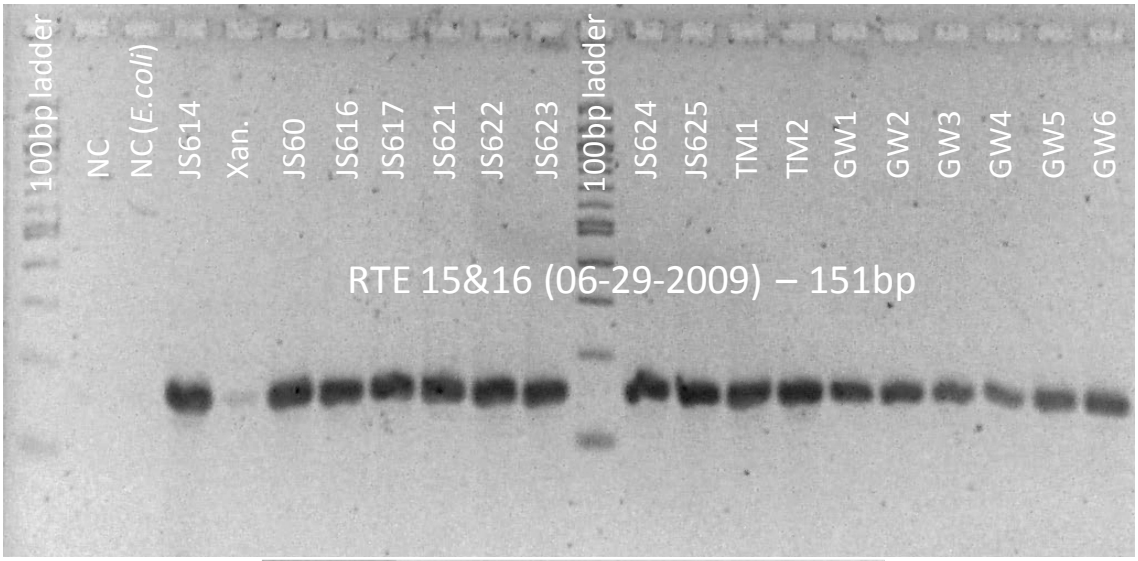

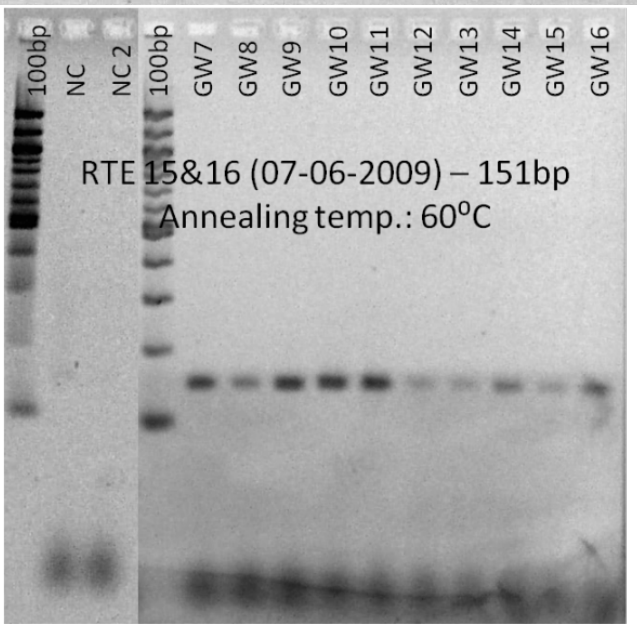

Figure 8**.** Specificity testing of the *etnE* primers RTE15 and RTE16 by standard PCR using DNA from pure cultures (E.coli, Xan. (propene-degrading *Xanthobacter* Py2), VC-assimilating strains JS614, JS60, JS616, JS617, JS621, TM1, TM2, etheneotrophic strains JS622, JS623, JS624, JS625, and 16 environmental samples (GW1-6 = Carver, MA samples; GW7-13 = Soldotna, AK samples; GW14-16 = NAS Oceana samples). In all cases a single band of the expected size was observed, a result which strongly suggested good primer specificity.

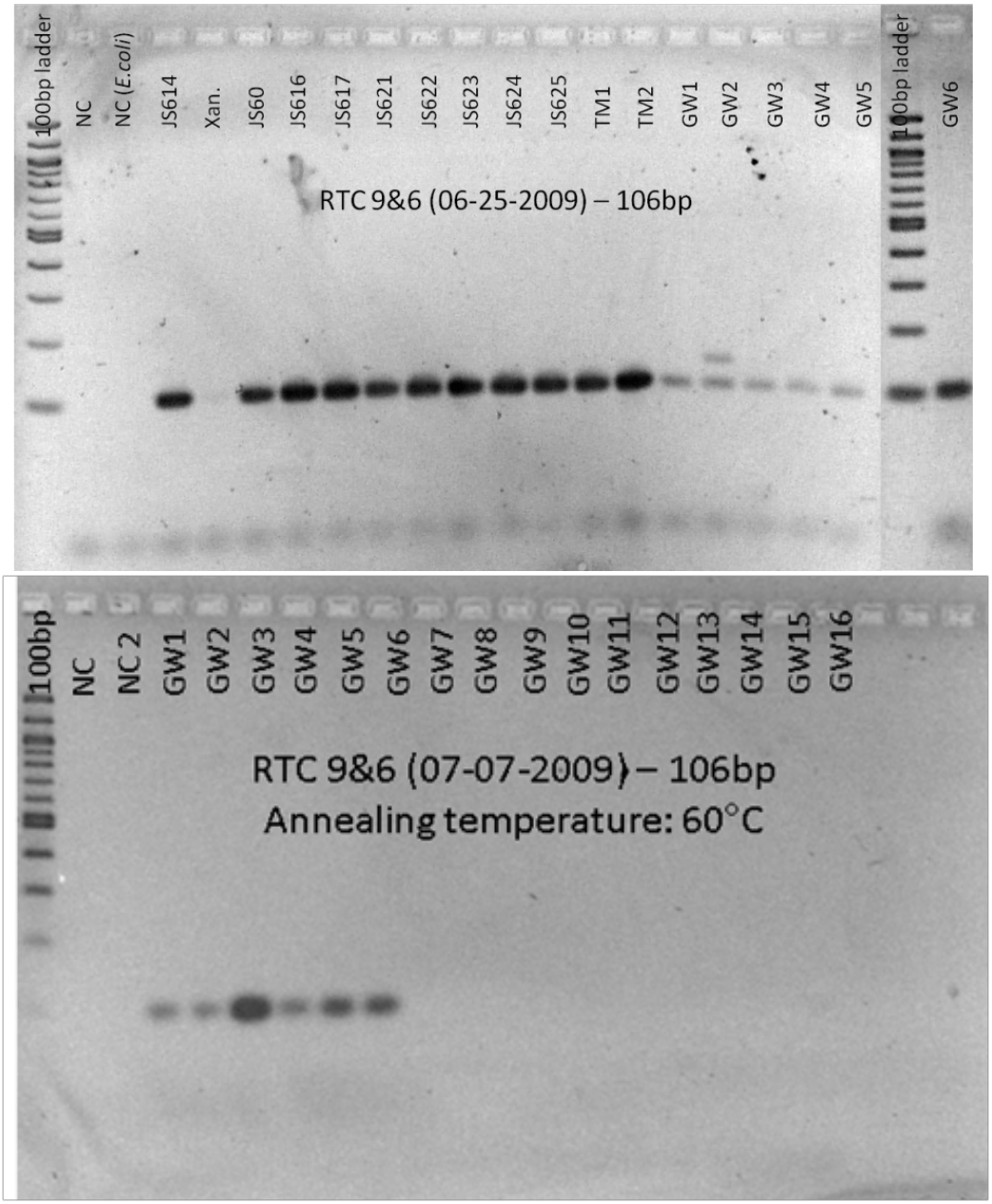

Figure 9. Specificity testing of the etnC primers RTC9 and RTC6 by standard PCR using DNA from pure cultures (*E.coli*, Xan. (propene-degrading Xanthobacter Py2), VC-assimilating strains JS614, JS60, JS616, JS617, JS621, TM1, TM2, etheneotrophic strains JS622, JS623, JS624, JS625, and 16 environmental samples (GW1-6 = Carver, MA samples; GW7-13 = Soldotna, AK samples; GW14-16 = NAS Oceana samples). The top gel image shows PCR products generated with a 55°C annealing temperature. At an annealing temperature of 60°C (bottom gel image), the larger incorrectly sized band disappears. However, no bands were observed initially in samples GW7-16, likely due to low target gene concentration. NC, NC2 = negative control (no template or E.coli template).

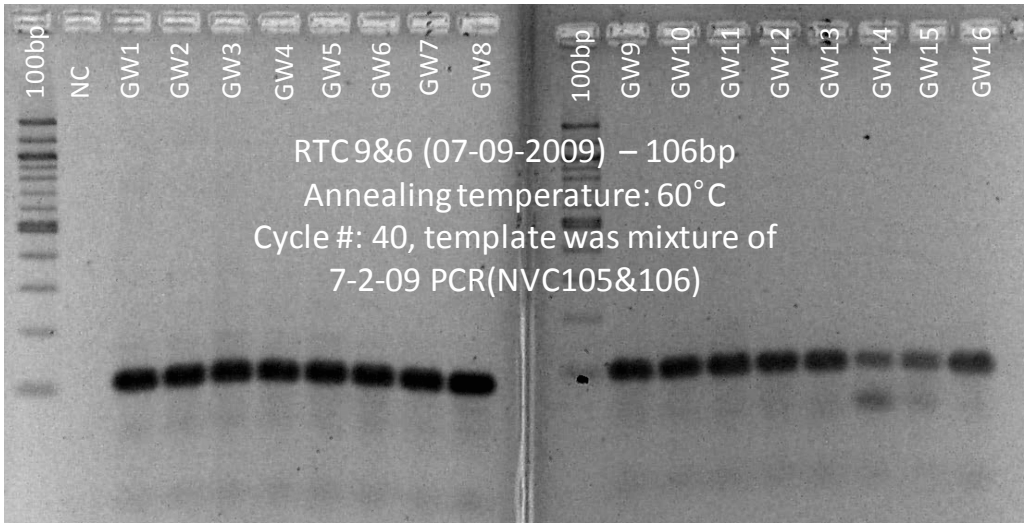

Figure 10**.** Results of a nested PCR experiment with *etnC* primers. The initial PCRs were carried out with environmental DNA and the primers NVC105 and NVC106 *(72)*. Then, 2 µl of each PCR was used as template in a second PCR with the RTC9 and RTC6 primer set. In all cases, a band of the expected size was noted, supporting the hypothesis that *etnC* concentrations were low in samples GW7-GW16. Note that GW1-6 = Carver, MA samples; GW7-13 = Soldotna, AK samples; GW14-16 = NAS Oceana samples. NC = negative control (no template).

Table 9**.** RTC PCR products sequencing results. Please refer to Table 1 and reference *(38)* for additional information about the pure cultures and clone sequences indicated in this table.

Sample	**Clone**	**Sequence Blast Results (% identity)**
RB46D (Carver, MA)	2	JS623 (100), NBB3 (95), NBB2 (95), NBB1 (95), E5-1 (95)
	3	JS623 (100), NBB3 (95), NBB2 (95), NBB1 (95), E5-1 (95)
	4	JS623 (100), NBB3 (95), NBB2 (95), NBB1 (95), E5-1 (95)
	5	JS623 (100), NBB3 (95), NBB2 (95), NBB1 (95), E5-1 (95)
	7	JS623 (100), NBB3 (95), NBB2 (95), NBB1 (95), E5-1 (95)
	8	JS623 (98), NBB3 (94), NBB2 (94), NBB1 (94), E5-1 (94)
	9	JS623 (100), NBB3 (95), NBB2 (95), NBB1 (95), E5-1 (95)
	10	JS623 (100), NBB3 (95), NBB2 (95), NBB1 (95), E5-1 (95)
	11	JS623 (100), NBB3 (95), NBB2 (95), NBB1 (95), E5-1 (95)
	13	JS623 (100), NBB2 (93), E5-1 (93), L10-1 (93), L10 (93)
MW20 (Soldotna, AK)	2	JS623 (97), NBB2 (92), E5-1 (92), L10-1 (92), L10 (92)
	3	JS623 (98), NBB2 (94), E5-1 (94), L10-1 (94), L10 (94)
	4	JS623 (98), NBB2 (93), E5-1 (93), L10-1 (93), L10 (93)
	9	RB73C09 (93), RB73C08 (93), RB73C07 (93), RB73C05 (93), RB73C02 (93)
	11	JS623 (100), NBB2 (95), E5-1 (95), L10-1 (95), L10 (95)
	13	JS60 (96), E1-1 (96), S20 (96), S19 (96), E1-5 (95)
	15	JS623 (98), NBB2 (93), E5-1 (93), L10-1 (93), L10 (93)
MW19 (NAS Oceana, VA)	3	JS623 (100), NBB3 (95), NBB2 (95), NBB1 (95), E5-1 (95)
	8	JS623 (99%), NBB2 (94), E5-1 (94), L10-1 (94), L10 (94)
	10	JS623 (100), NBB3 (95), NBB2 (95), NBB1 (95), E5-1 (95)
	16	JS623 (98), NBB2 (93), E5-1 (93), L10-1 (93), L10 (93)

We also investigated the specificity and diversity of *etnE* sequences amplified from Oceana, VA (MW19) and Soldotna, AK (MW20) groundwater samples using the RTE qPCR primer set (Table 10). Groundwater DNA was directly used for PCR templates using the primer specificity test conditions described previously. After PCR purification, ligation, and transformation, the products were sequenced. The actual product lengths were 150-152 bp (the expected product size was 151 bp). These 15 sequences were subjected to BLAST analysis using default search parameters (nucleotide blast). The top BLAST hits for 12 *etnE* sequences were 96-99% identical to *etnE* sequences from VC-assimilating strains JS623, JS622, and JS617, while one sequence was 97% identical to the ethene-assimilating *Mycobacterium* strain JS622 *etnE*, and one sequence was 97% identical to environmental *etnE* sequences RB63IE03, RB63IE02, and RB63IE01 retrieved from the Carver site during a previous study *(38)*. Like the *etnC* primer specificity experiments, all of the sequences retrieved during this experiment were specific products.

1.2.2 Melt curve analysis

Another approach to testing primer specificity during qPCR employing SYBR Green chemistry is the melt curve analysis. A melt-curve analysis is a quality assurance check that is performed by a real-time PCR instrument at the completion of the amplification stage. Following qPCR, the system will begin raising the temperature of the PCR mixture while measuring the rate of change in the fluorescence intensity. Because SYBR Green only binds double-stranded DNA, there will be a sharp rise followed by a sharp drop in the fluorescence intensity as the PCR product reaches its melting temperature and becomes single stranded. If the primers are specific, only one peak is expected. If there are multiple peaks then there are either non-specific PCR products or primer-dimers. Some representative melt-curves from qPCRs of environmental samples are shown in Figure 11, Figure 12 and Figure 13. In general, single peaks were most often observed, with the peak intensities of melt-curves generated from the RTE PCR products were stronger than those seen from RTC PCR products. In some instances, smaller peaks were observed in the RTE qPCRs at lower temperatures (Figure 12 and Figure 13). This suggests that a small amount of the SYBR green fluorescence could be attributed to primer dimer formation. However, we feel that these melt-curves are reasonable given the fact that we are analyzing environmental samples with relatively low target gene abundance. Further validation of the qPCR technique would involve additional analysis of the behavior of melt curves.

To date we have found no evidence that non-specific amplicons are produced with our qPCR primer sets, which increased our confidence in using SYBR Green as the real-time PCR chemistry for the remainder of this project.

Table 10**.** RTE PCR product sequencing results. Please refer to Table 1 and *(38)* for additional information about the pure cultures and clone sequences indicated in this table.

Site	**Clone**	**Sequence Blast Result (% identity)**
MW20 (Soldotna, AK)	1	JS623 (96), JS622 (94), JS61 (94), RB73E11 (92)
	2	JS621 (82), JS60 (82), *Ochrobactrum* sp. TD (82), *Pseudomonas putida* AJ (81)
	3	JS621 (99), JS60 (99), *Ochrobactrum* sp. TD (99), *Pseudomonas putida* AJ (98)
	4	JS621 (99), JS60 (99), *Ochrobactrum* sp. TD (99), *Pseudomonas putida* AJ (98)
	5	JS623 (96), JS622 (94), JS61 (95), RB73E11 (92)
	7	JS623 (97), JS622 (95), JS61 (95), RB73E11 (93)
	8	RB63IE03 (97), RB63IE02 (97), RB63IE01 (97), JS614 (93)
MW19 (NAS Oceana, VA)	2	JS623 (96), JS621 (94), JS61 (95), RB73E10
	3	JS623 (97), JS622 (96), JS61 (96), RB73E11 (94)
	4	JS622 (96), JS623 (93), JS61 (93), RB73E11(91)
	5	JS623 (98), JS622 (94), JS61 (95), RB73E11 (92)
	6	JS617 (97), JS625 (97), JS624 (97), JS619 (97)
	7	JS623 (98), JS622 (94), JS61 (95), RB73E11 (92)
	8	JS623 (96), JS622 (94), JS61 (94), RB73E11 (92)

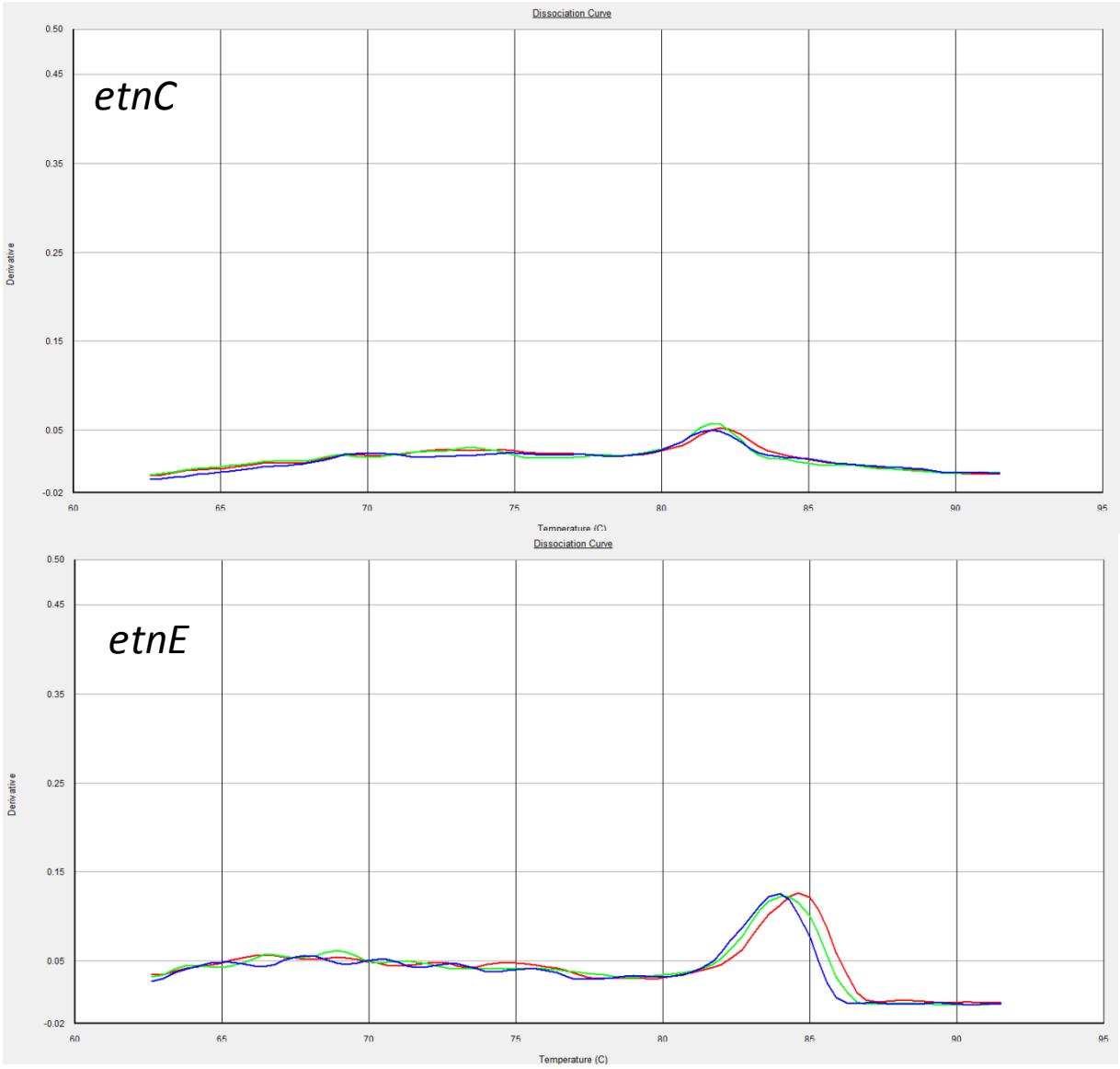

Figure 11. Melt-curve analysis (temperature vs. change in fluorescence intensity) of PCR products generated during qPCR analysis of DNA from Carver site well RB46D.

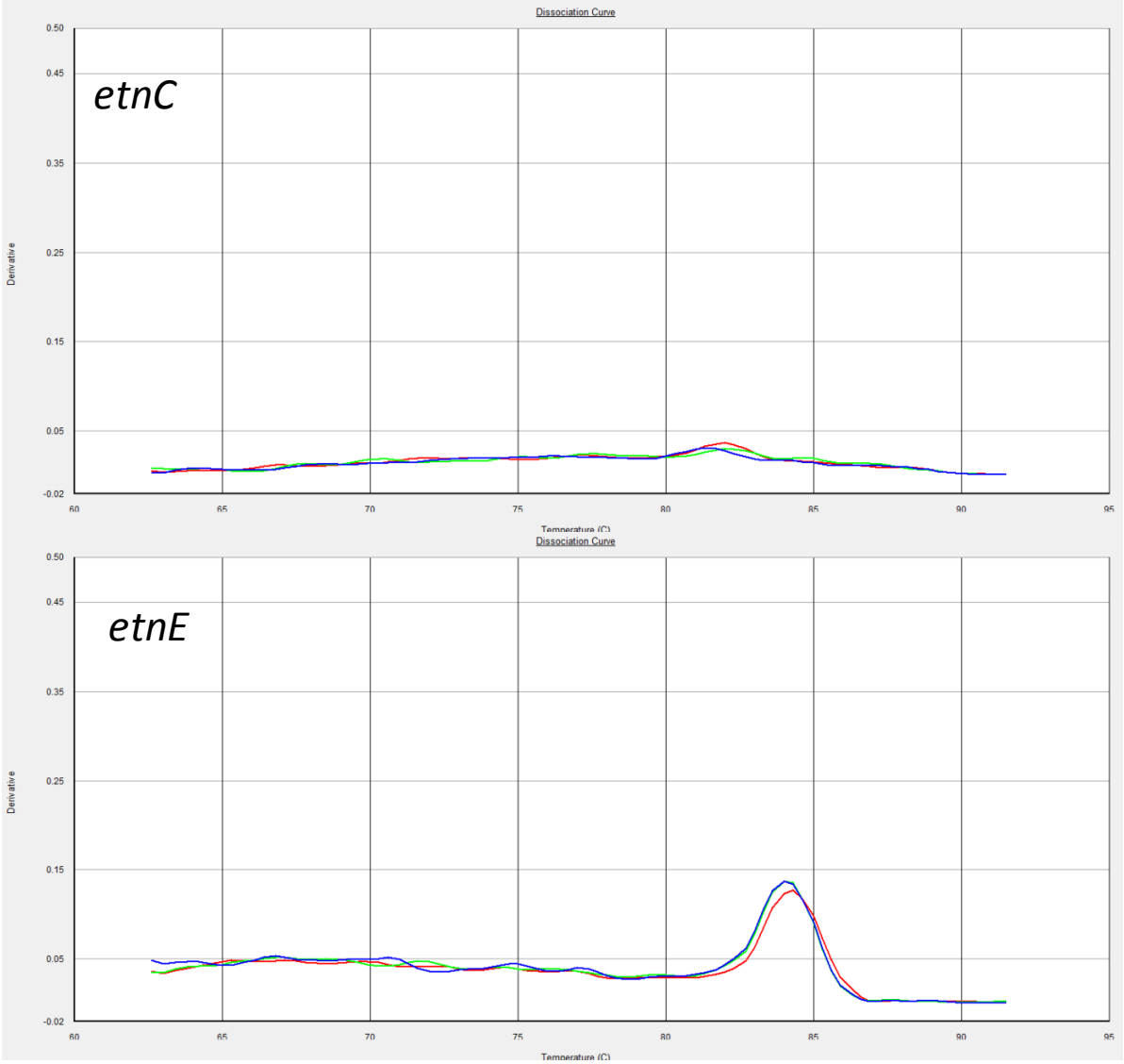

Figure 12. Melt-curve analysis (temperature vs. change in fluorescence intensity) of PCR products generated during qPCR analysis of DNA from NAS Oceana well MW25.

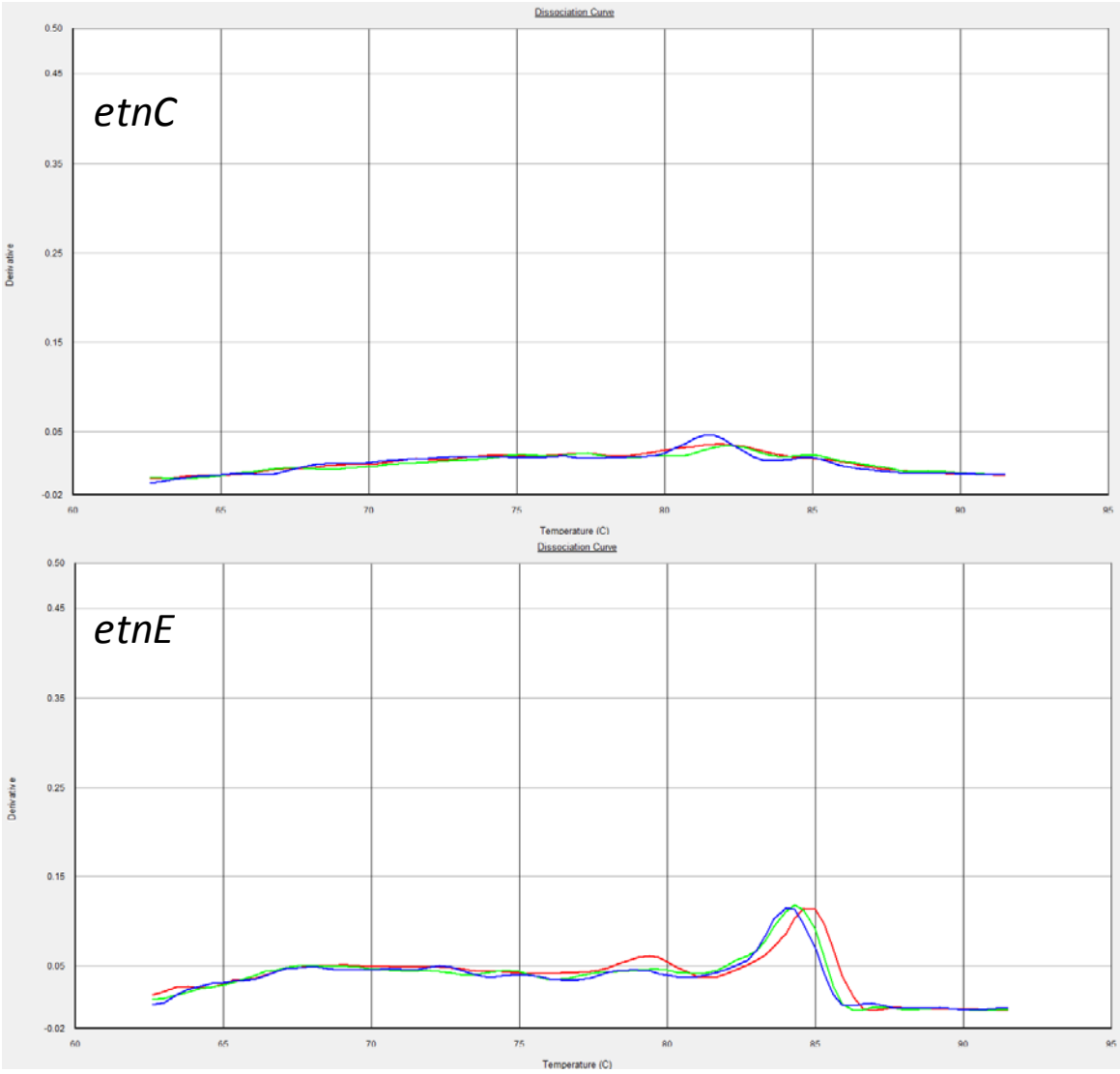

Figure 13. Melt-curve analysis (temperature vs. change in fluorescence intensity) of PCR products generated during qPCR analysis of DNA from Soldotna, AK well MW40.

When using the RTC and RTE primers in qPCR experiments with pure ethene-assimilating cultures (under the same conditions as described above) we noted that resulting *etnC/etnE* ratios were low (~0.1), when they were expected to be 0.5-2 (for example, the *etnC/etnE* ratio in *Nocardioides* JS614 is 0.5). Possible explanations for lower than expected *etnC/etnE* ratios are that *etnC* numbers are artificially low (due to primer bias) and/or that *etnE* numbers are artificially high (due to amplification of non-target sequences).

To further test primer specificity, we compared all possible primer combinations (16 for RTC and 128 for RTE) within the degenerate primers to GenBank with Primer-BLAST (www.ncbi.nlm.nih.gov/tools/primer-blast). Primer-BLAST indicated that none of the RTC primer combinations have unintended target sequences (data not shown), which suggests that these primers are highly specific to *etnC* sequences from known etheneotrophs and VC-assimilators. On the other hand, Primer-BLAST indicated three possible unintended RTE PCR products with expected sizes of 54 bp (*Vitis vinifera*, Genbank Acc. No. AM470838.2), 120 bp (*Chromohalobacter salexigens* peptidoglycan glycosyltransferase, Genbank Acc. No. CP000285.1), and 151 bp (*Rhodococcus rhodochrous* B-276 EaCoMT gene, Genbank Acc. No. AF426826.1). Generation of the 54 and 120 bp products is unlikely and can be excluded by melt-curve analysis. However, as the *etnE* from propene-oxidizing *Rhodococcus* B-276 is closely related to the *etnE* from VC-assimilating *Nocardioides* JS614, amplification of related sequences in groundwater DNA could occur.

Interestingly, all 16 RTC primer combinations returned 100% matches to target sequences, while only 3 RTE primer combinations did the same. Currently, there are 39 *etnC* and 23 *etnE* sequences in GenBank (and many of them are only partial sequences). Even though these primer combinations did not match target sequences 100%, we verified that PCR products of the correct size were generated with DNA from many pure cultures (as reported previously).

These Primer-BLAST results suggest that amplification of non-target sequences do not contribute to the low observed *etnC/etnE* ratios. Because a degenerate primer is actually a mixture of different primer sequences with variations at different locations on the oligonucleotide, it is possible that the degeneracies specified resulted in ineffective primer combinations when applied to DNA from pure cultures, thus leading to primer bias and erroneously low measured *etnC/etnE* ratios.

An alternative approach to developing degenerate primer sets entailed developing sequences specific to each target gene from each sequence in the database, identifying all the unique primer sequences (both forward and reverse), and then mixing the unique sequences together manually. This approach deviates from the typical degenerate primers design approach where a degenerate base is specified (e.g. a “K” indicates that a “G” or a “T” may be at that location). The typical procedure could result in primer combinations that are intended or even useful. Based on alignments of 39 *etnC* and 23 *etnE* sequences, we noted that 48 (8 forward x 6 reverse) different *etnC* primer combinations and 54 (6 forward x 9 reverse) different *etnE* primer combinations would represent all etheneotrophic *etnC* and *etnE* sequences currently in the database (Table 11). We named these new, “manually mixed” degenerate primers MRTC (for *etnC*) and MRTE (for *etnE*). Interestingly, this resulted in a more degenerate *etnC* primer set than our previously

described RTC primers (16 primer combinations) and a less degenerate primer set than our previously described RTE primers (128 primer combinations).

Primer-BLAST analysis of the MRTC and MRTE primers did not reveal any nonspecific MRTC PCR products. Primer-BLAST analysis did reveal that the MRTE primers could amplify EaCoMT genes from propene-assimilating bacteria, as determined previously for the RTE primers *(73)*.

We performed a laboratory analysis of the MRTC/MRTE primers (sequences in Table 11) to determine if they will facilitate more accurate estimation of *etnC/etnE* ratios in pure cultures than our previously described RTC/RTE primers. In these qPCRs, we used non-degenerate gene specific primers (GSPs) that were designed to amplify *etnE* or *etnC* from that strain's genomic DNA (Table 5). All qPCR conditions were the same as described previously, except for the GSP concentration (100 nM for each primer) and the template DNA concentration (1 ng per 25 μL reaction). Detailed qPCR parameters for this experiment are provided in Appendix B.

We quantified *etnC* and *etnE* abundance in four different pure cultures (VC- and ethene-assimilating strains JS60, JS614, JS617, and JS623) (Figure 14). Compared to gene abundance estimates with GSPs, gene abundance estimates with RTC primers were significantly different ($p<0.05$), while gene abundance estimates with RTE primers were not. The 2.7 fold (JS60) and 1.8 fold (JS623) deviation between *etnC/etnE* ratios estimated with GSPs and *etnC/etnE* ratios determined from genome sequences is currently not clear. Using MRTC primers results in a +46% (JS60), +21% (JS614), -32% (JS617), and +9% (JS623) deviation in estimated *etnC* abundance, and that using MRTE primers result in a +11% (JS60),+ 21% (JS614), 0% (JS617), and +2% (JS623) deviation in estimated *etnE* abundance, when compared to GSPs. Compared to gene abundance estimates with GSPs, gene abundance estimates with MRTC primers were significantly different ($p<0.05$) for only JS614 and JS623, while gene abundance estimates with MRTE primers were not.

Inspection of the genome sequences revealed that actual *etnC/etnE* ratios in the isolates studied are 1.0 (JS60), 0.5 (JS614), 2.0 (JS617), and 1.0 (JS623). Using GSPs, measured *etnC*/*etnE* ratios were 2.7 (JS60), 1.0 (JS614), 1.9 (JS617), and 1.8 (JS623). When using RTC and RTE primers, measured *etnC*/*etnE* ratios were 3.8 (JS60), 1.9 (JS614), 1.8 (JS617), and 2.6 (JS623). When using MRTC and MRTE primers, measured *etnC/etnE* ratios were 3.5 (JS60), 1.0 (JS614), 1.3 (JS617), and 2.0 (JS623).

Table 11. List of the “mixed real-time” (MRT) primers - a set of non-degenerate primers that account for all available *etnC* or *etnE* primer combinations at the same priming sites as the previously described “real-time” (RT) primers.

qPCR oligonucleotides (patent pending)	**Sequence (5′-3′)**	**Product size (bp)**	**Reference**
RTC_F (*etnC*)	ACCCTGGTCGGTGTKSTYTC	106	*(73)*
RTC_R (*etnC*)	TCATGTAMGAGCCGACGAAGTC		
RTE_F (*etnE*)	CAGAAYGGCTGYGACATYATCCA	151	*(73)*
RTE_R (*etnE*)	CSGGYGTRCCCGAGTAGTTWCC		
MRTC_F (*etnC*)	ACACTCGTCGGCGTTGTTTC ACCCTGGTCGGTGTGCTCTC ACGCTGGTCGGTGTTCTTTC GCTCTGGTCGGCGTTCTTTC ACTCTGGTCGGCGTTCTTTC ACCTTGGTTGGTGTGCTTTC ACCCTGGTCGGTGTGGTCTC ACCCTGGTCGGCGTGGTCTC	106	This study
MRTC_R (*etnC*)	TCATGTACGAGCCGACGAAGTC TCATGTAAGAGCCGACGAAGCC TCATGTAAGAGCCGACGAAGTC TCATGTAGGAGCCGACGAAGTC TCATGTAAGAACCGACGAAGTC TCATGTACGAACCGACGAAGTC		
MRTE_F (*etnE*)	CAGAATGGCTGTGACATTATCCA GACAACGGCTGCGACATCATCCA GACAACGGCTGCGACATCATTCA CAGAACGGCTGCGACATCATCCA CAGAACGGCTGCGACATCATTCA CAGAATGGTTGCGACATCATTCA	151	This study
MRTE_R (*etnE*)	CTGGTGTGCCGGAGTAGTTTCC CGGGTGTGCCGGAGTAGTTGCC CCGGCGTGCCGGAGTAGTTTCC CTGGTGTACCCGAGTAGTTTCC CGGGTGTGCCCGAGTAGTTTCC CGGGCGTGCCCGAGTAGTTTCC CCGGTGTACCCGAGTAGTTACC CCGGTGTACCCGCGTAGTTACC CCGGCGTACCTGAGTAGTTACC		

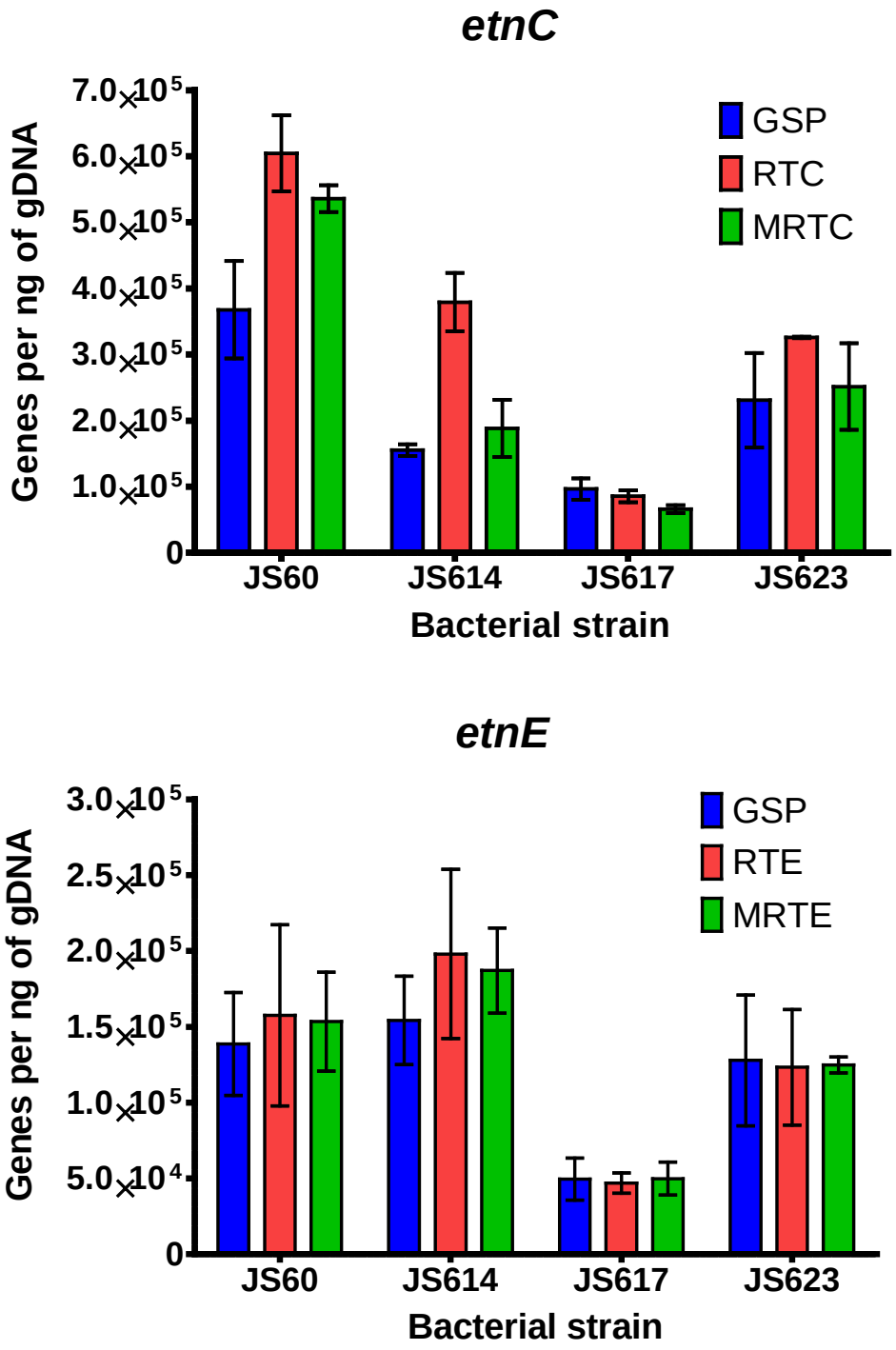

Figure 14**.** Comparison of *etnC* and *etnE* abundance (per ng of genomic DNA) in four different cultures (JS60, JS614, JS617, and JS623) estimated with non-degenerate GSPs and degenerate primer sets. Bar heights are the average of three analytical replicates and the error bars are the 95% confidence interval.

Subtask 1.3 Develop qPCR standard curves

The objectives of this subtask were to determine optimal primer concentrations, assess the performance of different standard templates (i.e. PCR products or plasmids), and determine if the resulting standard curve parameters are in the appropriate range for quantification. This is normally achieved by determining the PCR efficiency for the standard curve. The procedure for determining PCR efficiency begins with the preparation of 5 qPCRs containing defined template DNA (e.g. PCR product or plasmid) at a known concentration C_0 (and thus known gene abundance). Following real-time PCR, the data is analyzed at a particular fluorescence threshold. The cycle at which each real-time PCR curve crosses that threshold is designated the Ct for that particular sample or standard. Ct values are then plotted against the log of the template concentration (usually as gene copies). Performing a linear regression of the log C_0 vs. Ct data yields the slope and y-intercept of the regression line. If the PCR is 100% efficient over the range of samples (i.e. the template concentration exactly doubles after each amplification cycle), the slope of the regression line will be -3.32. Then PCR efficiency is calculated with the formula $E = (1-10^{(-1/slope)})$. However, achieving a 100% PCR efficiency is generally difficult due to experimental variability, so PCR efficiencies of 95-105% are generally considered acceptable for quantitation.

When using the qPCR primers we developed (called RTC and RTE for *etnC* and *etnE*, respectively) in regular PCRs with genomic DNA from VC-assimilating *Nocardioides* strain JS614, *Mycobacterium* strain JS60 and *Mycobacterium* strain JS623, partial *etnC* and *etnE* genes were amplified (expected sizes of PCR products are 106 bp and 151 bp for *etnC* and *etnE*, respectively), purified, cloned into the pDRIVE vector (Qiagen), and sequenced. The PCR products from strains JS60 and JS623 were as expected, but interestingly, the partial *etnE* from strain JS614 was 12 bp smaller than expected - a result that was repeated in two subsequent experiments. Our current hypothesis is that the RTE primer set did not anneal to the expected location. This result could be explained by the fact that there are two known *etnE* alleles in the JS614 genome *(74)*. However, most importantly, the target gene was amplified by the qPCR primers in all cases, and the plasmids generated were used for standard curve experiments.

Next, we determined optimal qPCR primer concentrations. The recommended primer concentration from the ABI system is 50-200 nM, but since we were working with degenerate PCR primers we screened a concentration range between 50-2,000 nM. We observed that amplification was not optimal when the qPCR primer concentration was less than 500 nM, but amplification significantly improved at primer concentrations of 750 nM and greater (for both RTC and RTE primers). At this primer concentration (750 nM) PCR product melting curves revealed one distinct peak, indicating that we had minimized the potential for primer dimers and non-specific amplicons. Therefore, we decided to use a primer concentration of 750 nM in future experiments. Initial qPCR standard curve experiments indicated that we can achieve R^2 values of 0.99, and that the standard curve dynamic range is 30-3,000,000 gene copies.

Standard curve parameters (i.e. slopes and Y-intercepts) derived when using plasmid templates containing genes cloned from strains JS60, JS614, and JS623 were initially highly variable when compared to each other. So, as an alternative strategy, we constructed standard curves by using PCR product templates. We first amplified *etnE* from JS60, JS623, and JS614 genomic DNA

with CoMF1L and CoMR2E primers (expected size 891 bp) *(16)*. We found the dynamic range of *etnE* standard curves using PCR product as template was 10-10,000,000 gene copies and that the slopes of the standards curve were very similar to the slopes observed with plasmid templates. Based on these favorable results, we elected to continue using PCR products as standard templates in all future experiments.

Next, we designed new *etnC* primer sets for VC-assimilating strains JS60 (product size 1043 bp), JS614 (product size 1138 bp), and JS623 (product size 1163 bp) (Table 5). These PCR products were used as templates to prepare qPCR standard curves. An initial comparison of these results indicated that JS60 PCR products had the best combination of dynamic range, R^2, and PCR efficiency (Table 12). Therefore, we decided to use JS60 *etnE* and *etnC* PCR products as template for all subsequent real-time PCR standard curves, at least during this phase of the project. Initially, we developed external standard curves with the intent of using an "inter-assay method" which means standards were developed on different plates than qPCR experiments with groundwater samples. However, after reading Smith, et al 2006, "Evaluation of quantitative polymerase chain reaction-bases approaches for determining gene copy and gene transcript numbers in environmental samples" *(75)*, we agreed that this practice could introduce additional variability in a procedure wrought with the potential for variability. To reduce potential error, we began using an "intra-assay method" which means that standard and groundwater samples were tested on same plate.

In later experiments, partial JS617 *etnC* sequences were generated with NVC105 and NVC106 primers for *etnC* (360 bp product) and partial *etnE* sequences were generated with CoMF1L and CoMR2E primers (891 bp product). Inter-assay (different plate) experiments were conducted, again in quintuplicate with BSA. The linear dynamic ranges were $5\text{-}3\times10^7$ for *etnC* primers (RTC) and $10\text{-}3\times10^7$ for *etnE* primers (RTE). The R^2 values for RTC and RTE were more than 0.99 and PCR efficiencies were 102.1% (RTC with Y-intercept 36.25) and 101% (RTE with Y-intercept 37.49). A comparison of these results suggested that using JS617 standards with BSA might be effective than using JS60 DNA as the standard template. However, the choice of standard template is probably somewhat arbitrary because there will be sequence diversity present in environmental samples. What appears to be more important is that the Y-intercepts of different standard curves should not vary significantly because this could lead to significant differences in gene abundance estimates.

1.3.1 Alleviation of potential PCR inhibition

We used this "inter-assay" standard curve approach with purified *etnC* (1043 bp) and *etnE* (891 bp) PCR products amplified from strain JS60 to test the effect of Bovine Serum Albumin (BSA) (400 ng/µL *(76)*) on PCR efficiency. We found that BSA had no effect on the linearity and dynamic range of the standard curves in triplicate experiments. When *etnC* primers were used, the PCR efficiency was 100% (without BSA) and 103% (with BSA), while the PCR efficiency was 100% in both the presence and absence of BSA when using the *etnE* qPCR primers. These results suggest that addition of BSA has little effect of qPCR standard curves and we plan to use BSA in all new qPCR experiments with DNA extracted from environmental samples.

Table 12. Inter-assay standard curve parameters for *etnC* (with RTC primers) and *etnE* (with RTE primers) using DNA template from *Mycobacterium* strain JS60, *Mycobacterium* strain JS623, and *Nocardioides* strain JS614. Data was collected in quintuplicate. BSA was not used in this experiment. The dynamic range is the range of gene copy numbers used in qPCR standards. The slope, R^2, and y-intercept were derived by a linear regression of log (initial gene copy numbers) vs. Ct data. Amplification efficiencies (AE) were calculated by the equation $10^{(-1/slope)} - 1$. Fluorescence thresholds were defined by manual operator adjustment in the Applied Biosystems Sequence Detection System software (version 1.2.3). These data represent the average of five replicates.

Strain	Primer set	Dynamic Range	Slope	R^2	Y-intercept	AE	Fluorescence threshold
JS60	RTC	$10 - 3\times10^7$	-3.1914	0.9996	36.0207	105.7	0.435
	RTE	$10 - 3\times10^7$	-3.3219	0.9984	35.7398	100.0	0.225
JS623	RTC	$10 - 3\times10^7$	-3.2473	0.9988	37.0559	103.2	0.7989
	RTE	$10 - 3\times10^7$	-3.2527	0.9986	36.8861	103.0	0.9878
JS614	RTC	$300 - 3\times10^7$	-3.3220	0.9968	41.9640	100.0	0.2285
	RTE	$30 - 3\times10^7$	-3.3220	0.9957	35.1315	100.0	0.1013

Note: PCR product dissociation curves revealed single peaks at melting temperatures of 81 - 84^{0}C, indicating that our qPCR primers were effective with each standard template.

1.3.2 Methanotroph qPCR

Another Subtask 1.3 objective was to develop a qPCR method for detecting the abundance and activity of methanotrophs in dilute VC groundwater plumes. Since methanotroph qPCR methods are not novel, we initially reviewed the scientific literature for qPCR primers targeting the methanotroph particulate methane monooxygenase (pMMO) functional genes. Particulate MMO was targeted because it is present in nearly all methanotrophs *(77)* and because methanotrophs can fortuitously degrade VC with pMMO. Thus, measuring levels of pMMO genomic DNA and mRNA in groundwater would allow for estimations of methanotroph abundance and activity. Initially, primers designed by Kolb et al *(51)*, which targeted the gene encoding the pMMO β-subunit (*pmoA*) were tested. However, reliable amplification of *pmoA* from pure culture methanotroph DNA using end point PCR techniques was not possible with these primers and thus, they were not used further. Experimental details that led us to this conclusion are described in Appendix A.

1.3.3 pmoA 178 and pmoA 330 Primer Validation

Other *pmoA* primers sets, pmoA 178 and pmoA 330, were discovered in the literature *(52)* and, though not specifically designed for qPCR, were rigorously evaluated to determine their usefulness in such assays. This was done by comparing *pmoA* abundance estimates against 16S rRNA abundance estimates with a set of 16S qPCR primers specific to Type I and Type II methanotrophs *(56)*. Since the copy numbers of PmoA and 16S rRNA genes are expected to be equal in pure methanotroph cultures, this comparison approach was deemed appropriate for qPCR primer validation. Prior to conducting this experiment, the primer concentrations and standard curve preparation techniques were optimized. The details of these experiments are described in Appendix A.

The primer validation experimental design entailed preparing mixtures of DNA from Type I and Type II methanotrophs. The 16S T1 and 16S T2 primer sets would then confirm the nature of the DNA mixtures and provide a basis for comparison with other qPCR primer sets, based on what we know about methanotrophs. The results of this experiment are shown in Table 13. As expected, when the amount of Type I methanotroph DNA decreased in each samples, so also did the 16S T1 quantifications (4.3×10^4 copies per ng DNA down to 0 copies per ng DNA). Likewise, as the amount of Type II methanotroph DNA increased in each samples, so also did the 16S T2 quantifications (0 copies per ng DNA up to 1.2×10^5 copies per ng DNA). These results demonstrated that 16S Type I and Type II primers were functioning as expected.

In comparison, pmoA 178 and 330 produced quantifications one to three orders of magnitude lower than the 16S primers. This was serious cause for concern because DNA extractions from environmental samples typically have low yields. As a result, to be able to detect methanotrophs in environmental samples, a primer set that can vigorously amplify from small quantities of DNA is necessary. Furthermore, the pmoA 178 primers seemed to be biased towards Type I methanotrophs. As the amount of Type I methanotroph DNA decreased in each sample, so also did the pmoA 178 quantifications (1.2×10^4 copies per ng DNA down to 2.0×10^2 copies per ng DNA). For both of these reasons, it was decided that neither the pmoA 178 nor the pmoA 330 were adequate primer sets for use in qPCR detection of methanotrophs.

Table 13. Average quantification results for known amounts of methanotrophic DNA amplified with 16S T1, 16S T2, pmoA 178, and pmoA 330 primer sets. The standard curve PCR efficiencies for the pmoA 178, pmoA 330, 16S T1, and 16S T2 primer sets were 95.8%, 94.5%, 95.5%, and 87.3%, respectively. The primer sets were used at 300 nM, 300 nM, 800 nM, and 200 nM, respectively (for more standard curve characteristics for this experiment, see Appendix A). Although the 16S T2 standard curve PCR efficiency is outside of the desirable range (95% to 105%) *(78)*, the most important issue raised by this experiment is the inefficient amplification of pure culture methanotroph template DNA by both pmoA primer sets. Dissociation curves for pmoA 178, pmoA 330, 16S T1, and 16S T2 qPCR assays can be found in Appendix A.

Sample	**16S T1**	**16S T2**	**pmoA 178**	**pmoA 330**
T1:T2	copies/ng DNA	copies/ng DNA	copies/ng DNA	copies/ng DNA
100 : 0	$4.3x10^4$	2	$1.2x10^3$	$6.8x10^2$
75 : 25	$3.0x10^4$	$8.7x10^4$	$1.3x10^3$	$3.4x10^2$
50 : 50	$2.1x10^4$	$1.4x10^5$	$9.3x10^2$	$2.5x10^2$
25 : 75	$1.1x10^4$	$1.4x10^5$	$6.2x10^2$	$1.9x10^2$
0 : 100	0	$1.2x10^5$	$2.1x10^2$	$1.0x10^2$

Note: Values represent the average of replicate measurements.

1.3.4 pmoA 472 and mmoX *Primer Validation*

Fortunately, a new set of *pmoA* qPCR primers (pmoA 472) in addition to a set qPCR primers (mmoX) that amplify a subunit of the soluble methane monooxygenase (sMMO) was located in the literature *(53, 54)*. We also located a qPCR primer set for universal detection of Bacteria *(55)*. These primer sets were used in a new validation experiment with the 16S T1 and T2 primer sets (Table 14). First, these results indicate that the *Methylocystis* sp. does not have *mmoX* (an sMMO gene). As the mass of *Methylocystis* DNA increased in each sample, the *mmoX* quantifications decreased from $1.3x10^5$ copies per ng DNA to 0 copies per ng DNA. This was confirmed by inspection of the recently published genome sequence of this strain *(79)*. The new pmoA 472 and mmoX primers did not produce the same quantification disparity as did the previous *pmoA* primer sets and were able to detect similar amounts of genomic DNA as the 16S T1 and T2 primers. In fact, the *pmoA* detection level was approximately 35% greater than the 16S T2 detection when the 100% T2 sample was probed (T2 ~ $8.8x10^5$ copies; pmoA ~ $1.2x10^6$ copies). This result could be explained by the fact that there are two copies of *pmoA* present in this methanotroph's genome. We concluded that both 16S primer sets and the *pmoA* primers were suitable for use evaluating environmental samples from contaminated groundwater.

With regard to the *mmoX* primers, it should be noted that there are two areas of concern. First, although the *mmoX* primers were able to produce significant levels of quantification, they were small when compared to the other primer sets. This could be explained by primer bias. Since only one species of methanotroph with the sMMO gene was used in these mixtures, if the primer set does not amplify that species well, then the quantifications will be lower. As mentioned before, this hypothesis would also need to be confirmed using lab experiments.

Table 14. Average quantification results for known amounts of methanotrophic DNA amplified using 16S T1, 16S T2, pmoA 472, and mmoX primer sets. Standard curves were constructed using the new pmoA 472, mmoX, and the 16S gene (16S U) primers. The primers were used at the same concentrations as stated in the original papers (300 nM for all) and were validated using the same technique as previously described. The standard curve PCR efficiencies for the pmoA 472, mmoX, 16S T1, and 16S T2 primer sets were 98.0%, 94.2%, 103%, and 101%, respectively (for more standard curve characteristics for this experiment, see Appendix A). Dissociation curves for pmoA 472, 16S T1, and 16S T2 qPCR assays can be found in Appendix A.

Dissociation curves for the mmoX experiment can be seen in Figure 16.

Sample T1:T2	**16S T1** copies/ng DNA	**16S T2** copies/ng DNA	**pmoA 472** copies/ng DNA	**mmoX** copies/ng DNA
100 : 0	$3.2x10^4$	0	$7.7x10^5$	$1.3x10^5$
75 : 25	$1.3x10^4$	$2.1x10^5$	$6.6x10^5$	$6.8x10^4$
50 : 50	$1.3x10^4$	$4.5x10^5$	$1.1x10^6$	$6.4x10^4$
25 : 75	$8.5x10^3$	$7.7x10^5$	$1.1x10^6$	$3.2x10^4$
0 : 100	3	$8.8x10^5$	$1.2x10^6$	0

Note: Values represent the average of replicate measurements.

Inspection of the *mmoX* dissociation curve showed two peak temperatures, 76.3°C and 85.8°C (Figure 16). Although the 76.3°C peak was much weaker than the 85.8°C peak, its presence implies possible primer-dimer artifacts or non-specific amplicons. Upon further inspection, it appeared that the 76.3°C peak only occurred in the dissociation curve related to the standard curve PCR products, while the dissociation curve associated with the Type I/Type II sample mixtures contained only the 85.8°C peak. Furthermore, it was observed that the no-template control contained only the 76.3°C peak. Since the no-template control is void of genetic material that would produce non-specific amplification, this peak implies a primer-dimer artifact. To confirm this suspected caveat, PCR products from these reactions should be gel analyzed and sequenced. Despite this, evaluation of environmental samples using the *mmoX* primers proceeded with caution. Additional details of the pmoA 472 and mmoX validation experiments are listed in Appendix A and shown in Figure 15 and Figure 16.

1.3.5 16S T1, T2 and Universal primer validation

Finally, the 16S T1 and 16S T2 primer sets were validated using the 16S universal qPCR primers and the same technique as previously stated. This showed that the 16S T2 primer quantifications matched well with the 16S U quantifications (Table 15). This shows that the 16S T2 primers are efficiently amplifying the methanotroph DNA. However, the 16S T1 primer set was producing much smaller quantifications than the 16S U. This suggests that the primer set is biased against the species of methanotroph that we have used in these mixtures. Additional details of the 16S T1 and T2 validation experiments are listed in Appendix A and shown in Figure 17.

The overall results from the pmoA 472, mmoX, 16S T1, 16S T2, and 16 U validation experiments suggest that the mmoX and 16S T1 primer sets can be used with caution until they can be further validated. However, quantifying environmental DNA with several sets of primers would be of benefit. Therefore, these five primer sets used to evaluate environmental samples from contaminated groundwater as further described under Subtask 1.4.

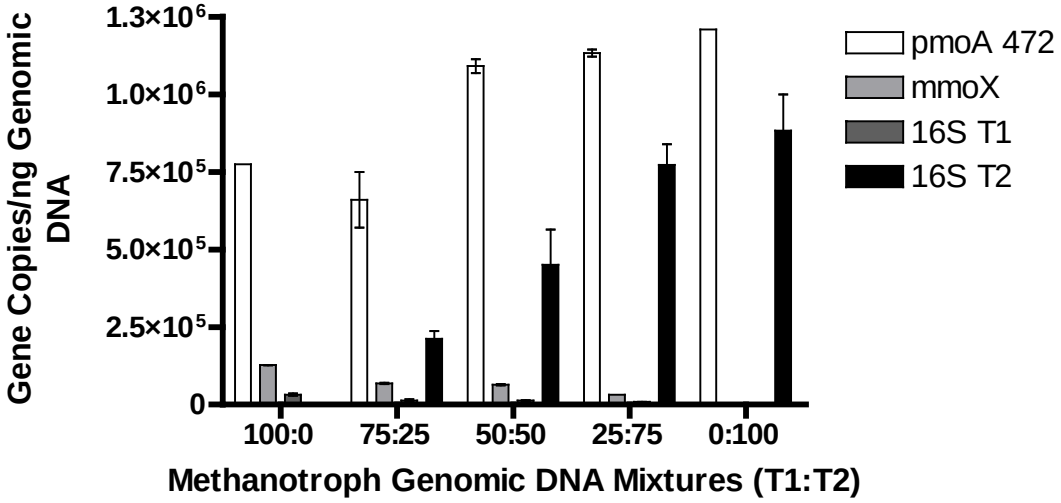

Figure 15. Comparison of average quantifications between pmoA 472, mmoX, 16S T1, and 16S T2 primer sets amplifying known amounts of genomic DNA. Type I DNA was extracted from *Methylococcus capsulatus* pure culture. Type II DNA was extracted from *Methylocystis* sp. strain Rockwell. The bar heights for each sample are the average of replicate measurements and error bars represent the range of data.

Table 15. Average quantification results for known amounts of methanotrophic DNA amplified using 16S T1, 16S T2, and 16S U primer sets. The standard curve PCR efficiencies for the 16S T1, 16S T2, and 16S U primer sets were 101%, 99.2%, and 102%, respectively. The primer sets were used at 800 nM, 200 nM, and 300 nM, respectively (for all standard curve characteristics for this experiment, see Appendix A). Dissociation curves for the 16S T1, 16S T2, and 16S U primer assays can be found in Appendix A.

Sample T1:T2	**16S T1** copies/ng DNA	**16S T2** copies/ng DNA	**16S U** copies/ng DNA
100 : 0	6.0×10^4	0	9.7×10^5
75 : 25	2.3×10^4	1.6×10^5	6.9×10^5
50 : 50	1.7×10^4	4.1×10^5	6.5×10^5
25 : 75	1.2×10^4	6.9×10^5	1.0×10^6
0 : 100	1	9.5×10^5	9.5×10^5

Note: Values represent the average of replicate measurements.

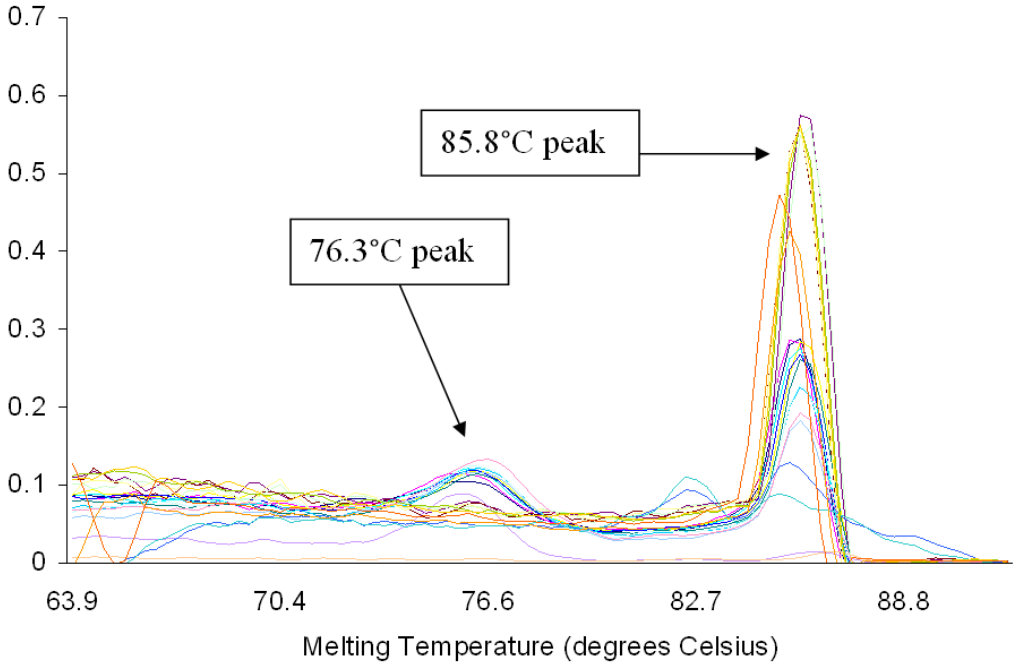

Figure 16. Dissociation curve for *mmoX* primer set amplifying *Methylococcus* sp. (Type I) and *Methylocystis* sp. (Type II). Multiple peaks were observed, implying primer-dimer artifacts or non-specific amplification.

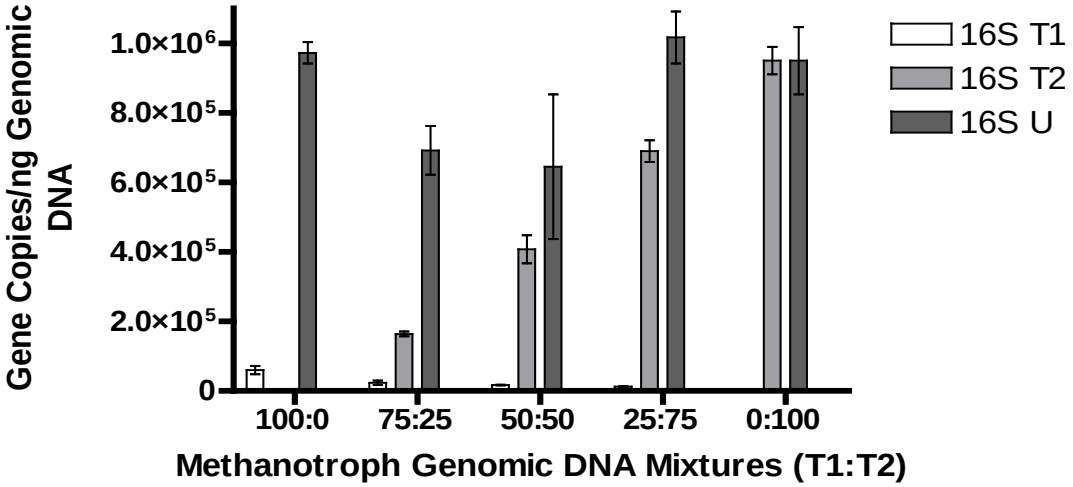

Figure 17. Comparison of average quantifications between 16S T1, 16S T2 and 16S U primer sets amplifying known amounts of genomic DNA. Type I DNA was extracted from *Methylococcus capsulatus* pure culture. Type II DNA was extracted from *Methylocystis* sp. strain Rockwell. The bar heights for each sample are the average of replicate measurements and error bars represent the range of data.

Subtask 1.4 Testing qPCR primer sets on environmental samples

1.4.1 Assessment of PCR inhibition potential

Based on the positive results of subtasks 1.1, 1.2, and 1.3 we proceeded to subtask 1.4, where the goal was to begin quantifying functional gene abundance in environmental samples. PCR inhibition is an important issue to address when working with environmental samples. Preliminary inhibition tests were done by constructing several serial dilutions of template DNA (i.e. dilution factors of 2, 6, 18, 54, 162, and 486) and then performing qPCR with our RTC (*etnC*) and RTE (*etnE*) qPCR primer sets. Our hypothesis was that if PCR inhibitors are present, then they will become less effective with serial dilution of the template. If the amplification efficiency from environmental samples is in the range of inter-assay standard curve PCR efficiency (95-105%), we could safely conclude that PCR inhibitors are not present at a significant concentration in the DNA extracts.

When using the RTC primer for PCR inhibition tests, two samples (MW18 and MW19 from NAS Oceana, VA) were in the appropriate efficiency range (95-105%), but amplification efficiencies of 66-173% were noted in the rest of the samples. On the other hand, all PCR inhibition tests with the RTE primer set showed PCR efficiencies far from the desired range. Only one sample (RB64I Carver, MA) had an efficiency near the desired range (117%). In some cases (e.g. MW9, MW20 from Soldotna, AK and MW25 from NAS Oceana, VA), Ct values were very similar regardless of dilution. Initial experiments involving a dilution suggested that PCR inhibitors were present in many of the groundwater DNA samples, even though the DNA extraction method employed is designed to remove PCR inhibitors.

A comprehensive PCR inhibition test was performed using two groundwater samples from Carver, MA (RB46D, RB64I), two samples from Soldotna, AK (MW6, MW40), and three samples from NAS Oceana, VA (MW18, MW19, MW25. The goal was to compare the amplification efficiency and R^2 of each set of dilutions in the presence and absence of BSA, a known alleviator of PCR inhibition *(49)*. These results (Table 16) led us to modify our qPCR protocol to include BSA at all times.

1.4.2 Testing the RTC and RTE primer sets on environmental samples

With this modified protocol, quantification of *etnC* and *etnE* was performed, in triplicate on any qPCR plate, using groundwater DNA template extracted from filter samples taken from six different wells at three different sites (Table 17). In an attempt to minimize analytical variability, we only quantified gene copies from environmental samples against standards included on the same assay plate (i.e. intra-assay standards) rather than from an external (inter-assay) standard curve as advised in a previous study *(80)*. Despite this, we occasionally observed significant variability in triplicate qPCR assays on the same plate (up to 45% (*etnC*) and 15% (*etnE*) (Table 18).

Because we used SYBR Green chemistry, dissociation curves were generated after qPCR to assess amplification quality. In general, dissociation curves of PCR products amplified from groundwater DNA templates displayed single peaks with melting temperatures near those observed in the standards. However, in contrast to the standard, additional minor peaks were

often observed (data not shown). We also observed that when using RTC primers, the resulting dissociation curve peak intensities were lower than that with RTE. Despite these observations, the dissociation curves did not indicate any significant formation of primer dimers and non-specific amplicons. Additional details concerning the amount of groundwater sampled, DNA yield and gene abundance per reaction are provided in Table 18.

Comparing *etnC* and *etnE* abundance in samples with VC and ethene concentrations in groundwater at the time of sampling suggests that *etnC* and *etnE* abundance is elevated in samples where VC and ethene concentrations were also higher (Table 17). However, more qPCR data from environmental samples is required before firm conclusions can be drawn about the relationships between *etnC* and *etnE* abundance and VC and ethene concentrations.

Measuring both *etnC* and *etnE* abundance in environmental samples also allowed us to estimate the *etnE/etnC* ratio, which ranged from 1.1 to 17.8. This ratio is 2 in *Nocardioides* strain JS614 *(17, 74)*, and range from 0.5 to 1.0 in other VC- and ethene-assimilating Mycobacteria, as noted in this report. Other possible explanations for high *etnE/etnC* ratios in environmental samples include primer bias and amplification of *etnE* sequences from propene-assimilating bacteria. For instance, a high *etnE/etnC* ratio could result if the RTC primers were biased against *etnC* sequences present in these samples. Conversely, amplification of *etnE* from propene-assimilating bacteria would lead to an overestimation of *etnE* abundance in comparison to *etnC* abundance. Primer-BLAST analysis of the RTE primers suggests that *etnE* sequences related to those found in propene-assimilating *Rhodococcus* strain B-276 could be amplified. This is not unexpected as the deduced EtnE in strain B-276 shares 83% amino acid identity to the deduced EtnE in VC-assimilating *Nocardioides* strain JS614 *(17)*.

Overall, these qPCR results presented here clearly indicate the potential for aerobic degradation of VC in and around monitoring wells at each of the three sites studied. This qPCR assay will facilitate detailed studies of microbial community functionality at VC-contaminated sites and help determine if the abundance of these functional genes is correlated with measured VC degradation rates. For example, an increase in *etnC* and/or *etnE* abundance in the same well over a relevant time series would suggest that natural attenuation of VC is occurring somewhere in the vicinity of that well's zone of influence. Ideally, these approaches will be conducted with mRNA extracted from environmental samples to reveal gene expression levels and provide stronger evidence of metabolic functionality (addressed during Task 2).

Table 16. Effect of BSA addition (400 ng/µL) on amplification efficiencies (AE) in six different groundwater DNA extracts. The RTC and RTE primer sets were used. Template DNA was diluted by 5X, 10X, 20X, and 40X for the purpose of estimating standard curve linearity (via R^2 from a linear regression analysis) and amplification efficiencies (via analysis of the slope of the regression line). Amplification efficiencies were calculated by plotting log (dilution) vs. Ct, determining the slope of a linear regression line with the data, and using the equation: $10^{(-1/slope)} - 1$.

Site	Well	Primer set	AE (%)	
			No BSA	BSA added
Carver, MA	RB46D	RTC	139.8	91.9
		RTE	104.4	106.5
	RB64I	RTC	122.3	101.6
		RTE	139.1	110.4
Soldotna, AK	MW6	RTC	179.2	84.5
		RTE	119.0	93.4
	MW40	RTC	6091.5	81.4
		RTE	266.8	123808.9
NAS Oceana, VA	MW18	RTC	80.3	89
		RTE	181.4	120.8
	MW25	RTC	201.4	85.8
		RTE	113.6	99.6

Table 17. Abundance of *etnC* and *etnE* in groundwater samples collected from monitoring wells at three VC-contaminated sites. DNA from single Sterivex filter samples was extracted and analyzed from each well. The number of gene copies reported for each sample is the average of three analytical replicates ± the standard deviation. The lowest C_t values in the no template controls (NTCs) were 35.7 (*etnC*) and 35.2 (*etnE*).)). Intra-assay standard PCR efficiencies were 105.5% when using *etnC* primers (-slope = 3.21, R^2 = 0.999; Y-intercept = 38.55, threshold = 0.21) and 100.0% when using *etnE* primers (-slope = 3.32, R^2 = 0.998; Y-intercept = 38.53, threshold = 0.24). Using these intra-assay standard curves, along with template DNA concentrations (ng/µL), groundwater sample volume (L), and mass (ng) of DNA per L of groundwater, we calculated *etnC* and *etnE* gene copies per liter of groundwater. Additional detail concerning sampling, DNA extraction, and analysis of gene copy abundance is provided in Table 18.

Site (sampling date)	Well	VC (µg/L)[a]	Ethene (µg/L)[a]	Gene copies/L of groundwater[b]	
				etnC	*etnE*
Carver, MA (09/29/2009)	RB46D	3.9	1.4	$7.0\times10^3\pm2.0\times10^3$	$1.2\times10^5\pm1.4\times10^4$
	RB64I	BDL	BDL	$1.6\times10^3\pm1.1\times10^2$	$1.9\times10^4\pm2.9\times10^3$
Soldotna, AK (05/06/2009)	MW6	9.6	50	$3.5\times10^4\pm 1.6\times10^3$	$6.3\times10^5\pm2.9\times10^3$
	MW40	9.4	72	$1.0\times10^5\pm3.5\times10^3$	$1.6\times10^5\pm4.2\times10^3$
NAS Oceana,VA (08/05/2009)	MW18	0.8	BDL	$3.8\times10^3\pm1.7\times10^3$	$4.3\times10^3\pm5.2\times10^2$
	MW25	46	BDL	$1.9\times10^3\pm4.6\times10^2$	$2.4\times10^4\pm9.3\times10^2$

[a]These values were obtained via personal communication from Sam Fogel, Bioremediation Consulting, Inc. (Carver), the May 2009 Groundwater Monitoring Report, River Terrace RV Park, Soldotna, AK, Alaska Department of Environmental Conservation, and the 2009 Long Term Monitoring Report for SMWUs 2B, 2C, and 2E, NAS Oceana, Virginia Beach, VA, CH2MHill. BDL: Below detection limit.

[b]The number of gene copies per liter of groundwater was calculated via this formula:

$$\frac{\textbf{Gene copies}}{\textbf{L of groundwater}} = \left(\frac{70\ \mu\text{L DNA per filter}}{\text{ng DNA per filter}}\right)\left(\frac{\text{reaction}}{2\ \mu\text{L DNA}}\right)\left(\frac{\text{Gene copies}}{\text{reaction}}\right)(\text{ng DNA per L of groundwater})$$

Table 18. Additional information concerning sampling, DNA extraction, and analysis of gene copy abundance in environmental samples. DNA extracted from each filter was eluted with 70 µL buffer as described in the materials and methods.

Site (sampling date)	Well	Volume GW filtered (L)	DNA yield from filter (ng)	DNA yield (ng/L GW)	Gene copies per reaction		Std. Dev./ Mean (%)	
					etnC	*etnE*	*etnC*	*etnE*
Carver, MA	RB46D	3.0	546	182	604±179	10,410±1,226	30	12
	RB64I	3.0	138.3	46	138±9	1,590±245	7	15
Soldotna, AK	MW6	0.26	2,688	10,338	263±12	4,677±214	5	5
	MW40	0.7	579.6	8,280	201±7	323±8	3	3
NAS Oceana, VA	MW18	2.0	151.2	76	216±98	248±30	45	12
	MW25	2.4	1,778	741	132±33	1,617±64	25	4

1.4.3 Testing the MRTC and MRTE primer sets on environmental samples

To further validate the degenerate MRTC and MRTE primer sets (first described in the Subtask 1.2 section), *etnC* and *etnE* quantification was conducted with groundwater DNA described previously (for comparative purposes). Functional gene abundance estimates with MRTC and MRTE primers (expressed as gene copies per liter of groundwater) were 9-149 times (*etnC*) and 1-8 times (*etnE*) greater than those previously estimated with RTC and RTE primers (Table 19). In addition, *etnC*/*etnE* ratios estimated with MRTC and MRTE primers were 0.8 - 2.6 with the exception of MW40 (8.1) and MW25 (5.1). Post amplification melt curve analysis indicated no evidence of non-specific products (data not shown). These suggest that 4 viable sets of degenerate qPCR primers are available for use with environmental samples, and that the MRTC/MRTE primer sets may have some advantages over the original RTC/RTE primer sets.

Table 19. Comparison of estimated abundance of *etnC* and *etnE* in groundwater samples collected from monitoring wells at three VC-contaminated sites using two different degenerate primer sets. PCR efficiencies of the standard curves in this experiment were 105.0% (MRTC) and 108.1% (MRTE) with R^2>0.99. The linear dynamic range of the MRTC and MRTE standards were 100-3×10^7. Primer concentrations used: 800 µM for MRTC_F, 600 µM for MRTC_R, 600 µM for MRTE_F, and 900 µM for MRTE_R.

Site	Well	Gene copies/L of groundwater with RTC/RTE		Gene copies/L of groundwater with MRTC/MRTE		MRTC /RTC	MRTE /RTE
		etnC	*etnE*	*etnC*	*etnE*	*etnC*	*etnE*
Carver, MA	RB46D	7.0×10^3	1.2×10^5	2.3×10^5	8.8×10^4	33	1
	RB64I	2.0×10^3	1.9×10^4	5.0×10^4	4.3×10^4	31	2
Soldotna, AK	MW6	3.5×10^4	6.3×10^5	9.5×10^5	1.2×10^6	27	2
	MW40	1.0×10^5	1.6×10^5	2.0×10^6	2.4×10^5	20	2
NAS Oceana, MA	MW18	4.0×10^3	4.0×10^3	3.6×10^4	3.6×10^4	9	8
	MW25	2.0×10^3	2.4×10^4	2.9×10^5	5.6×10^4	149	2

1.4.4 Methanotroph qPCR in Environmental Samples

Soldotna, AK

Community DNA extracted from Soldotna groundwater samples (Site map – Figure 3) was assayed for the presence of methanotrophs (i.e. for *pmoA* and *mmoX* abundance) (Table 20). Each of the wells tested contained detectable amount of both genes, although in some wells estimated gene abundance was both above and below the dynamic range of the standard curves. Monitoring well 40 (MW40), which is located in an area considered to be favorable for reductive dechlorination, experienced a 99% decrease in gene abundance; down from $3.9x10^7$ copies/L groundwater (copies/LGW) to $1.7x10^5$ copies/LGW. Specific geochemical data for this well illustrated a decrease in both VC (20.7 μg/L to 9.4 μg/L) and methane (12,400 μg/L to 4,380 μg/L) from 2008 to 2009, and the presence of ethene (90 μg/L and 72 μg/L) at both time points *(81)*. Even though some oxygen was present in the well (~1.29 mg/l in 2008), the qPCR data do not suggest that the drop in methane was due to methane oxidation by methanotrophs. Rather, it suggests that the surrounding aquifer was anaerobic, but that methane production in the vicinity of that well decreased during the time period studied. However, we should stress that because there are very few groundwater and geochemical samples being considered, we are speculating and cannot draw any definitive conclusions, or links, between the specific geochemical data and the qPCR gene abundance results.

Regarding MW6, although quantifications at both time points were within the same order of magnitude, MW 6, which is located on an aerobic/anaerobic boundary, experienced an increase in the *pmoA* gene abundance by 438%. From 2008 to 2009, *pmoA* gene abundance in MW 6 increased from $1.6x10^4$ copies/LGW to $6.3x10^4$ copies/LGW. The DO in the well was 0.35 mg/L in 2008. During the same time period, a steady presence of VC (8.89 μg/L to 9.64 μg/L), and methane and ethene concentrations of 7,650 μg/L and 50 μg/L, respectively were observed. Collectively, the qPCR results would seem to fit with the geochemical data trends in this well, which indicate MW6 to be near an aerobic/anaerobic interface. These aerobic/anaerobic interfaces are thought to be conducive to methanotrophic VC oxidation, because they are likely to contain ample amounts of methane and O_2.

For the *mmoX* gene, from 2008 to 2009, MW 6 and MW 40 experienced a 170% increase ($1.5x10^3$ copies/LGW to $2.6x10^3$ copies/LGW) and a 52% decrease ($2.0x10^5$ copies/LGW to $9.7x10^4$ copies/LGW) in gene abundance, respectively. As previously stated, these results coincide with the overall trends of these wells; however, it is extremely difficult to draw any definitive conclusions, or links, between the specific geochemical data and the qPCR gene abundance results. Full results for Soldotna are displayed in Table 20, Figure 18, Figure 19, Figure 20, and Figure 21. In addition to geochemical data, Soldotna results were also compared to data from a tracer study conducted at the site. Real-time PCR results coincide with the tracer study, which demonstrated DCE and VC were being oxidized to CO_2 near MW 6 *(81, 82)*. The presence of *pmoA* and *mmoX* genes in these wells could indicate that methanotrophs producing pMMO and sMMO enzymes are responsible for the oxidative degradation of VC.

With regard to the mmoX dissociation curve, results showed the presence of the standard-curve double peak that was previously mentioned; however, in this instance the 76°C peak was much larger than those observed in the previous experiment (Figure 22). The presence of this

suspected primer-dimer artifact in the standard curve would falsely elevate the fluorescence in these wells, ultimately leading to decreased sample quantification. The environmental sample melt curve contained a single peak at the 86°C (Figure 23).

Table 20. Average methanotroph gene abundance at the Soldotna, Alaska contaminated site. Standard curve PCR efficiencies for each primer set were 101 % and 97.6 %, respectively (for more standard curve characteristics, see Appendix A. Dissociation curves for the pmoA 472 primer assays can also be found in Appendix A.

Monitoring Well	***pmoA 472***		***mmoX***	
	2008	**2009**	**2008**	**2009**
	copies/L groundwater		copies/L groundwater	
MW 6	$1.6x10^4$	$6.3x10^4$	$1.5x10^3$ **	$2.6x10^3$ **
MW 40	$3.9x10^7$ *	$1.7x10^5$	$2.0x10^5$	$9.7x10^4$

Note: Samples marked with "**" were detected at quantities below the dynamic range of the standard curve (100 copies/reaction). Samples marked with "*" were detected at quantities above the dynamic range of the standard curve ($1.0x10^5$ copies/reaction).

Note: Each sample was run in duplicate.

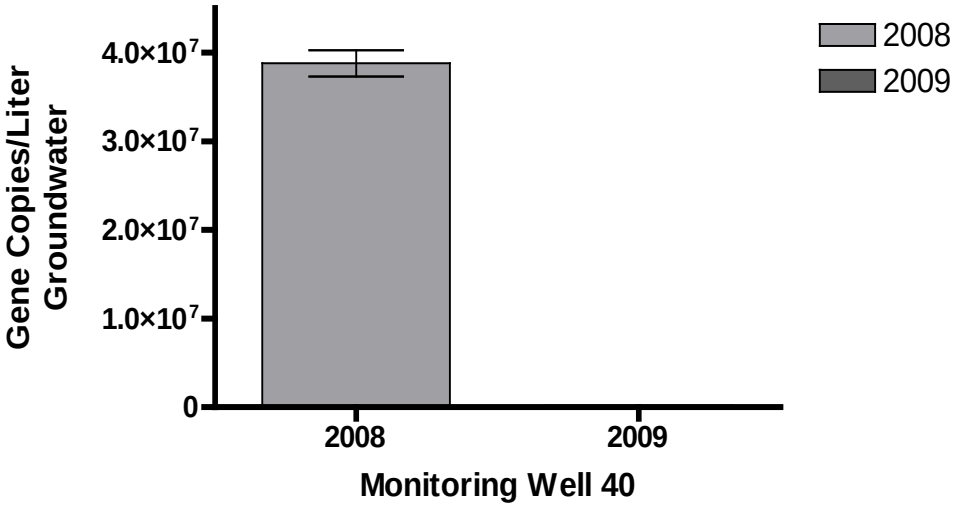

Figure 18. Change in average *pmoA* gene abundance in contaminated groundwater from MW 40 in Soldotna, AK. The bar heights for each sample are the average of replicate measurements and error bars represent the range of data.

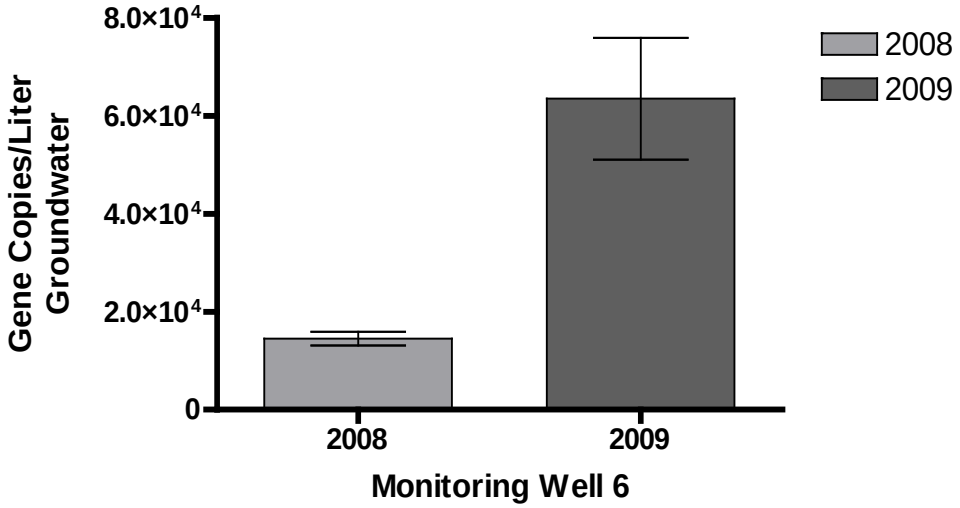

Figure 19. Change in average *pmoA* gene abundance in contaminated groundwater from MW 6 in Soldotna, AK. The bar heights for each sample are the average of replicate measurements and error bars represent the range of data.

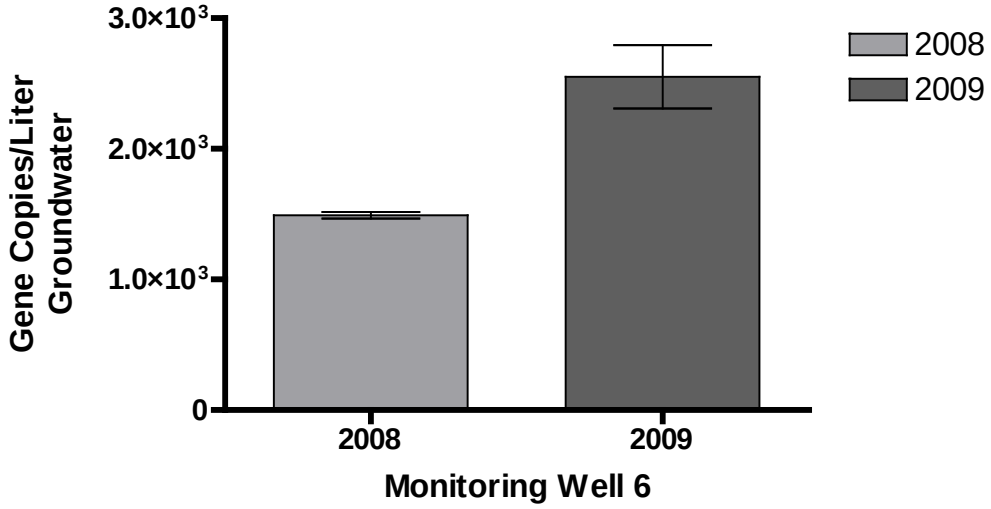

Figure 20. Change in average *mmoX* gene abundance in contaminated groundwater from MW 6 in Soldotna, AK. The bar heights for each sample are the average of replicate measurements and error bars represent the range of data.

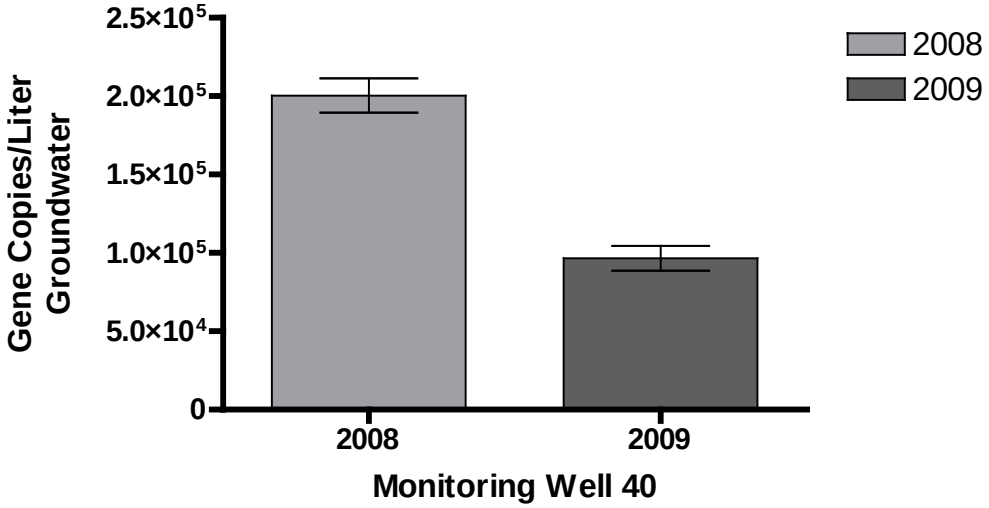

Figure 21. Change in average *mmoX* gene abundance in contaminated groundwater from MW 40 in Soldotna, AK. The bar heights for each sample are the average of replicate measurements and error bars represent the range of data.

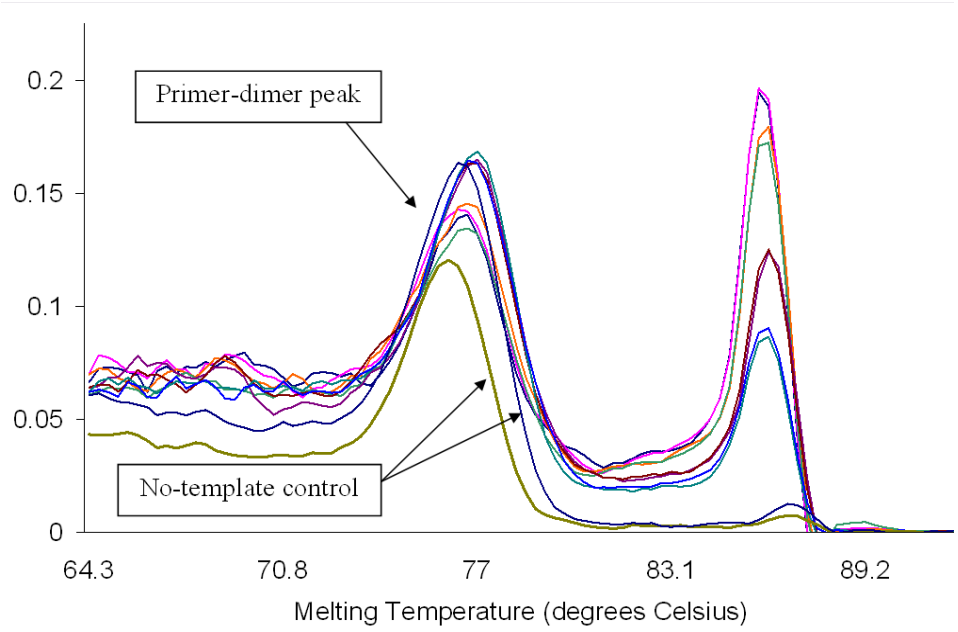

Figure 22. Dissociation curve for *mmoX* primer set standard curve. Multiple peaks were observed and appear to be primer-dimer artifacts since the no-template control contains only one peak quantification. The environmental sample melt curve contained a single peak at the 86°C (Figure 23).

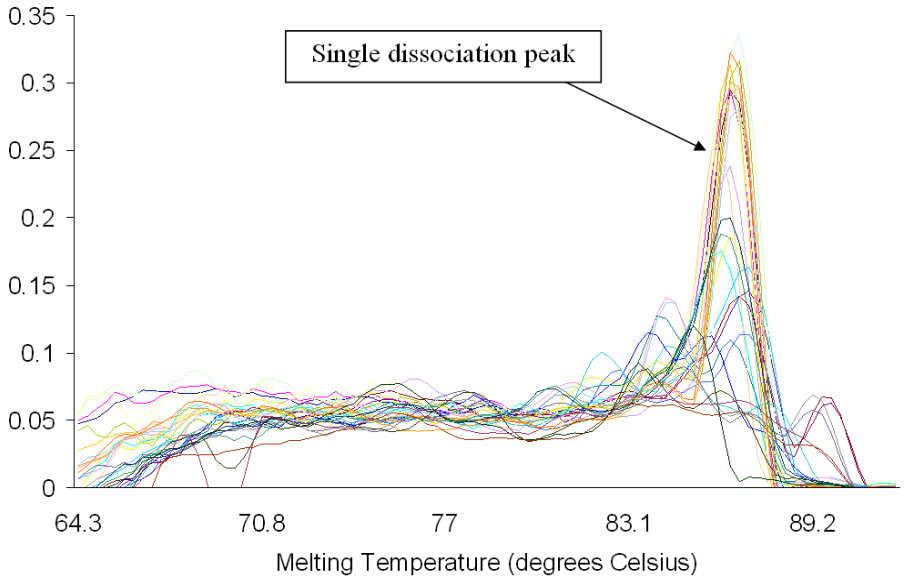

Figure 23. Dissociation curve for *mmoX* primer set amplifying environmental samples from the Soldotna, AK site. The single dissociation peak demonstrates absence of primer-dimer artifacts.

<u>NAS Oceana, VA</u>

Environmental samples collected in 2008 and 2009 from Naval Air Station Oceana (Site map – Figure 2) site in Virginia Beach, VA were also tested for the presence of methanotrophs. Genomic DNA from groundwater samples (wells MW18, MW19, and MW25) were qPCR assayed using the pmoA 472, mmoX, 16S T1, and 16S T2 primer sets. Nearly all wells tested contained detectable amounts of *pmoA*, *mmoX*, 16S T1, and 16S T2 genes, indicating that methanotrophs are present at this site.

Geochemical data from well 18, spanning 2008 to 2009, showed a decrease in CH_4 and VC (2.8 mg/L – 1.0 mg/L and 22 µg/L – 0.83 µg/L, respectively), and a steady presence of dissolved O_2 (1.28 mg/L – 1.89 mg/L). From 2008 to 2009, *pmoA*, *mmoX*, and 16S T1 gene abundance decreased by 99%, 98%, and 83%, respectively. Data from MW19, spanning 2008 to 2009, showed an increase in CH_4 and VC (1.8 mg/L – 5.8 mg/L and 7.2 µg/L – 11.2 µg/L, respectively) and steady presence of dissolved O_2 (1.3 mg/L – 1.26 mg/L). Samples from MW19 also saw an increase in abundance for all targeted genes by 3 orders of magnitude. Data from MW 25, 2008 to 2009, showed an increase in CH_4 and VC (2.5 mg/L – 7.6 mg/L and 19 µg/L – 46 µg/L, respectively) and steady presence of dissolved O_2 (1.2 mg/L – 1.44 mg/L). Likewise, samples from MW 25 saw an increase in *pmoA*, *mmoX*, and 16S T1 gene abundance by an order of magnitude and steady presence of methanotroph 16S T2 rRNA genes, with abundances varying from 2.0×10^5 copies/L GW to 4.2×10^5 copies/L GW. Full results for NAS Oceana are displayed in Table 21.

Table 21. Average methanotroph gene abundance (copies/L groundwater) at NAS Oceana. Primer concentrations were 300 nM, 300 nM, 800 nM, and 200 nM, respectively, and produce standard curve PCR efficiencies of 100 %, 99.4 %, 102 %, and 94.5 %, respectively. The 16S T2 PCR efficiency fell below the desired range (95% to 105%) and implies slightly decreased amplification efficiency for that primer set. This decrease in efficiency will cause the 16S T2 quantifications to appear smaller than they would otherwise in a qPCR reaction amplifying at 100%. For more standard curve characteristics and dissociation curves, see Appendix A.

Monitoring Well	***pmoA***		***mmoX***	
	2008	**2009**	**2008**	**2009**
MW18	$9.6x10^5$	$1.2x10^4$	$4.3x10^3$	$1.3x10^2$ **
MW19	$1.4x10^4$	$1.9x10^7$*	0	$4.3x10^4$
MW25	$2.1x10^5$	$1.1x10^6$	$6.6x10^4$	$4.8x10^5$
	16S T1		**16S T2**	
	2008	**2009**	**2008**	**2009**
MW18	$1.9x10^4$ **	$3.0x10^3$ **	$6.5x10^5$	$5.3x10^3$
MW19	$1.0x10^3$ **	$1.6x10^6$	$9.4x10^3$	$5.2x10^6$
MW25	$1.0x10^4$	$4.8x10^5$	$2.0x10^5$	$4.2x10^5$

Note: Samples marked with "*" were detected at quantities above the dynamic range of the standard curve (10^5 copies/reaction). Samples marked with "**" were detected at quantities below the dynamic range of the standard curve (100 copies/reaction).
Note: Values are the average of replicate measurements.

Carver, MA

Environmental samples from the Carver, MA site were also tested for the presence of methanotrophs (Table 22) *(46)*. Relative abundance was calculated by adding the Type I methanotroph quantifications with the Type II methanotroph quantifications and then dividing by the universal bacterial quantifications (16S T1+16S T2/16S U). For each monitoring well, the relative abundance was as follows: 46D – 0.95%, 52I – 0.18 %, 58I – 6.56%, and 64I – 0.48% (Table 23. Well 63I was not analyzed due to lack of available sample. This data suggests that methanotrophs make up a very small portion of the total microbial community in these wells, with 58I having the highest abundance of methanotrophs.

Table 22. Average methanotroph gene abundance at Carver contaminated site estimated using the 16S universal, 16S T1, and 16S T2 primer sets. Sampling date: 6/23/2009Primer concentrations were 300 nM, 800 nM, 200 nM, and 100 nM, respectively, and produce standard curve PCR efficiencies of 99.4 %, 99.3 %, 99.9 %, and 99.8 %, respectively. For more standard curve characteristics and dissociation curves, see Appendix A.

Monitoring Well	**16S U**	**16S T1**	**16S T2**
		copies/L groundwater	
46 D	$6.1x10^{7}$	$5.3x10^{5}$	$5.3x10^{5}$*
52 I	$5.0x10^{9}$ *	$3.9x10^{6}$	$3.9x10^{6}$
58 I	$1.0x10^{8}$ *	$5.1x10^{7}$	$5.1x10^{7}$
64 I	$9.2x10^{8}$ *	$1.4x10^{6}$	$1.4x10^{6}$

Note: Samples marked with "*" were detected at quantities above the dynamic range of the standard curve (10^{5} copies/reaction).
Note: Values are the average of replicate measurements

Table 23. Methanotroph relative abundances as determined by qPCR.

Monitoring Well	**Methanotroph Population as a % of Total Organisms**	**Type I Methanotrophs as a % of Total Methanotrophs**	**Type II Methanotrophs as a % of Total Methanotrophs**
46 D	0.95	97.7	2.31
52 I	0.18	43.7	56.3
58 I	6.56	76.0	24.0
64 I	0.48	34.8	65.2

Note: Each sample was quantified in duplicate and quantifications were averaged before calculating relative abundances.

Task 2 Develop RT-qPCR technique for etheneotrophs

The objective of this task was to extend our qPCR technique to include absolute quantification of mRNA transcript abundance in pure cultures and environmental samples. This will allow us to determine whether or not etheneotrophs (and methanotrophs) are *functional* (i.e. expressing their functional genes) in any of these environmental samples. The extended technique involves RNA extraction, addition of internal control nucleic acids, and reverse-transcription of mRNA into cDNA. Real-time PCR is conducted with both cDNA and DNA templates. Gene expression is estimated quantitatively in terms of the transcript per gene ratio.

Subtask 2.1 Develop a RNA extraction protocol suitable for groundwater samples

The results presented in Subtask 1.4 indicate that etheneotrophs (and methanotrophs) are present in quantifiable amounts in selected wells at each of the three different sites studied. Since ethene and/or VC is present it is plausible that these microbes could participate in cometabolic (or even metabolic oxidation, in the case of etheneotrophs) of VC. In order for this approach to be successful, an effective protocol for extracting RNA from environmental samples was developed first.

We postulated that extracting RNA and DNA simultaneously from a Sterivex filter (Figure 5) would remove variability and thus improve accuracy of gene and transcript abundance estimates compared to DNA and RNA extraction from separate Sterivex filters (Figure 4). Initial testing of simultaneous RNA and DNA extraction from Sterivex filters was performed with the PowerWater RNA Isolation Kit (PRI kit, MOBIO) using ethene-grown *Mycobacterium* JS60 cultures. Normally when extracting RNA a DNA digestion step is performed to remove contaminating DNA. To achieve simultaneous extraction of RNA and DNA, we divided the extract into two equal volumes prior to the DNA digestion step and then followed the kit protocol for RNA extraction, excluding the DNAse step in one of the tubes. To understand how much RNA and DNA was lost during extraction, we compared the PowerWater RNA Isolation from Sterivex filters against a beadbeating (BB) method with pelleted cells. In this case we presumed that extraction of RNA and DNA from pelleted cells via beadbeating would provide maximal yields. We used triplicate 10 ml *Mycobacterium* strain JS60 cultures (OD_{600} = 0.067) in this experiment. Cultures were pelleted and resuspended in STE lysis buffer prior to starting the beadbeating protocol, while cultures were filtered through Sterivex filters prior to initiating the PRI kit protocol. The RNA/DNA ratio was measured by fluorometry.

Following beadbeating, 66.7% of the starting volume was lost and the RNA/DNA ratio was 86.9%. Using the PRI method, the RNA/DNA ratio was 61.0%, 60.7%, and 74.9% (in triplicate experiments). The PRI/BB ratio for RNA was 18.3%, 16.2%, and 18.8% (Avg.17.8% ± 1.4%). The PRI/BB ratio for DNA was 26.0%, 26.8%, and 21.8% (Avg. 24.9% ± 2.7%). These results indicate that, when using the same starting amount of cells, the DNA and RNA yields from filtered cells with the PRI kit were relatively low in comparison to beadbeating the same amount of pelleted cells. In other words, a high percentage of the cells appear to not be released from the filters, thus decreasing yield.

With the introduction of the PowerWater Sterivex kit from MoBio, we subsequently embarked on an evaluation of several RNA extraction kits and protocol modifications with pure VC-assimilating cultures (*Mycobacterium* JS60 and *Nocardioides* JS614) as the reference strains.

The experimental design is similar to that described for DNA kit comparison in Subtask 1.1. Here, we compared RNA yields from *Mycobacterium* JS60 and *Nocardioides* JS614 cultures when using Beadbeating RNA extraction (followed by phenol/chloroform/isoamyl alcohol purification; BB), PowerSoil RNA Isolation (PS), Modified PowerSoil RNA Isolation (MPS), PowerWater RNA Isolation (PW), Modified PowerWater RNA Isolation (MPW), and PowerWater Sterivex RNA Isolation (PWS). All kits were produced by MoBio. In general, original protocols were applied to (PS), (PW), and (PWS). "Modified" indicated that addition of 0.1 mm zirconia/silica beads (300 µL and 1,500 µL for (MPS) and (MPW), respectively).

The results of this experiment are shown in Figure 24A. Based on this extracted RNA mass comparison, a Modified PowerWater Sterivex RNA Isolation Kit procedure appears to be the most effective product for purifying RNA from our reference strains. Transcripts were also quantified in mid-exponential phase ethene-grown JS614 and JS60 cultures using our published qPCR methods and unpublished RT-qPCR method (which will be described in more detail in the next section) Figure 24B. This approach also suggested that the PowerWater Sterivex kit gave the best combination of quantity and quality of RNA template for qPCR. However, we noted that the Powersoil kit also yielded good quality RNA even though the yields were less.

However, it should be noted that RT-qPCR experiments with environmental samples described later in Task 2 were performed prior to the analysis described in Figure 25. DNA and RNA samples for this experiment were extracted with the MoBio PowerWater DNA and RNA extraction kits.

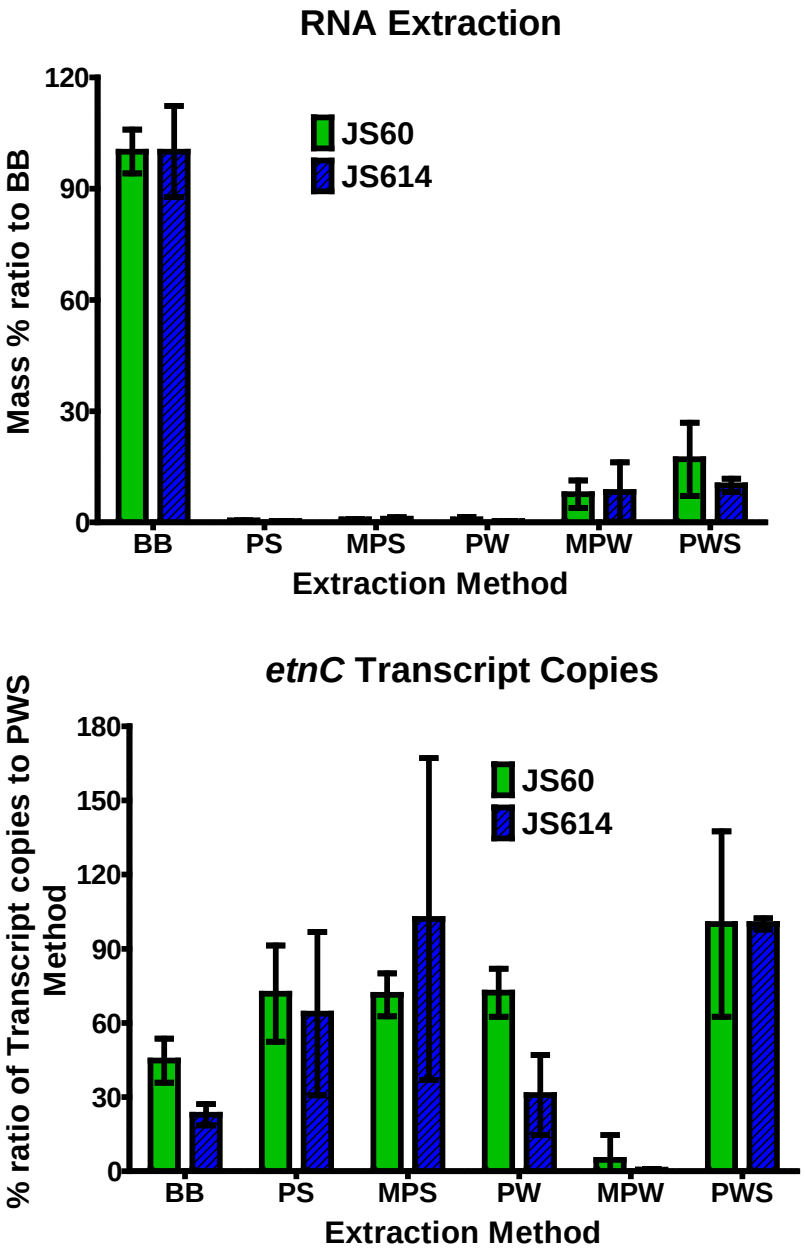

Figure 24. Top graph: Nucleic acid mass recovery following RNA extraction from pure cultures of VC-assimilating *Mycobacterium* JS60 (clear greeen bars) and *Nocardioides* JS614 (hatched blue bars) using a variety of extraction methods and kits. The mass of RNA recovered was normalized to the BB method. The bar height is the average of three replicates and the error bars are the 95% confidence interval. Bottom graph: Comparison of estimated *etnC* transcript abundance by RT-qPCR following RNA extraction. The *etnC* abundance was normalized to the abundance estimated in the PWS RNA extract. Abbreviations: BB: Nucleic acid extraction by bead beating, followed by phenol:chloroform:isoamyl alcohol extraction. PS: Mo Bio Powersoil extraction kit. MPS: Mo Bio Powersoil extraction kit with additional zirconium/silica beads added. PW: Mo Bio PowerWater extraction kit. MPW: Mo Bio PowerWater extraction kit with additional zirconium/silica beads added. PWS: MoBio PowerWater Sterivex extraction kit.

Subtask 2.2 Develop etheneotroph RT-qPCR method

The primary goal of this subtask was to develop a reverse transcription (RT)-qPCR method for *etnC* and *etnE* expression using an absolute quantitation approach. We also aimed to apply the same approach to look at *pmoA* and *mmoX* expression in methanotrophs. First, we adopted the "exogenous internal reference technique" using luciferase mRNA *(62)*. We are currently most concerned about minimizing sources of variability in the approach. For example, incomplete cell lysis, RNA/DNA loss during purification steps, and reverse transcription efficiency should be taken into account when attempting to quantify mRNA from environmental samples. Based on the results of Subtask 2.1, we expect that 82.2% of the RNA and 75.1% of the DNA would be lost following extraction from Sterivex filters with the PRI kit. Addition of a known mass of ref mRNA to the sample following the PRI kit cell lysis step and then quantifying the number of ref cDNA gene copies after the protocol was complete would allow us to estimate both the RNA loss from extraction and the RT efficiency.

2.2.1 Ref mRNA quantification

The first step in this process was to develop a ref mRNA qPCR standard curve. It is described in the materials and methods section. Next we designed an experiment to test the effect of different parameters on the quantification of ref mRNA. Starting with a known amount of ref mRNA transcripts, we converted them to cDNA and measured the gene copy number by qPCR. The difference between the starting and final gene abundance reflects the efficiency at which mRNA is converted to cDNA and other mRNA losses (e.g. from purification) and is expressed as a percentage. The parameters studied included using either gene-specific primers (refSTF and refSTR) or random primers during the RT step. Since we expect PCR inhibitors to be present in groundwater, we also tested the effect of BSA (400 ug/mL) on the recovery efficiency using both random and gene-specific RT primers. Finally we tested the effect of a PCR purification step following the RT step. When using random primers, the cDNA recovery was 51.6% ± 3.6%. When BSA was added, the recovery dropped to 43.3% ± 2.8%. When a purification step was added the recovery was 28.3% ± 0.9% (no BSA present) and 14.2% ± 1.4% (BSA present). When using the gene-specific primers, the cDNA recovery was 97.1% ± 10.9%. When BSA was present, the recovery was 114.2%. When a purification step was added the recovery dropped to 40.0 % ± 4.6% (no BSA present) and 36.3% (BSA present).

Overall, the ref mRNA recovery, when using random primers, was 50% of the recovery observed when using gene-specific primers. The ref mRNA recovery in the presence of BSA was 86% of the recovery when BSA was absent. Finally, the ref mRNA recovery with purification was 40% of that obtained when no purification was done. Even though the use of random primers and BSA resulting in decreased quantitation of ref mRNA, we determined that these two steps are necessary when applying a RT-qPCR method to groundwater samples. Random primers must be used because it is not possible to use GSPs in an environmental sample. BSA must be used because PCR inhibitors may also inhibit the activity of reverse transcriptase.

2.2.2 Addressing DNA contamination in RNA extracts by qPCR

An important quality control procedure is to determine if genomic DNA contamination is present in RNA extracts from Sterivex filters when using PowerWater RNA Isolation Kit (PRI kit, MOBIO). In this kit, an “on-column" DNA digestion step (with DNase I) is performed following RNA extraction. We tested the efficiency of the DNase I step according to incubation time with

RNA extracted from *Mycobacterium* strain JS60 cultures. Cultures were grown on 1/10-strength trypticase soy agar + 1% glucose, resuspended into minimum salts medium and then filtered onto 9 different Sterivex filters. All samples were processed according the PRI kit protocol except that the DNase I incubation time was varied from 15 min (protocol value) to 120 min. A control sample with no DNase I added was also analyzed so that we could make comparisons between treatments. This experiment revealed that the 15 min DNA digestion step removed 93.2% of the DNA contamination from the RNA. Approximately 13.5% of the RNA was also lost during this step. There appeared to be very little effect of incubation time on the amount of DNA remaining in the RNA extracts, but this could be a result of DNA and RNA cross-reactions in the different fluorometry assays. So, we PCR-tested the RNA itself (with CoMF1L/R2E primers (Table 5) because PCR is a very sensitive measure of DNA presence and RNA is not used as a template by Taq polymerase. PCR products were observed in every RNA extract except the sample incubated for 105 min with DNAse, indicating that the on-column DNAse digestion step is relatively ineffective in removing DNA contamination to levels not detectable by PCR.

To further investigate this issue, we analyzed the commercially-provided luciferease mRNA stock using qPCR primers we designed in-house (called refSTF and refSTR). First, we tested the commercial mRNA stock for the presence of DNA contamination by using it as a template for PCR. DNA polymerases do not use RNA as a template, so any positive result in these PCRs would indicate DNA contamination. DNA contamination was confirmed by PCR, and then quantified by qPCR, which showed that there were only about 600-800 luciferase genes per million transcripts. Since this is such a low percentage, it can be considered negligible. However, to address the possibility of DNA contamination in any of our RNA extract, we plan to include RNA template as a negative control in all future RT-qPCR experiments.

2.2.3 Analysis of the transcript per gene ratio in Nocardioides sp. strain JS614 cultures
With a working RT-qPCR method in place, we chose to study *etnC* and *etnE* expression in acetate-, ethene-, and VC-grown *Nocardioides* sp. strain JS614 cultures (ATCC BAA-499). In addition to helping us validate the RT-qPCR method, it also allowed us to investigate some observations made in a previous study. For example, EaCoMT activities in cell free extracts of VC-grown JS614 were found to be higher than in ethene-grown JS614 cultures *(17)*. We sought to confirm this observation by comparing *etnC* and *etnE* transcript abundance in ethene- and VC-grown JS614 cultures. Because etheneotrophs and VC-assimilators are known to repress ethene and VC biodegradation gene expression while growing on acetate *(9, 15, 17, 36, 83)*, we determined basal levels of *etnC* and *etnE* expression in acetate-grown JS614 cultures. Transcript per gene ratios in acetate-grown JS614 cultures were 0.5 (*etnC*) and 0.6 (*etnE*) (Figure 25). However, when JS614 is growing on ethene or VC, transcript per gene ratios range from approximately 3-11 for *etnC* and 2-12 for *etnE*. Overall, this experiment suggests that when the transcript per gene ratio is less than one, then the cells within the sample are not likely to be fully induced.

We also investigated the quantitative effect of VC and ethene starvation on *etnC* and *etnE* expression in JS614 (Figure 25). Transcript per gene ratios were between 0.1-0.2 for *etnC* and *etnE* respectively, significantly lower than induced conditions (2-12) and also lower than acetate-grown conditions (0.5-0.6). This indicates that the transcript per gene ratio was sensitive enough to yield relevant information about the activity status of a pure culture in the laboratory.

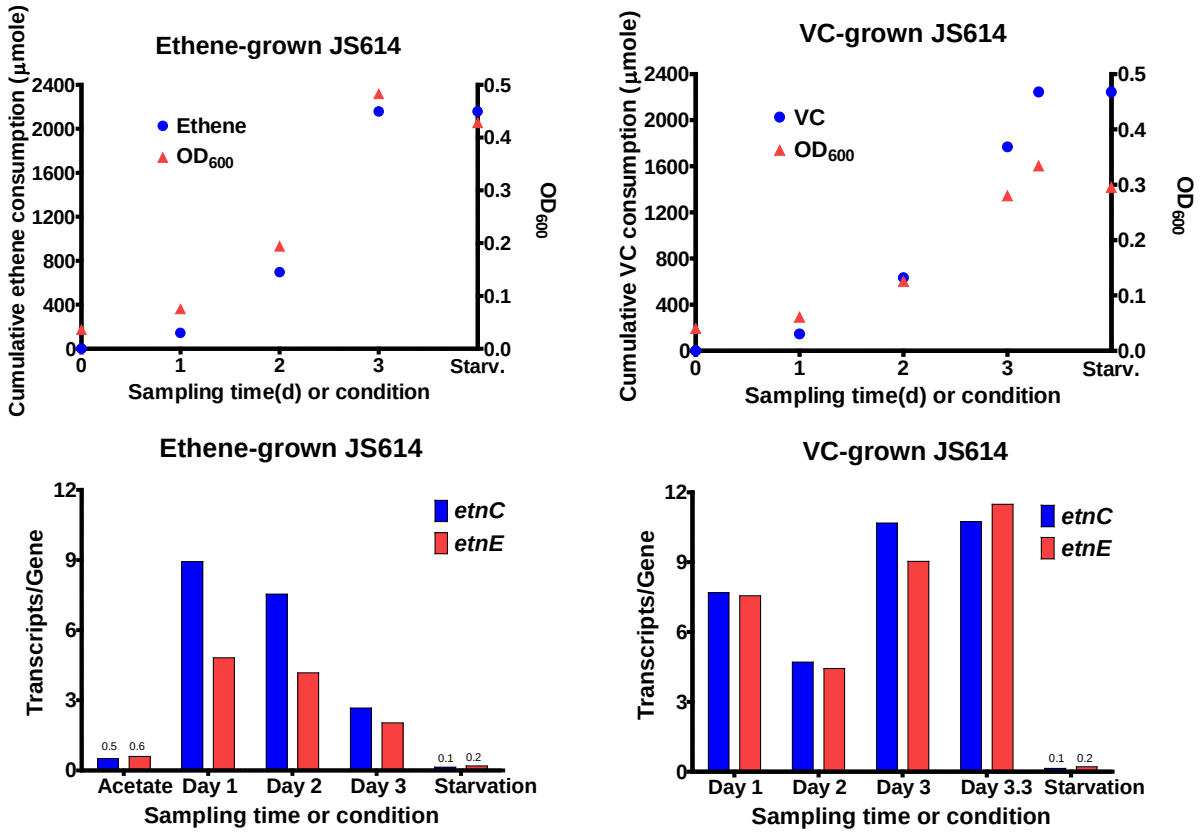

Figure 25**.** These experiments, conducted with ethene- and VC-grown cultures of the VC-assimilating *Nocardioides* sp. strain JS614, illustrate the relationship between growth on VC, ethene, and acetate (as well as VC and ethene starvation) and the transcript/gene ratio for both functional genes (*etnC* and *etnE*). Liquid samples were taken periodically, DNA and RNA were extracted simultaneously from liquid samples, and extracts were subjected to RT-qPCR analysis with internal controls. (A) This graph shows accumulative ethene consumption and resulting microbial growth (measured indirectly by the optical density at 600 nm wavelength (OD_{600}) with time. Liquid samples were taken at the times where data points are shown. (B) This graph shows accumulative VC consumption and resulting microbial growth with time. Liquid samples were taken at the times where data points are shown. (C) The transcripts per gene ratio for functional genes (*etnC* and *etnE*) vs. sampling time and condition when JS614 was grown on ethene or acetate, (D) The transcripts per gene ratio for functional genes (*etnC* and *etnE*) vs. sampling time and condition when JS614 was grown on VC.

2.2.4 RT-qPCR analysis of groundwater samples

Using the knowledge gained with laboratory culture experiments, the RT-qPCR method was also applied to groundwater samples to examine whether this approach can be used to assess individual wells at two different VC-contaminated sites Carver, MA and NAS Oceana SWMU 2C.

2.2.4.1 Carver, MA samples (collected in 2010 and 2011). For this experiment, Sterivex filter samples were obtained from three different monitoring wells at the Carver, MA site (RB63I, RB64I, and RB46D). Filters for RNA analysis were preserved with RNAlater as described in the materials and methods. DNA and RNA were separately extracted from three individual filters from each well, combined in to a single DNA and RNA stock for each well to RT-qPCR for *etnC* and *etnE*. Transcript/gene ratios were estimated as follows: 0.4 for both *etnC* and *etnE* in RB46D, 0.7 for *etnC* and 0.8 for *etnE* in RB63I, and 5.7 for *etnC* and 2.2 for *etnE* in RB64I (Figure 26).

In light of the laboratory experiments with acetate-grown, ethene-grown, and VC-grown JS614 cells, these results can be interpreted as follows. The microbial community harboring etnC and etnE (i.e. etheneotrophs) in well RB46D was expressing these genes only at basal levels and cannot be considered as active. The same conclusion can be reached for well RB63I, since the transcript per gene ratio was less than one. However, the etheneotrophs present in well RB64I appeared to be active at the time of sampling since transcript/gene ratios were greater than 1 for both *etnC* and *etnE*. This very promising result suggests that RT-qPCR can be a useful diagnostic tool to determine the physiological status of specific groups of microorganisms (e.g. etheneotrophs) in groundwater sampled from monitoring wells.

It should be noted that since the RNA extracts were converted to cDNA and pooled, we could not perform a control PCR on these RNA extracts (sampled March 2010). Therefore, the possibility that the RNA extracts were contaminated by genomic DNA cannot be excluded. However, several subsequent independent RNA extraction experiments using pure cultures indicated that DNA contamination was insignificant. Because the DNA yields from pure cultures were much higher (and thus the potential for DNA contamination of RNA extracts was also higher) this result suggests to us that any DNA contamination in the RNA extracts from environmental samples is negligible.

In a later experiment, DNA and RNA was extracted from Carver well RB73 samples (September 2010 and March 2011 sampling dates) with the PowerWater DNA and RNA Isolation Kits. All qPCR analyses were performed on the same plate to facilitate comparisons. Standard curve amplification efficiencies were 105.0% (MRTC), 107.4% (MRTE), and 103.7% (ref) with a good linear fit in all cases. The linear dynamic ranges were $30\text{-}3\times10^7$ copies for functional gene and reference gene standards (JS614 DNA was used for *etnC* and *etnE* standards and Luciferase PCR product was used for reference standard). We calculated that there were 5,800 ± 2,300 *etnC* and 500 ± 100 *etnE* per L of groundwater (September 2010) and 5,400 ± 1,900 *etnC* and 1,900 ± 200 *etnE* per L of groundwater (March 2011). This corresponds to *etnC*/*etnE* ratios of 10.9 (2010) and 2.8 (2011). In addition, the recovery of reference mRNA (as cDNA) added to the extracts was 0.6% (2010) and 5.9% (2011). We calculated that there were $1.86\times10^4 \pm 4.9\times10^3$ *etnC* transcripts and $2.44\times10^4 \pm 5.6\times10^3$ *etnE* transcripts per L of groundwater in the March 2011

samples. The data indicate the transcripts per gene were 9.33 (*etnC*) and 12.16 (*etnE*) for March 2011 samples. September 2010 transcript and gene abundance were not quantifiable since the data did not fall within the calibration curve values.

We attempted to extract RNA from samples taken from these same Carver, MA wells at later time points in 2011, but were not successful. There are several possible explanations for these results. First, since the filters were not processed soon after sampling, it is possible that the preservation technique, which employs RNAlater and freezing at -80C, could have led to RNA degradation over time. Second, we were not present during the groundwater sampling. It is possible the sampling crew mishandled the filters and the RNA was not preserved appropriately. We recommend that more experimentation be conducted to confirm an appropriate sample preservation protocol and more control over the sampling protocol needed in future experiments of this nature.

2.2.4.2 NAS Oceana samples (collected in 2008, 2009). Sterivex filter samples collected in 2008 and 2009 from wells MW18, MW19, and MW25 at NAS Oceana SWMU 2C were also subjected to RT-qPCR analysis. Like the Carver, MA samples filters for RNA analysis were preserved with RNAlater as described in the materials and methods. DNA and RNA were separately extracted from three individual filters from each well, combined in to a single DNA and RNA stock for each well to RT-qPCR for *etnC* and *etnE*. However, some RNA was not converted to cDNA and instead used in control qPCRs to assess the possibility of DNA contamination in the extracts.

In general, the results of this experiment were not as intriguing as at the Carver site, but still showed some promise. First of all, there was little evidence for the presence or expression of *etnC* in these samples. However, *etnE* was present at low levels in all three wells. Evidence of *etnE* expression was noted in the 2009 MW19 sample, suggesting there might have been active etheneotrophs at the time of sampling.

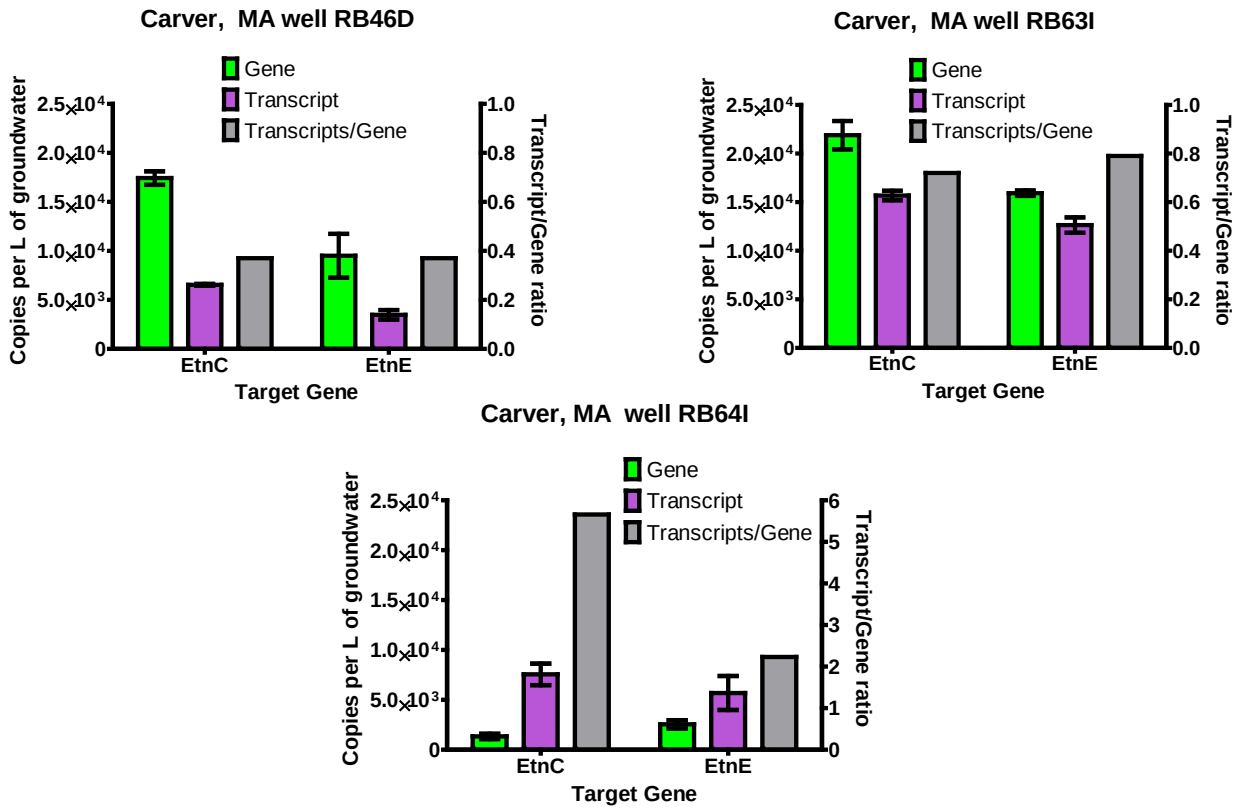

Figure 26. These graphs illustrate the application of our RT-qPCR method to groundwater samples from a VC-contaminated site (Carver, MA). Biomass was collected on Sterivex filters. Filters from RNA analysis were preserved with RNA later. DNA and RNA were extracted separately from a total of 6 filters per well (3 each for DNA and RNA) using the Mo Bio PowerWater DNA and PowerWater RNA kits, respectively, using slightly modified protocols. Internal controls were added, RT-qPCR was performed for both functional genes (*etnC* and *etnE*), and the transcript/gene ratio calculated. This analysis was performed with samples from three different monitoring wells: RB46D (A), RB63I (B), and RB64I (C). The error bars represent the 95% CI. The calculated gene copies were 1.7×10^4 *etnC* and 9.5×10^3 *etnE* per L of groundwater (RB46D), 2.4×10^4 *etnC* and 1.6×10^4 *etnE* per L of groundwater (RB63I), and 1.3×10^3 *etnC* and 2.5×10^3 *etnE* per L of groundwater (RB64I). The calculated transcripts were 6.5×10^3 *etnC* and 3.5×10^3 *etnE* per L of groundwater (RB46D), 1.6×10^4 *etnC* and 1.3×10^4 *etnE* per L of groundwater (RB63I), and 7.6×10^3 *etnC* and 5.7×10^3 *etnE* per L of groundwater (RB64I). For the DNA plate, standard curve amplification efficiencies were 100.8% (MRTC), 104.3% (MRTE), and 96.6% (ref) with a good linear fit and $R^2>0.99$ in all cases. The linear dynamic range for DNA were $10\text{-}3\times10^5$ copies for both *etnC* and *etnE* standard and $30\text{-}3\times10^7$ copies for reference gene standard. Reference DNA(2.3×10^8 copies) was added and the fractional recoveries were 32.7% (RB46D), 67.6% (RB63I) and 15.9% (RB64I). For the cDNA plate, standard curve amplification efficiencies were 102.2% (MRTC), 112.7% (MRTE), and 102.4% (ref) with a good linear fit and $R^2>0.99$ in all cases. The linear dynamic ranges for cDNA were $10\text{-}3\times10^5$ copies for both *etnC* and *etnE* standard and $30\text{-}3\times10^7$ copies for reference gene standard. Reference mRNA(4.1×10^9 copies) was added and the fractional recoveries were 4.4% (RB46D), 1.2% (RB63I) and 2.3% (RB64I).

2.2.5 RT-qPCR for methanotrophs

Samples from Carver, MA wells 64I, 63I, and 46D were also subject to RT-qPCR analysis for methanotrophs. Transcript per gene ratios were calculated compared for *pmoA* and *mmoX*. For both *pmoA* and *mmoX*, the transcripts/gene ratio was less than one for all wells (Table 24). Thus, the VC oxidation occurring in these wells is not likely attributed to methanotrophic bacteria, since their functional gene expression is very low.

Table 24: *pmoA* and *mmoX* transcript per gene ratios. Primer concentrations were 300 nM for both functional genes (pmoA 472 and mmoX) and 100 nM for the Luciferase control gene Standard curve PCR efficiencies for each primer set were of 98.6 %, 96.7 %, and 100 %, respectively. Percent recoveries for the Luciferase control gene ranged from 9.3 % to 60.1 %. For more standard curve characteristics and detailed Luciferase recovery ratios, see Appendix A. With regard to the mmoX dissociation curve, results mirrored those of Soldotna, with the presence of the standard-curve double peak at 76°C and 86°C. Environmental samples contained two peak temperatures as well. It is suspected that the primer-dimer artifact in environmental samples is due to low target gene abundance. Dissociation curves for the pmoA 472, mmoX, and Luciferase primer assays can be found in Appendix A).

Monitoring Well	**Transcript per gene ratio**			
	***pmoA* 472**		***mmoX***	
64I	0.18	0.10	0.27	0.26
63I	0.02	0.01	0.00	0.00
46D	0.02	0.01	0.28	0.20

Note: Each sample was quantified in duplicate and quantifications were averaged before calculating relative abundances.

Task 3 Investigate the normalized rate of VC oxidation

The overall purpose of this task was to determine the factors that would contribute to the rate of VC oxidation at contaminated site and explore how our qPCR method could be used to determine a normalized rate of VC oxidation. We chose to work with the Carver, MA site, primarily because BCI had access to groundwater samples on a quarterly basis.

Subtask 3.1 Preliminary Carver microcosm study (2009)

BCI first conducted a preliminary microcosm study of groundwater samples collected from 14 wells at the Carver, MA site in September 2009. The goal of BCI's initial experiment is to obtain data on the chemical composition and presence of methanotrophs and etheneotrophs in each of the fourteen Carver site monitoring wells (named RB-35I, -39I, -46D, -47D, -73, -58I, -63D, -63I, -64D, -64I, -78, -79, -80, and -81) located in and around the dilute VC plume (Figure 1). Groundwater was sampled by EST Associates Inc. (Needham, MA) on September 28th and 29th, 2009. Samples were received at BCI on September 29th and 30th and were refrigerated until use.

For geochemical characterization, three composite samples were prepared by compositing 14 well samples as follows:

"U" (up-gradient)	wells	78,	79,	80,	81	
"D" (down-gradient)	wells	58-I	63-D	63-I	64-D	64-I
"M" (mid-gradient)	wells	35-I	39-I	46-D	47-D	73

Composites were sent to Eastern Analytical for trace element analysis. Cd and Cr, which are not desirable, were not detected. Other elements required by bacteria were present, except Mo, which was < 1 µg/L in the mid- and down-gradient composites. Selenium was also not present, but may not be required. The groundwater samples were analyzed for Cl^-, NO_3^-, SO_4^{2-}, ammonia-N, PO_4^{3-} and organic acids. Nitrate and organic acids were below the detection limit (<0.6 mg/L). Field ORP ranged from -10 mV (RB-79) to 165 mV (RB-64I) suggesting that the groundwater is slightly anoxic to slightly oxic. Field pH ranged from 5.9 (RB-46D) to 8.8 (RB-78) with the majority of the wells between pH 7-8. Overall, these analyses confirmed that the Carver, MA site was an appropriate test site for this project.

VC concentrations ranged from below detection (<1 µg/L, wells RB-64I and RB-78) to 3.4 µg/L (RB-81) with an average VC concentration of 1.5 µg/L. Therefore, this VC can be considered dilute. Ethene concentrations ranged from below detection (<0.1 µg/L, RB-64I, RB-78, and RB-58I) to 3.9 µg/L (RB-46D) with an average of 0.7 µg/L. Methane concentrations ranged from 0.3 µg/L (RB-64I) to 1,490 µg/L (RB-73) with an average of 567 µg/L. Ethane concentrations ranged from below detection (<0.1 µg/L, wells RB-58I, 64I, and 78) to 0.5 µg/L (RB-81) with an average of 0.2 µg/L. CO_2 concentrations ranged from 64-216 mg/L with an average of 138 mg/L.

Presence/Absence (P/A) microcosms were constructed at BCI on October 13-15, 2009. Analysis of methane/ethene/VC degradation, O_2 use, and CO_2 production was provided at 3 time points during the test. Methanotrophs were found to be present in all 14 samples. Etheneotrophs were

in all wells except 64D, 35I, 39I, and 58I. As of Day 154, five well samples (63-I, 63-D, 67, 79, and 80) had shown significant utilization of the added VC. Two of the microcosms (63-I and 78) were fed an additional 2.7 µmol/bottle VC. By 3/24/2010, both of these bottles had consumed that second VC spike. These results (provided in Appendix C) are significant in that they show the potential for etheneotrophs at the Carver site to develop into VC-assimilating bacteria. The RB-63I VC microcosm, the source of a VC enrichment culture, which was developed and used for subsequent experiments, described later in this report.

Subtask 3.2 Microcosm study of groundwater from Carver well RB63-I (2010 and 2011)

*3.2.1 Estimates of etheneotroph and methanotroph abundance in well 63-I groundwater sampled in 2010 and 2011***.**

The relative abundance of etheneotrophs and methanotrophs in well 63-I groundwater used for microcosm experiments was estimated by qPCR analysis of functional genes (Table 25). The gene copy estimates further confirm the presence of etheneotrophs and methanotrophs in well 63-I, and suggest that methanotrophs outnumbered etheneotrophs by 2-3 orders of magnitude. The functional gene abundance data also suggest that both methanotrophs and etheneotrophs increased in abundance between the 2010 and 2011 sampling events.

Table 25. Functional gene copy abundance for etheneotrophs and methanotrophs in well RB63I, as estimated by qPCR and expressed as Gene copies per liter of groundwater as described previously *(61)*.

Sample date	Etheneotrophs		Methanotrophs	
	etnC	*etnE*	*pmoA*	*mmoX*
3/2010	5.7×10^{3}	1.5×10^{4}	6.2×10^{6}	1.6×10^{6}
3/2011	1.7×10^{4}	8.1×10^{4}	2.6×10^{7}	6.2×10^{6}

3.2.2 Interactions of native methanotrophs, etheneotrophs and VC-assimilators in microcosms containing methane, ethene, and VC singly and in mixtures.

Having demonstrated that methanotrophs, etheneotrophs, and VC-assimilators were present and functional in well 63-I groundwater, microcosm experiments were conducted to determine the effect of substrate mixtures on substrate degradation by the native mixture of these microbial groups. The amounts of methane, ethene and VC fed to each microcosm were selected to be consistent with historical concentrations at the site. We expected that microcosms containing only one substrate would have lag times and 50% degradation times characteristic of the type and concentration of each substrate. For microcosms fed a second or third substrate, the lag times for substrate utilization and times for 50% degradation were compared to those observed when each substrate was fed singly. Differences in these parameters were interpreted to elucidate the interactions of methanotrophs, etheneotrophs and VC-assimilators in the microcosms.

3.2.3. Microcosms with a single substrate.
When methane, ethene, and VC were fed separately to microcosms containing well 63-I groundwater collected in 2010 and 2011, oxidation of these compounds was observed after lag periods ranging from 9 to 20 days. In the 2011 microcosms, degradation of each of the three substrates alone was investigated in duplicate microcosms (Figure 27a-c). Similar results were obtained in the 2010 single substrate microcosms (Figure 28). Estimated lag times for methane, ethene, or VC utilization, and times for 50% degradation of each substrate are summarized in Table 26 (2011 experiments) and Table 27 (2010 experiments). However, the results of the 2010 and 2011 single substrate experiments cannot be compared directly because estimated methanotroph and etheneotroph abundances were greater in 2011 (Table 25). However, the data are useful in interpreting the results for substrate mixtures for a given year.

The mechanism controlling the lag period in these samples is likely the time required for the growth of a small microbial population to cause noticeable changes in substrate concentrations. It is notable, however, that certain etheneotrophs and VC-assimilators are known to exhibit lag periods following periods of carbon starvation *(9, 84)*. Proteomic analysis of ethene-enriched microcosms constructed in 2007 and 2008 revealed thirteen EtnE peptides identical to those found in VC-assimilating *Nocardioides* sp. strain JS614 *(38)*. JS614 is known to exhibit an extended lag before resuming activity after VC starvation *(9, 84)*, similar to that reported here for the VC-assimilators.

3.2.4. Behavior with VC and methane mixtures
Methanotrophs growing on methane are known to cometabolize VC *(6, 7, 85, 86)*. Therefore we expected that feeding well 63-I groundwater methane and VC mixtures would result in substrate utilization patterns consistent with VC cometabolism. Based on previous reports we also expected methanotrophs to be reversibly inhibited by VC *(65, 85, 87)*.

3.2.5 VC with methane (2011 experiments)
VC degradation in the presence of 1 µM methane (Figure 27-d) was faster than with VC alone (Figure 27-a). With methane present, the lag time for VC utilization decreased from 14 days to 11 days, and the 50% degradation time decreased from 43 days to 30 days (Table 26). In these 2-substrate microcosms, methane utilization was initiated at about the same time as VC degradation. These observations indicate that VC degradation in these bottles is mainly the result of cometabolic oxidation by methanotrophs rather than utilization by VC-assimilators, as the lag time for degradation of VC as sole substrate was at least 13 days.

3.2.6 VC with increasing concentrations of methane (2010 experiments)
With initial aqueous concentrations of 0.47 µM VC and 0.45 µM methane, the lag time for initiation of methane use increased from 20 days for methane alone to about 43 days with VC present, and the time for 50% methane use also increased from 40 days to 53 days (Table 27, Figure 29). This suggests that methane utilization by methanotrophs was inhibited when VC was at an aqueous concentration similar to that of methane.

In bottles fed the same amount of VC (0.47 µM), but with increasing amounts of methane, the lag time for methane use decreased, and the time for 50% methane degradation also decreased

(Table 27, Figure 29) . These results suggest that VC inhibition of methanotrophs is overcome at increasing ratios of methane to VC.

Comparing VC degradation in the same microcosms, we observed that the lag times for VC degradation decreased, and the times for 50% VC degradation also decreased (Table 27, Figure 29). This data indicates that VC degradation in the presence of higher methane concentrations in this groundwater is primarily cometabolic.

3.2.7 Behavior with VC and ethene mixtures

Etheneotrophs are known to cometabolize VC to chlorooxirane, and use chlorooxirane as a growth substrate while growing on ethene *(8, 24, 88)*. VC-assimilators metabolize VC in the same manner without a requirement for ethene. Because etheneotrophs and VC-assimilators are present in well 63-I groundwater, we expected that feeding ethene and VC mixtures to microcosms would result in substrate utilization patterns consistent with VC cometabolism and VC assimilation.

3.2.8 Effect of ethene on VC degradation (2011 experiments)

For the duplicate microcosms with VC alone (Figure 27a), the average lag time for VC use by VC-assimilators was about 14 days and time for 50% use was 43 days. In triplicate microcosms fed both VC and ethene (Figure 27e) the initiation of VC consumption was similar, about 16 days, but after day 32, the rate of VC oxidation increased notably, resulting in 50% use by day 38 and 77% by day 43 (Table 26). The data indicates that at least after day 32, etheneotrophs made a significant contribution to the degradation of VC. In these microcosms, there appears to be a slight stimulation by VC on ethene use, perhaps due to VC being used as a carbon source and stimulating etheneotroph growth.

3.2.9 VC with increasing concentrations of ethene (2010 experiments)

Comparing bottles fed 0.47 µM VC, and increasing concentrations of ethene, the lag time for VC use did not change significantly (Table 27, Figure 30). However, the time for 50% VC degradation increased, indicating competition between VC and ethene for the alkene monooxygenase (Table 27). VC degradation with all three concentrations of ethene tested was faster than that obtained with VC alone.

3.2.10 Behavior with methane and ethene mixtures without VC

Our initial experiments with microcosms fed substrates separately indicated that methanotrophs, etheneotrophs and VC-assimilators are present in this groundwater. In these next experiments we asked how the microbial groups would respond to mixtures of methane and ethene. We expected methanotrophs expressing MMO to cometabolize ethene in the presence of methane *(5)*, while etheneotrophs expressing AkMO are not known to degrade methane. In the 2010 microcosm fed a mixture of methane and ethene, the lag times and days for 50% degradation of either substrate were similar to when both substrates were fed alone (Table 27, Figure 31). In 2011 microcosms (Figure 27f), the time for 50% degradation of ethene in the mixture was much shorter than the time measured for ethene alone (Table 26). In contrast, the time for 50% degradation of methane in the mixture was longer than for methane alone (Table 26).

Faster ethene loss in the presence of methane could be explained by cometabolic oxidation of ethene by methanotrophs. Hou et al. *(89)* reported that methane-grown cells could oxidize ethene at a rate similar to that of methane oxidation, and that epoxyethane accumulated in the medium. Interestingly, MMO in crude extracts of methane-grown *Methylococcus capsulatus* (Bath) cells oxidized ethene nearly twice as quickly as methane *(90)*. The data is also consistent with the idea that the epoxyethane generated by methanotrophs is utilized by the etheneotrophs. Epoxyethane is known to induce AkMO gene expression and activity in VC and ethene-assimilating *Nocardioides* sp. strain JS614 cultures *(84)*. The slower degradation of methane in the ethene/methane mixture is explained by the idea that methane and ethene are competing for the active site on the methanotroph MMO.

3.2.11 Behavior with mixtures of methane, ethene, and VC

Having demonstrated that VC degradation proceeds as least partly via cometabolism in the presence of either methane or ethene, and shown that ethene degradation is enhanced by the presence of methane, but methane degradation is slower in the presence of ethene, we asked what effect the presence of both methane and ethene would have on VC degradation in this groundwater.

In 2010 experiments, when VC was tested with three ratios of methane to ethene, the mixture containing 1.3 µM methane and 3.8 µM ethene showed 50% VC degradation in 19 days, much faster than for VC alone (44 days), as well as faster than with only 1.3 µM methane or with only 3.8 µM ethene (Table 27; Figure 32a-c). In all three microcosms, the degradation of VC was simultaneous with the utilization of ethene, and did not reflect the methane utilization. In fact, in the microcosm containing the lowest concentration of methane, its utilization was inhibited for > 70 days, possibly because its low concentration made methanotrophs susceptible to VC inhibition.

In 2011 experiments, when VC was present with both methane and ethene (Figure 27g), the time for 50% degradation (20 days) was much shorter than that for VC alone (43 days), as well as shorter than with either methane (30 days) or ethene (38 days) (Table 26). As in 2010, when all three substrates were present, VC degradation occurred simultaneously with ethene use.

In a mixture containing methane and ethene, in which VC degradation appears to be carried out by etheneotrophs, utilization of added methane appears to improve the rate of VC degradation compared to that obtained when only ethene is added. A possible explanation is that methanotrophs may be able to “stimulate” etheneotrophs by oxidizing some of the ethene to epoxyethane, which induces AkMO in etheneotrophs *(84)*.

The role of methanotrophs and etheneotrophs in the natural attenuation of chlorinated ethenes in aerobic groundwater has received relatively little attention although these aerobic processes are well suited to the bioremediation of dilute plumes of VC. The Carver site, the source of samples for the present study, is perhaps the first full-scale in situ bioremediation effort in which ethene injections into the groundwater were used to stimulate ethenotrophic biodegradation of VC *(37, 39)*.

The interaction of native methanotrophs and etheneotrophs in groundwater from a VC-contaminated site undergoing natural attenuation was first studied by Freedman et al *(65)* using microcosms containing sediment and groundwater without mineral amendment. The initial ethene concentration was similar to that used here, but the concentrations of the other substrates were much higher - methane at 12.5 µM (35.6 µmol/bottle) and VC at 42 µM (5.9 µmol/bottle). Initial results were similar to those reported here in that lag times for VC degradation with ethene or methane were about 15 days, and the rate of VC degradation was faster in the presence of both ethene and methane than with either substrate alone.

Our microcosm experiments were designed to address groundwater scenarios with relatively low concentrations ethene, methane and VC (all less than 100 µg/L) which are typical for groundwater down gradient of sites having previously undergone reductive dechlorination of chlorinated ethenes. We have observed that when both methane and ethene are present, is that there is an enhanced potential for VC to be completely degraded. We conclude that substrate interactions during VC cometabolism in groundwater systems will be site-specific and depend highly on the abundance of methanotrophs and etheneotrophs as well as the concentrations of VC, ethene, and methane present (assuming oxygen is not limiting the process). These factors should be considered in the design of future VC bioremediation strategies involving cometabolism by applying the tools described here.

Table 26. Observed lag periods and times for 50% degradation of VC, methane, and/or ethene in microcosms constructed in 2011. Lag and 50% degradation times are averages of duplicate or triplicate measurements ± the range.

Number of replicates	VC (µM) Initial aqueous	methane (µM) initial aqueous	ethene (µM) initial aqueous	VC lag time (days)	Days for 50% VC degradation	methane lag time (days)	Days for 50% methane degradation	Ethene lag time (days)	Days for 50% ethene degradation
2	0	1.0	0	**-**	**-**	**9 ±1**	**19 ± 0**	**-**	**-**
2	0	0	3.0	**-**	**-**	**-**	**-**	**18 ± 3**	**39 ± 3**
3	0	1.0	3.0	**-**	**-**	**12 ± 2**	**26 ± 2**	**12 ± 2**	**21 ± 2**
2	0.47	0	0	**14 ±1**	**43 ±3**	**-**	**-**	**-**	**-**
3	0.47	1.0	0	**11 ± 1**	**30 ± 2**	**10 ±1**	**22 ± 1**	**-**	**-**
3	0.47	0	3.0	**16 ± 3**	**38 ± 3**	**-**	**-**	**17 ± 3**	**32 ± 3**
3	0.47	1.0	3.0	**18 ± 1**	**20 ± 2**	**16 ± 1**	**28 ± 1**	**13 ± 2**	**19 ± 1**

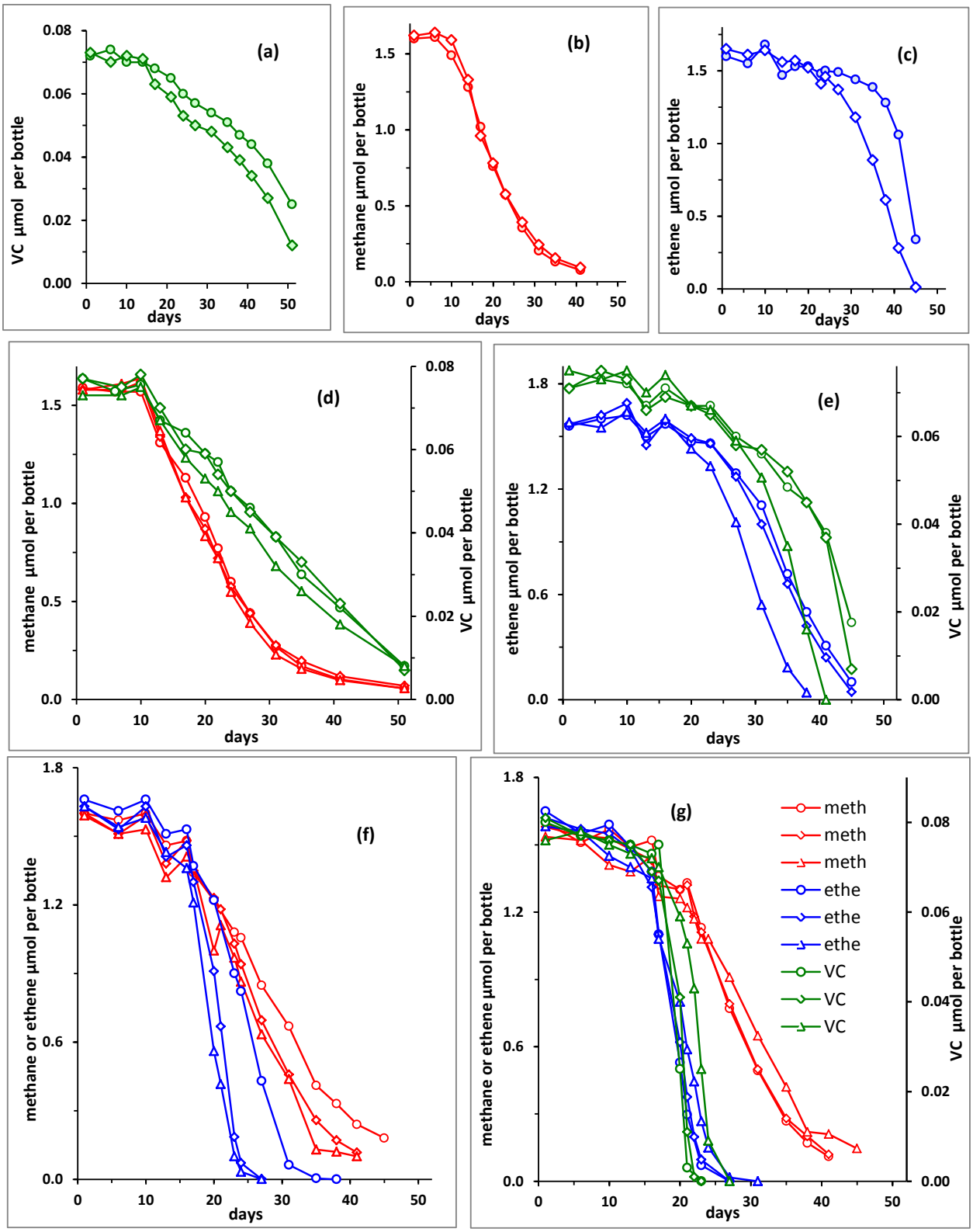

Figure 27. Aerobic biodegradation of VC, methane, and/or ethene added to microcosms constructed with groundwater from the Carver site containing methanotrophs, ethenotrophs, and vinyl chloride-assimilating bacteria. Single substrate bottles were constructed in duplicate. Multiple substrate bottles were conducted in triplicate. The results from duplicate or triplicate

bottles are shown separately for clarity. (a) VC added, (b) Methane added (c) Ethene added, (d) Methane and VC added, (e) Ethene and VC added, (f) Methane and ethene added, (g) Methane, ethene, and VC added. The symbol legend in panel (g) applies to all panels. Comparison of substrate utilization under different conditions was based on lag time and days for 50% utilization. VC was degraded faster in the presence of both methane and ethene (g), than in the presence of either methane alone (d) or ethene alone (e). Abbreviations: meth: methane, ethe: ethene

Table 27. Observed lag periods and times for 50% degradation of VC, methane, and/or ethene in single microcosms constructed in 2010.

Number of replicates	VC (µM) initial aqueous	methane (µM) initial aqueous	ethene (µM) initial aqueous	VC lag time (days)	Days for 50% VC degradation	methane lag time (days)	Days for 50% methane degradation	Ethene lag time (days)	Days for 50% ethene degradation
1	0	0.45	0	-	-	20	40	-	-
1	0	0	1.3	-	-	-	-	14	18
1	0	**1.3**	**3.8**	-	-	20	30	13	21
1	0.47	0	0	20	44	-	-	-	-
1	0.47	0.45	0	18	37	43	53	-	-
1	0.47	1.3	0	15	32	15	24	-	-
1	0.47	3.60	0	12	22	12	17	-	-
1	0.47	0	1.3	15	19	-	-	15	18
1	0.47	0	3.8	19	23	-	-	18	22
1	0.47	0	10.7	16	38	-	--	16	28
1	0.47	0.45	3.8	14	21	35	> 70	13	20
1	0.47	1.3	1.3	16	18	18	28	15	17
1	0.47	1.3	3.8	13	19	24	33	13	18

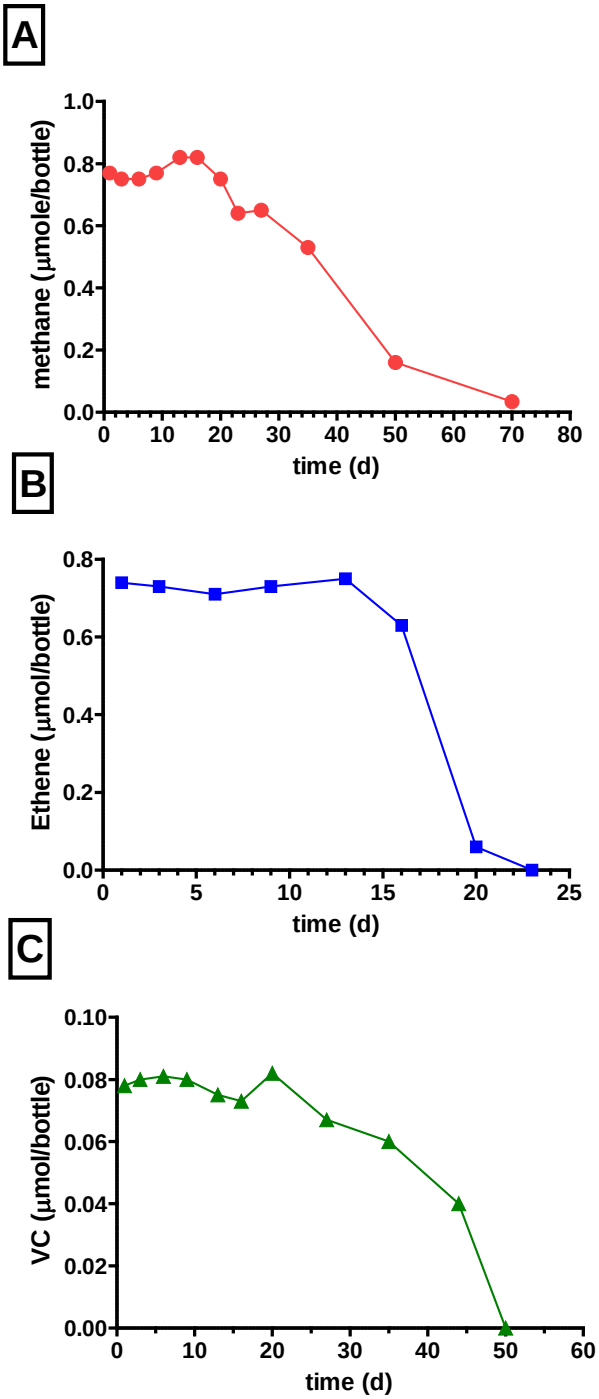

Figure 28. Aerobic biodegradation of A) methane (red circles), B) ethene (blue squares), and C) VC (green triangles) added singly to microcosms constructed with groundwater from the Carver site containing methanotrophs, etheneotrophs, and vinyl chloride-assimilating bacteria. Comparison of substrate utilization under different conditions was based on lag time and days for 50% utilization.

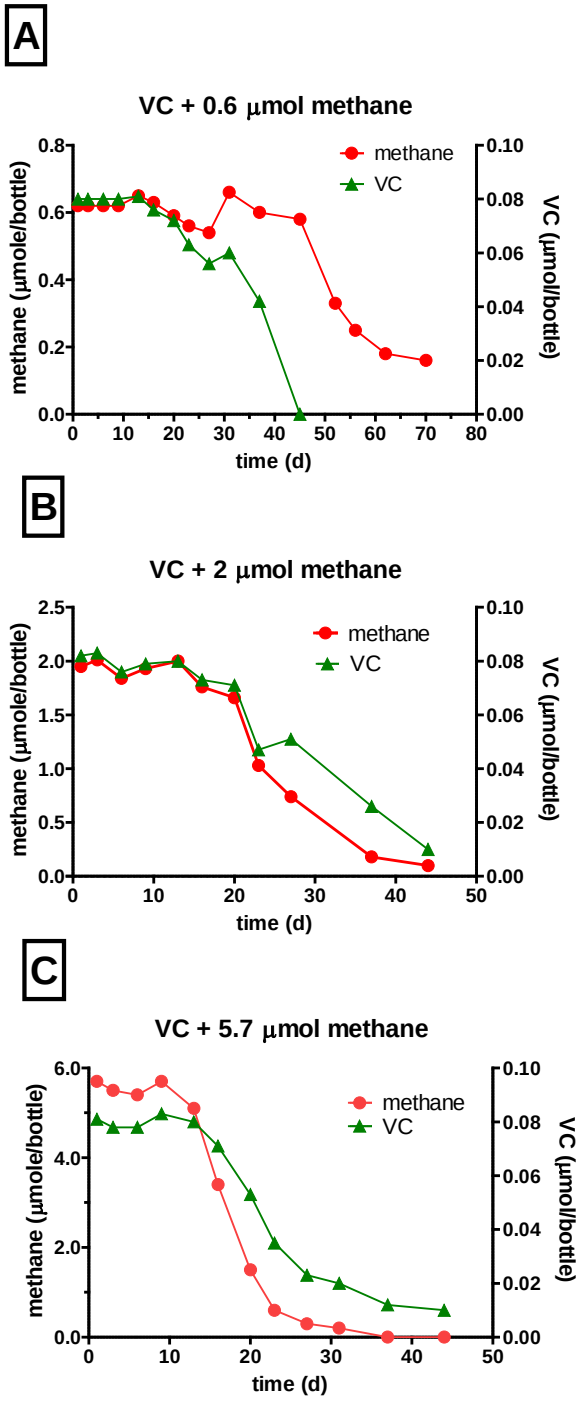

Figure 29. Aerobic biodegradation of 0.08 umol VC in the presence of a range of methane concentrations in microcosms constructed with groundwater from the Carver site containing methanotrophs, etheneotrophs, and vinyl chloride-assimilating bacteria. Comparison of substrate utilization under different conditions was based on lag time and days for 50% utilization.

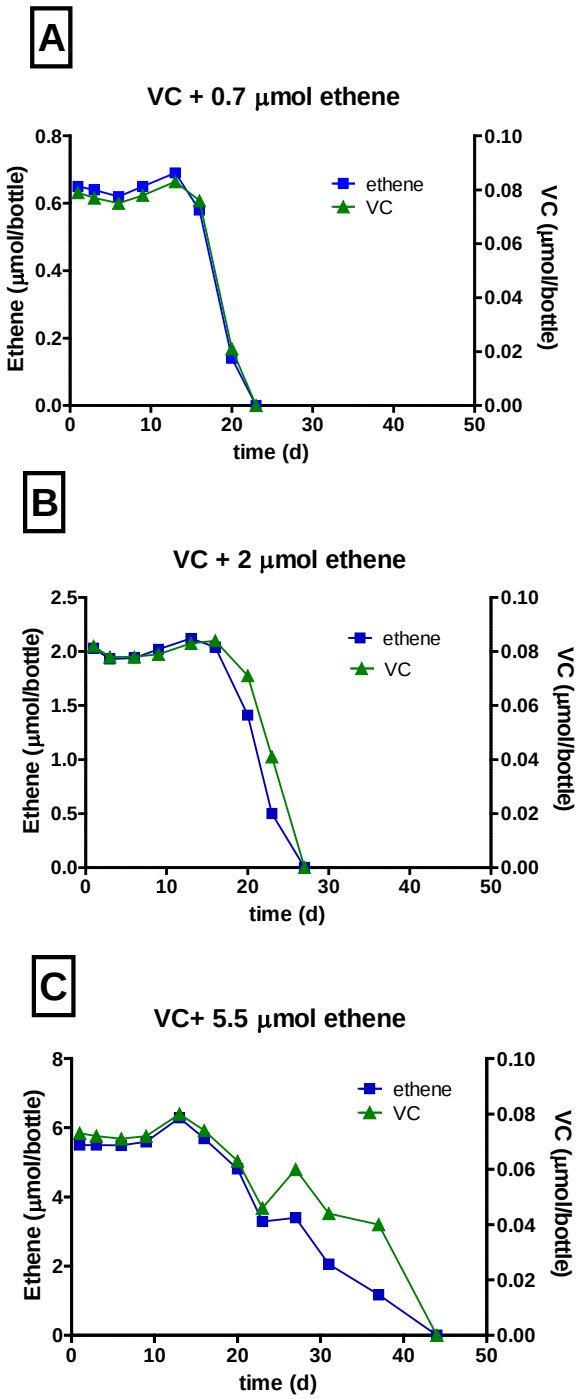

Figure 30. Aerobic biodegradation of 0.08 umol VC in the presence of a range of ethene concentrations in microcosms constructed with groundwater from the Carver site containing methanotrophs, etheneotrophs, and vinyl chloride-assimilating bacteria. Comparison of substrate utilization under different conditions was based on lag time and days for 50% utilization.

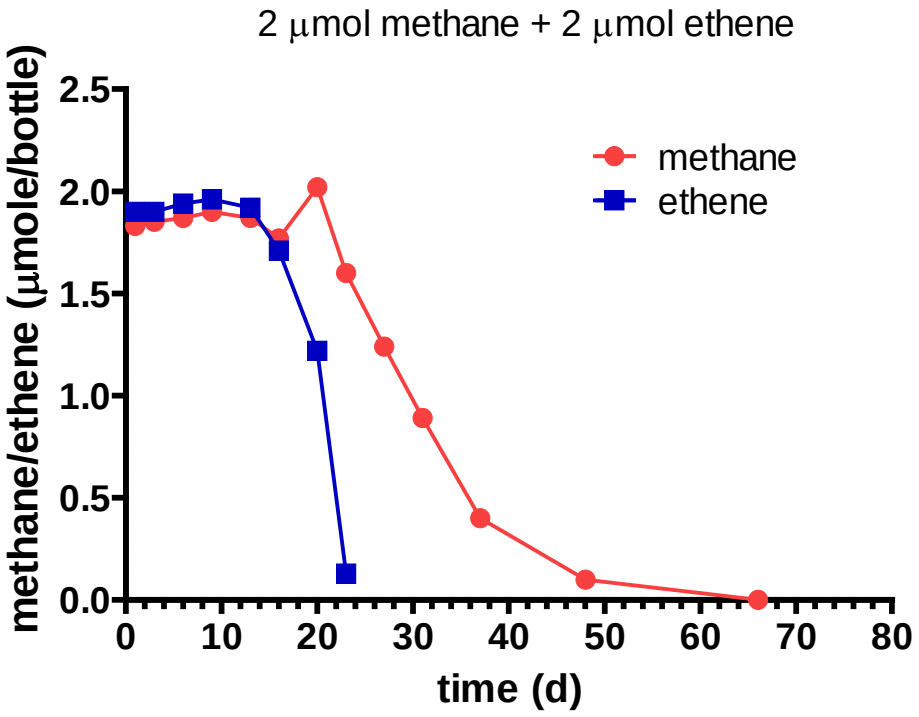

Figure 31. Aerobic biodegradation of 2 µmol methane and 2 µmol ethene in a microcosm constructed with groundwater from the Carver site containing methanotrophs, etheneotrophs, and vinyl chloride-assimilating bacteria. Comparison of substrate utilization under different conditions was based on lag time and days for 50% utilization.

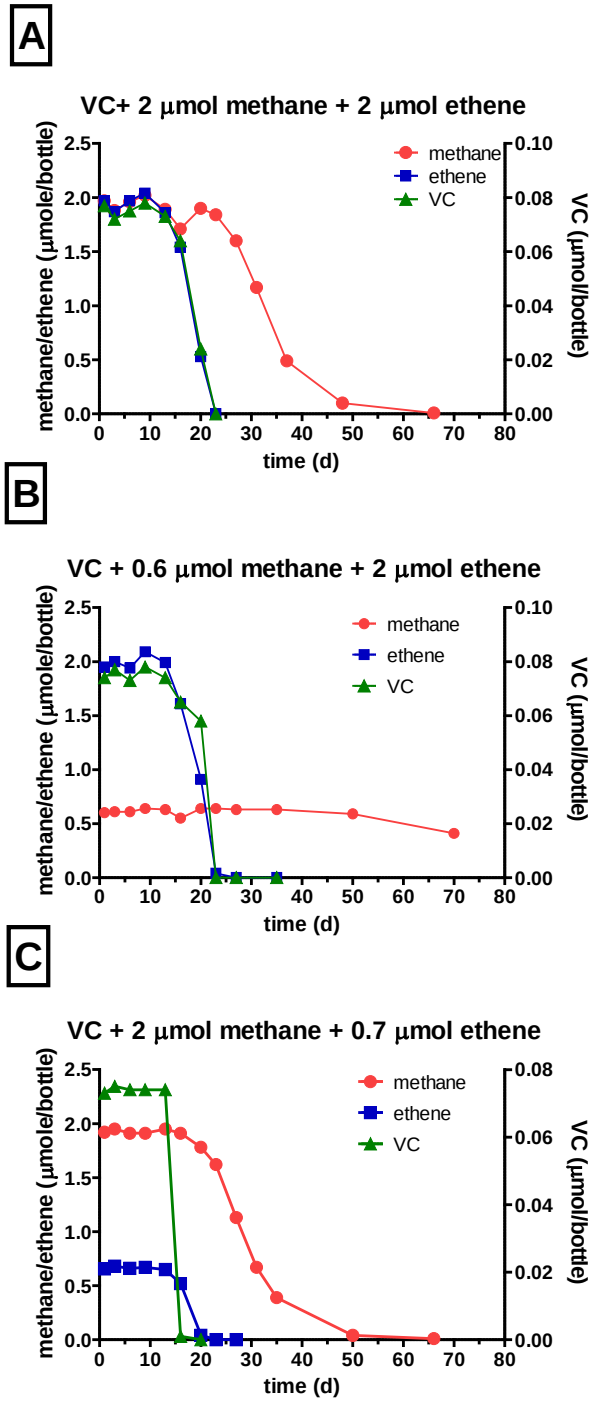

Figure 32. Aerobic biodegradation of 0.08 µmol VC in the presence of a range of methane and ethene concentrations in microcosms constructed with groundwater from the Carver site containing methanotrophs, etheneotrophs, and vinyl chloride-assimilating bacteria. Comparison of substrate utilization under different conditions was based on lag time and days for 50% utilization.

Subtask 3.3 Methane, ethene, and VC enrichment cultures from Carver site well RB63-I

Enrichment cultures were created in order to conduct additional experiments with selected microbial types and to assist in interpretations of previous BCI microcosm experiments with groundwater containing a mixture of types. These cultures could be further purified and/or genetically evaluated, since it may be of interest to know their relationship to organisms used for publications, as well as to commercially-available cultures. Using these enrichment cultures we tested some specific questions, as described below.

3.3.1 Methanotroph enrichment culture from Carver site well 63-I

Groundwater from well 63 I was obtained March 24, 2011 and refrigerated. On April 15, 2011, an enrichment culture for methanotrophs was initiated by adding 1 ml of groundwater to 100 ml of mineral media in 160 ml serum bottles, and feeding with 3 ml of methane (also 3 ml air). After methane was consumed, on 5/20/11, the bottle headspace was flushed to remove CO_2, then re-sealed and given additional 3 ml methane. Additional subculturing steps are summarized below:

- Subculturing, 1/100. On 9/12/11, one ml of the above enrichment culture was transferred to 100 ml of mineral media in a 160 ml serum bottle, and fed with 3 cc methane.
- Subculturing, 1/100. On 12/23/11, one ml of the above enrichment culture was transferred to 100 ml of mineral media in a 160 ml serum bottle, and fed with 3 cc methane.
- Subculturing, 1/100. On 3/1/12, one ml of the above enrichment culture was transferred to 100 ml of mineral media in a 160 ml serum bottle, and fed with 9 ml methane
- Subculturing 1/1000. On 3/13/12, subculturing was conducted using 0.1 ml of culture into 100 ml of mineral media, and feeding 9 ml methane.
- Subculturing 1/1000. On 4/4/12, feeding 3 ml methane, fed again 5/15 (6 ml) and 6/6 (9 ml).
- Subculturing 1/1000. On 4/24/12, feeding 3 ml methane fed again 5/15, 6 ml methane (June 6), divided with media 50:50, kept both bottles. Fed 7/9/12 with 6 ml methane.
- Total dilution since 3/24/11 is 10^{17}-fold

3.3.2 Enrichment culture Experiment #1: "Do Carver Methanotrophs Oxidize VC in the Absence of Methane?"

The Carver methanotroph enrichment dated 4/4/12 was used as a source of culture for this experiment. At the time that 0.2 ml aliquots of culture were removed from this source, the culture was in 'log phase' growth with 55 µmol/bottle methane present. To initiate the experiment, 0.2 ml of culture was transferred to each of three 160 ml microcosm bottles containing 100 ml of mineral media and 60 ml air headspace.

There was a 1 to 2-hour delay before adding methane and VC to these experimental bottles. Bottles #1 and #3 then received 36 µL methane, and bottles #2 and #3 received 15 µL dilute VC (the same concentrations as used in the 2011 microcosm experiments described above). The experimental bottles were put on a slow orbital shaker. Analyses were conducted starting on day 1, after overnight equilibration.

Methane was utilized starting around day 3 (Figure 33). Without VC, 97.5% used by day 12 With VC, 94% of methane was used. By day 12, without methane, VC was not oxidized. With methane, 20% of the VC was oxidized.

Because 1-2 hr elapsed before the methane was added to the experimental bottles, it was possible that the methane monooxygenase became un-induced. For that reason, the experiment was repeated on 5/22/12, as described below.

The Carver methanotroph enrichment dated 4/24/12 was used as a source of culture for the repeat experiment. At the time that 0.3 ml aliquots of culture were removed from this source, the culture was in 'log phase' growth with 35 µmol/bottle methane present.

The experimental bottles contained 100 ml of mineral media and 60 mL air headspace. Prior to adding culture to the experimental bottles, bottles #1 (methane only) and #3 (methane + VC) received 36 µL methane, bottles #2 (VC only) and #3 (methane + VC) received 14 µL dilute VC, both injected into the media. Then 0.3 ml of culture was transferred to each of three 160 ml microcosm bottles. Thus, there was no occasion for the MMO to become un-induced. Bottles were incubated on a slow orbital shaker. Analyses were conducted starting on day 1, after overnight equilibration of gases.

Methane was extensively utilized by day 3, consistent with no lag. By day 7, without VC, 95.4% of methane was used. With VC, 94.7% of methane was used. In bottle #2, by day 21, without methane, VC was at most 4% oxidized. In bottle #3, by day 10, when methane had been nearly fully utilized, VC was 31% oxidized. By day 21, during 11 days with no methane, an additional 10% of the VC had been oxidized (Figure 34).

The results indicate that VC oxidation by well-fed methanotrophs, after methane is nearly depleted, may continue at a very low rate for several days. The results are consistent with our interpretation of the 2011 microcosm data that starved methanotrophs did not carry out oxidation of VC in the absence of methane.

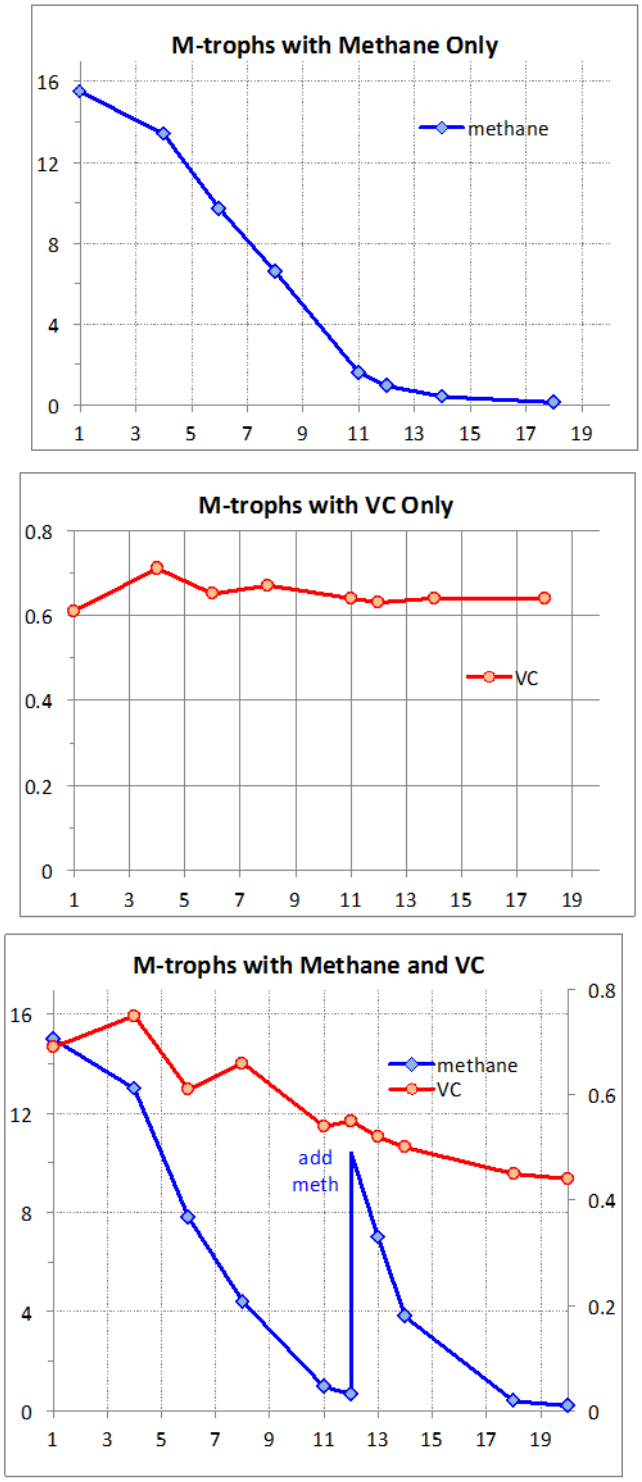

Figure 33. Biodegradation of methane, VC and a methane+VC mixture by methane enrichment cultures derived from Carver well RB63I. These results indicate that the methanotrophs in this culture cannot degrade VC in the absence of methane, and slowly cometabolize VC in the presence of methane.

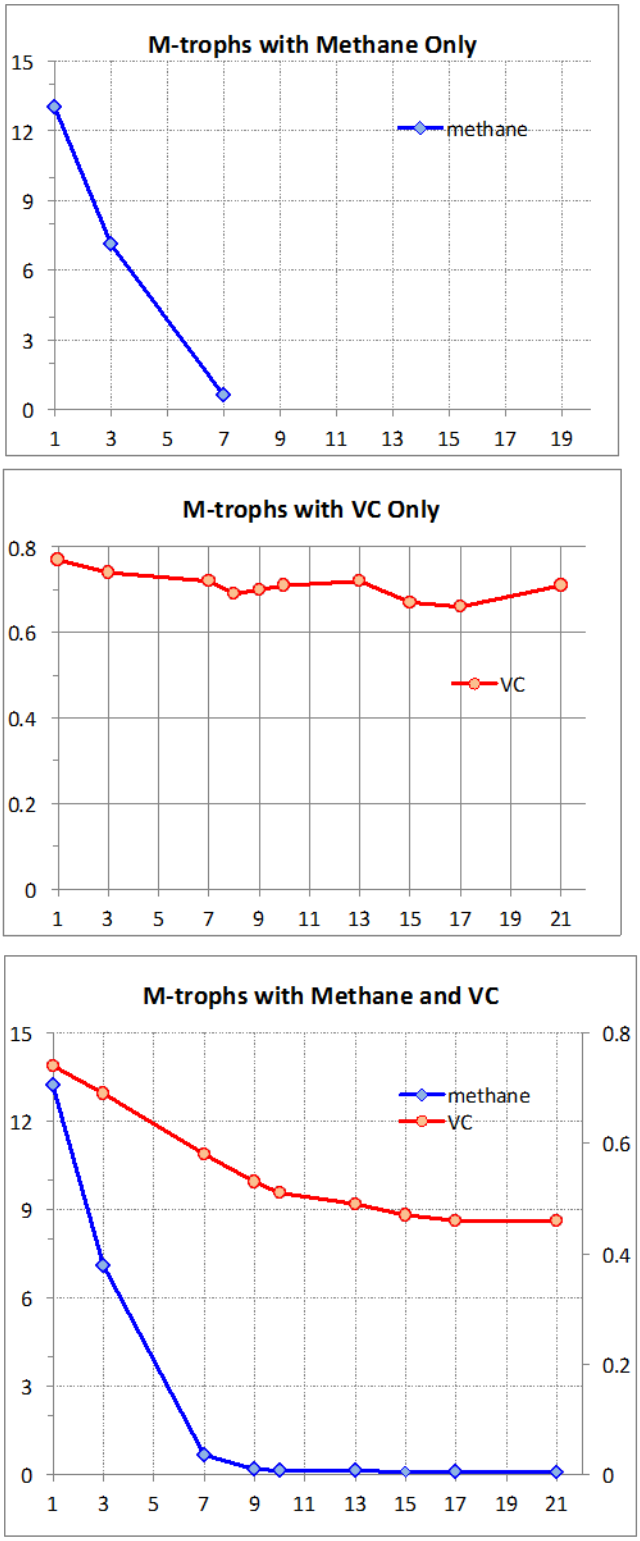

Figure 34. Biodegradation of methane, VC and a methane+VC mixture by methane enrichment cultures derived from Carver well RB63I. These results are a repeat of the experiment depicted in Figure 33 and confirm that the methanotrophs in this culture cannot degrade VC in the absence of methane, and slowly cometabolize VC in the presence of methane.

3.3.3 Enrichment culture Experiment #2, 6/11/12 "Do Carver Site methanotrophs oxidize ethene to epoxyethane?"

This experiment was conducted at a much higher methane concentration, and a much higher culture density (milky–appearing culture vs. clear-appearing culture), although the cell density was not estimated. This was done because the gas chromatographic detection limit for epoxyethane is very high (6 µM).

The experiment used a methanotroph culture which had been without methane for about 5 days. On 6/6/12, the entire culture was divided into two experimental bottles by using 50 ml of culture and 50 ml of mineral media in each bottle, which were then given 9 ml of methane. Growth on methane was observed for 4 days. On day 4.5, when the methane concentration was about 3,000 µM, 50 µL of ethene was injected into bottle #1 only. The initial concentration of ethene was calculated. Additional O_2 (6 mL) was added to bottle #1 on day 4.5, and to bottle #2 on day 5.5. Ethene was rapidly oxidized by the methanotrophs (7 µM in 3 hours), and that 7 µM epoxyethane was produced during that time (Figure 35).

Ethene was > 99% oxidized in 24 hours, but a molar equivalent of epoxyethane was not present likely because it had already been further oxidized by the methanotrophs. The epoxyethane was completely oxidized by day 7.5. These results demonstrate that Carver methanotrophs *can* oxidize ethene to epoxyethane, which is consistent with our interpretation of the results obtained for our 2011 microcosm experiment.

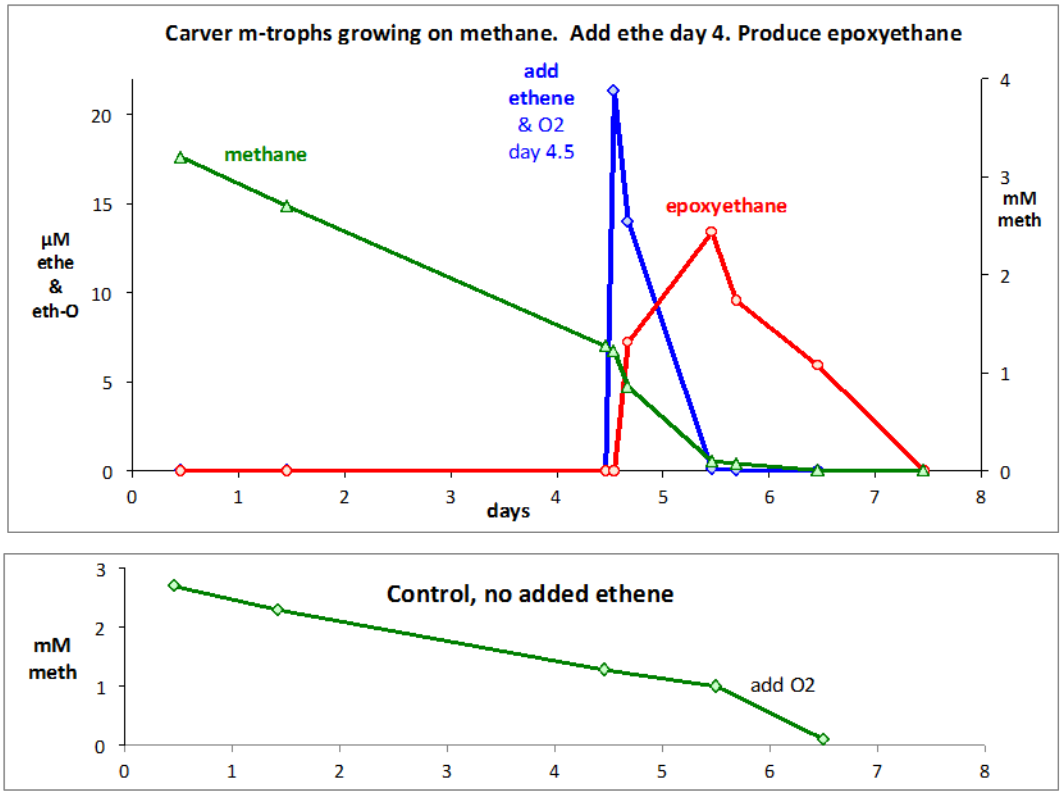

Figure 35. Biodegradation of ethene and formation of epoxyethane by methane enrichments cultures from the Carver site. This indicates that methanotrophs can produce epoxyethane, a molecule known to stimulate etheneotroph gene expression.

3.3.4 Etheneotroph enrichment culture from Carver site well 63-I

- Initial enrichment 1:100. Groundwater from well 63I was obtained March 24, 2011 and refrigerated. On April 15, 2011, an enrichment culture for ethenotrophs was initiated by adding 1 ml of groundwater to 100 ml of mineral media in 160 ml serum bottles, and feeding with 1 cc of ethene (also 5 cc air). After ethene was consumed, on 5/20/2011, the bottle headspace was flushed to remove CO_2, then re-sealed and given additional 1 cc ethene.
- Subculturing, 1:100. On 9/12/2011, one ml of the above enrichment culture was transferred to 100 ml of mineral media in a 160 ml serum bottle, and fed with 1 cc ethene.
- Subculturing, 1:100. On 12/23/2011, one ml of the above enrichment culture was transferred to 100 ml of mineral media in a 160 ml serum bottle, and fed with 1 cc ethene
- Subculturing, 1:100. On 1/25/2012, one ml of the above enrichment culture was transferred to 100 ml of mineral media in a 160 ml serum bottle, and fed with 1 cc ethene
- Subculturing, 1:100. On 3/1/2012. one ml of the above enrichment culture was transferred to 100 ml of mineral media in a 160 ml serum bottle, and fed with 1 cc ethene
- Subculturing 1:1000. On 3/13/2012, subculturing was conducted using 0.1 ml of culture into 100 ml of mineral media, and feeding 1 cc ethene.
- Subculturing 1:1000. On 3/27/2012, 1 cc ethene
- Subculturing 1:1000. On 4/24/2012, 1 cc ethene

Total dilution as of 4/24 = 10^{19}-fold.

- Subculturing 1:330. On 7/9/2012, 2 cc ethene

This culture was used as the inoculum for the following set of experiments.

3.3.5 Enrichment culture experiment #3: Effect of epoxyethane on starving Carver etheneotrophs to resume ethene use.

In preparation for this experiment, BCI tested the etheneotroph culture after varying starvation periods to determine the length of starvation required to cause a lag after when subcultured into new media containing ethene. The experiment was conducted when a lag time of at least 6 days could be achieved following ethene starvation. In this initial experiment, three different epoxyethane concentrations were tested. A slight decrease in the time for 50% ethene use in the presence of increasing amounts of epoxyethane was observed (Figure 36, Table 28).

Table 28. The effect of epoxyethane concentration on time for 50% ethene use in Carver well 63I derived ethene enrichment cultures that were subjected to ethene starvation. Bottles contained mineral media and 82 µmols ethene/bottle, with 0.3 ml ethenotroph culture added per bottle at the start of the experiment.

microcosm	Epoxyethane µmols/bottle	Time (days) for 50% use of ethene
1	0	10.2
2	0	9.0
3	0.7	8.6
4	2.1	8.4
5	6.2	8.3

Because epoxyethane was also being consumed during the experiment (presumably by etheneotrophs) a repeat experiment was conducted with the same setup, except that 3 bottles received no epoxyethane, and 3 bottles received 6 µmole/bottle epoxyethane. This more clearly shows that epoxyethane, which can be produced by methanotrophs in the presence of ethene, can stimulate etheneotrophs and reduce the time for ethene use in a starved etheneotroph culture (Figure 37).

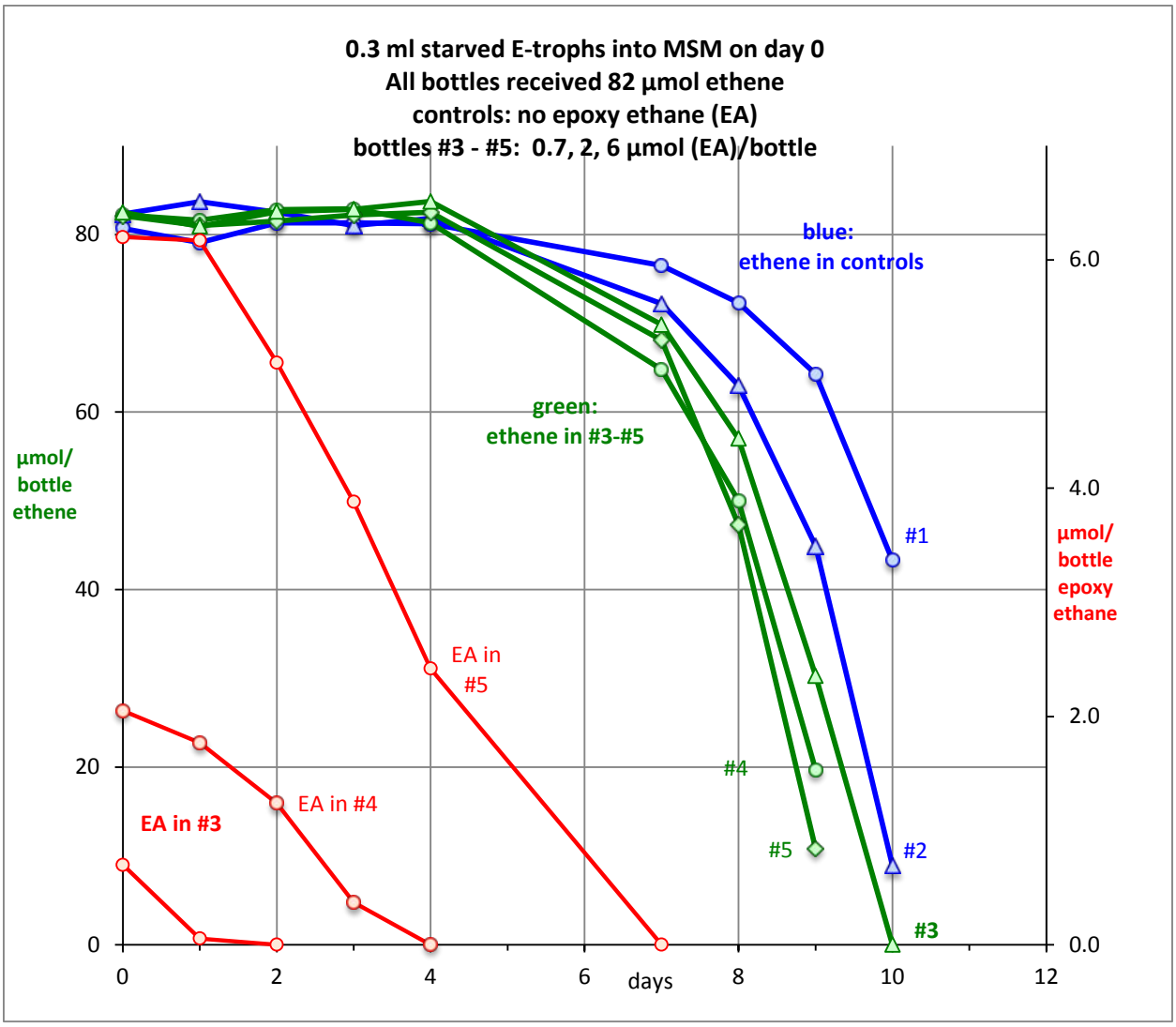

Figure 36. The effect of epoxyethane concentration on time for 50% ethene use in Carver well 63I derived ethene enrichment cultures that were subjected to ethene starvation.

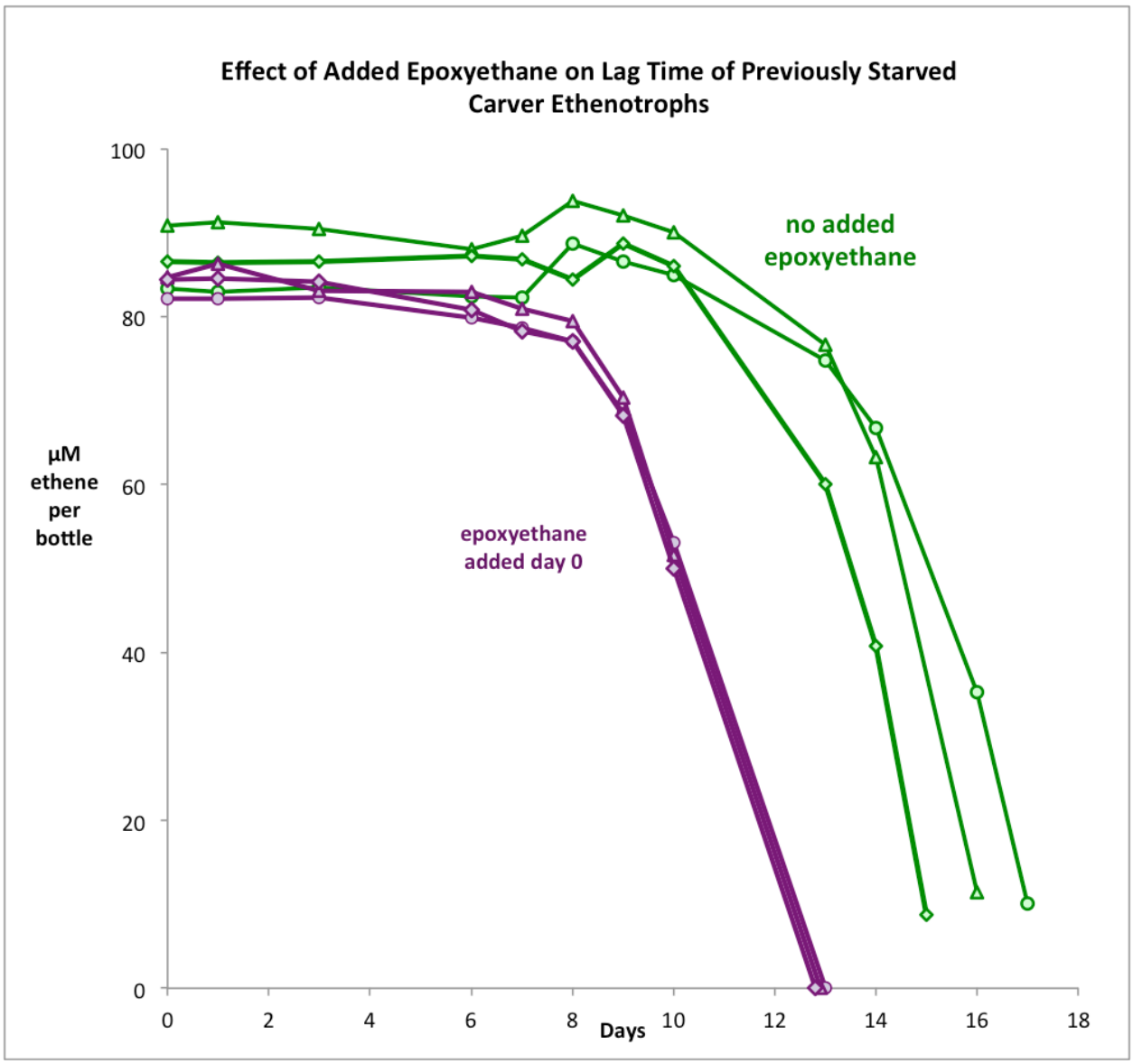

Figure 37. The effect of epoxyethane concentration on time for 50% ethene use in Carver well 63I derived ethene enrichment cultures that were subjected to ethene starvation. Three bottles received no epoxyethane (green lines) , and 3 bottles received 6 µmole/bottle epoxyethane (purple lines).

3.3.6 VC Assimilators (VCA) from Carver site well 63-I

- Initial enrichment 4:10 Groundwater from well 63 I was obtained Sept 28, 2009, and refrigerated. On Oct 15, 2009, an enrichment culture for VCA (Presence / Absence Tests) was initiated by adding 40 ml of groundwater to 60 ml of mineral media in 160 ml serum bottles. To remove native ethene and methane, the groundwater/media was flushed with air at 100 cc/min for at least 2 min. After sealing the bottles, VC was added by injecting 0.25 cc of dilute VC gas stock (prepared by adding 0.85 ml of VC in methanol solution from Restek, to a sealed 160 ml serum bottle containing 77 ml of distilled water) to give 10 µM. Additional 30 µM was injected into the same bottle on 2/2/10, 3/3/10, 3/25/10, 5/14/10, 7/15/10, 9/17/10, 11/23/10.
- Subculturing 1:100 The above enrichment culture was subcultured on 1/25/11 by transferring one ml into 100 ml of mineral media and fed 40 µM VC. The same bottle was re-fed with 50 µM VC on 3/2 and on 3/9.
- Subculturing 1:500. This culture was again sub-cultured, 0.2 ml into 100 ml media on 3/13/12, and fed 50 µM VC.
- Subculture 1:1000. The above culture was subcultured 1:1000 on 3/27/12. Fed 50 µM VC.
- Subculture 1:1000. The above culture was subcultured 1:1000 on 4/24/12. Fed 50 µM VC. Fed again 6/6/12 and on 7/9/2 both 50 µM VC.

Total dilution since 9/28/09 = 1.25×10^{11}.

All enrichment cultures were shipped from BCI to the University of Iowa, where we continue to maintain them for purposes of isolating new VC-assimilating strains and to be available for additional experimentation.

Subtask 3.4 Pure culture experiments with *Mycobacterium* strain JS622 and pMMO-expressing *Methylocystis* sp. ATCC 49242

To further interpret the results of the BCI microcosm and enrichment cultures studies, we initiated experiments with mixtures of methanotrophic and etheneotrophic pure cultures. The rationale behind these experiments was that we could examine the cometabolic behavior of cultures alone and in mixtures, control the amount of methane, ethene, and VC present in the bottles, and also control the relative amount of each microbial group in the experiments. We obtained two methanotrophic cultures (Type I *Methylococcus capsulatus* and Type II *Methylocystis* sp. ATCC49242) from the ATCC. In preliminary experiments we found that the *Methylococcus capsulatus* strain did not grow well at room temperature, while the *Methylocystis* strain grew well at room temperature in MSM. Thus we used *Methylocystis* sp. ATCC49242 for the remainder of the study. We also used ethene-assimilating *Mycobacterium* strain JS622 in this study.

We found that under aerobic conditions, both AkMO-expressing *Mycobacterium* strain JS622 and pMMO-expressing *Methylocystis sp.* ATCC 49242 are able to cometabolize VC separately. Different concentrations of methane, ethene and VC were provided in order to test how the metabolism (of ethene and methane respectively) and cometabolism of VC in the two microorganisms would be affected. The effect of different ratios of the two microbial groups on VC degradation patterns was also examined.

3.4.1 Biodegradation of equal masses of methane, ethene and VC by Mycobacterium strain JS622

In initial experiments we evaluated the cometabolic activity of ethene-oxidizing *Mycobacterium* strain JS622 in the presence of equal masses of methane, ethene and VC (40 µmol each; Table 2). However, due to the diverse values of dimensionless Henry's Law constants: methane (24.4), ethene (7.15) and VC (1.0) *(65)*, the aqueous concentrations of VC were 5-fold higher than ethene and more than 10-fold higher than methane approximately. The theoretical aqueous concentrations of methane, ethene, and VC were: 18 µM, 57 µM, and 250 µM. However, the actual amount of gases that were added into the bottles were often smaller than the theoretical values. We suspect that this resulted from an imprecise VOC delivery method.

We did not expect that ethene-grown *Mycobacterium* JS622 would degrade methane as the AkMO is not known to accept C_1 compounds as substrates. Indeed, methane was not degraded in the presence of 10 µM methane (Figure 38a). JS622 rapidly oxidized the initial ethene (39 µM) at the rate of 31 µmol/day (Figure 38b), and VC (20 µM) was degraded at the initial rate of 6 µmol/day (Figure 38c). This quick degradation of the VC in this bottle likely led to an erroneous measurement for the VC oxidation rate as described below.

Studies have shown that AkMO catalyzes the initial steps of the aerobic microbial VC and ethene biodegradation pathways *(71)*. The similar chemical structure between ethene and VC apparently allows AkMO to catalyze VC oxidation, even though the organisms are not dependent on VC as a carbon and energy source *(36)*.

In bottles containing equal masses of methane and VC, 182 µM VC was degraded at the initial rate of 16 µmol/day, which was faster than VC was being degraded alone (6 µmol/day), while 13 µM of methane remained (Figure 39a). Since methane appears to have no effect on AkMO activity in JS622, this experiments suggests that our initial estimate of VC degradation alone was inaccurate.

In the bottle that received equal masses of ethene and VC, 217 µM VC was degraded at the initial rate of 11.5 µmol/day. On the other hand, 40 µM of ethene was degraded at the rate of 23 µmol/day (slower than when present as a single substrate). Ethene was degraded more quickly than VC at VC concentrations about 5-fold higher than ethene, suggesting that the active site of the JS622 AkMO preferentially accepts ethene over VC. However, the presence of VC did appear to compete for the AkMO active site as evidenced by the slower ethene degradation rate in the presence of VC (Figure 39b).

When methane and ethene were both present in a bottle containing strain JS622, 37 µM ethene was degraded at a rate of 30 µmol/day, and methane was not degraded, which confirms that AkMO does not degrade methane given that the initial degradation rate of ethene remained the same (Figure 39c). The presence of methane did not affect the ethene degradation rate. This is consistent with degradation behavior seen in other bottles. When all three substrates were present, JS622 VC and ethene oxidation rates and degradation patterns were similar to those in the presence of ethene (10.5 µmol/day for VC (176 µM) degradation and 22 µmol/day for ethene (35 µM) degradation (Figure 39d)).

Overall, this experiment demonstrates that ethene-grown *Mycobacterium* strain JS622, at the cell concentration employed (initial OD_{600} = 0.1):

- does not degrade methane
- metabolizes ethene at a rate of ~ 30 µmol/day when present alone or with methane
- cometabolizes VC (20-182 µM) at a rate of ~6-16 µmol/day when present alone or with methane
- metabolizes ethene (35-40 µM) at a diminished rate of ~22 µmol/day in the presence of VC (176-217 µM)
- cometabolizes VC (217 µM) a rate of (~11 µmol/day) when present with ethene (~40 µM)
- when VC and ethene are both present, their degradation rates are slower than when they are present singly, suggesting competitive inhibition for the AkMO active site occurs at these concentrations.

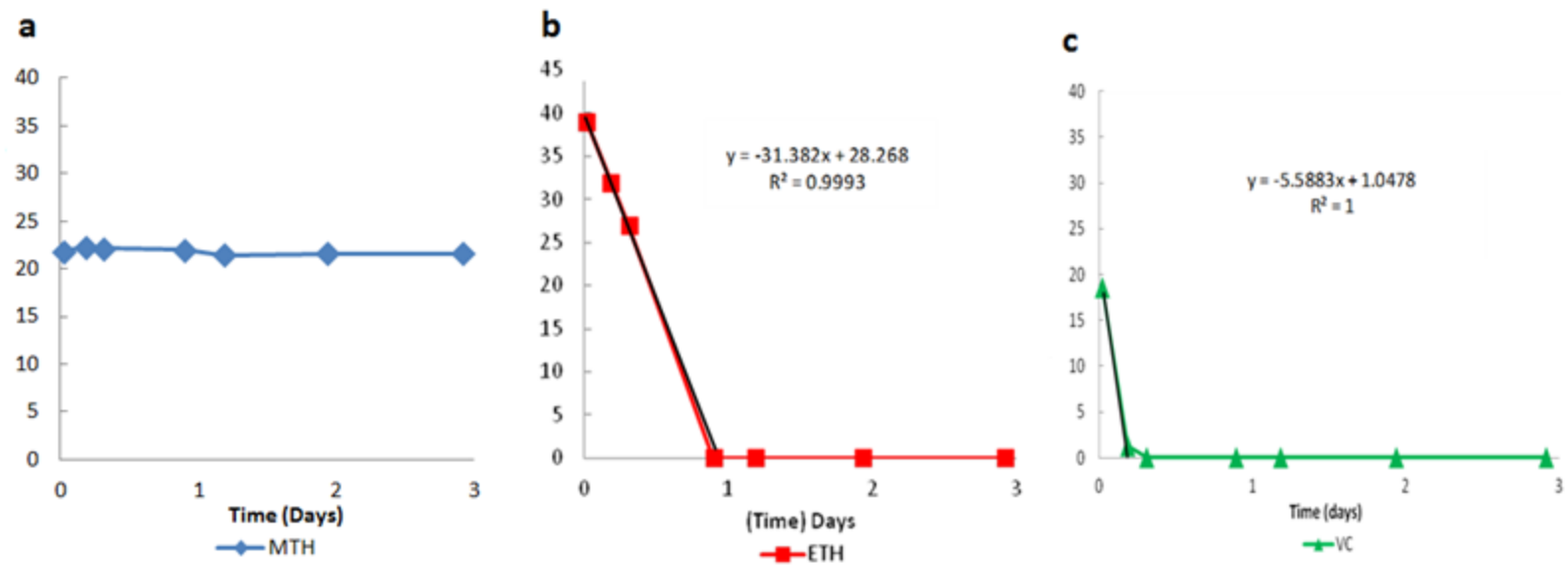

Figure 38**.** Degradation of methane (a) ethene (b) and VC (c) as single substrates for ethene-grown JS622 cells in separate bottles. All values shown are in µM. The slopes of the regression lines shown represent the degradation rates (initial OD_{600} = 0.1).

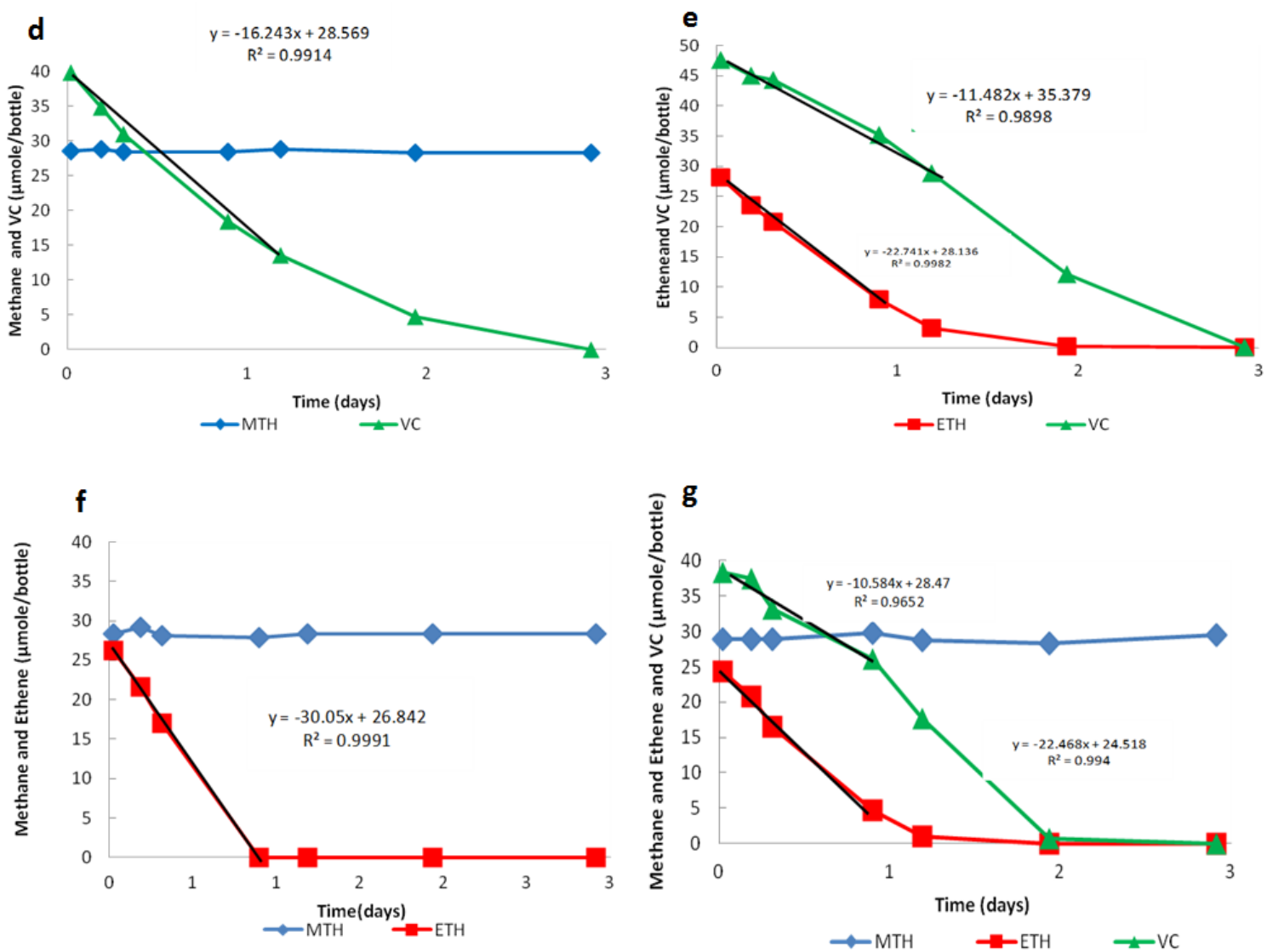

Figure 39. Aerobic biodegradation of methane+VC (d), ethene+VC (e), methane+ethene (f), methane+ethene+VC (g) by ethene-grown JS622. The slopes represent the degradation rates.

3.4.2 Biodegradation of equal mass of methane, ethene and VC by Methylocystis strain ATCC 49242

The same experimental design was used to evaluate the cometabolic activity of pMMO-expressing *Methylocystis sp.* ATCC 49242 in the presence of equal initial masses (40 µmol) of methane, ethene and VC. The calculated theoretical initial aqueous concentrations of methane, ethene, and VC were: 18 µM, 57 µM, and 250 µM.

Methylocystis sp. degraded 11 µM of methane at the rate of 75 µmol/day (Figure 40a). Methane grown *Methylocystis sp.* produces particulate methane monooxygenase (pMMO) that can bind and fortuitously oxidize ethene and chloroethenes *(6, 91)*. However, 39 µM of ethene was degraded at the rate of 22 µmol/day suggesting that methane starvation reduced the pool of active enzyme available for the degradation of ethene (Figure 40b). Therefore, when the concentration of ethene was about 3-fold higher than methane, the degradation rate decreased a little more than 3 fold. Gradual degradation of 10 µM of VC (3 µmol/day) in the absence of methane shows that *Methylocystis sp.* can also cometabolize VC (Figure 40c).

In the bottle with 12 µM of methane and 101 µM of VC, 38% of methane was degraded at the rate of 9 µmol/day, and 63% of VC was degraded at a rate of 13 µmol/day, respectively, by *Methylocystis sp.*, suggesting that VC inhibits methane degradation. This result is consistent with the BCI microcosm experiments fed only methane and VC, where methane utilization by methanotrophs was inhibited by an aqueous VC concentration more than 10-fold higher than methane (Figure 41d)*(86)*. In the bottle fed with 41µM ethene and 156 µM VC, *Methylocystis sp.* only degraded 12% of the ethene at a rate of 16 µmol/day and 23% of the VC at a rate of 3 µmol/day because no necessary cofactors are generated during the transformation of the cosubstrate (Figure 41e). When 14 µM methane and 38 µM ethene were present in the bottle, ethene was degraded at a rate of 30 µmol/day and methane was degraded at a rate of 14 µmol/day by *Methylocystis sp.*, 5-fold slower than when methane was being oxidized alone. This result suggests that the presence of ethene not only slowed the rate of methane consumption by its obligate degrader, but also competed for the active site (Figure 41f). In the bottle that contained 12 µM of methane, 24 µM of ethene, and 39 µM of VC, 72% of the ethene, 41% of the VC, and 23% of the methane was degraded by *Methylocystis sp.* at the rate of 17 µmol/day, 2 µmol/day and 6 µmol/day respectively (Figure 41g).

Overall, these results suggest that the ability of methane-grown *Methylocystis* strain ATCC 49242 at the cell concentration employed (initial OD_{600} = 0.1):

- rapidly metabolizes methane (75 µmol/day) as a single substrate
- cometabolizes ethene (22 µmol/day) and VC (3 µmol/day) as single substrates
- displays substantially impaired methane metabolism in the presence of ethene and/or VC, suggesting that ethene and VC compete for the *Methylocystis* pMMO active site.
- Ethene and VC cometabolism is enhanced by the presence of methane, although it is likely that pMMO is damaged by the generation of epoxide products of pMMO that are known to be toxic to methanotrophs (epoxyethane and chlorooxirane, respectively) *(71)*.

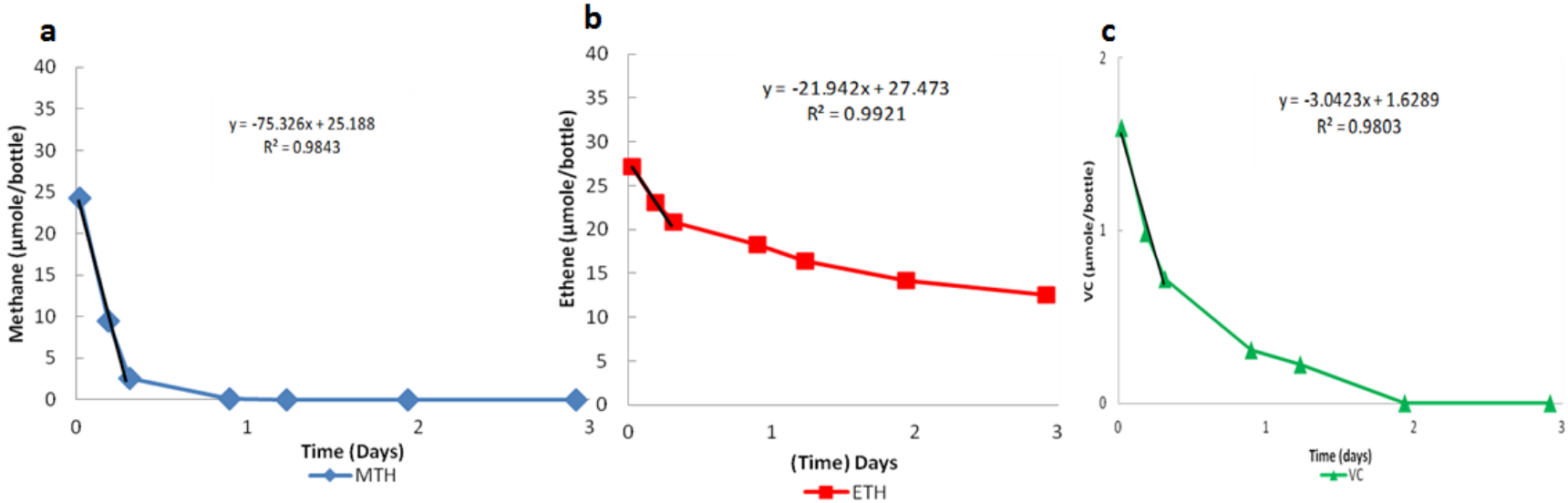

Figure 40**.** Degradation of a) methane, b) ethene, and c) VC as single substrates for methane-grown *Methylocystis* sp. ATCC49242 in separate bottles. The slopes of the regression lines shown represent the degradation rates.

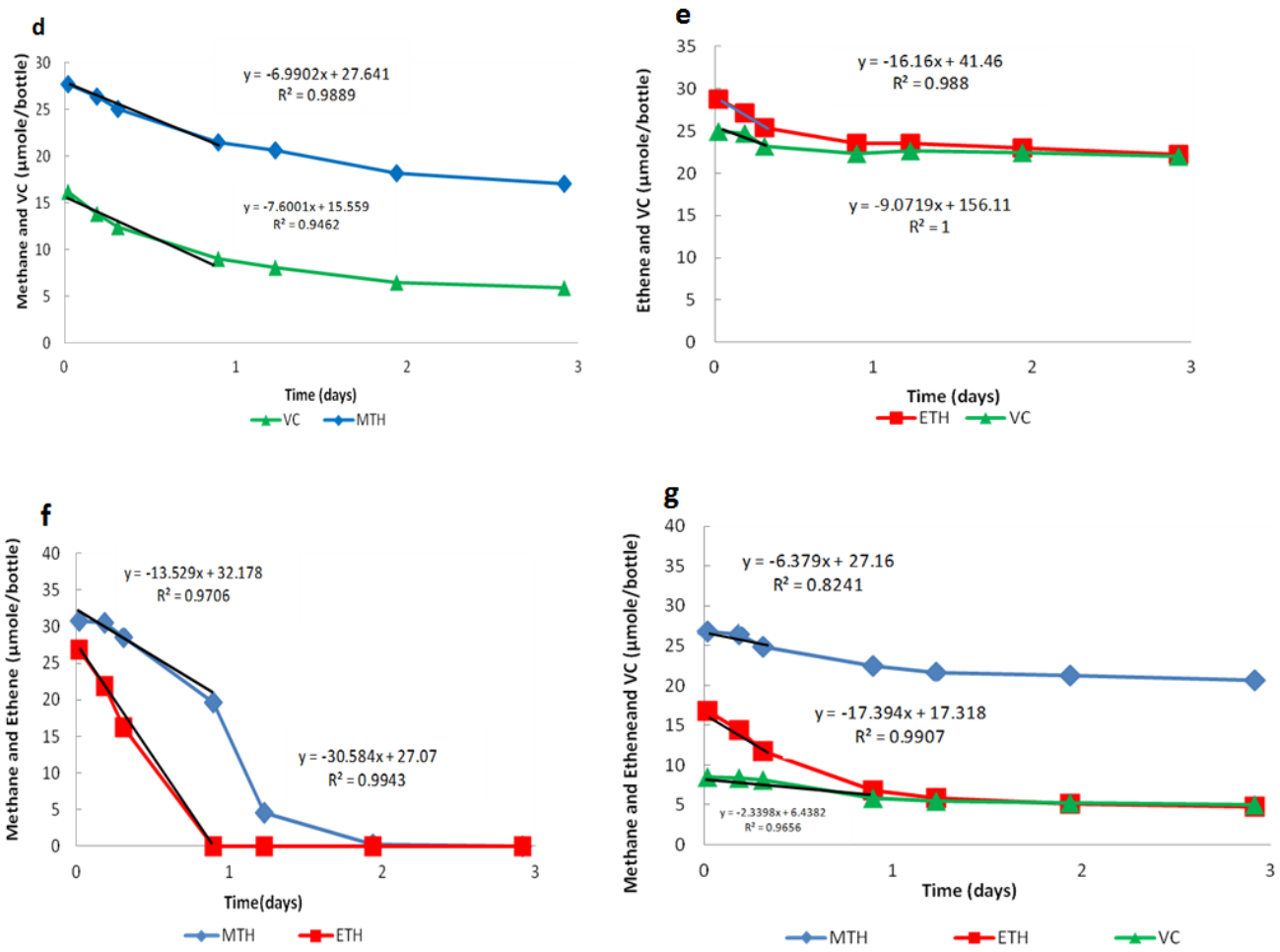

Figure 41**.** Aerobic biodegradation of methane+VC(d), ethene+VC (e), methane+ethene (f), methane+ethene+VC (g) by *Methylocystis* ATCC49242. The slopes of the regression lines shown represent substrate degradation rates.

3.4.3 Biodegradation of equal masses of methane, ethene and VC by a mixture of JS622 and Methylocystis ATCC 49242

Having investigated the cometabolic behavior of ethene-oxidizing *Mycobacterium* strain JS622 and methane-oxidizing *Methylocystis sp.* ATCC 49242 as pure cultures, we asked how the presence of both microbial groups in a single culture will affect VC cometabolism. As an initial basis of comparison, we used equal masses (40 µmol) of methane, ethene and VC. This corresponded to aqueous concentrations of 18 µM (methane), 57 µM (ethene), and 250 µM (VC). The ratio of JS622 to *Methlocystis sp.* in this experiment was 1:1.

In this mixture, we expect that *Methylocystis sp.* will be solely responsible for methane degradation. As expected, 12 µM of methane was rapidly oxidized at a rate of 69 µmol/day, which was similar to the rate observed with *Methylocystis sp.* alone (11 µM at 75 µmol/day) (Figure 42a). In a separate bottle, 40 µM ethene was degraded at a rate of 30 µmol/day (Figure 42b). This is the same rate as observed when 40 µM ethene was degraded by JS622 alone, but the cell concentration of JS622 in this experiment was 50% of the cell concentration in the JS622 only experiment. This result suggests that both strain JS622 and strain ATCC 49242 were participating in ethene degradation. VC (43 µM) degradation occurred at a rate of 6 µmol/day, which was the same rate when degraded by pure JS622 culture, but 3 µmol/day faster than being degraded by the *Methylocytis* culture (Figure 42c).

In the bottle that contained 14 µM of methane and 106 µM of VC, VC was completely degraded at the rate of 12 µmol/day and 42% of methane was degraded at the rate of 11 µmol/day (Figure 43d). This result indicated that methane degradation was inhibited in the presence of a VC concentration approximately 10-fold higher than methane, similar to what was observed when being degraded by pure *Methylocystis sp.* VC cometabolism in the presence of methane was slower when compared to degradation by JS622 alone (182 µM VC, 12 µmol/day), but improved in the presence of methane by ATCC49242 alone since only 63% of the VC was degraded at a rate of 9 µmol/day.

In the bottle that received 40 µM of ethene and 74 µM of VC, ethene was degraded at a rate of 23 µmol/day, and VC was 11 µmol/day. With the same initial concentration of ethene (40 µM), ethene was degraded slower (by 2 µmol/day) in the mixed culture compared to consumption by JS622 alone, and 7 µmol/day faster when being consumed by ATCC49242 alone at its initial degradation rate (Figure 43e). In comparison to VC cometabolism in the presence of ethene by JS622, 74 µM of VC was degraded slower by 7 µmol/day (VC conc. 217 µM), only 12% of VC was being degraded in three days by pure culture of ATCC49242.

When 14 µM of methane and 40 µM of ethene were both present, ethene was degraded at the rate of 28 µmol/day, and methane was degraded at a rate of 13 µmol/day. At the same concentration, the rate of ethene oxidation (30 µmol/day) and methane oxidation (13 µmol/day) similar in comparison to degradation by 100% *Methylocystis sp*, and by 100% JS622 (31 µmol ethene/day).This result suggests that both microbial groups metabolize their respective primary substrates without much interference (Figure 43f).

In the bottle that contained 42 µM of ethene, 147 µM of VC, and 10 µM of methane, 38% of the ethene, 15% of the VC, and 7% of the methane was degraded by both bacterial groups at initial

degradation rates of 15 µmol/day, 2 µmol/day and 3 µmol/day, respectively (Figure 43g). The results resembled the behavior of pure ATCC49242 cultures fed with the three gases, suggesting that ATCC49242 did play a role in ethene and VC cometabolism. Comparing degradation of the ethene and VC by pure JS622 cultures, the ethene degradation rate was 6 µmol/day slower and VC degradation rate was 9 µmol/day slower. These contrasts suggest that pMMO activity was inhibited in the presence of a VC concentration 10-fold higher than methane, which also affects the ability of the *Methylocystis* sp. to cometabolize ethene and VC (Figure 43g).

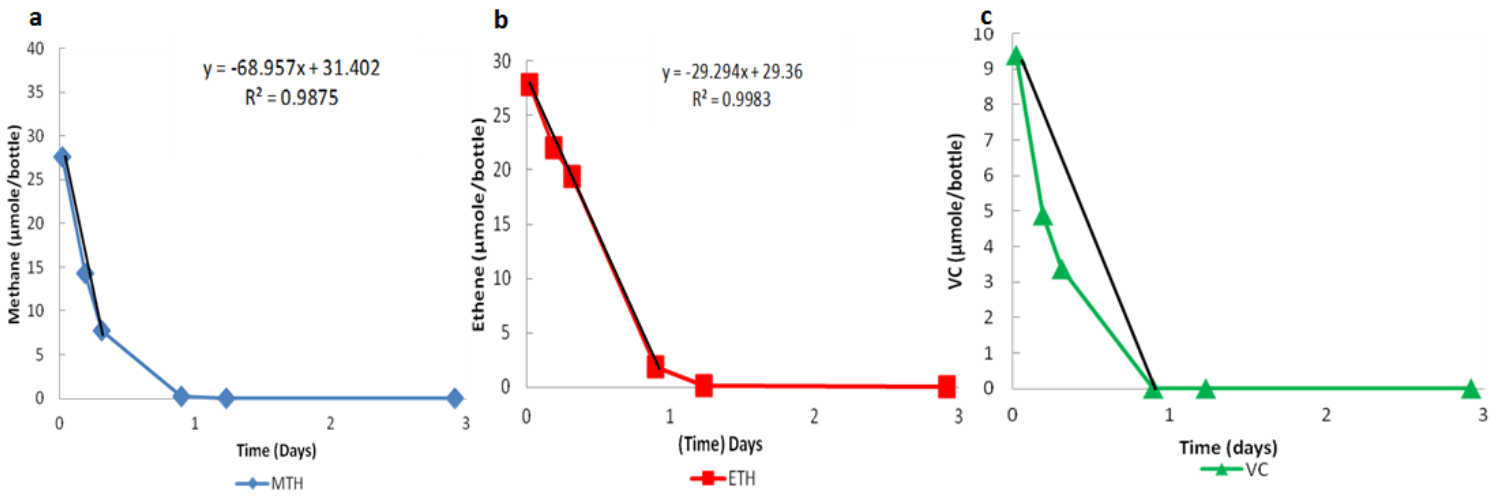

Figure 42**.** Degradation of methane (a), ethene (b), VC (c) as a sole substrate for a 1:1 JS622 and ATCC49242 mixture (initial OD_{600} = 0.1). The slopes of the regression lines represent the degradation rates.

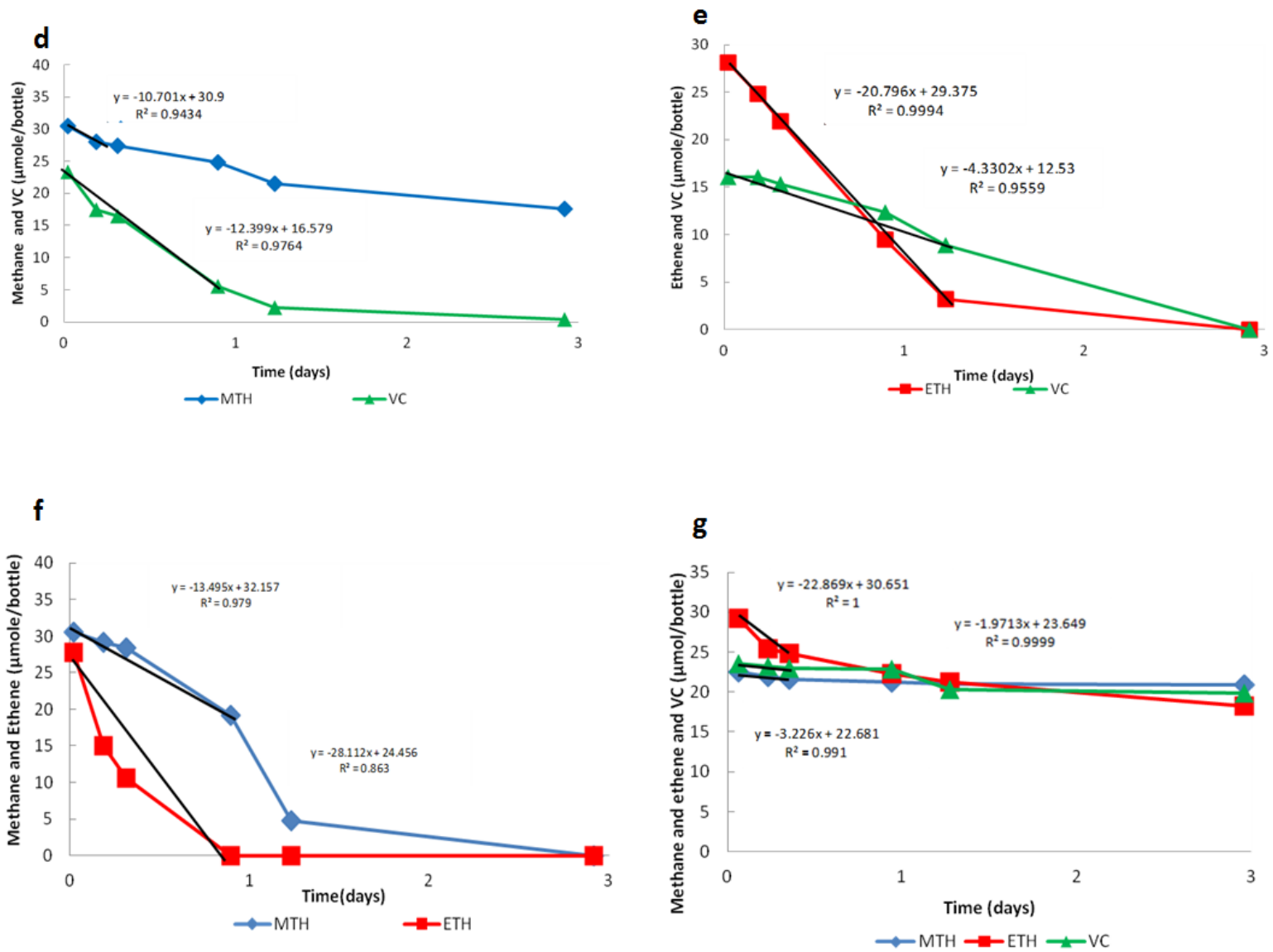

Figure 43. Aerobic biodegradation of methane+VC (d), ethene +VC (e), methane+ethene (f), methane+ethene+VC (g) by a JS622 and ATCC49242 (1:1) mixture. The slopes represent the degradation rates.

3.4.4 Biodegradation of 400 µmol of methane, 400 µmol of ethene and 20 µmol of VC by Mycobacterium strain JS622

In March 2010 and March 2011, Bioremediation Consulting, Inc. performed microcosm studies from groundwater taken from a VC-contaminated site in Carver, MA (well 63-I) to determine how the native mixed population of methanotrophs, etheneotrophs and VC-assimilating bacteria biodegrade VC under varying concentrations of methane alone and ethene alone, and mixtures of these substrates *(39)*. In 2011 experiments, the microcosms were fed with methane, ethene, and VC in the following concentration: 1.6, 1.6 and 0.08 µmol/bottle, which corresponded to 1 µM, 3 µM, and 0.47 µM respectively (i.e. the methane and ethene masses tested were 20 times greater than VC). Therefore in the following experiments, we utilized the same mass ratio of methane and ethene to VC to better align our experimental design with pure cultures to the BCI experimental design in groundwater microcosms. In this experiment the theoretical initial aqueous concentrations of methane, ethene, and VC were: 180 µM, 570 µM, and 125 µM. The reason why we conducted these experiments with a 20-fold higher concentration than used in the Bioremediation Consulting, Inc. microcosm study was because we were also using much higher cell concentrations in order to obtain the data within reasonable time period.

We did not expect that ethene-grown *Mycobacterium* JS622 would be able to degrade methane as the AkMO is not known to accept C_1 compounds as substrates. As expected, methane was not degraded in the presence of 170 µM methane (Figure 44a). JS622 rapidly oxidized 476 µM ethene at the rate of 197 µmol/day. However, JS622 degraded ethene slowly within the first two days (24 µmol/day) and increased after the second day, resulting a distinct degradation curve compared to that of 40 µmol ethene (Figure 44b). In the bottle that contained 21 µM of VC, it was degraded at the rate of 13 µmol/day because AkMO was already induced (Figure 44c), which was the average degradation rate of VC when pure JS622 culture was fed with 170 µM of VC (Figure 42c).

In the bottle that contained 176 µM of methane and 37 µM of VC, VC was not inhibited by methane and degraded at the rate of 11 µmol/day (Figure 45a). In the bottle that received 491 µM of ethene and 49 µM of VC, VC was initially degraded at the rate of 0.5 µmol/day, then increased to a rate of 9 µmol/day, similarly, ethene was initially degraded at an initial rate of 32 µmol/day, that increased to a rate of 204 µmol/day. The highly similar degradation curves suggested that ethene and VC oxidation was occurring simultaneously (Figure 45b).

When methane and ethene were both present in the bottle containing pure JS622, 507 µM ethene was degraded slowly initially at 32 µmol/day, then increased to a rate of 179 µmol/day, The fact that methane was not degraded is consistent with degradation behavior seen in other bottles that ethene metabolism by JS622 was not inhibited by methane (Figure 46a).

When all three substrates were present, the VC and ethene oxidation rate and degradation pattern by JS622 were similar to that in the presence of ethene, 54 µM of VC was degraded at the maximum rate of 10 µmol/day, and 512 µM of ethene was degraded at the maximum rate of 209 µmol/day (Figure 46b). The fact that ethene and VC degradation rate were very similar in the presence and in the absence of methane, suggesting that methane did not affect the oxidation of VC and ethene by JS622 at any concentration.

3.4.5 Biodegradation of 400 µmol of methane, 400 µmol of ethene and 20 µmol of VC by Methylocystis strain ATCC 49242

In this experiment the same initial aqueous concentrations of methane (180µM), ethene (570 µM), and VC (125 µM) were used in the present of a pure culture of *Methylocystis sp.* We were interested in investigating the behavior of ATCC49242 under the situation that ethene aqueous concentration was 3-fold higher, but VC aqueous was 3-fold lower.

Methylocystis sp. degraded 151 µM of methane rapidly at the rate of 176 µmol/day (Figure 44m). The cometabolic activity of *Methylocystis sp.* on ethene (469 µM) was not very effective in comparison to JS622; the ethene oxidation rate was 28 µmol/day, and only 14% was degraded in 4 days (Figure 44n). This result suggests that pMMO activity is inhibited in the presence of relatively high concentrations of ethene. In the bottle that contained 28 µM VC, VC was cometabolized gradually at a rate of 3 µmol/day because pMMO was induced (Figure 44o). When compared to the VC degradation rate by pure JS622, which was 13 µmol/day for 21 µM of VC, the results suggest that AkMO cometabolized VC at a rate greater than that of pMMO.

In the bottle that contained 170 µM of methane and 57 µM of VC, methane was metabolized at the rate of 193 µmol/day, and VC was degraded at a rate 6 µmol/day. The fact that the VC cometabolic rate was the almost the same in comparison to its degradation rate alone, and the methane metabolic rate was slightly decreased in the presence of VC, suggests that VC competes for active binding site of pMMO even when the concentration was about 3-fold lower than methane (Figure 45i).

In the bottle that contained ethene (489 µM) and VC (44 µM) ATCC49242 degraded 14% of the ethene (at 31 µmol/day) and 11% of the VC (at 0.5 µmol/day) within 4 days (Figure 45j). In the bottle that contained methane (167 µM) and ethene (494 µM), ethene appeared to inhibit pMMO activity of *Methylocystis sp.* at this relatively high concentration, with 26% of the ethene and 18% of the methane being degraded within 4 days.

In the bottle that contained all three gases, the initial aqueous concentrations of methane, ethene, and VC were 173 µM, 516 µM, and 66 µM, respectively. The result indicates inhibition of pMMO activity, resulting in 20% ethene, 14% methane, and 11% of VC degradation within 4 days (Figure 46j).

3.4.6 Biodegradation of 400 µmol of methane, 400 µmol of ethene and 20 µmol of VC by different ethenenotroph/methanotroph ratios

Mixtures of these substrates at the initial aqueous concentrations of methane (180 µM), ethene (570 µM), and VC (125 µM) in the presence of different JS622/ATCC49242 cell ratios were tested to investigate how the various combined metabolic activities of the two organisms affect the VC biodegradation process.

In the bottles that contained approximately 170 µM of methane, the methane degradation rate increased from 98 to 176 µmol/day as the ratios of ATCC49242 increased from 25% to 100% (Figure 44a, d, g, j, m). Bottles that received approximately 470 µM of ethene, the average

maximum degradation rate decreased steadily as JS622 ratios decreased from 100% to 0% as follows: 197 µmol/day, 118 µmol/day, 113 µmol/day, 27 µmol/day (Figure 44b, e, h, k, n).

When VC was present, the average initial aqueous concentration was about 30 µM, but the cometabolic rates of VC degradation did not show an obvious trend as the ratio of JS622 decreased. Pure JS622 degraded VC the fastest at 13 µmol/day, followed by 75% JS622 and 75%ATCC49242 degraded VC at about 11 µmol/day, and 50% JS622 and 0% JS622 only degraded VC at 3 µmol/day (Figure 44c, f, i, l, o).

In the bottles that contained about 170 µM of methane and 45 µM of VC, the rate of methane degradation increased from 86 µmol/day to about 200 µmol/day as the ratio of ATCC49242 culture increased to 75%. Pure ATCC49242 degraded methane in the presence of VC a bit slower at 193 µmol/day, which could be due to an inhibitory effect of VC epoxide accumulation since no JS622 was present in the bottle (note: VC epoxide was not measured). On the other hand, VC degradation rates showed no obvious decreasing trend. The highest degradation rate (about 11.5 µmol/day) was by 100% JS622, 75% JS622 and 75% ATCC49242, with the slowest VC cometabolic rate reached by 50% JS622 (6.8 µmol/day) and 0% JS622 (6.4 µmol/day) (Figure 45a, c, e, g, i). The results observed from bottles that contained VC alone and methane+VC suggested when the methanotroph and etheneotroph cell concentrations were equal, AkMO and pMMO were not synergistic with each other.

In separate bottles that contained about 500 µM of ethene and approximately 40 µM of VC, ethene degradation decreased steadily from 205 µmol/day to 31 µmol/day as the JS622 fraction decreased from 100% JS622 to 0% JS622. However, the highest VC degradation rate was observed in the pure JS622 bottle (9 µmol/day), while the rest of the mixtures degraded VC at average of 3 µmol/day (Figure 45b, d, f, h, i). VC degradation also appeared to be inhibited until ethene dropped below 100 µmol/bottle. This suggests that high concentrations of ethene lead to competitive inhibition of VC for the AkMO binding site. Furthermore, VC degradation rates were lower in the presence of ethene than of methane, indicating that although pMMO participated in ethene and VC cometabolism, it was also apparently inhibited by ethene.

When ethene concentrations were about 500 µM and methane concentrations were about 170 µM, pMMO activity in the methanotroph appeared to be strongly inhibited as methane degradation rates only slightly increased from 23 µmol/day to 35 µmol/day as ATCC49242 fractions increased from 25% to 75%. On the other hand, ethene degradation rates decreased from 179 µmol/day to 50 µmol/day as the percent JS622 in the culture decreased (Figure 46a, c, e, g, i). At aqueous concentrations of methane, ethene, and VC were about 170 µM, 500 µM, and 50µM respectively. As expected, ethene degradation rates decreased from 209 µmol/day to 52 µmol/day, and methane still showed no obvious trend of degradation as ATCC49242 fractions increased (degraded at the rate~18 µmol/day). The cometabolic VC degradation rate still appeared to be controlled by the % JS622 in the bottles - 100% JS622 had the highest VC degradation rate (10 µmol/day), followed by 75% JS622 (9 µmol/day), 50% JS622 (4 µmol/day), and 25% JS622 (2 µmol/day) (Figure 46b, d, f, h, i).

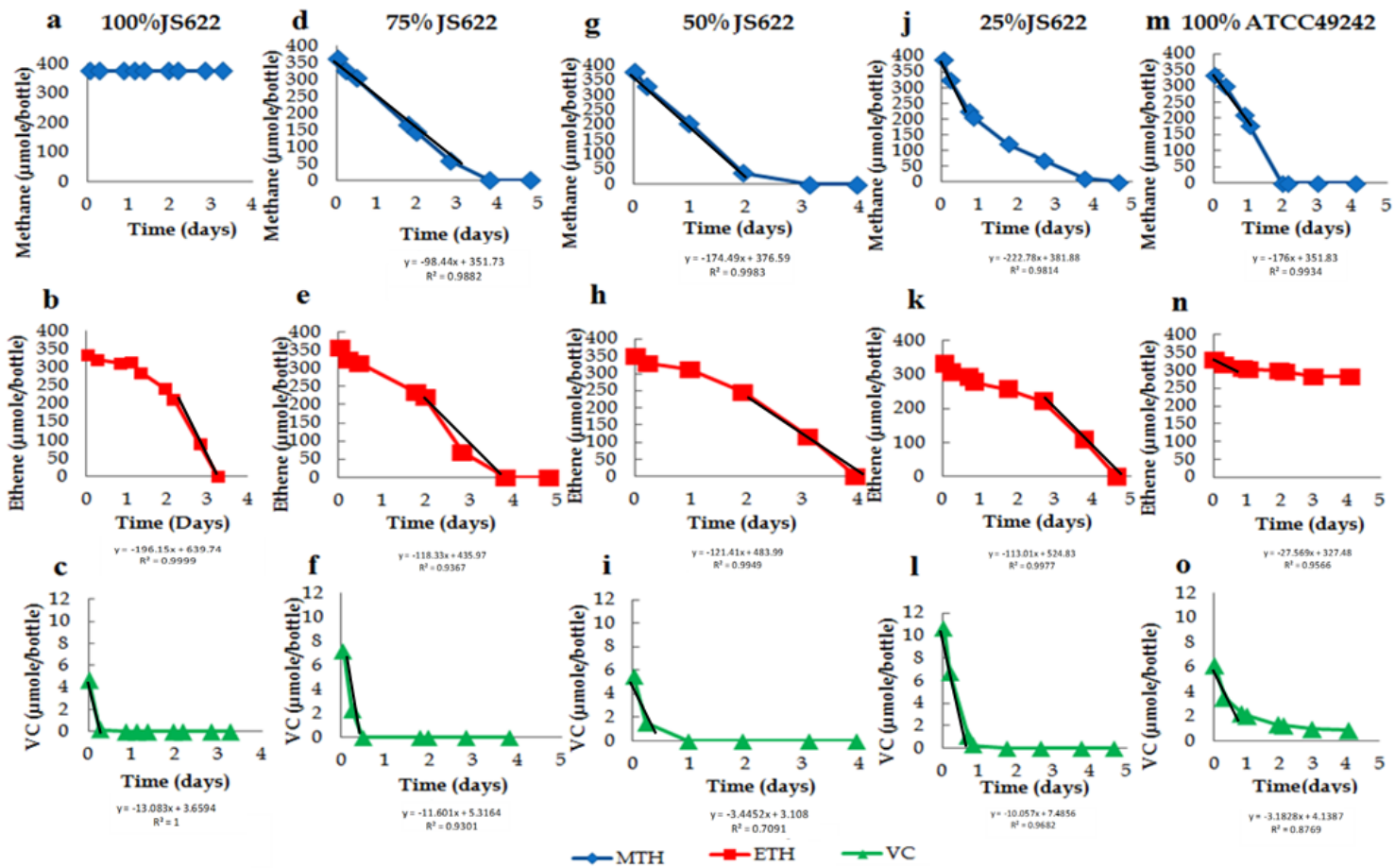

Figure 44. The degradation patterns of methane, ethene, VC as single substrate by different JS622/ATCC49242 ratios. The slopes represent the degradation rates.

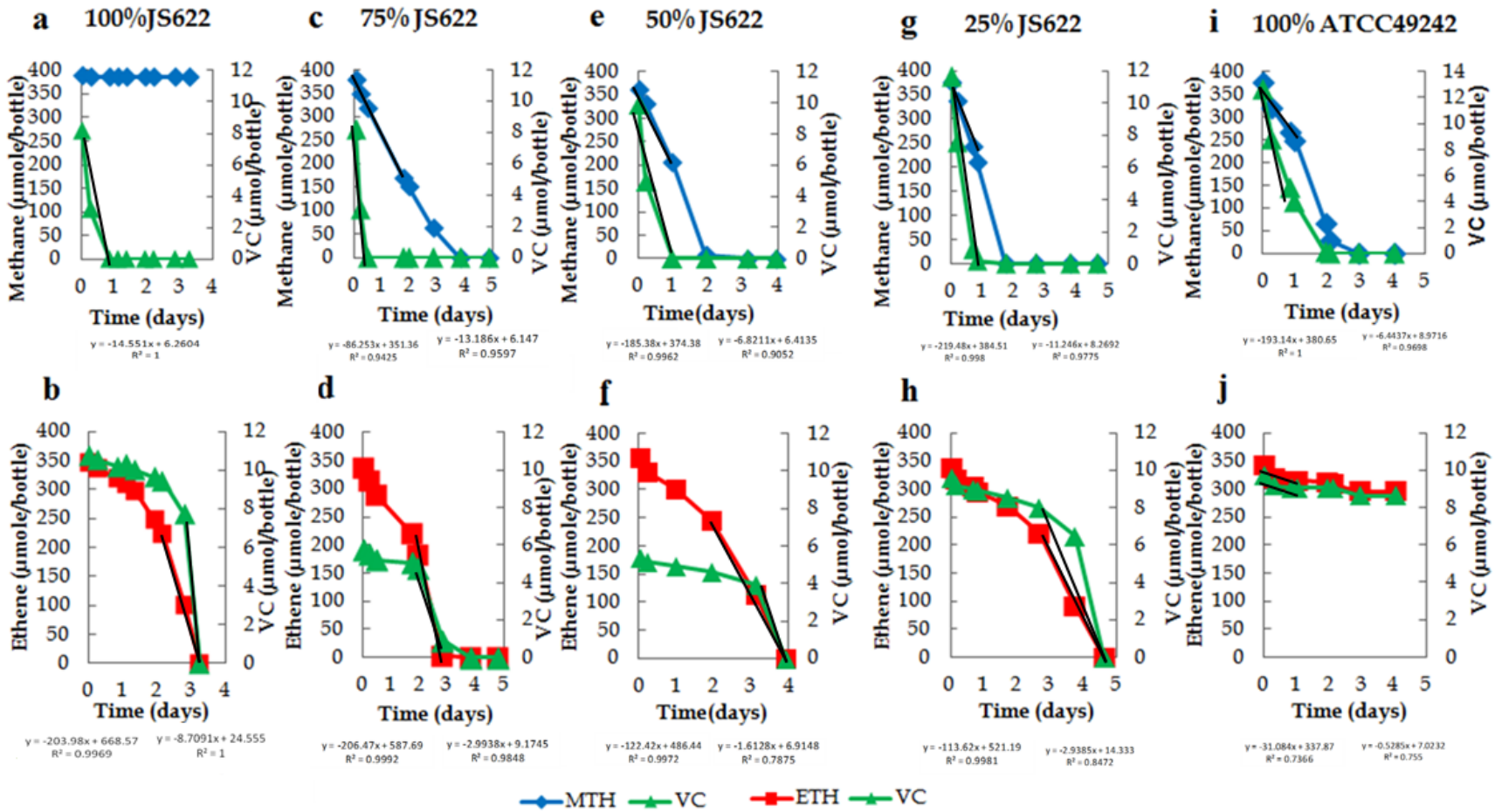

Figure 45. The degradation patterns of methane+VC and ethene+VC by different JS622/ATCC49242 ratios. The slopes represent the degradation rates.

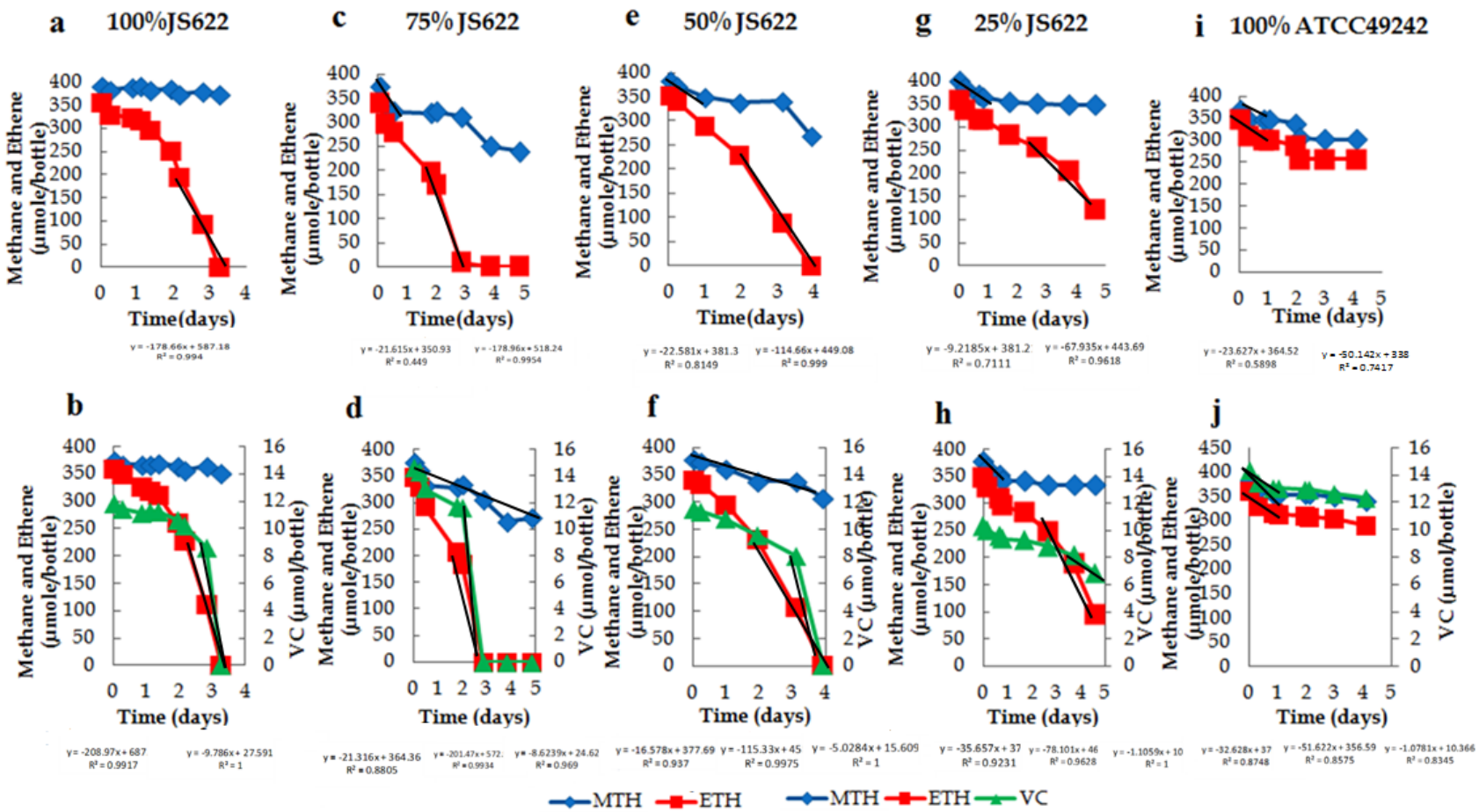

Figure 46. The degradation patterns of methane+ ethene and methane+ ethene+ VC by different JS622/ATCC49242 ratios. The slopes represent the degradation rates.

3.4.7 Biodegradation of 400 µmol of methane, 40 µmol of ethene, and 20 µmol of VC by different etheneotroph/methanotroph ratios

The previous set of experiments showed that high ethene concentrations inhibit methanotrophs (i.e. pMMO activity) in a Type II methanotroph (strain ATCC49242). These experiments were repeated using a methane:ethene:VC = 10:1:0.5 gas volume ratio, which corresponds to aqueous concentrations of methane (180 µM), ethene (57 µM), and VC (125 µM) respectively. These ratios were selected because they may more accurately reflect the relative abundance of these compounds at a contaminated site – i.e. there is typically much more methane than ethene or VC. Furthermore, because etheneotrophs like JS622 could play a significant role in VC cometabolism, but may not be in high abundance in the environment in comparison to methanotrophs, two additional smaller JS622 fractions were tested, giving the seven different cell concentration ratios as follows: (1) 100% JS622 (2) 75% JS622 (3) 50% JS622 (4) 25% JS622 (5) 10% JS622 (6) 5% JS622, and (7)100% ATCC49242.

In the bottles that contained approximately 170 µM of methane, it was expected that ATCC49242 would metabolize methane. Indeed, the initial rate of methane degradation increased gradually as follows: 34, 80, 128, 200, 274 µmol/day as the fraction of ATCC49242 in the mixed culture increased from 25% to 95%. However, the bottle containing 100% ATCC49242 degraded methane at a rate of 141 µmol/day (Figure 47a, d, g, j, m, p, s).

In the bottles that received approximately 30 µM of ethene, the ethene degradation rate decreased from 24 µmol/day to 14 µmol/day as the JS622 fraction decreased to 5%. The fact that only 61% of the ethene was cometabolized (rate of 9 µmol/day) suggested that pMMO was either failed to work due to lack of energy source, or the accumulative epoxyethane inhibited pMMO activity (Figure 47b, e, h, k, n, q, t). Cultures fed with approximately 45 µM VC displayed a similar phenomenon observed in the previous experiment (Figure 45a, c, e, g, i), where the lowest VC degradation rates was in the 50% JS622/50% ATCC49242 and 100%ATCC49242 bottles. The remaining bottles displayed VC degradation rates about 1-4 µmol/day higher (Figure 47c, f, i, l, o, r, u).

In the bottles fed about 170 µM methane and 50 µM VC, the rate of methane degradation did not steadily increase as the ATCC49242 fraction increased from 25% to 95%. This suggests that when VC concentration are about 3-fold lower than methane, competitive inhibition by VC is evident (Figure 48a-g). On the other hand, the same lowest VC degradation rate (8 µmol/day) was observed in the 50% JS622/50% ATCC49242 and 25% JS622 bottles. Higher VC cometabolic rates (2-6 µmol/day higher) were observed in the bottles that contained 75% JS622, 90% and 95% ATCC49242.

In the bottles fed 35 µM ethene and 60 µM VC the apparent ethene degradation rate decreased from 18 µmol/day to 8 µmol/day as the JS622 fraction decreased from 75% to 0%. VC degradation rates also decreased slightly from 4 µmol/day to 2 µmol/day as the ratio of JS622 decreased from 75% to 0% (Figure 49a-g).

In comparison to the experiments where the aqueous concentrations of ethene and VC were approximately 500 µM and 50 µM, we noticed that the average VC degradation rate was 3

μmol/day in the presence of ethene (both 500 μM and 30 μM) in bottles with 75%, 50%, and 25% JS622 (Figure 45d, f, h). VC cometabolism was more efficient when ethene concentrations were about 2-fold lower than VC.

In the bottles fed approximately 170 μM methane and 30 μM ethene, methane degradation rates increased from 30, 52, 58, 128 to 195 μmol/day as the ATCC49242 fraction increased from 25% to 95%. However, these rates were about 50% of those observed when methane was being degraded alone, and only 22% of the methane and 70% of the ethene was degraded within a week by 100% ATCC49242, suggesting ethene concentrations that are 3-fold smaller than methane inhibited pMMO activity more than VC. Comparing the degradation patterns of methane and ethene in the bottles with 50%, 25% and 5% JS622, methane concentrations decreased rapidly after ethene was completely utilized, further illustrating the effect of ethene inhibition on pMMO activity (Figure 50a-g).

Similarly, the bottles fed about 170 μM methane, 30 μM ethene, and 60 μM VC, the degradation rates and patterns were the combined results of methane alone and of ethene+VC were fed in the bottles. The fact that in a week only 20% of methane, 70% of ethene, and 40% of VC were degraded by pure ATCC49242, suggesting that pMMO was strongly inhibited by the combined toxic intermediates of epoxyethane and chloroxirane. In addition, the rate of ethene degradation did not decrease as the ratio of JS622 decreased, 40 μM of ethene was degraded at the average rate of 16 μmol/day, VC degradation rates appeared to very low at the average of 5 μmol/day throughout all the culture ratio bottles. No obvious trend and rank were observed from the bottles that contained low concentrations of ethene and VC (Figure 51a-g).

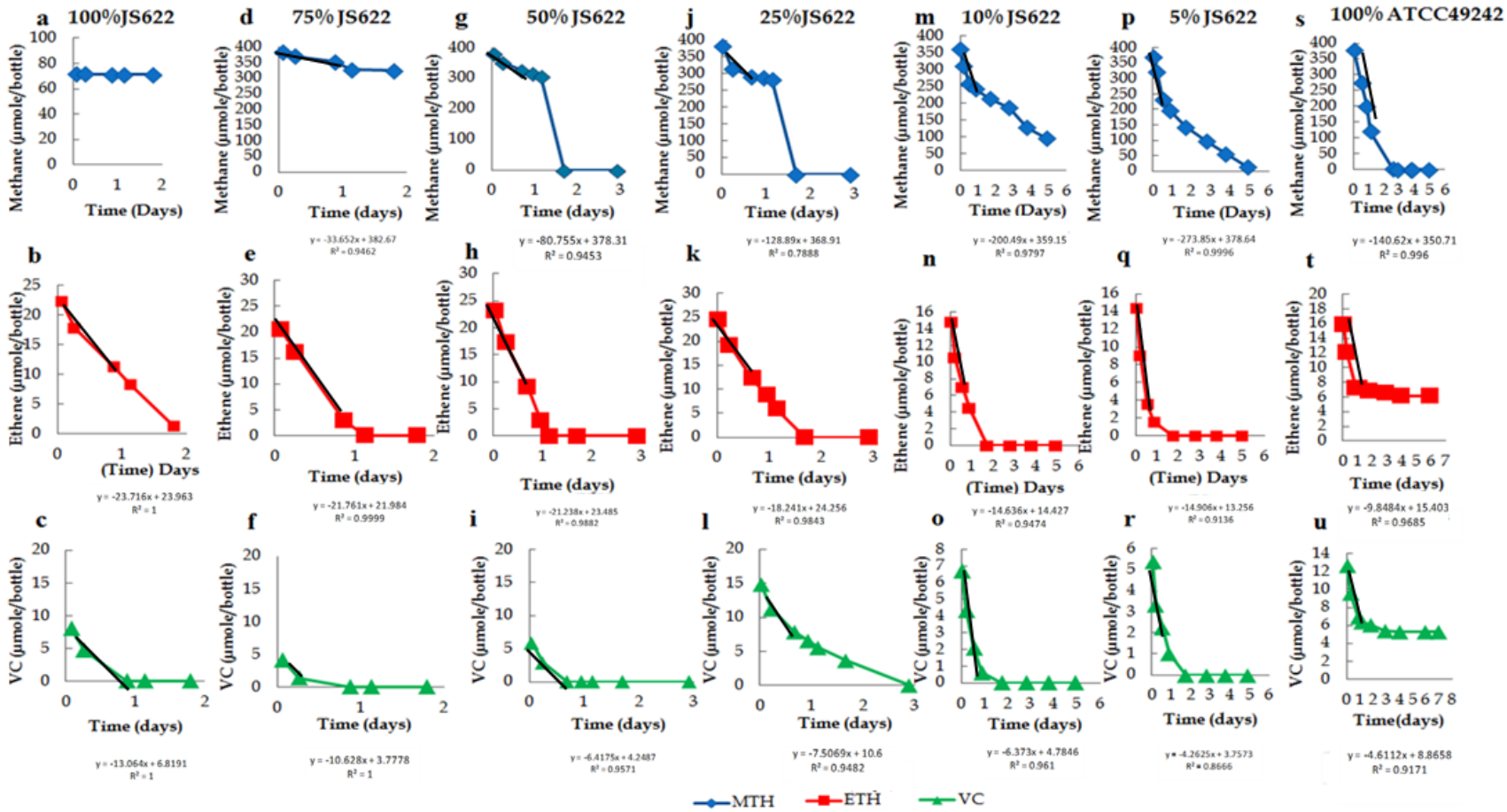

Figure 47. The degradation patterns of methane, ethene, VC as single substrate by different JS622/ATCC49242 ratios. The slopes represent the degradation rates

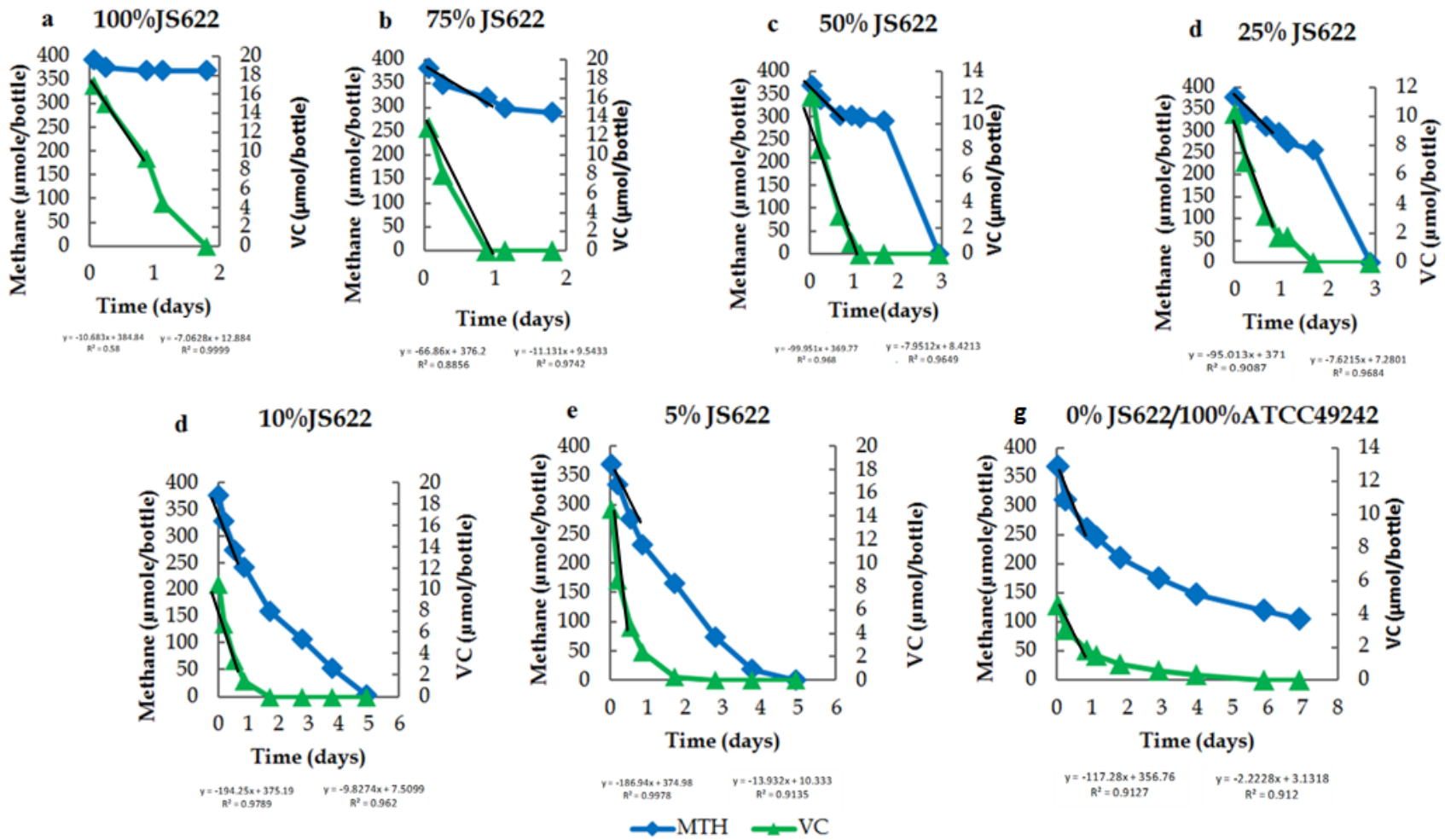
a
100%JS622
Methane (µmole/bottle)
VC (µmol/bottle)
Time (days)
y = -10.683x + 384.84
R² = 0.58
y = -7.0628x + 12.884
R² = 0.9999
b
75% JS622
Methane (µmole/bottle)
VC (µmol/bottle)
Time (days)
y = -66.86x + 376.2
R² = 0.8856
y = -11.131x + 9.5433
R² = 0.9742
c
50% JS622
Methane (µmole/bottle)
VC (µmol/bottle)
Time(days)
y = -99.951x + 369.77
R² = 0.968
y = -7.9512x + 8.4213
R² = 0.9649
d
25% JS622
Methane (µmole/bottle)
VC (µmol/bottle)
Time (days)
y = -95.013x + 371
R² = 0.9087
y = -7.6215x + 7.2801
R² = 0.9684
d
10%JS622
Methane (µmole/bottle)
VC (µmol/bottle)
Time (days)
y = -194.25x + 375.19
R² = 0.9789
y = -9.8274x + 7.5099
R² = 0.962
e
5% JS622
Methane (µmole/bottle)
VC (µmol/bottle)
Time (days)
y = -186.94x + 374.98
R² = 0.9978
y = -13.932x + 10.333
R² = 0.9135
g
0% JS622/100%ATCC49242
Methane(µmole/bottle)
VC (µmol/bottle)
Time (days)
y = -117.28x + 356.76
R² = 0.9127
y = -2.2228x + 3.1318
R² = 0.912
MTH
VC

Figure 48**.** The degradation patterns of methane+VC by different JS622/ATCC49242 ratios where the mass of methane fed is 20 times that of VC. The slopes of the regression lines represent the degradation rates discussed in the text.

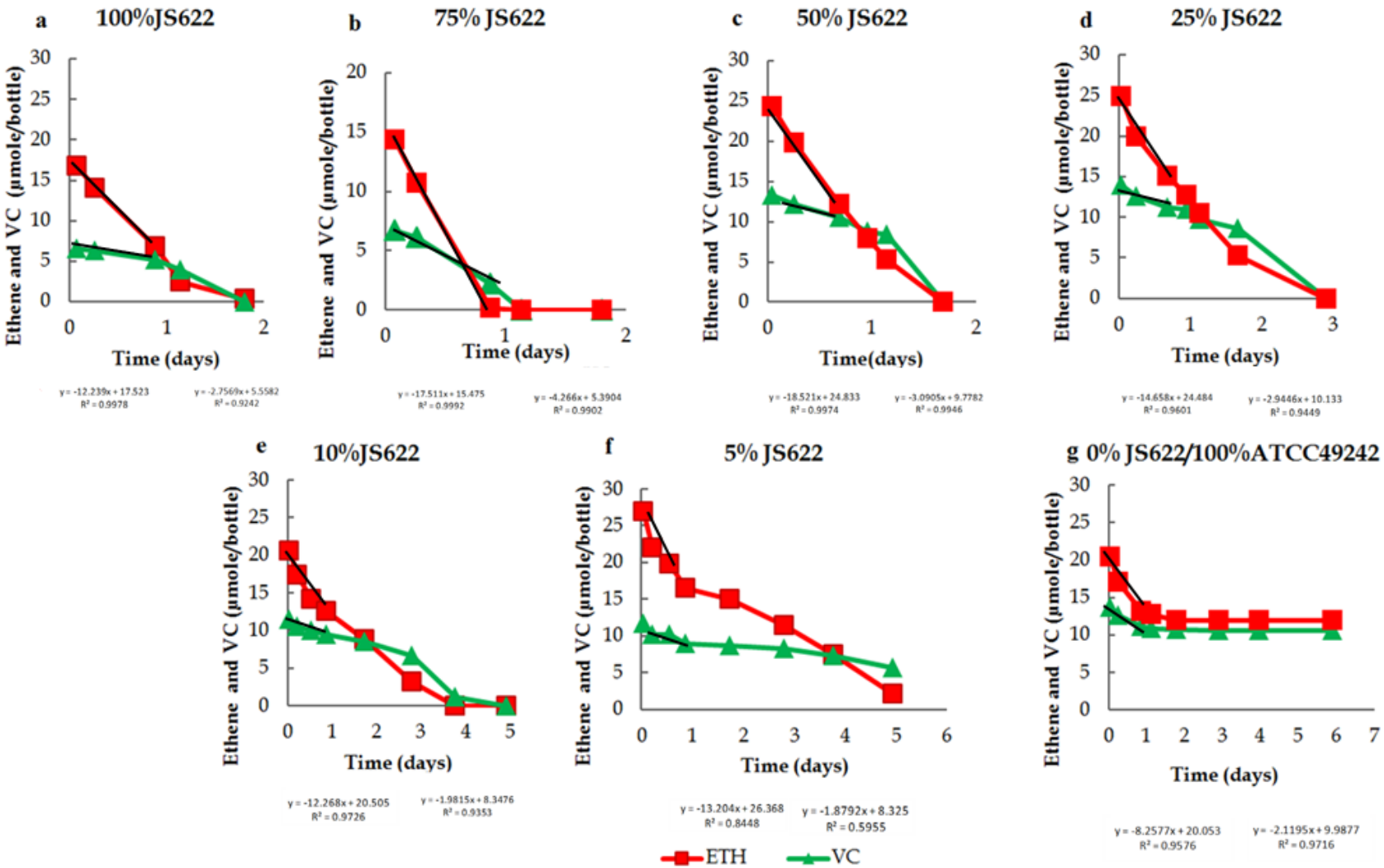
a
100%JS622
Ethene and VC (µmole/bottle)
Time (days)
y = -12.239x + 17.523
R² = 0.9978
y = -2.7569x + 5.5582
R² = 0.9242
b
75% JS622
Ethene and VC (µmole/bottle)
Time (days)
y = -17.511x + 15.475
R² = 0.9992
y = -4.266x + 5.3904
R² = 0.9902
c
50% JS622
Ethene and VC (µmole/bottle)
Time(days)
y = -18.521x + 24.833
R² = 0.9974
y = -3.0905x + 9.7782
R² = 0.9946
d
25% JS622
Ethene and VC (µmole/bottle)
Time (days)
y = -14.658x + 24.484
R² = 0.9601
y = -2.9446x + 10.133
R² = 0.9449
e
10%JS622
Ethene and VC (µmole/bottle)
Time (days)
y = -12.268x + 20.505
R² = 0.9726
y = -1.9815x + 8.3476
R² = 0.9353
f
5% JS622
Ethene and VC (µmole/bottle)
Time (days)
y = -13.204x + 26.368
R² = 0.8448
y = -1.8792x + 8.325
R² = 0.5955
ETH
VC
g 0% JS622/100%ATCC49242
Ethene and VC (µmole/bottle)
Time (days)
y = -8.2577x + 20.053
R² = 0.9576
y = -2.1195x + 9.9877
R² = 0.9716

Figure 49**.** The degradation patterns of ethene+VC by different JS622/ATCC49242 ratios in the gas ratio of 2:1. The slopes represent the degradation rates.

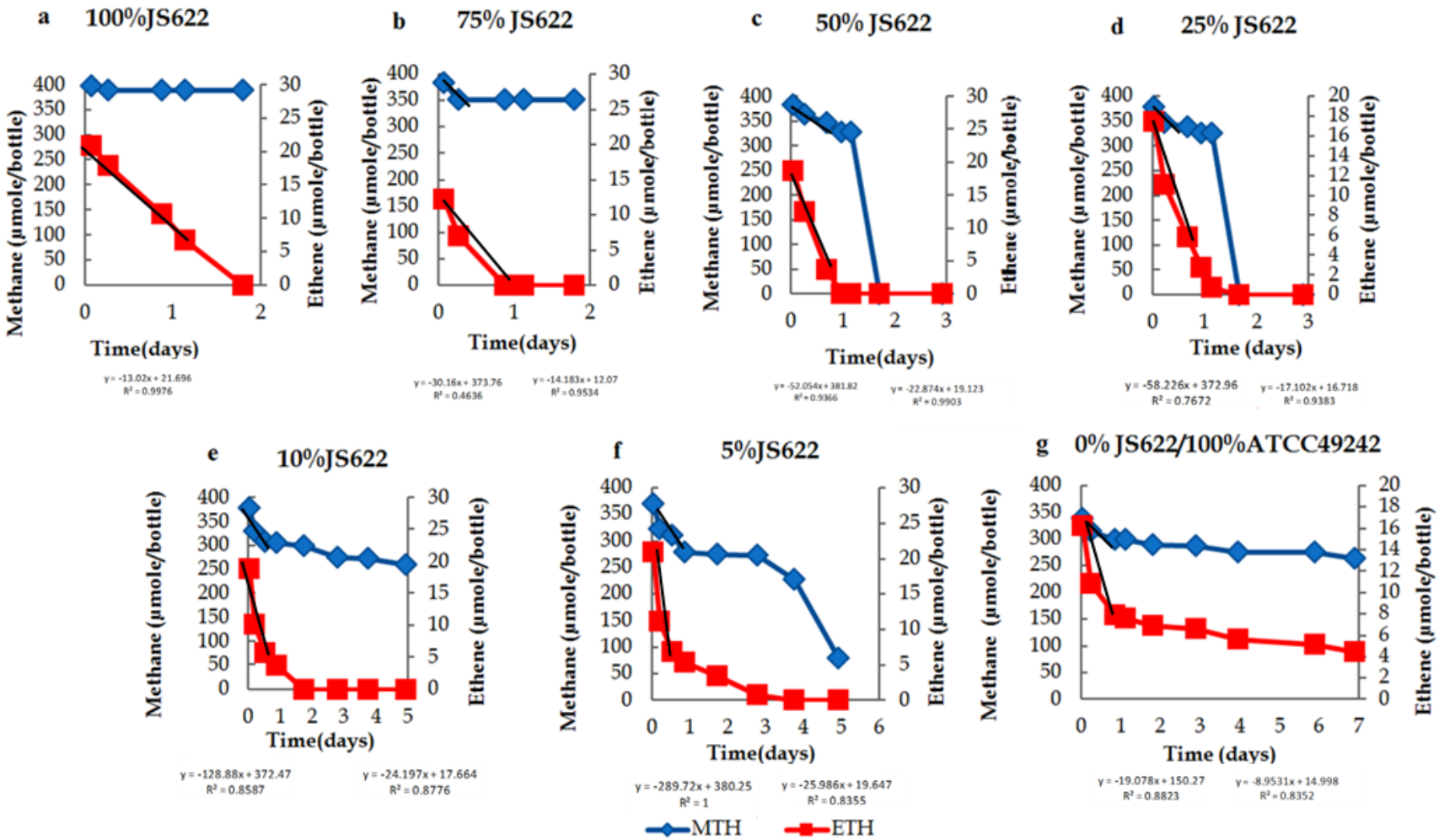

Figure 50. The degradation patterns of methane+ethene by different JS622/ATCC49242 ratios in the gas ratio of 10:1. The slopes represent the degradation rates.

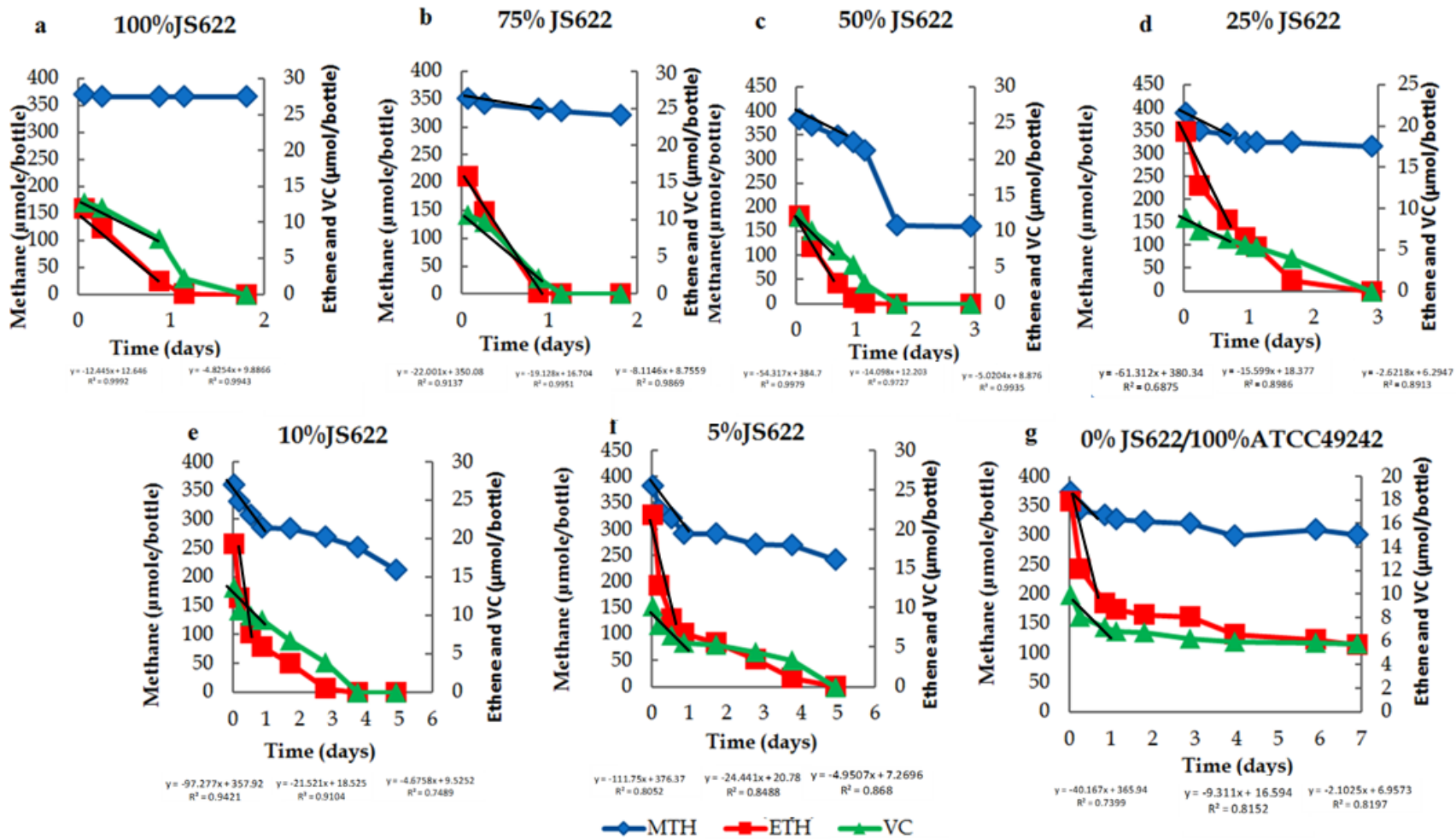

Figure 51. The degradation patterns of methane+VC and ethene+VC by different JS622/ATCC49242 ratios in the gas ratio of 20:2:1. The slopes of the regression lines represent the initial degradation rates.

Conclusions and Implications for Future Research/Implementation

Based on the results presented in this report we can make the following conclusions:

Development of a qPCR method for etheneotrophs

- We have developed effective protocols for DNA extraction from groundwater, where the biomass is sampled using Sterivex filters. Initially we utilized a modified Mo Bio PowerSoil DNA extraction kit protocol. Later we utilized a modified Mo Bio PowerWater DNA extraction kit protocol. A comparison of these methods along with the new Mo Bio PowerWater Sterivex kit protocol revealed that DNA yields from pure cultures were comparable. The DNA quality, tested via qPCR, was also comparable among these protocols. In future studies, we recommend that a single effective protocol be adopted so that results among and within sites can be reasonably compared.

- We have developed two different sets of degenerate qPCR primers, each targeting two different etheneotrophic functional genes (*etnC* and *etnE*). The specificity of the initial primer sets, named RTC (for *etnC*) and RTE (for *etnE*), was tested extensively on pure cultures and groundwater samples. To date, after using several independent approaches such as PCR analysis, melt-curve analysis, cloning and sequencing, and Primer BLAST, we have found no evidence that the primers amplify non-target sequences or form primer dimers when interrogating environmental samples.

- The second set of primers, named MRTC and MRTE was directly compared to the RTC and RTE primers using pure cultures and environmental samples. These results indicated that the MRTC and MRTE primers could provide improved gene abundance estimates (in comparison to RTC and RTE. However, until further field validation of these primers is completed we conclude that all primer sets are useful for studies of pure cultures and estimating gene abundance in environmental samples.

- Since it is our overall goal to interrogate environmental samples with these qPCR primers and because we are interested in capturing the diversity of *etnC* and *etnE* sequences that are present in the environment, we found that the use of degenerate primers and SYBR green qPCR chemistry is a valid approach.

- Constructing standard curves for real-time PCR quantitation was successful (i.e. PCR efficiencies were within the range of 95-105%) when using PCR products as the templates. Using PCR products amplified from *Mycobacterium* strain JS60 or JS617 was found to be acceptable. An intra-assay standard curve approach was adopted. This means that a standard curve is prepared for every qPCR plate run.

- PCR inhibitors were noted in DNA extracted from environmental samples. This issue was overcome by adding 400 ng/µL BSA to qPCRs

- The qPCR method for etheneotrophs was successfully applied to 9 different samples from three different VC-contaminated sites, in some cases over a 3 year period. The abundance of *etnC* ranged from 1.3×10^3 – 1.0×10^5 genes per liter of groundwater (LGW).

The abundance of *etnE* ranged from $1.9\times10^3 – 6.3\times10^5$ genes per LGW. Because field application of this method is limited, conclusions regarding these gene abundances cannot be made other than the fact that etheneotrophs were found to be present at all three sites.

Methanotroph qPCR protocol

- A search of the literature for methanotrophs qPCR primers yielded several candidate primer sets for laboratory testing. We determined that four primer sets, which amplify Type I 16S rRNA, Type II 16S rRNA, *pmoA*, and *mmoX* genes, respectively, can be useful for estimating the abundance of different methanotrophic groups in groundwater samples.

- Application of *pmoA* and *mmoX* qPCR primer sets to 8 samples from 3 different sites revealed that pmoA abundance ranged from $1.6\times10^4 – 4.1\times10^7$ genes/LGW and that *mmoX* abundance ranged from $2.5\times10^2 – 6.5\times10^6$ genes/LGW. The *pmoA* qPCR data suggest that methanotrophs are more abundant at VC-contaminated sites than etheneotrophs. This is expected since methane concentrations are typically much higher than ethene and VC concentrations at the sites examined.

RT-qPCR method development and applications

- A protocol for simultaneous RNA/DNA extraction from Sterivex filters was developed. This protocol was based on the MoBio PowerWater RNA extraction kit. This protocol was useful when working with pure cultures, however in environmental samples DNA and RNA were extracted from separate Sterviex filters.

- Using pure cultures, a comparison of several Mo Bio RNA extraction kit protocols suggested that the PowerWater Sterivex kit provides the best combination of RNA yield and quality.

- Extending the qPCR method for etheneotrophs to mRNA analysis entailed adding reference nucleic acids (luciferase mRNA) into the samples following the extraction step and then performing the reverse-transcription step. Standard curves for the reference nucleic acids were developed so that quantitation of ref mRNA could be conducted. The ref mRNA recovery allows us to assess losses of sample RNA during steps in the protocol (e.g. during the RT step).

- Even though the use of random primers and BSA resulting in decreased quantitation of ref mRNA, these two steps are necessary when applying a RT-qPCR method to groundwater samples.

- RT-qPCR was applied to *Nocardioides* sp. strain JS614 cultures grown on acetate, ethene, and VC as well as to starved JS614 cultures. Both transcript and gene abundances were measured and the results expressed as “transcripts per gene”. These experiments indicated that when JS614 was starved, transcript per gene ratios were low (0.1-0.2). Acetate-grown JS614 cultures displayed transcript per gene ratios of 0.5-0.6. In contrast ethene- and VC-grown JS614 cultures displayed transcript per gene ratios of

2-12. This suggests that when the transcript per gene ratio is greater than 1, then the bacteria expressing *etnC* and/or *etnE* are active.

- RT-qPCR was successfully applied to 4 different groundwater samples from the Carver site. Transcript/gene ratios were estimated as follows: 0.4 for both *etnC* and *etnE* in RB46D, 0.7 for *etnC* and 0.8 for *etnE* in RB63I, 5.7 for *etnC* and 2.2 for *etnE* in RB64I, and 9.3 for *etnC* and 12.6 for *etnE* in RB73. These promising results suggest that RT-qPCR could be useful for interrogating the physiological status of etheneotrophs within the zone of influence of monitoring wells.

- RT-qPCR for methanotrophs was also performed on the same samples from Carver wells RB46D, RB63I, and RB64I. Transcript/gene ratios were estimated as follows: 0.02 for *pmoA* and 0.24 for *mmoX* in RB46D, 0.02 for *pmoA* and 0.00 for *mmoX* in RB63I, and 0.11 for *pmoA* and 0.2 for *mmoX* in RB64I. These values are substantially lower than the etheneotroph transcript per gene ratios estimated in the same samples. This suggests that although methanotrophs were more abundant in these wells, they were not necessarily more active than the less abundant etheneotrophs. We recommend that additional studies be conducted to better delineate the differences in methanotroph/etheneotroph abundance and gene expression in environmental samples.

- Effective RNA extraction was not always possible from Sterivex filters that had been preserved with RNAlater and stored at -80C for a period of time prior to analysis. This is currently a drawback to the RT-qPCR method. Based on anecdotal reports it is possible that freezing filters preserved with RNAlater could lead to rapid RNA degradation. Ideally, nucleic acids are to be extracted from filters as soon as possible after sampling and freezing should be avoided. We recommend that more work be done to determine the appropriate sample preservation and handling procedures for filtered groundwater samples.

Microcosm study with VC-contaminated well 63-I groundwater from the Carver, MA site

- Our microcosm experiments were designed to address substrate interactions during VC cometabolism in groundwater scenarios with relatively low concentrations of ethene, methane and VC (all less than 100 µg/L) which are typical for groundwater down gradient of sites having previously undergone reductive dechlorination of chlorinated ethenes.

- In these experiments, when methane and ethene were present, the lag time for initiation of ethene degradation and the time for 50% ethene degradation were lower than in microcosms with ethene alone. We hypothesized that these observations could be explained by methanotrophs cometabolizing the ethene and producing epoxyethane, which could in turn stimulate ethene degradation by etheneotrophs.

- These hypotheses were tested with methane and ethene enrichment cultures developed from the same groundwater. Methanotrophs were shown to produce epoxyethane when fed a mixture of methane and ethene. Etheneotrophs were shown to initiate ethene degradation more quickly when epoxyethane was present.

- Overall, we have observed that when both methane and ethene are present, is that there is an enhanced potential for VC to be completely degraded. We conclude that substrate interactions during VC cometabolism in groundwater systems will be site-specific and depend highly on the abundance of methanotrophs and etheneotrophs as well as the concentrations of VC, ethene, and methane present (assuming oxygen is not limiting the process). These factors should be considered in the design of future VC bioremediation strategies involving cometabolism by applying the tools described here.

Pure culture experiments of substrate interactions between a methanotroph and an etheneotroph

- The purpose of this study was to investigate how known ratios of methanotrophs and etheneotrophs in culture behave when cometabolizing VC using different gas volume ratios of methane: ethene: VC. The 20:20:1 ratio is similar to that observed in a groundwater system at the Carver, MA site. The results of this study highlighted the issues that may arise and the potential synergistic interactions that occur when methanotrophs and etheneotrophs are present together in a system containing mixtures of methane, ethene, and VC.

- VC degradation had the highest potential to be fully degraded in mixed cultures when methane and ethene are both present. The highest VC degradation rates (8-10 μmol/day) were observed in the bottles that contained 75% JS622, and the VC oxidation rate decreased as the percentage of etheneotrophs decreased. Based on qPCR results, the abundance of etheneotrophs is likely to be an order of magnitude or more less than methanotrophs. This has implications for the normalized rate of VC oxidation in the environment.

- The relative aqueous concentrations of methane, ethene, and VC are essential elements that determine the behavior of the two microbial groups. Methane degradation by *Methylocystis sp.* was readily inhibited in the presence of VC (50-170 μM) and ethene (~50 μM). However, the presence of methane does not affect the activity of the etheneotrophic *Mycobacterium* JS622 strain. This suggests that etheneotrophs have an advantage over methanotrophs for aerobic cometabolism of VC in these systems.

- However, by enhancing VC cometabolism by etheneotrophs, the toxic inhibition of VC and epoxyethane to methanotrophs may also be reduced so that VC cometabolism by methanotrophs is also enhanced.

Synthesis of overall results and conclusions of this research

We have developed and refined a qPCR method for etheneotrophs which can yield rapid information concerning presence and abundance of this microbial group using an absolute DNA quantification approach (Jin and Mattes 2010; Jin and Mattes 2011). The method employs degenerate oligonucleotide primers that target the functional genes *etnC* and *etnE*, both of which are known to be involved in the aerobic VC and ethene biodegradation pathways of etheneotrophs. The gene *etnC* encodes the alpha subunit of alkene monooxygenase (AkMO), the

enzyme utilized by etheneotrophs in their initial attack on VC. The gene *etnE* encodes the epoxyalkane:coenzyme M transferase (EaCoMT). AkMO converts VC and ethene to epoxide intermediates, while EaCoMT detoxifies and transforms these epoxides into compounds that can enter central metabolic pathways (Mattes, Alexander et al. 2010). While the presence of either functional gene may indicate the presence and abundance of etheneotrophs, quantifying both functional genes is more definitive and allows analysis of *etnC/etnE* ratios, which are expected to be between 0.5 and 3.0 based on our the genomes of etheneotrophs that are currently sequenced (Jin and Mattes 2011).

We have also extended our original qPCR method to include the ability to assess functionality of etheneotrophs by quantifying expression of *etnC* and *etnE* in environmental samples. The method extension includes procedures for RNA extraction from filtered groundwater samples, addition of internal control DNA and RNA to track nucleic acid losses during the process, reverse transcription (RT) of RNA into cDNA, and qPCR analysis of *etnC*, *etnE*, and the luciferase internal control gene, using both DNA and cDNA templates. This absolute quantification approach for both transcripts and genes allows estimation of gene expression levels based on the transcript per gene ratio. The extension of the technology to include mRNA analysis allows assessment of microbial activity in the subsurface, which can provide a crucial line of evidence that VC oxidation is occurring.

Therefore, it is our opinion that we have successfully completed Tasks 1 and 2 of this project. Additional research into sampling, handling, sample preservation and extraction of nucleic acids from environmental samples would be helpful, particularly with RNA extraction. More field application of the qPCR and RT-qPCR techniques is also warranted.

Task 3 was not conducted as described in the original proposal. This is primarily because the scope of the experiments were more complex than originally anticipated and so we focused much of the work on groundwater from one well. However, we made significant progress in addressing knowledge gaps associated with the normalized rate of VC oxidation. In groundwater microcosms, we noted the synergistic effects of the simultaneous presence of methanotrophs and etheneotrophs. Enrichment cultures helped us better understand the role of epoxyethane in ethene oxidation. Finally, the pure culture studies highlighted the effects of competitive inhibition and VC toxicity on the activity of methanotrophs. We were poised to perform normalized rate studies on pure culture mixtures of methanotrophs and etheneotrophs using qPCR and RT-qPCR, but the project funding was expended by that point. Additional research on the normalized rate of VC oxidation in these culture systems should be performed, and the potential role of epoxides in stimulating ethene and VC oxidation by etheneotrophs should also be delineated in pure culture experiments.

Potential for direct implementation by DoD and others

VC plumes are present at many DoD sites, and there are significant costs associated with their clean-up, primarily because they are often dilute and require extensive long-term monitoring to determine if remediation is progressing satisfactorily. VC oxidation, mediated by both etheneotrophs and methanotrophs, may be occurring within or at the fringes of VC plumes at many sites, including those that are ideal for anaerobic reductive dechlorination processes.

The qPCR technology that we developed in this project has the potential to provide rapid molecular biology-based information concerning the presence and activity of etheneotrophs (and also methanotrophs). This technology could potentially be applied at any DoD site where VC oxidation might be occurring. Based on the results presented here, we believe that we should continue working to demonstrate and validate our quantitative, real-time PCR (qPCR) technologies at VC-contaminated sites where geochemical conditions are favorable for VC oxidation. The demonstration and validation of this technology would entail regularly collecting groundwater from multiple locations at one or more VC-contaminated sites over a period of several years. Ideally, the groundwater samples will be subjected to both qPCR analysis and chemical analysis for VOCs (i.e. VC, ethene, and methane) as well as other relevant geochemical parameters (i.e. terminal electron acceptors). This will allow us to build a data set that describes how the abundance and functionality of etheneotrophic (and methanotrophic) bacteria change both spatially and temporally at several locations in a VC plume. Analysis of this data set will allow us to assess the performance of the qPCR (and RT-qPCR) technology in a real field application, as well as how the molecular biology data correlates to the rate of VC degradation in a particular monitoring well. We expect that the results of this potential demonstration will demonstrate that application of molecular biology tools during long term monitoring of VC-contaminated groundwater will yield useful and cost-effective information for site managers.

The environmental impact will be realized by providing a new capability to document VC natural attenuation at many sites instead of relying on random aerobic VC oxidation in the plume to reduce plume size and mass. This new capability may then ultimately lead to site closure in shorter time periods. We argue that there may be significant value to the DoD for adding RT-qPCR analyses for etheneotrophs and methanotrophs to long-term groundwater monitoring plans at VC-contaminated sites in that these analyses have the potential to decrease overall life cycle costs for clean-up.

A microcosm test approach is currently the only option available to site managers for documenting aerobic VC oxidation processes at contaminated sites. Microcosm tests can only show that the appropriate organisms are present and possibly functional in the sample. In contrast to RT-qPCR analyses, microcosms provide no abundance information and no direct confirmation of microbial activity. Groundwater must be shipped back to a laboratory where a technician prepares the microcosms and monitors them for some period of time (i.e. 60 days or more for etheneotrophs). Combined presence/absence microcosm tests for methanotrophs and etheneotrophs cost between $1,000- $1,350 per sample, depending on site specific parameters such as presence of other chlorinated solvents or excess oxygen demand. Because of the labor involved in microcosm construction and monitoring, there is generally no decrease in unit cost as sample size increases.

Gene abudnace estimateate for both methanotrophs and etheneotrophs (via qPCR analysis) would cost $350 per sample and that mRNA analysis adds another $500 per sample, for a total unit cost of $850 per sample that can be decreased with increased sample size. These analyses can be performed much more rapidly than microcosm tests (within a few days). It should be noted that RT-qPCR analysis need not be applied to every single sample, but could instead be applied in a more targeted fashion to demonstrate activity, thus reducing overall costs. This initial estimate indicates that significant cost savings can already be realized if

etheneotroph/methanotroph microcosm tests are supplanted by RT-qPCR analysis. During the proposed demonstration we will tabulate RT-qPCR operating costs over a 2 year sampling and analysis period, ascertain options for decreasing unit costs and further compare these costs to those required for microcosm testing. This will allow us to better estimate life cycle costs, the expected return on investment in RT-qPCR technologies and time for payback if the technology is implemented on a larger scale following the demonstration. An estimate of life cycle costs for a VC remediation project, both with and without the use of RT-qPCR analysis will be especially useful for quantifying DoD benefit.

Literature Cited

(1) Bucher, J. R.; Cooper, G.; Haseman, J. K.; Jameson, C. W.; Longnecker, M.; Kamel, F.; Maronpot, R.; Matthews, H. B.; Melnick, R.; Newbold, R.; Tennant, R. W.; Thompson, C.; Waalkes, M. *Ninth report on carcinogens*; U.S. Dept. of Health and Human Services, National Toxicology Program. [http://ehis.niehs.nih.gov/roc/ninth/known/vinylchloride.pdf]: 2001.

(2) Squillace, P. J.; Moran, M. J.; Lapham, W. W.; Price, C. V.; Clawges, R. M.; Zogorski, J. S., Volatile organic compounds in untreated ambient groundwater of the United States, 1985-1995. *Environ. Sci. Technol.* **1999,** *33*, 4176-4187.

(3) Davis, J. W.; Carpenter, C. L., Aerobic degradation of vinyl chloride in groundwater samples. *Appl. Environ. Microbiol.* **1990,** *56*, 3878-3880.

(4) Edwards, E. A.; Cox, E. E., Field and laboratory studies of sequential anaerobic-aerobic chlorinated solvent biodegradation. In *In Situ and On-Site Bioremediation*, Alleman, B. C., and Leeman, A., Ed. Battelle Press: Columbus, OH, 1997; Vol. 3, pp 261-265.

(5) Lee, M. D.; Odom, J. M.; Buchanan, R. J. J., New perspectives on microbial dehalogenation of chlorinated solvents: insights from the field. *Annu. Rev. Microbiol.* **1998,** *52*, 423-452.

(6) Fogel, M. M.; Taddeo, A. R.; Fogel, S., Biodegradation of chlorinated ethenes by a methane-utilizing mixed culture. *Appl. Environ. Microbiol.* **1986,** *51*, 720-724.

(7) van Hylckama Vlieg, J. E. T.; de Koning, W.; Janssen, D. B., Transformation kinetics of chlorinated ethenes by *Methylosinus trichosporium* OB3b and detection of unstable epoxides by on-line gas chromatography. *Appl. Environ. Microbiol.* **1996,** *62*, 3304-312.

(8) Freedman, D. L., and S. D. Herz, Use of ethylene and ethane as primary substrates for aerobic cometabolism of vinyl chloride. *Water Env. Res.* **1996,** *68*, 320-328.

(9) Coleman, N. V.; Mattes, T. E.; Gossett, J. M.; Spain, J. C., Phylogenetic and kinetic diversity of aerobic vinyl chloride-assimilating bacteria from contaminated sites. *Appl. Environ. Microbiol.* **2002,** *68*, (12), 6162-6171.

(10) Danko, A. S.; Luo, M.; Bagwell, C. E.; Brigmon, R. L.; Freedman, D. L., Involvement of linear plasmids in aerobic biodegradation of vinyl chloride. *Appl. Environ. Microbiol.* **2004,** *70*, (10), 6092-6097.

(11) Hartmans, S.; de Bont, J. A. M., Aerobic vinyl chloride metabolism in *Mycobacterium aurum* L1. *Appl. Environ. Microbiol.* **1992,** *58*, 1220-1226.

(12) Verce, M. F.; Ulrich, R. L.; Freedman, D. L., Characterization of an isolate that uses vinyl chloride as a growth substrate under aerobic conditions. *Appl. Environ. Microbiol.* **2000,** *66*, 3535-3542.

(13) Cupples, A. M., Real-time PCR quantification of *Dehalococcoides* populations: Methods and applications. *Journal of Microbiological Methods* **2008,** *72*, (1), 1-11.

(14) Coleman, N. V.; Bui, N. B.; Holmes, A. J., Soluble di-iron monooxygenase gene diversity in soils, sediments and ethene enrichments. *Environmental Microbiology* **2006,** *8*, (7), 1228-1239.

(15) Coleman, N. V.; Spain, J. C., Epoxyalkane:Coenzyme M transferase in the ethene and vinyl chloride biodegradation pathways of *Mycobacterium* strain JS60. *J. Bacteriol.* **2003,** *185*, (18), 5536-5545.

(16) Coleman, N. V.; Spain, J. C., Distribution of the coenzyme M pathway of epoxide metabolism among ethene- and vinyl chloride-degrading *Mycobacterium* strains. *Appl. Environ. Microbiol.* **2003,** *69*, (10), 6041-6046.

(17) Mattes, T. E.; Coleman, N. V.; Gossett, J. M.; Spain, J. C., Physiological and molecular genetic analyses of vinyl chloride and ethene biodegradation in *Nocardioides* sp. strain JS614. *Arch. Microbiol.* **2005,** *183*, 95-106.

(18) Danko, A. S.; Saski, C. A.; Tomkins, J. P.; Freedman, D. L., Involvement of coenzyme M during aerobic biodegradation of vinyl chloride and ethene by *Pseudomonas putida* strain AJ and *Ochrobactrum* sp. strain TD. *Appl. Environ. Microbiol.* **2006,** *72*, (5), 3756-3758.

(19) Kikuchi, T.; Iwasaki, K.; Nishihara, H.; Takamura, Y.; Yagi, O., Quantitative and rapid detection of the trichloroethylene-degrading bacterium Methylocystis sp. M in groundwater by real-time PCR. *Applied Microbiology and Biotechnology* **2002,** *59*, (6), 731-736.

(20) Kolb, S.; Knief, C.; Stubner, S.; Conrad, R., Quantitative Detection of Methanotrophs in Soil by Novel pmoA-Targeted Real-Time PCR Assays. *Appl. Environ. Microbiol.* **2003,** *69*, (5), 2423-2429.

(21) Hartmans, S.; de Bont, J. A. M.; Tramper, J.; Luyben, K. C. A. M., Bacterial degradation of vinyl chloride. *Biotech. Lett.* **1985,** *7*, 383-388.

(22) Verce, M. F.; Ulrich, R. L.; Freedman, D. L., Transition from cometabolic to growth-linked biodegradation of vinyl chloride by a *Pseudomonas* sp. isolated on ethene. *Environ. Sci. Technol.* **2001,** *35*, 4242-4251.

(23) Tsien, H. C.; Brusseau, G. A.; Hanson, R. S.; Waclett, L. P., Biodegradation of trichloroethylene by *Methylosinus trichosporium* OB3b. *Appl. Environ. Microbiol.* **1989,** *55*, (12), 3155-61.

(24) Koziollek, P., Bryniok, D., and H. -J. Knackmuss, Ethene as an auxiliary substrate for the cooxidation of *cis*-dichloroethene and vinyl chloride. *Arch. Microbiol.* **1999,** *172*, 240-246.

(25) Phelps, T. J.; Malachowsky, K.; Schram, R. M.; White, D. C., Aerobic mineralization of vinyl chloride by a bacterium of the order Actinomycetales. *Appl. Environ. Microbiol.* **1991,** *57*, (4), 1252-4.

(26) Wackett, L. P.; Brusseau, G. A.; Householder, S. R.; Hanson, R. S., Survey of microbial oxygenases : trichloroethylene degradation by propane-oxidizing bacteria. *Appl. Environ. Microbiol.* **1989,** *55*, 2960-2964.

(27) Malachowsky, K. J., T. J. Phelps, A. B. Teboli, D. E. Minnikin, and D. C. White, Aerobic mineralization of trichloroethylene, vinyl chloride and aromatic compounds by *Rhodococcus* species. *Appl. Environ. Microbiol.* **1994,** *60*, 542-548.

(28) Saeki, H.; Akira, M.; Furuhashi, K.; Averhoff, B.; Gottschalk, G., Degradation of trichloroethene by a linear-plasmid-encoded alkene monooxygenase in *Rhodococcus corallinus* (*Nocardia corallina*) B-276. *Microbiology* **1999,** *145*, (Pt 7), 1721-30.

(29) Ensign, S. A.; Hyman, M. R.; Arp, D. J., Cometabolic degradation of chlorinated alkenes by alkene monooxygenase in a propylene-grown *Xanthobacter* strain. *Appl. Environ. Microbiol.* **1992,** *58*, 3038-3046.

(30) Vannelli, T., M. Logan, D. M. Arciero, and A. B. Hooper, Degradation of halogenated aliphatic compounds by the ammonia-oxidizing bacterium *Nitrosomonas europaea*. *Appl. Environ. Microbiol.* **1990,** *56*, 1169-1171.

(31) Semprini, L., Strategies for the aerobic co-metabolism of chlorinated solvents. *Curr. Opin. Biotechnol.* **1997,** *8*, 296-308.
(32) McCarty, P. L.; Goltz, M. N.; Hopkins, G. D.; Dolan, M. E.; Allan, J. P.; Kawakami, B. T.; Carrothers, T. J., Full-scale evaluation of in situ cometabolic degradation of trichloroethylene in groundwater through toluene injection. *Environ. Sci. Technol.* **1998,** *32*, 88-100.
(33) Habets-Crützen, A. Q. H.; de Bont, J. A. M., Inactivation of alkene oxidation by epoxides in alkene- and alkane-grown bacteria. *Appl. Microbiol. Biotechnol.* **1985,** *22*, 428-433.
(34) Cai, H.; Guengerich, F. P., Acylation of protein lysines by trichloroethylene oxide. *Chem. Res. Toxicol.* **2000,** *13*, (5), 327-35.
(35) Guengerich, F. P.; Langouet, S.; Mican, A. N.; Akasaka, S.; Muller, M.; Persmark, M., Formation of etheno adducts and their effects on DNA polymerases. *IARC Sci Publ* **1999**, (150), 137-45.
(36) Jin, Y. O.; Mattes, T. E., Adaptation of aerobic, ethene-assimilating *Mycobacterium* strains to vinyl chloride as a growth substrate. *Environ. Sci. Technol.* **2008,** *42*, (13), 4784-4789.
(37) Begley, J. F.; Hansen, E.; Wells, A. K.; Fogel, S.; Begley, G. S., Assessment and monitoring tools for aerobic bioremediation of vinyl chloride in groundwater. *Remediation Journal* **2009,** *20*, (1), 107-117.
(38) Chuang, A. S.; Jin, Y. O.; Schmidt, L. S.; Li, Y.; Fogel, S.; Smoler, D.; Mattes, T. E., Proteomic analysis of ethene-enriched groundwater microcosms from a vinyl chloride-contaminated site. *Environ. Sci. Technol.* **2010,** *44*, (5), 1594-1601.
(39) Begley, J. F.; Czarnecki, M.; Kemen, S.; Verardo, A.; Robb, A. K.; Fogel, S.; Begley, G. S., Oxygen and ethene biostimulation for a persistent dilute vinyl chloride plume. *Ground Water Monitoring & Remediation* **2011**, DOI:10.1111/j.1745-6592.2011.01371.x.
(40) Fogel, S.; Begley, J. F.; LeBlanc, C. R. In *Stimulation of vinyl chloride biodegradation in groundwater at low concentrations with ethene under aerobic conditions*, The 8th International Symposium on In Situ and On-site Bioremediation Baltimore, MD, 2005; Alleman, B. C.; Kelley, M. E., Eds. Battelle Press: Baltimore, MD, 2005.
(41) Cook, L. J.; Hickman, G.; Chang, A.; Landin, P.; Reisch, T., Comparison of aerobic and anaerobic biotreatments of low-level vinyl chloride. In *Remediation of chlorinated and recalcitrant compounds. Battelle, Monterey, CA*, 2006.
(42) Contaminated Sites Program, River Terrace RV Park, Second Five Year Review of the Record of Decision, August 4, 2010. Alaska Department of Environmental Conservation http://www.dec.state.ak.us/spar/csp/docs/rivterr/DOC009.pdf (Accessed September 21, 2010),
(43) Begley, G. S.; Fogel, S.; Begley, J. F., Microbiological Performance Monitoring for Aerobic Bioremediation of a Low Concentration Vinyl Chloride Plume. In.
(44) CH2MHill *Treatability Study Report SWMUs 2B, 2C, and 2E, Naval Air Station, Oceana, Virginia Beach, Virginia*; 2007.
(45) Owens, C. R.; Karceski, J. K.; Mattes, T. E., Gaseous alkene biotransformation and enantioselective epoxyalkane formation by *Nocardioides* sp. strain JS614. *Appl. Microbiol. Biotechnol.* **2009,** *84*, (4), 685-692.
(46) Johnson, D. R.; Lee, P. K. H.; Holmes, V. F.; Alvarez-Cohen, L., An Internal Reference Technique For Accurately Quantifying Specific mRNAs by Real-Time PCR With an

Application to the tceA Reductive Dehalogenase Gene. *Appl Environ Microb* **2005,** *71*, (7), 3866-3871.

(47) Chenna, R.; Sugawara, H.; Koike, T.; Lopez, R.; Gibson, T. J.; Higgins, D. G.; Thompson, J. D., Multiple sequence alignment with the Clustal series of programs. *Nucl. Acids Res.* **2003,** *31*, (13), 3497-3500.

(48) Jin, Y. O.; Cheung, S.; Coleman, N. V.; Mattes, T. E., Association of missense mutations in epoxyalkane coenzyme M transferase with adaptation of *Mycobacterium* sp. strain JS623 to growth on vinyl chloride. *Appl. Environ. Microbiol.* **2010,** *76*, (11).

(49) Kreader, C., Relief of Amplification Inhibition in PCR with Bovine Serum Albumin or T4 Gene 32 Protein. *Appl. Environ. Microbiol.* **1996,** *62*, (3), 1102-1106.

(50) V. Wintzingerode, F.; Göbel, U. B.; Stackebrandt, E., Determination of Microbial Diversity in Environmental Samples: Pitfalls of PCR-Based rRNA Analysis. *Fems Microbiology Reviews* **1997,** *21*, (3), 213-229.

(51) Kolb, S.; Knief, C.; Stubner, S.; Conrad, R., Quantitative Detection of Methanotrophs in Soil by Novel pmoA-Targeted Real-Time PCR Assays. *Appl Environ Microb* **2003,** *69*, (5), 2423-2429.

(52) Cheng, Y. S.; Halsey, J. L.; Fode, K. A.; Remsen, C. C.; Collins, M. L. P., Detection of Methanotrophs in Groundwater by PCR. *Appl Environ Microb* **1999,** *65*, (2), 648-651.

(53) Holmes, A. J.; Costello, A.; Lidstrom, M. E.; Murrell, J. C., Evidence That Particulate Methane Monooxygenase and Ammonia Monooxygenase May Be Evolutionarily Related. *Fems Microbiol Lett* **1995,** *132*, (3), 203-208.

(54) Lyew, D.; Guiot, S., Effects of Aeration and Organic Loading Rates on Degradation of Trichloroethylene in a Methanogenic-Methanotrophic Coupled Reactor. *Applied Microbiology and Biotechnology* **2003,** *61*, (3), 206-213.

(55) Nadkarni, M. A.; Martin, F. E.; Jacques, N. A.; Hunter, N., Determination of Bacterial Load by Real-Time PCR Using a Broad-Range (Universal) Probe and Primers Set. *Microbiology* **2002,** *148*, (Pt 1), 257-66.

(56) Martineau, C.; Whyte, L. G.; Greer, C. W., Stable Isotope Probing Analysis of the Diversity and Activity of Methanotrophic Bacteria in Soils from the Canadian High Arctic. *Appl Environ Microb* **2010,** *76*, (17), 5773-5784.

(57) Yergeau, E.; Hogues, H.; Whyte, L. G.; Greer, C. W., The Functional Potential of High Arctic Permafrost Revealed by Metagenomic Sequencing, qPCR and Microarray Analyses. *Isme J* **2010,** *4*, (9), 1206-1214.

(58) Fuse, H.; Ohta, M.; Takimura, O.; Murakami, K.; Inoue, H.; Yamaoka, Y.; Oclarit, J. M.; Omori, T., Oxidation of Trichloroethylene and Dimethyl Sulfide by a Marine *Methylomicrobium* Strain Containing Soluble Methane Monooxygenase. *Biosci Biotech Bioch* **1998,** *62*, (10), 1925-1931.

(59) Johnson, D. R.; Lee, P. K.; Holmes, V. F.; Alvarez-Cohen, L., An internal reference technique for accurately quantifying specific mRNAs by real-time PCR with application to the *tceA* reductive dehalogenase gene. *Appl. Environ. Microbiol.* **2005,** *71*, (7), 3866-71.

(60) Jin, Y. O.; Mattes, T. E., A Quantitative PCR Assay for Aerobic, Vinyl Chloride- and Ethene-Assimilating Microorganisms in Groundwater. *Environ. Sci. Technol.* **2010,** *44*, (23), 9036-9041.

(61) Jin, Y. O.; Mattes, T. E., A Quantitative PCR Assay for Aerobic, Vinyl Chloride- and Ethene-Assimilating Microorganisms in Groundwater. *Environmental Science & Technology* **2010,** *44*, (23), 9036-9041.
(62) Johnson, D. R.; Lee, P. K. H.; Holmes, V. F.; Alvarez-Cohen, L., An internal reference technique for accurately quantifying specific mRNAs by real-time PCR with application to the *tceA* reductive dehalogenase gene. *Appl. Environ. Microbiol.* **2005,** *71*, (7), 3866-3871.
(63) Jin, Y. O.; Mattes, T. E., Assessment and modification of degenerate qPCR primers that amplify functional genes from etheneotrophs and vinyl chloride-assimilators. *Lett. Appl. Microbiol.* **Accepted**.
(64) Stanley, S. H.; Prior, S. D.; Leak, D. J.; Dalton, H., Copper stress underlies the fundamental change in intracellular location of methane mono-oxygenase in methane-oxidizing organisms: Studies in batch and continuous cultures. *Biotechnology Letters* **1983,** *5*, (7), 487-492.
(65) Freedman, D. L.; Danko, A. S.; Verce, M. F., Substrate interactions during aerobic biodegradation of methane, ethene, vinyl chloride and 1,2-dichloroethenes. *Water Sci. Technol.* **2001,** *43*, 333-40.
(66) Gossett, J. M., Measurement of Henry's Law constants for C_1 and C_2 chlorinated hydrocarbons. *Environ. Sci. Technol.* **1987,** *21*, 202-208.
(67) Verce, M. F.; Ulrich, R. L.; Freedman, D. L., Characterization of an isolate that uses vinyl chloride as a growth substrate under aerobic conditions. *Appl. Environ. Microbiol.* **2000,** *66*, (8), 3535-3542.
(68) Ritalahti, K. M.; Hatt, J. K.; Petrovskis, E.; Löffler, F. E., Groundwater sampling for nucleic acid biomarker analysis. In *Handbook of Hydrocarbon and Lipid Microbiology*, Timmis, K. N., Ed. Springer Berlin Heidelberg: 2010; pp 3407-3418.
(69) Jin, Y. O.; Mattes, T. E., Assessment and modification of degenerate qPCR primers that amplify functional genes from etheneotrophs and vinyl chloride-assimilators. *Letters in Applied Microbiology* **2011,** *53*, (5), 576-580.
(70) Jin, Y. O.; Mattes, T. E., Assessment and modification of degenerate qPCR primers that amplify functional genes from etheneotrophs and vinyl chloride-assimilators. *Lett. Appl. Microbiol.* **2011,** *53*, (5), 576-580.
(71) Mattes, T. E.; Alexander, A. K.; Coleman, N. V., Aerobic biodegradation of the chloroethenes: pathways, enzymes, ecology, and evolution. *FEMS Microbiol. Rev.* **2010,** *34*, (4), 435-475.
(72) Coleman, N. V.; Bui, N. B.; Holmes, A. J., Soluble di-iron monooxygenase gene diversity in soils, sediments and ethene enrichments. *Environ. Microbiol.* **2006,** *8*, (7), 1228-1239.
(73) Jin, Y. O.; Mattes, T. E., A quantitative PCR assay for aerobic, vinyl chloride- and ethene-assimilating microorganisms in groundwater. *Environ. Sci. Technol.* **2010,** *44*, (23), 9036-41.
(74) Chuang, A. S.; Mattes, T. E., Identification of polypeptides expressed in response to vinyl chloride, ethene, and epoxyethane in *Nocardioides* sp. strain JS614 by using peptide mass fingerprinting. *Appl. Environ. Microbiol.* **2007,** *73*, (13), 4368-4372.
(75) Smith, C. J.; Nedwell, D. B.; Dong, L. F.; Osborn, A. M., Evaluation of quantitative polymerase chain reaction-based approaches for determining gene copy and gene

transcript numbers in environmental samples. *Environmental Microbiology* **2006,** *8*, (5), 804-815.

(76) Kreader, C. A., Relief of amplification inhibition in PCR with bovine serum albumin or T4 gene 32 protein. *Appl. Environ. Microbiol.* **1996,** *62*, (3), 1102-6.

(77) Semrau, J. D.; DiSpirito, A. A.; Yoon, S., Methanotrophs and Copper. *Fems Microbiology Reviews* **2010,** *34*, (4), 496-531.

(78) Ten Most Common Real-Time qPT-PCR Pitfalls. http://www.invitrogen.com/site/us/en/home/References/Ambion-Tech-Support/rtpcr-analysis/general-articles/top-ten-pitfalls-in-quantitative-real-time-pcr-primer.html

(79) Stein, L. Y.; Bringel, F.; DiSpirito, A. A.; Han, S.; Jetten, M. S. M.; Kalyuzhnaya, M. G.; Kits, K. D.; Klotz, M. G.; den Camp, H. J. M. O.; Semrau, J. D.; Vuilleumier, S.; Bruce, D. C.; Cheng, J. F.; Davenport, K. W.; Goodwin, L.; Han, S. S.; Hauser, L.; Lajus, A.; Land, M. L.; Lapidus, A.; Lucas, S.; Medigue, C.; Pitluck, S.; Woyke, T., Genome Sequence of the Methanotrophic *Alphaproteobacterium Methylocystis* sp Strain Rockwell (ATCC 49242). *J Bacteriol* **2011,** *193*, (10), 2668-2669.

(80) Smith, C. J.; Nedwell, D. B.; Dong, L. F.; Osborn, A. M., Evaluation of quantitative polymerase chain reaction-based approaches for determining gene copy and gene transcript numbers in environmental samples. *Environ. Microbiol.* **2006,** *8*, (5), 804-15.

(81) United States Geological Survey, Chloroethene Biodegradation Potential in the "Lower" Contaminant Plume, River Terrace RV Park, Soldotna, Alaska. In Survey, U. S. G., Ed. 2004.

(82) Bradley, P. M.; Richmond, S.; Chapelle, F. H., Chloroethene Biodegradation in Sediments at 4 Degrees C. *Appl Environ Microb* **2005,** *71*, (10), 6414-6417.

(83) Mattes, T. E.; Coleman, N. V.; Chuang, A. S.; Rogers, A. J.; Spain, J. C.; Gossett, J. M., Mechanism controlling the extended lag period associated with vinyl chloride starvation in *Nocardioides sp*. strain JS614. *Arch. Microbiol.* **2007,** *187*, (3), 217-26.

(84) Mattes, T. E.; Coleman, N. V.; Chuang, A. S.; Rogers, A. J.; Spain, J. C.; Gossett, J. M., Mechanism controlling the extended lag period associated with vinyl chloride starvation in *Nocardioides* sp. strain JS614. *Arch. Microbiol.* **2007,** *187*, (3), 217-226.

(85) Chang, H.; Alvarez-Cohen, L., Biodegradation of individual and multiple chlorinated aliphatic hydrocarbons by methane-oxidizing cultures. *Appl. Environ. Microbiol.* **1996,** *62*, (9), 3371-3377.

(86) Anderson, J.; McCarty, P., Transformation yields of chlorinated ethenes by a methanotrophic mixed culture expressing particulate methane monooxygenase. *Appl. Environ. Microbiol.* **1997,** *63*, (2), 687-693.

(87) van Hylckama Vlieg, J. E.; De Koning, W.; Janssen, D., Effect of Chlorinated Ethene Conversion on Viability and Activity of *Methylosinus trichosporium* OB3b. *Appl. Environ. Microbiol.* **1997,** *63*, (12), 4961-4964.

(88) Verce, M. F.; Ulrich, R. L.; Freedman, D. L., Transition from cometabolic to growth-linked biodegradation of vinyl chloride by a *Pseudomonas* sp. isolated on ethene. *Environ. Sci. Technol.* **2001,** *35*, (21), 4242-4251.

(89) Hou, C. T.; Patel, R.; Laskin, A. I.; Barnabe, N., Microbial oxidation of gaseous hydrocarbons: epoxidation of C2 to C4 n-alkenes by methylotrophic bacteria. *Appl. Environ. Microbiol.* **1979,** *38*, (1), 127-134.

(90) Colby, J.; Stirling, D. I.; Dalton, H., The soluble methane mono-oxygenase of *Methylococcus capsulatus* (Bath). Its ability to oxygenate n-alkanes, n-alkenes, ethers, and alicyclic, aromatic and heterocyclic compounds. *Biochem. J.* **1977,** *165*, (2), 395-402.

(91) Burrows, K. J.; Cornish, A.; Scott, D.; Higgins, I. J., Substrate specificities of the soluble and particulate methane mono-oxygenases of *Methylosinus trichosporium* OB3b. *J. Gen. Microbiol.* **1984,** *130*, (12), 3327-3333.

Appendices

Appendix A – Methanotroph qPCR primer selection and optimization experiments

Kolb Primer Results

When used to amplify *Methylocystis* sp. and *Methylococcus* sp. pure cultures genomic DNA, the Kolb primer set produced either two PCR products or no PCR product, respectively. This was cause for concern. To begin to resolve the issue, the PCR products were excised from the agarose gel and then sequenced. Sequence data revealed the Kolb were amplifying non-specific PCR products. Due to the difficulties of amplifying from pure culture methanotrophs, coupled with the fact that, when able to amplify, these primers were amplifying non-specifically, the Kolb primers were not used in the remainder of this qPCR method development. These results suggest that we should abandon the Kolb primer set.

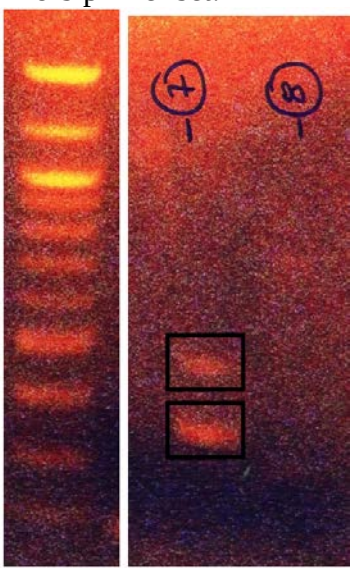

Figure A52: End point PCR products of Kolb primers and *Methylococcus* (lane 7) and *Methylocystis* (lane 8) template DNA.

pmoA 178 and pmoA 330 PCR Efficiency Variations

Reproducibility of the methanotrophs standard curve on each plate was an issue of concern. The PCR efficiencies of the standard curves varied between plates considerably, from 70% to 125%. One possible cause for this variation may be related to the freshness of the standard curve. Experiments show that when the standards are made with in 48 hrs of use, the PCR efficiencies are closer to 100% (115% for *Methylocystis* and *Methyloccocus* when amplifying with pmoA 178, 102% for *Methylocystis* and 107% for *Methyloccocus* when amplifying with pmoA 330 M, 98.8% for *Methylocystis* and 97.0% for *Methyloccocus* when amplifying with the pmoA 330 primer set). When an older standard curve was used (stored at -20 for 3 weeks) the PCR efficiencies were less than desirable (125% for *Methylocystis* and *Methyloccocus* when amplifying with pmoA 178, 70% for *Methylocystis* and *Methyloccocus* when amplifying with pmoA 330). In order to increase their reproducibility, the standards must be made fresh for every experiment.

Methanotroph qPCR Primer Optimization

Optimizing pmoA 178 and pmoA 330 Primer Concentrations

The goal of this experiment was to determine the optimal standard templates, primer set, and primer concentration so that a single standard curve can be used in the remainder of our methanotroph qPCR experiments. To that end, standard curves were constructed using both pmoA 178 and pmoA 330 primer sets, amplifying from both isolates of methanotroptophs (*Methylococcus* and *Methylocystis*), and with primer concentrations varying from 200 nM to 1000 nM. To ensure equal comparison between primer sets, template species, and primer concentrations, the standard curve dynamic ranges were limited to 100-10^6 copies per reaction and data was analyzed using the "auto CT analysis" function of the proprietary Applied Biosystems 7000 System software.

The results of this experiment revealed that, when *Methylocystsis* sp. and *Methylococcus* sp. template DNA was amplified, the optimal standard curves for the pmoA 178 primer set occurred when the primer concentrations were 300 nM and 200 nM, respectively, yielding PCR efficiencies of 107%* and 103% (Table A29, Table A30, Figure A 53, and Figure A54). For the pmoA 330 primer set, when *Methylocystsis* sp. and *Methylococcus* sp. template DNA was amplified, the optimal standard curves for both species occurred when the primer concentrations were 300 nM, yielding PCR efficiencies of 100% in both cases (Table A31, Table A32, Figure A55, Figure A56).

When comparing results between species, there was no noticeable difference between standard curves amplified using *Methylocystis* sp. or *Methylococcus* sp. template DNA. Due to the lack of discernable variation, and because the *Methylocystis* sp. is easier to culture in the lab, it was decided that *Methylocystis* sp. would be the best choice for template DNA in standard curves. Table A29 and Figure A 53 contain the standard curve results for the pmoA 178 primer set amplifying *Methylocystis* sp. template DNA, while Table A30 and Figure A54 contain the standard curve results for *Methylococcus* sp. template DNA. Table A31 and Figure A55 contain the standard curve results for the pmoA 330 primer set amplifying *Methylocystis* sp. template DNA, while Table A32 and Figure A56 contain the standard curve results for *Methylococcus* sp. template DNA.

Analysis of the dissociation curves of PCRs with the pmoA 178 and the pmoA 330 primer sets revealed 2 or more peaks in both cases (Figure A 59 - Figure A 61). In most cases, these double peaks were found in the no template control suggesting they were primer dimer artifacts (which is not ideal for qPCR with SYBR Green). In one case, both double peaks in Figure A62 (with the highest melting temperature) were found to correspond to the PmoA gene. These issues with the dissociation curves contributed to our decision to abandon these primer sets for use in methanotroph qPCR in this study.

Optimizing 16S Type I and 16S Type II Primer Concentrations

After the appropriate primer concentrations and template species were determined, the pmoA 178 and pmoA 330 primer sets needed to be validated. In order to do this, a set of 16S qPCR primers specific to Type I and Type II methanotrophs were taken from the literature *(56)*. However, before performing the validation experiment, the 16S qPCR primer concentrations were also optimized.

Standard curves were constructed using both 16S T1 and 16S T2 primer sets, amplifying from *Methylococcus* sp. (Type I methanotroph) and *Methylocystis* sp. (Type II methanotroph), respectively. Primer concentrations varied from 200 nM to 1000 nM. To ensure equal comparisons between primer concentrations, the standard curve dynamic ranges were limited to 100-10^6 copies per reaction and were analyzed using the "auto CT analysis". The results of this experiment revealed that the optimal standard curve for the 16S T1 primer set occurred when the primer concentration was 800 nM, yielding a PCR efficiency of 101% (Table A33 and Figure A57). For the 16S T2 primer set, the optimal standard curve occurred when the primer concentration was 300 nM, yielding a PCR efficiency of 100% (Table A34 and Figure A58). Table A33 and Figure A57 contain the standard curve results for the 16S T1 primer set, and Table A34 and Figure A58 contain the standard curve results for the 16S T2 primer set. Dissociation curves for the Type I and Type II primers are shown in Figure A 63 and Figure A64.

Table A29: Average standard curve characteristics for primer set pmoA 178 amplifying template DNA from *Methylocystis* sp. strain Rockwell.

nM	**Dynamic Range**	**Slope**	**R^2**	**PCR Efficiency (%)**	**Y-intercept (cycle #)**
200	100 - 10^6	-3.34	0.993	99.3	38.0
300	100 - 10^6	-3.16	0.994	107	36.1
400	100 - 10^6	-2.97	0.988	117	34.4
500	na	na	na	na	na
600	na	na	na	na	na
700	100 - 10^6	-3.00	0.994	115	34.2
800	100 - 10^6	-2.89	0.989	121	33.7
900	100 - 10^6	-2.86	0.987	123	33.5
1000	100 - 10^6	-2.75	0.981	131	33.3

Note: Cells marked "na" were not included in these result due to the 10^3 portion of the standard curve amplifying poorly, resulting in standard curves that were unusable.

Note: Values represent the average of triplicate measurements.

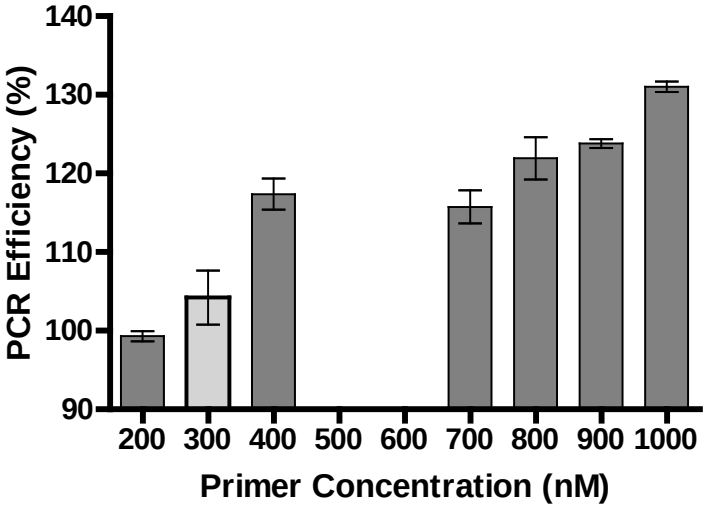

Figure A 53: Comparison of pmoA 178 PCR efficiencies as related to varying primer concentrations. Template DNA was from *Methylocystis* sp. strain Rockwell. Bolded borders indicate optimal primer concentration, and light grey bars represent chosen template species for the indicated primer set. The bar heights at each concentration are the average of triplicate measurements and error bars represent standard deviations.

Table A30: Average standard curve characteristics for primer set pmoA 178 amplifying template DNA from *Methylococcus capsulatus*.

nM	Dynamic Range	Slope	R^2	PCR Efficiency (%)	Y-intercept (CT)
200	100 - 10^6	-3.23	0.994	104	36.5
300	100 - 10^6	-3.14	0.995	108	35.5
400	100 - 10^6	-2.91	0.984	121	33.5
500	100 - 10^6	-3.08	0.993	111	34.5
600	100 - 10^6	-3.03	0.991	114	34.2
700	100 - 10^6	-2.93	0.986	120	33.9
800	100 - 10^6	-2.87	0.979	123	33.7
900	100 - 10^6	-2.78	0.968	129	33.3
1000	100 - 10^6	-2.68	0.959	136	32.9

Note: Values represent the average of triplicate measurements.

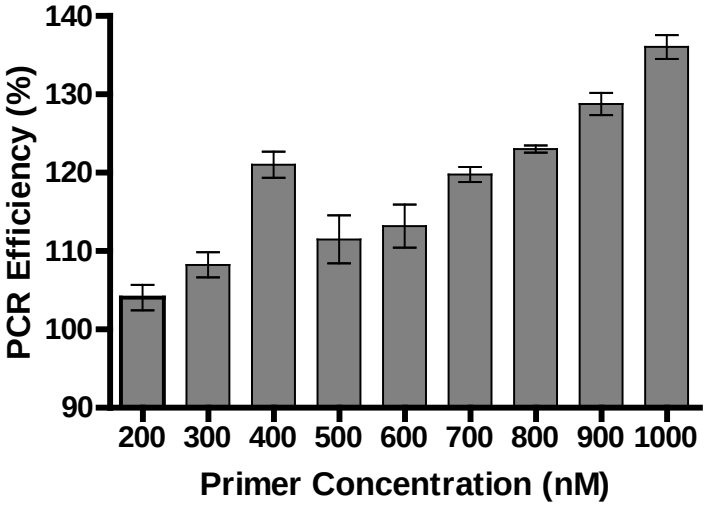

Figure A54: Comparison of pmoA 178 PCR efficiencies as related to varying primer concentrations. Template DNA was from *Methylococcus capsulatus*. Bolded borders indicate optimal primer concentration. The bar heights are the average of triplicate measurements and the error bars represent standard deviations.

Table A31: Average standard curve characteristics for primer set pmoA 330 amplifying template DNA from *Methylocystis* sp. strain Rockwell.

nM	Dynamic Range	Slope	R^2	PCR Efficiency (%)	Y-intercept (CT)
200	100 - 10^6	-3.35	0.998	98.9	35.9
300	100 - 10^6	-3.31	0.999	101	35.6
400	100 - 10^6	-3.26	0.998	103	35.5
500	100 - 10^6	-3.20	0.995	105	35.3
600	100 - 10^6	-3.22	0.997	105	35.4
700	100 - 10^6	-3.22	0.999	104	35.2
800	100 - 10^6	-3.14	0.998	108	35.1
900	100 - 10^6	-3.05	0.999	113	34.9
1000	100 - 10^6	-3.09	0.998	111	35.4

Note: Values represent the average of triplicate measurements.

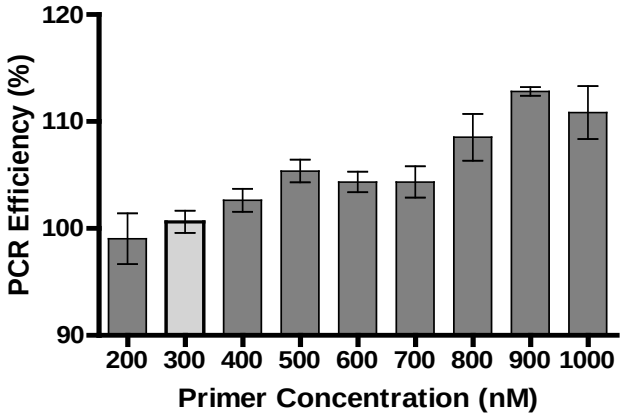

Figure A55: Comparison of pmoA 330 PCR efficiencies as related to varying primer concentrations. Template DNA was from *Methylocystis* sp. strain Rockwell. Bolded borders indicate optimal primer concentration, and light grey bars represent chosen template species for the indicated primer set. The bar heights at each concentration are the average of triplicate measurements and error bars represent standard deviations.

Table A32: Average standard curve characteristics for primer set pmoA 330 amplifying template DNA from *Methylococcus capsulatus.*

nM	Dynamic Range	Slope	R^2	PCR Efficiency (%)	Y-intercept (CT)
200	100 - 10^6	-3.32	0.999	100	35.5
300	100 - 10^6	-3.31	0.999	101	35.3
400	100 - 10^6	-3.23	0.999	104	35
500	na	na	na	na	na
600	na	na	na	na	na
700	100 - 10^6	-3.20	0.997	106	35.1
800	100 - 10^6	-3.15	0.995	108	35.2
900	100 - 10^6	-3.03	0.997	114	34.4
1000	100 - 10^6	-3.08	0.994	111	35.0

Note: Cells marked "na" were not included in these result because the 10^3 portion of the standard curve amplified poorly, resulting in standard curves that were unusable.
Note: Values represent the average of triplicate measurements.

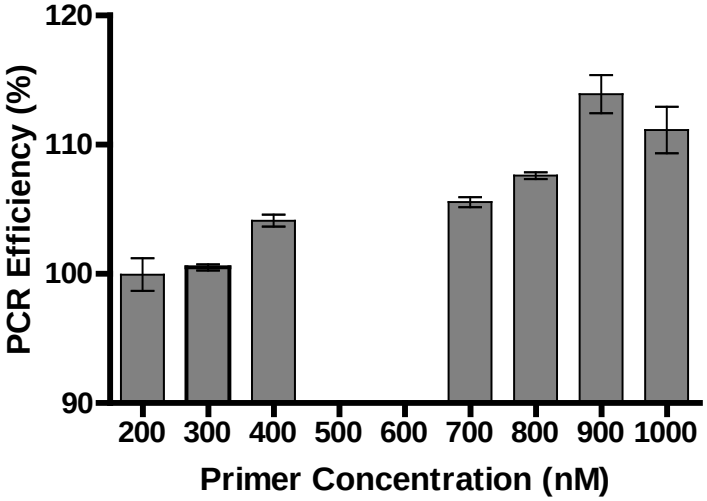

Figure A56: Comparison of pmoA 330 PCR efficiencies as related to varying primer concentrations. Template DNA was from *Methylococcus capsulatus*. Bolded borders indicate optimal primer concentration. The bar heights at each concentration are the average of triplicate measurements and error bars represent standard deviations.

Table A33: Average standard curve characteristics for 16S T1 primer set amplifying template DNA from *Methylococcus capsulatus*.

nM	Dynamic Range	Slope	R^2	PCR Efficiency (%)	Y-intercept (CT)
200	100 - 10^6	-3.96	0.998	78.8	42.8
300	100 - 10^6	-3.62	0.999	88.9	39.2
400	100 - 10^6	-3.46	0.999	94.7	37.3
500	100 - 10^6	-3.46	0.999	94.7	36.5
600	100 - 10^6	-3.42	1.000	96.0	35.9
700	100 - 10^6	-3.35	0.999	99.0	35.6
800	100 - 10^6	-3.30	0.999	101	35.1
900	100 - 10^6	-3.31	0.999	101	34.8
1000	100 - 10^6	-3.34	0.999	99.3	35.0

Note: The standard curve at each concentration was run in triplicate.

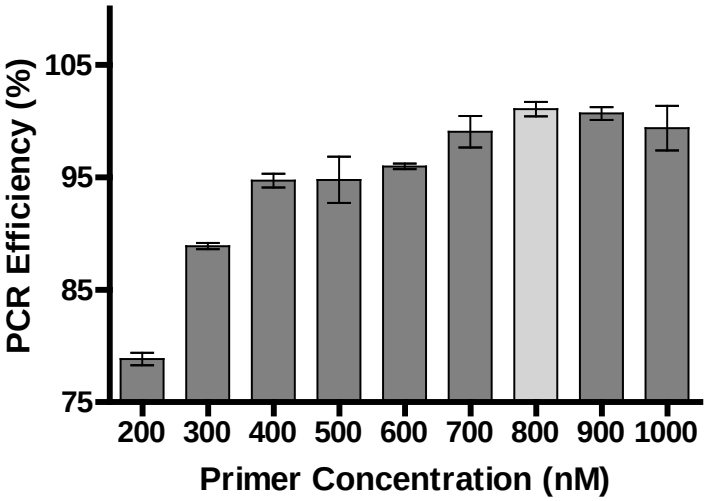

Figure A57: Comparison of 16S T1 PCR efficiencies as related to varying primer concentrations. Template DNA was from *Methylococcus capsulatus*. Light grey bars indicate optimal primer concentration. The bar heights at each concentration are the average of triplicate measurements and error bars represent standard deviations.

Table A34: Average standard curve characteristics for 16S T2 primer set amplifying template DNA from *Methylocystis* sp. strain Rockwell.

nM	Dynamic Range	Slope	R^2	PCR Efficiency (%)	Y-intercept (CT)
200	100 - 10^6	-3.36	0.999	98.6	35.8
300	100 - 10^6	-2.97	0.989	117	33.2
400	100 - 10^6	-3.05	0.994	113	33.1
500	100 - 10^6	-3.27	0.999	102	34.2
600	100 - 10^6	-3.26	0.994	103	34.0
700	100 - 10^6	-3.16	0.997	108	33.7
800	100 - 10^6	-3.18	0.998	107	33.2
900	100 - 10^6	-3.24	0.999	104	34.1
1000	100 - 10^6	-3.24	0.999	103	34.1

Note: The standard curve at each concentration was run in triplicate.

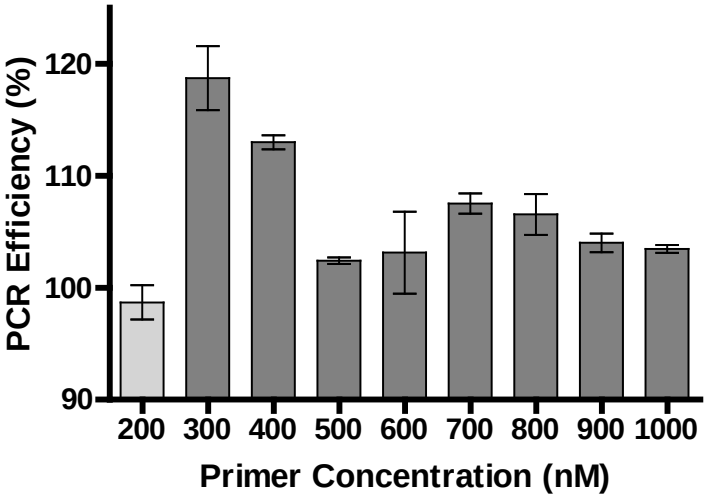

Figure A58: Comparison of 16S T2 PCR efficiencies as related to varying primer concentrations. Template DNA was from *Methylocystis* sp. strain Rockwell. Light grey bars indicate optimal primer concentration. The bar heights at each concentration are the average of triplicate measurements and error bars represent standard deviations.

qPCR product disssocation curves

This section provides supporting data for methanotroph qPCR experiments conducted under Subtasks 1.3 and 1.4. The dissociation curves are a quality assurance/quality control step that indicates qPCR specificity when using the non-specific DNA binding dye SYBR green.

pmoA 178/330 Dissociation Curves

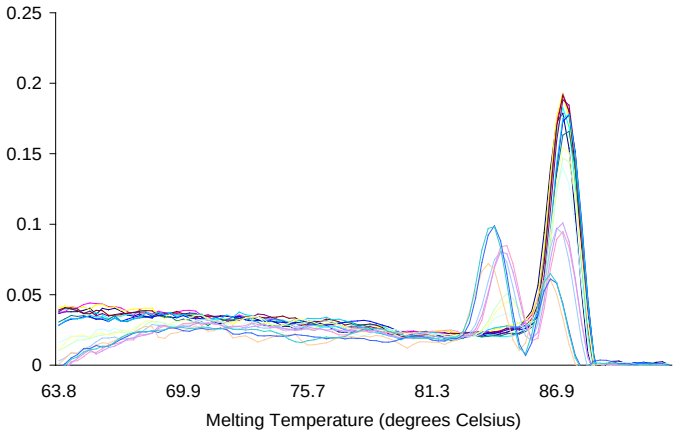

Figure A 59: Dissociation curve for primer set pmoA 178 amplifying template DNA from *Methylocystis* sp. strain Rockwell at a primer concentration of 300 nM. Double peaks are seen in samples containing little (10^2) to no (no-template control) template DNA, indicating probable primer-dimer artifacts.

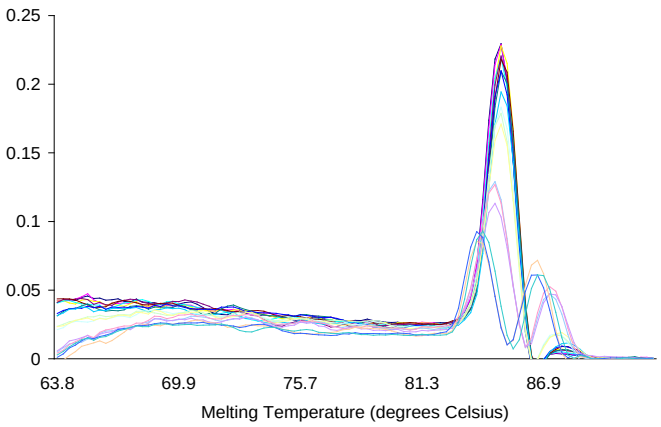

Figure A 60: Dissociation curve for primer set pmoA 178 amplifying template DNA from *Methylococcus capsulatus* at a primer concentration of 300 nM. Double peaks are seen in samples containing little (10^2) to no (no-template control) template DNA, indicating probable primer-dimer artifacts.

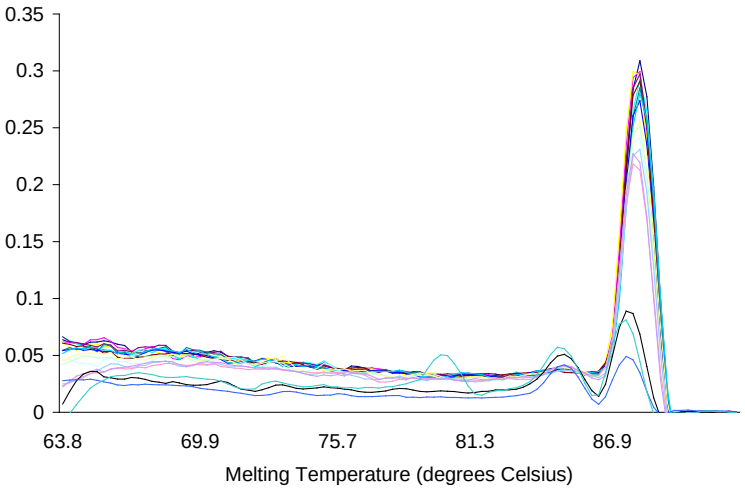

Figure A 61: Dissociation curve for primer set pmoA 330 amplifying template DNA from *Methylocystis* sp. strain Rockwell at a primer concentration of 300 nM. Double peaks are seen in no-template control samples indicating probable primer-dimer artifacts.

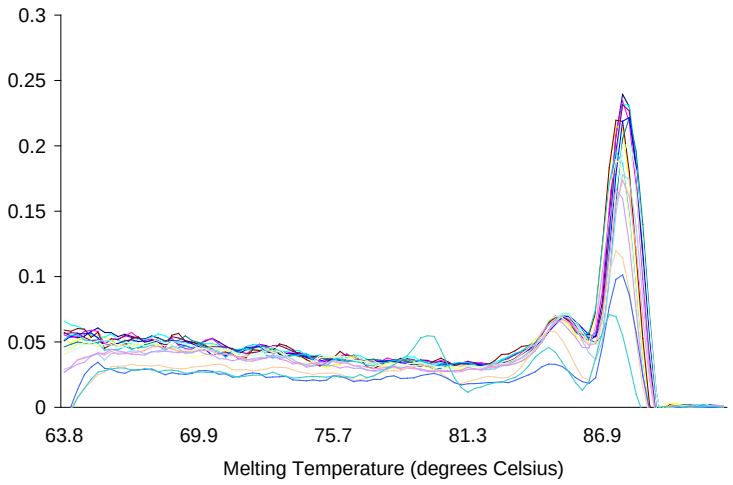

Figure A62: Dissociation curve for primer set pmoA 330 amplifying template DNA from *Methylococcus capsulatus* at a primer concentration of 300 nM. Double peaks are seen in all samples. PCR products were purified and sequence results indicated that both peaks represented the *pmoA* gene.

Optimization Experiments:
16S T1 and 16S T2 Dissociation Curves

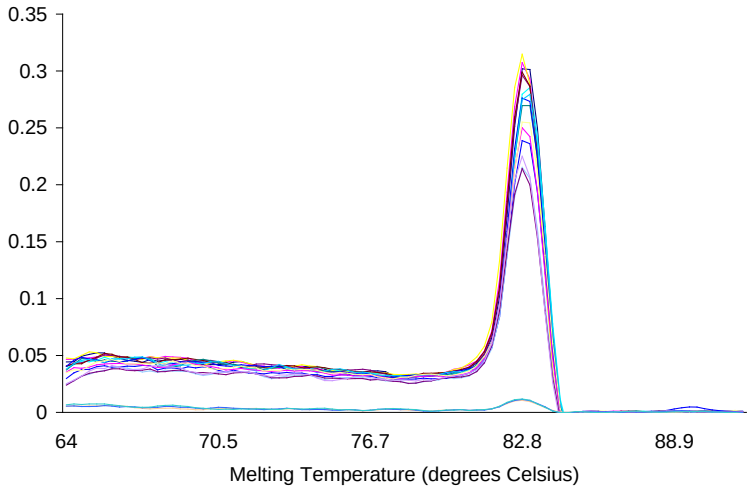

Figure A 63: Dissociation curve for primer set 16S T1 amplifying template DNA from *Methylococcus capsulatus* at a primer concentration of 800 nM.

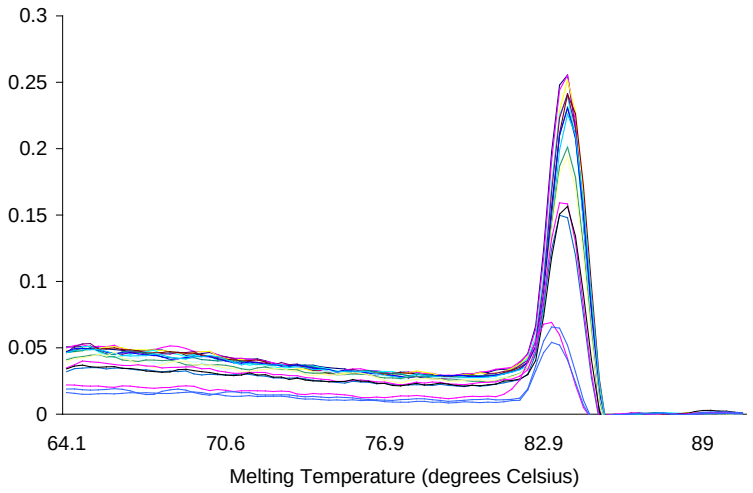

Figure A64: Dissociation curve for primer set 16S T2 amplifying template DNA from *Methylocystis* sp. strain Rockwell at a primer concentration of 200 nM.

Primer Validation

To validate the pmoA primer sets for qPCR, known amounts of methanotrophic DNA were quantified using the pmoA 178, 330, 16S T1, and T2 primer sets and subsequently compared. Assuming there is one copy of each gene per organism genome, this technique would be expected to validate the qPCR primers because the gene abundance derived from them would be with in the same order of magnitude. Genomic DNA was extracted from *Methylococcus capsulatus* (Type I) and *Methylocystis* sp. strain Rockwell (Type II) and used to assemble 5 different mixtures of Type I and Type II methanotroph DNA. The mixtures were as follows: 100% (T1); 75:25 (T1:T2); 50:50 (T1:T2); 25:75 (T1:T2), and 100% (T2). Important details of this experiment are reported in the main text under subtask 1.3. Average standard curve characteristics for pmoA 178 and pmoA 330 primer validation experiments are shown in Table A 35 Product dissociation curves for this experiment are presented in Figure A 65 through Figure A 68. These indicate, once again, that qPCR with the 178 and 330 *pmoA* primer sets is not as effective as it is with the T1 and T2 16S primer sets. This led us to search for a better *pmoA* qPCR primer set in the literature.

Table A 35. Average standard curve characteristics for pmoA 178 and pmoA 330 primer validation experiments.

	Dynamic Range	**Slope**	**R^2**	**PCR Efficiency (%)**	**Y-intercept (cycle #)**
T1	100 - 10^7	-3.43	0.999	95.54	36.52
T2	100 - 10^6	-3.67	0.991	87.33	38.21
pmoA 178	100 - 10^7	-3.43	0.998	95.83	37.16
pmoA 330	100 - 10^7	-3.46	0.996	94.47	36.03

Note: Each standard curve was run in duplicate.

Validation Experiments:
pmoA 178/pmoA 330 Dissociation Curves

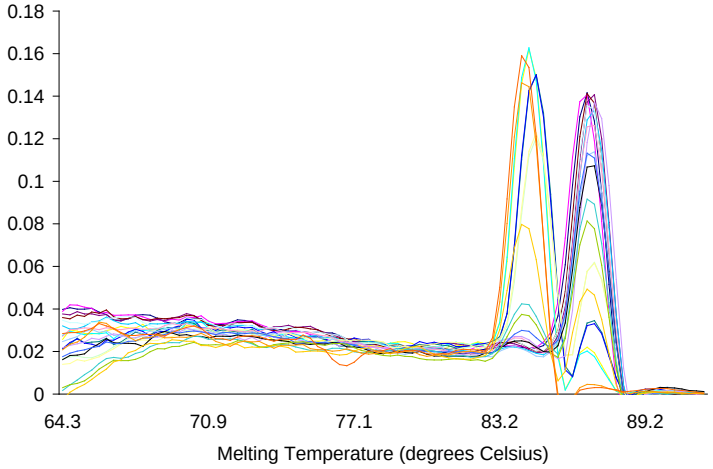

Figure A 65: Dissociation curve for primer set pmoA 178. The ~89°C peak represents standard curve melting temperatures, while the ~84°C peak represents melting temperature of the Type I/Type II sample mixtures.

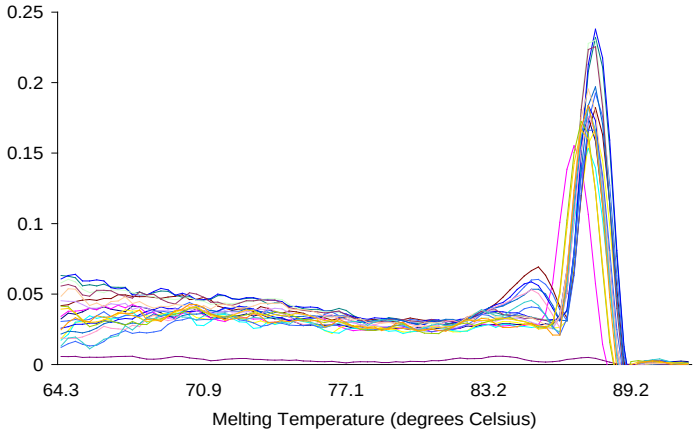

Figure A 66: Dissociation curve for primer set pmoA 330 amplifying standard curve template DNA and Type I/Type II sample mixtures at a primer concentration of 300 nM.

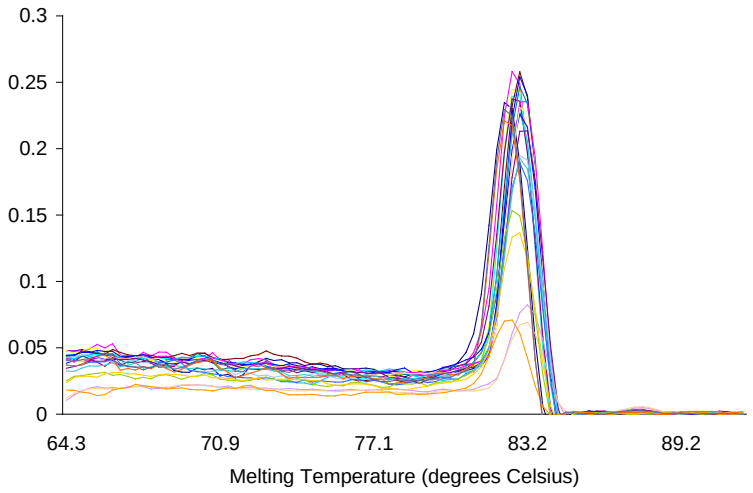

Figure A67: Dissociation curve for primer set pmoA 16S T1 amplifying standard curve template DNA and Type I/Type II sample mixtures at a primer concentration of 800 nM.

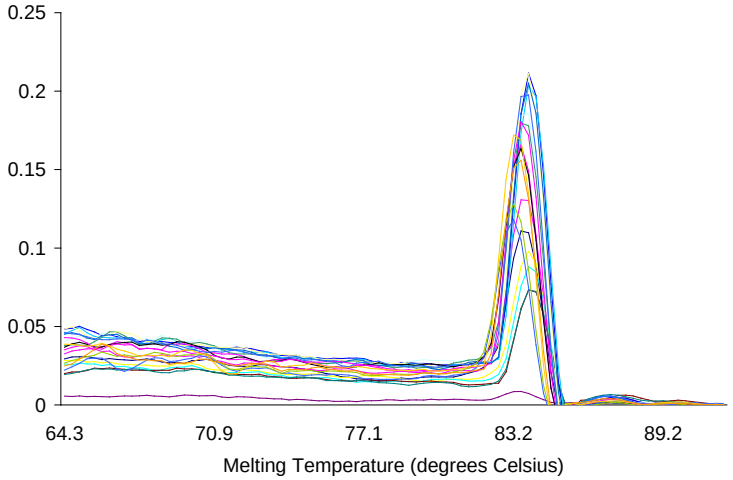

Figure A 68: Dissociation curve for primer set pmoA 16S T2 amplifying standard curve template DNA and Type I/Type II sample mixtures at a primer concentration of 200 nM.

pmoA 472 and mmoX primer set Validation Experiments

The following dissociation curves illustrate that SYBR Green qPCR with the pmoA472 (Figure A69), and the two methanotroph specific 16S rRNA primer sets for Type I (T1) (Figure A70) and Type II methanotrophs (T2) (Figure A 71) are specific when amplifying standard curve template DNA and Type I/TypeII methanotroph DNA mixtures. Table A 36 and Table A 37 illustrate that the qPCR standard curves are linear and other parameters (e.g. PCR efficiency) are within acceptable ranges.

Dissociation Curves

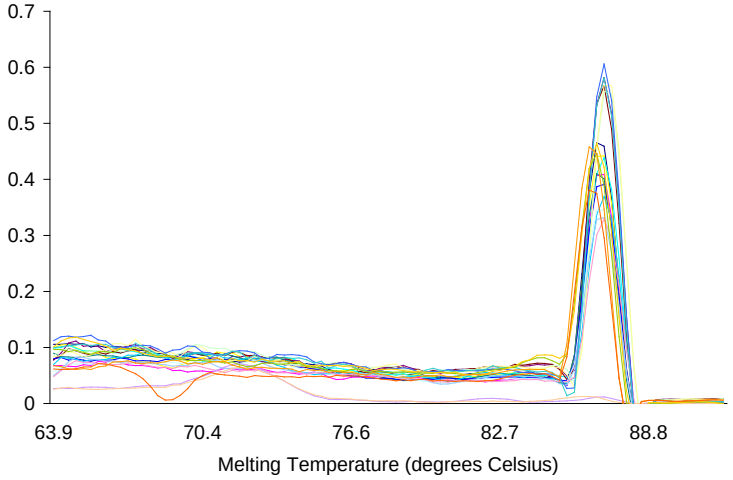

Figure A69: Dissociation curve for primer set pmoA 472 amplifying standard curve template DNA and Type I/Type II sample mixtures at a primer concentration of 300 nM. This curve is associated with the data presented in Table 20.

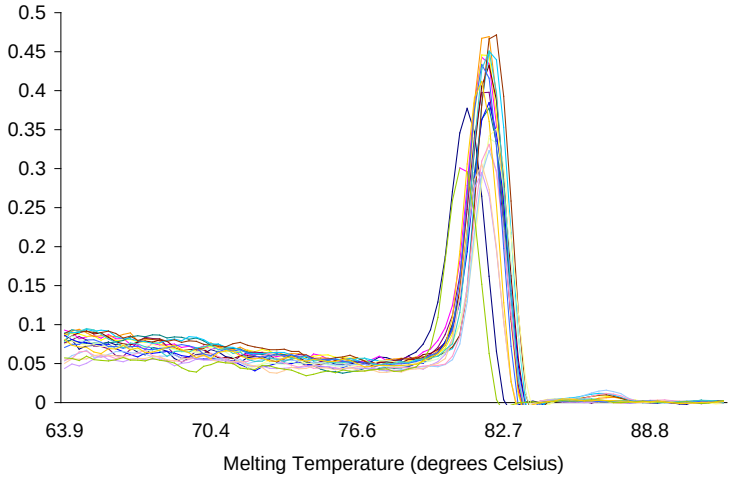

Figure A70: Dissociation curve for primer set 16S T1 amplifying standard curve template DNA and Type I/Type II sample mixtures at a primer concentration of 800 nM.

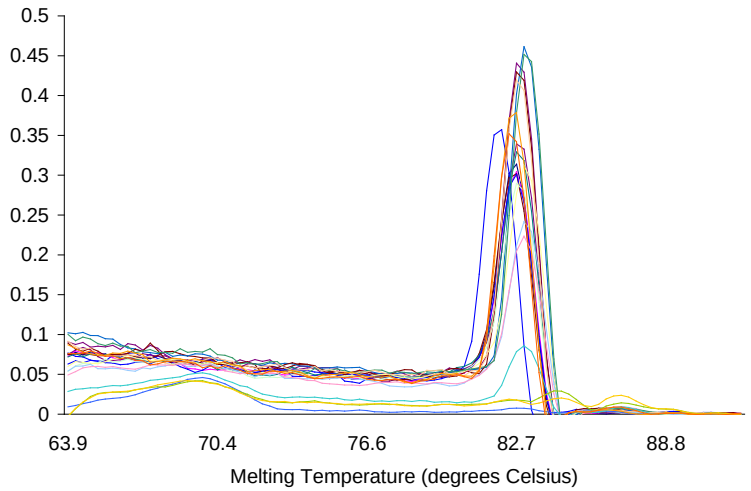

Figure A 71: Dissociation curve for primer set primer set 16S T2 amplifying standard curve template DNA and Type I/Type II sample mixtures at a primer concentration of 200 nM.

Standard Curve Characteristics - pmoA 472 and mmoX Validation Experiments

Table A 36. Average standard curve characteristics for pmoA 472 and mmoX primer validation experiment.

	Dynamic Range	Slope	R^2	PCR Efficiency (%)	Y-intercept (cycle #)
T1	1000 - 10^6	-3.25	0.997	102.93	34.75
T2	100 - 10^6	-3.30	0.999	100.94	35.43
pmoA 472	100 - 10^6	-3.37	0.998	98.05	36.36
mmoX	100 - 10^6	-3.47	0.999	94.18	35.80

Note: Each standard curve was run in duplicate.

Table A 37. Average standard curve characteristics for 16S T1 and 16S T2 primer validation experiment.

	Dynamic Range	Slope	R^2	PCR Efficiency (%)	Y-intercept (cycle #)
T1	100 - 10^6	-3.30	0.997	100.80	35.53
T2	100 - 10^6	-3.34	0.999	99.17	35.58
16S U	10^4 - 10^6	-3.27	0.999	102.22	34.79

Note: Each standard curve was run in duplicate.

16S T1, T2 and Universal primer validation

The following figures indicate SYBR Green qPCR with the methanotroph-specific 16S rRNA qPCR primer 16S T1 (Figure A 72), 16S T2 (Figure A 73), and "universal" 16S rRNA primer (16SU; Figure A 74) is appropriately specific when amplifying standard curve template DNA and Type I/TypeII methanotroph DNA mixtures.

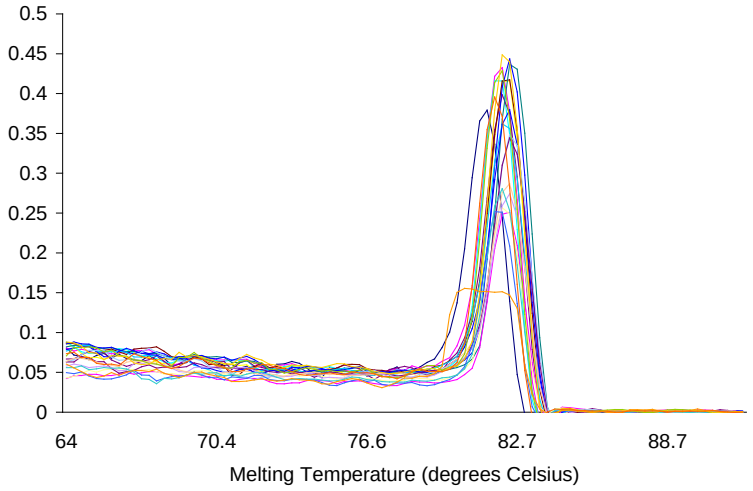

Figure A 72: Dissociation curve for primer set 16S T1 amplifying standard curve template DNA and Type I/Type II sample mixtures at a primer concentration of 800 nM.

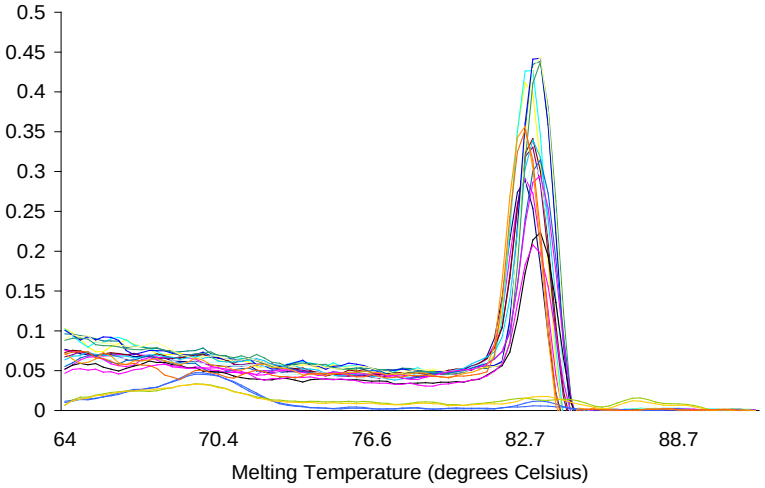

Figure A 73: Dissociation curve for primer set 16S T2 amplifying standard curve template DNA and Type I/Type II sample mixtures at a primer concentration of 200 nM.

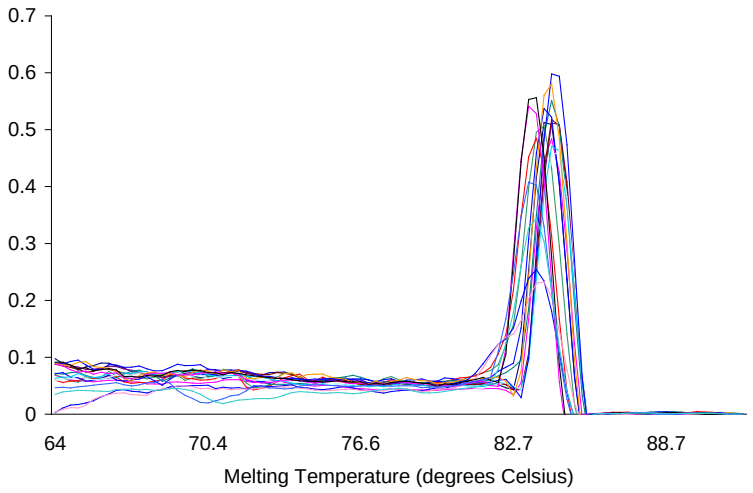

Figure A 74: Dissociation curve for primer set 16S U amplifying template DNA from *Methylocystis* sp. strain Rockwell at a primer concentration of 300 nM.

Soldotna, AK Environmental Samples – methanotroph qPCR

The following information shows standard curve parameters (Table A 38), no template control Ct values (Table A 39) (using pmoA47 and mmoX qPCR primers) and dissociation curves for the pmoA 472 products (Figure A 75) when performing methanotroph qPCR on DNA extracted from Soldotna, AK samples.

Table A 38. Average standard curve characteristics for pmoA 472 and mmoX in Soldotna, AK environmental sample qPCR assay.

	Dynamic Range	**Slope**	**R^2**	**PCR Efficiency (%)**	**Y-intercept (cycle #)**
pmoA 472	100 - 10^5	-3.31	0.998	100.62	36.28
mmoX	100 - 10^6	-3.38	0.999	97.64	35.80

Note: Each standard curve was run in duplicate.

Table A 39. No Template Control (NTC) Ct values for Soldotna, AK standard curves.

	No Template Control	
	Duplicate 1 (cycle #)	Duplicate 2 (cycle #)
pmoA 472	35.3	35.02
mmoX	35.69	33.61

Note: Each NTC was run in duplicate.

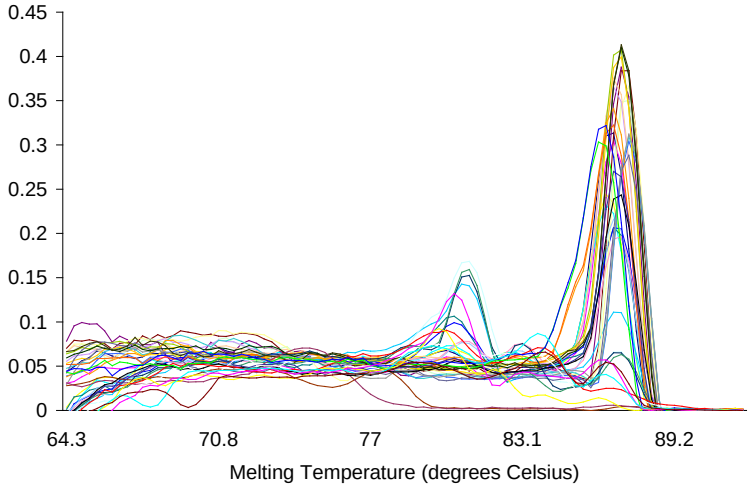

Figure A 75: Dissociation curve for primer set pmoA 472 amplifying standard curve template DNA and environmental samples from VC contaminated groundwater in Soldotna, AK.

Naval Air Station Oceana, Virginia Environmental Samples

The following information shows standard curve parameters (Table A 40), no template control Ct values (Table A 41) (using pmoA47, mmoX, 16S T1, and 16S T2 qPCR primers) and dissociation curves for the pmoA 472 products (Figure A 76) and mmoX products (Figure A 77) when performing methanotroph qPCR on DNA extracted from NAS Oceana, VA samples.

Table A 40. Average standard curve characteristics for pmoA 472, mmoX, 16 T1, and 16S T2 in NAS Oceana, VA environmental sample qPCR assay.

	Dynamic Range	Slope	R^2	PCR Efficiency (%)	Y-intercept (cycle #)
pmoA 472	100 - 10^5	-3.29	0.997	101.17	36.90
mmoX	100 - 10^6	-3.34	0.979	99.44	35.72
16S T1	1000 - 10^6	-3.28	0.998	101.88	35.31
16S T2	100 - 10^6	-3.46	0.999	94.53	38.66

Note: Each standard curve was run in duplicate.

Table A 41. No Template Control (NTC) Ct values for NAS Oceana, VA standard curves.

	No Template Control	
	Duplicate 1 (cycle #)	Duplicate 2 (cycle #)
pmoA 472	36.37	undetectable
mmoX	undetectable	undetectable
16S T1	33.17	33.6
16S T2	36.93	36.76

Note: Each NTC was run in duplicate.

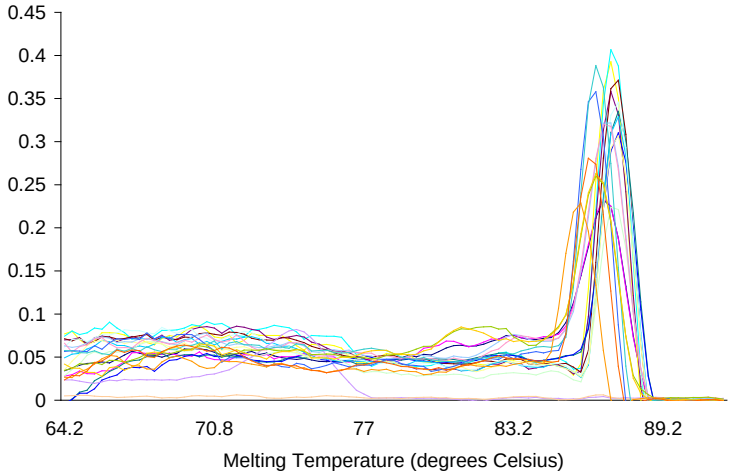

Figure A 76: Dissociation curve for primer set pmoA 472 amplifying standard curve template DNA and environmental samples from VC contaminated groundwater in NAS Oceana, VA.

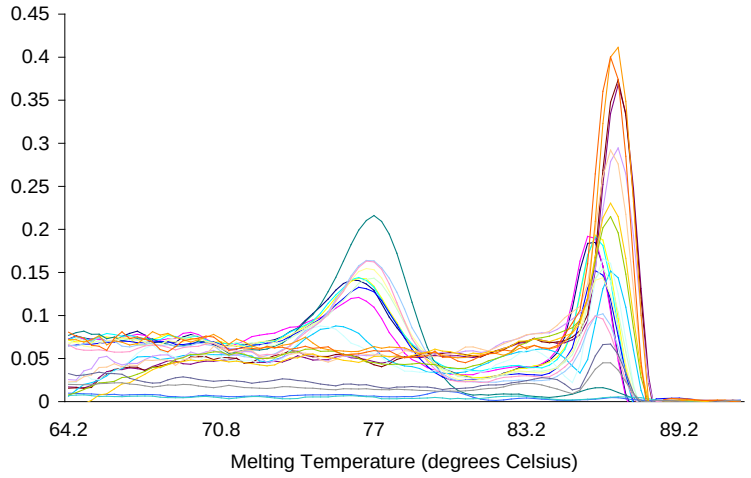

Figure A 77: Dissociation curve for primer set mmoX amplifying standard curve template DNA and environmental samples from VC contaminated groundwater in NAS Oceana, VA.

Carver, MA Environmental Samples

The following information shows standard curve parameters (Table A 42), no template control Ct values (Table A 43) (using pmoA47 and mmoX qPCR primers) and dissociation curves for the pmoA 472 products (Figure A 76) when performing methanotroph qPCR on DNA extracted from Soldotna, AK samples.

Table A 42: Average standard curve characteristics for 16S U, 16 T1, 16S T2 and Luciferase in Carver, MA environmental sample qPCR assay.

	Dynamic Range	**Slope**	**R^2**	**PCR Efficiency (%)**	**Y-intercept (cycle #)**
16S U	100 - 10^6	-3.34	0.990	99.40	36.04
16S T1	100 - 10^6	-3.34	0.998	99.26	36.03
16S T2	100 - 10^6	-3.32	0.998	99.88	36.20
Luciferase	100 - 10^6	-3.33	0.998	99.80	35.91

Note: Each standard curve was run in duplicate

Table A 43: No Template Control (NTC) results for Carver, MA standard curves shown in Table A 42.

	No Template Controls	
	Duplicate 1 (cycle #)	Duplicate 2 (cycle #)
16S U	33.56	33.85
16S T1	34.37	33.79
16S T2	35.00	35.33
Luciferase	undetectable	undetectable

Note: Each NTC was run in duplicate.

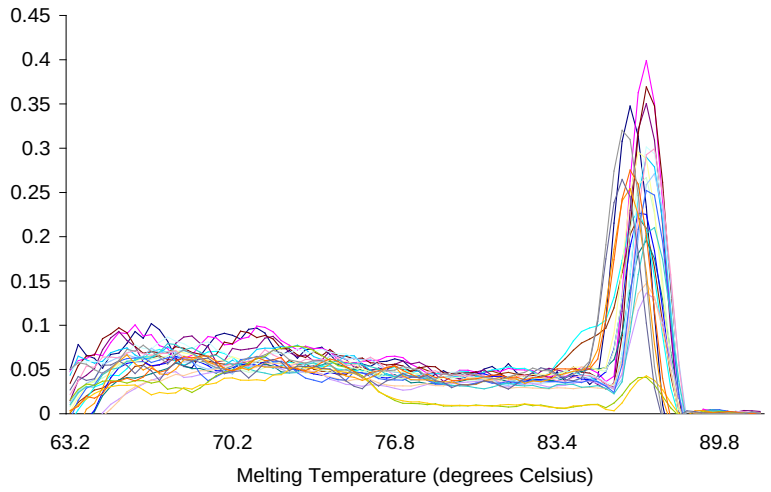

Figure A 78: Dissociation curve for pmoA 472 primer set amplifying standard curve template DNA and environmental samples from VC contaminated groundwater in Carver, MA.

Carver, MA – Task 2 cDNA Experiment

The data below, including luciferase gene recovery ratios (Table A 44), standard curve characterisitics (Table A 45), and NTC Ct values (Table A 46), and mmoX and luciferase primer product dissociation curves (Figure A 79, Figure A 80 and Figure A 81) supports the information presented in section 2.2.5, where RT-qPCR for methanotrophs was described.

Table A 44. Luciferase gene recovery ratios for Carver, MA qPCR experiments.

Monitoring Well	Injected Reference Gene Copies	Reference Gene Copies Recovered	Recovery Ratio
64I	225,000,000	25,392,468	0.112855
63I	225,000,000	20,950,970	0.093115
46D	225,000,000	21,836,357	0.09705
64I cDNA	225,000,000	61,151,264	0.271783
63I cDNA	225,000,000	31,010,226	0.137823
46D cDNA	225,000,000	135,332,755	0.601479

Note: Each sample was run in duplicate and average quantifications were used to calculate recovery ratios.

Table A 45. Average standard curve characteristics for 16S U, 16 T1, 16S T2 and Luciferase in Carver, MA environmental sample qPCR assay.

	Dynamic Range	Slope	R^2	PCR Efficiency (%)	Y-intercept (cycle #)
pmoA 472	$100 - 10^6$	-3.36	0.992	98.62	37.38
mmoX	$100 - 10^6$	-3.40	0.999	96.69	36.04
Luciferase	$300 - 3x10^6$	-3.29	0.999	101.38	35.27

Note: Each standard curve was run in duplicate.

Table A 46: No Template Control (NTC) results for Carver, MA standard curves shown in Table A 45.

	No Template Controls	
	Duplicate 1 (cycle #)	Duplicate 2 (cycle #)
pmoA 472	34.02	35.49
mmoX	31.19	31.56
Luciferase	undetectable	undetectable

Note: Each NTC was run in duplicate.

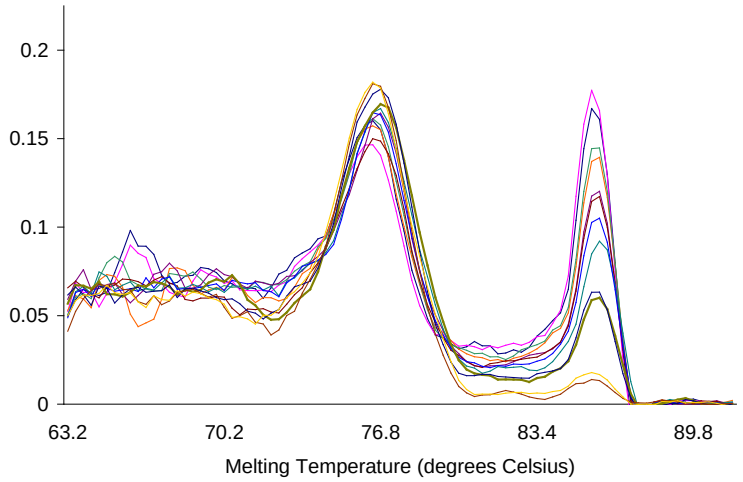

Figure A 79: Dissociation curve for *mmoX* primer set standard curve Carver, MA cDNA experiment. Multiple peaks were observed and appear to be primer-dimer artifacts since the no-template control contains only one peak.

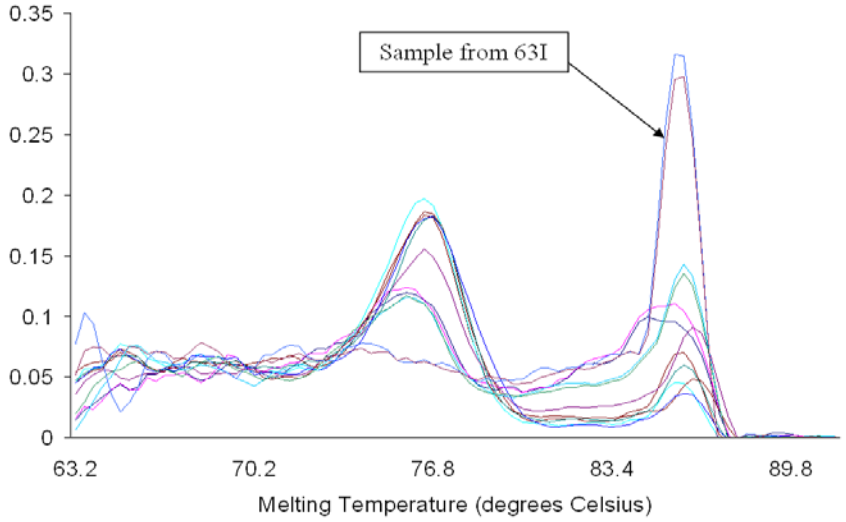

Figure A 80: Dissociation curve for *mmoX* primer set amplifying environmental samples from Carver, MA cDNA experiment. Multiple peaks were observed and appear to be primer-dimer artifacts caused by low target gene abundances. Sample 63I showed high quantities of the target gene, which could explain why it did not have a melting temperature associated with the primer-dimer peak.

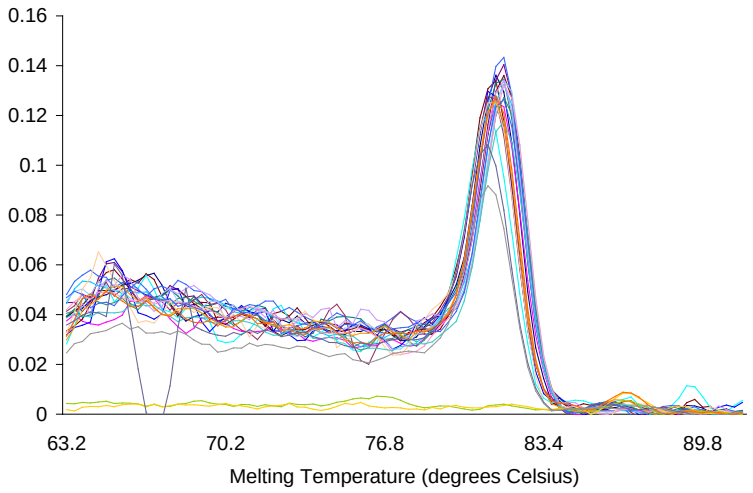

Figure A 81: Dissociation curve for Luciferase primer set amplifying standard curve template DNA and environmental samples from VC contaminated groundwater in Carver, MA.

Appendix B qPCR standard curve parameters

Table B 47**.** qPCR standard curve parameters using different primer sets and template DNA from pure cultures. ABI 7000 System SDS Software (Applied Biosystems) was used to analyze real-time PCR fluorescence data. The "auto baseline" function was used in all situations. All fluorescence threshold numbers for each set of standards and samples were manually optimized as described previously. PCR efficiency was derived by $E = (1-10^{(-1/slope)})$. The linear dynamic range for all standards was between 3×10^2-3×10^7 gene copies.

(A) Gene specific primer qPCR standard curve parameters for the primer bias experiment

Target Gene	Primer	Standard	Template	Fluorescence threshold (Ft)	Slope (-)	PCR Efficiency	R^2	Y-intercept	Gene copies per ng template
etnC	JS60 *etnC* GSP	JS60 *etnC* product	JS60 gDNA	0.014	3.3212	100.0%	0.9986	36.1553	368,000
	JS614 *etnC* GSP	JS614 *etnC* product	JS614 gDNA	0.078	3.2500	103.1%	0.9984	36.1931	155,000
	JS617 *etnC* GSP	JS617 *etnC* product	JS617 gDNA	0.075	3.2126	104.8%	0.9975	35.7803	96,000
	JS623 *etnC* GSP	JS623 *etnC* product	JS623 gDNA	0.02	3.3355	99.4%	0.9986	36.3040	231,000
etnE	JS60 *etnE* GSP	JS60 *etnE* product	JS60 gDNA	0.01	3.3296	99.7%	0.9981	32.3866	139,000
	JS614 *etnE* GSP	JS614 *etnE* product	JS614 gDNA	0.225	3.3218	100.0%	0.9974	36.3321	154,000
	JS617 *etnE* GSP	JS617 *etnE* product	JS617 gDNA	0.01	3.4527	94.8%	0.9982	34.1678	50,000
	JS623 *etnE* GSP	JS623 *etnE* product	JS623 gDNA	0.02	3.3697	98.0%	0.9986	34.3121	128,000

(B) RTC and RTE qPCR standard curve parameters for the primer bias experiment

Target Gene	Primer[a]	Standard	Template	Fluorescence threshold (Ft)	Slope (-)	PCR Efficiency	R^2	Y-intercept	Gene copies per ng template
etnC	RTC	JS60 *etnC* PCR product	JS60 gDNA	0.04	3.2176	104.5%	0.9987	37.1106	604,000

		JS614 *etnC* PCR product	JS614 gDNA	0.18	3.1913	105.8%	0.9991	43.9579	379,000
		JS617 *etnC* PCR product	JS617 gDNA	0.16	3.2477	103.2%	0.9983	36.4225	86,000
		JS623 *etnC* PCR product	JS623 gDNA	0.07	3.3385	99.3%	0.9901	37.6656	326,000
		JS60 *etnE* PCR product	JS60 gDNA	0.027	3.3234	99.9%	0.9925	34.3077	157,000
		JS614 *etnE* PCR product	JS614 gDNA	0.11	3.3286	99.7%	0.9978	37.9529	198,000
etnE	RTE	JS617 *etnE* PCR product	JS617 gDNA	0.07	3.3243	99.9%	0.9922	37.1397	47,000
		JS623 *etnE* PCR product	JS623 gDNA	0.021	3.3251	99.9%	0.9956	34.5063	123,000

(C) MRTC and MRTE qPCR standard curve parameters for the primer bias experiment

Target Gene	Primer	Standard	Template	Fluorescence threshold (Ft)	Slope (-)	PCR Efficiency	R^2	Y-intercept	Gene copies per ng template
		JS60 *etnC* PCR product	JS60 gDNA	0.31	3.2615	102.6%	0.9987	38.5402	536,000
etnC	MRTC	JS614 *etnC* PCR product	JS614 gDNA	0.4	3.1746	106.5%	0.9991	37.1226	188,000
		JS617 *etnC*	JS617	0.4	3.2459	103.3%	0.9984	36.5575	66,000

		PCR product	gDNA						
		JS623 *etnC* PCR product	JS623 gDNA	0.31	3.2528	103.0%	0.9953	38.4899	251,000
		JS60 *etnE* PCR product	JS60 gDNA	0.16	3.5399	91.6%	0.9990	36.7274	153,000
		JS614 *etnE* PCR product	JS614 gDNA	0.23	3.3235	99.9%	0.9996	35.0851	187,000
etnE	MRTE	JS617 *etnE* PCR product	JS617 gDNA	0.1	3.4049	96.6%	0.9984	35.0547	50,000
		JS623 *etnE* PCR product	JS623 gDNA	0.1	3.4781	93.9%	0.9947	35.9271	125,000

Appendix C - Data from Carver, MA VC-assimilation microcosms

35-I	
day	VC
1	1.19
14	1.14
36	1.19
101	1.05
133	1.03

39-I	
day	VC
1	1.04
14	1.13
36	1.18
104	1.11
133	1.10

46-D	
day	VC
1	0.97
56	0.93
101	0.88
133	0.85

47-D	
day	VC
1	1.04
56	1.06
101	1.00
133	0.95

58-I	
day	VC
1	1.04
102	0.94
132	0.96

63-D	
day	VC
1	0.86
14	0.86
36	0.85
56	0.87
102	0.66
132	0.19
139	0.07
146	0

63-I	
day	VC
1	1.04
14	1.02
56	1.01
104	0

64-D	
day	VC
1	1.03
14	1.00
102	0.99
132	0.98

64-I	
day	VC
1	1.04
14	1.03
100	0.98
133	0.99

64-I	**Killed**
day	VC
1	1.03
56	1.04
100	1.01
133	0.99

73	
day	VC
1	1.10
14	1.09
56	1.11
100	1.05
133	0.95

78	
day	VC
1	1.04
57	0.93
99	0.80
132	0.28
140	0.02
147	0

78	**Killed**
day	VC
1	0.98
14	0.95
36	0.97
100	0.93
132	0.91

79	
day	VC
1	1.14
14	1.12
36	1.12
101	0.99
133	0.60
140	0.41
147	0.23
154	0.12

80	
day	VC
1	1.04
14	1.07
36	1.10
100	0.99
133	0.79
140	0.70
147	0.58
154	0.56

81	
day	VC
1	0.98
14	0.95
36	0.97
100	0.93
132	0.91

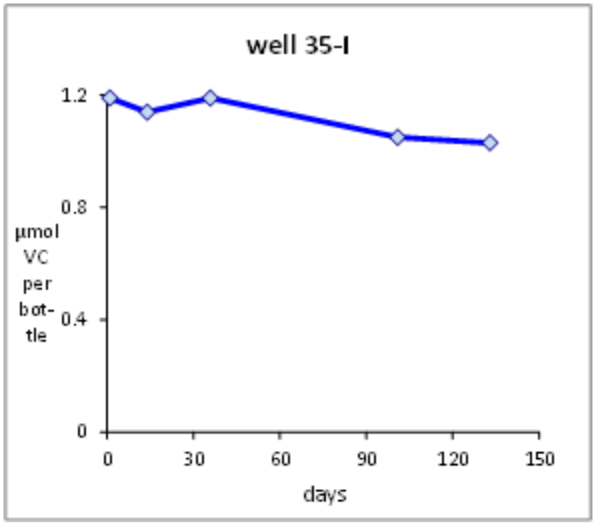
well 35-I
1.2
0.8
0.4
0
µmol VC per bot-tle
0
30
60
90
120
150
days

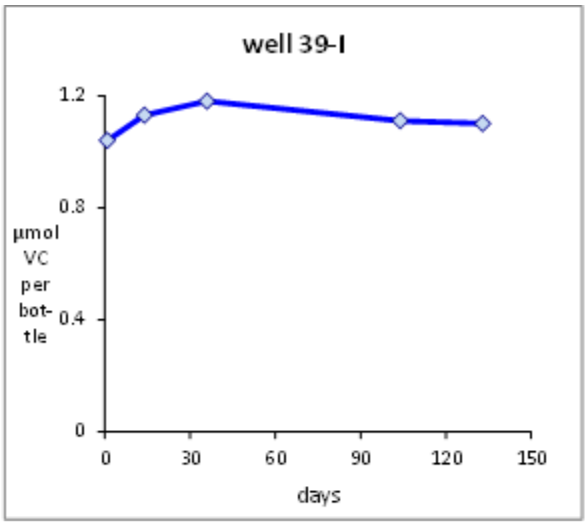
well 39-I
1.2
0.8
0.4
0
µmol VC per bot-tle
0
30
60
90
120
150
days

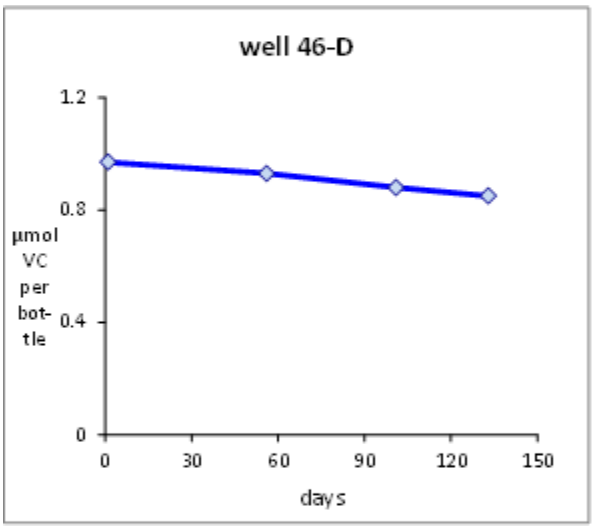
well 46-D
1.2
0.8
0.4
0
µmol VC per bot-tle
0
30
60
90
120
150
days

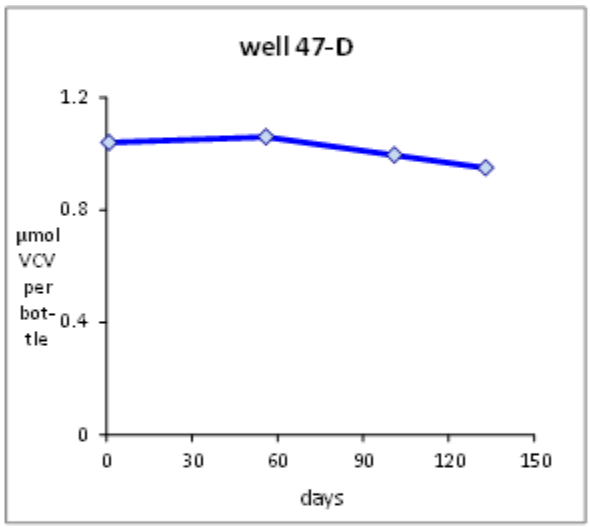
well 47-D
1.2
0.8
0.4
0
µmol VCV per bot-tle
0
30
60
90
120
150
days

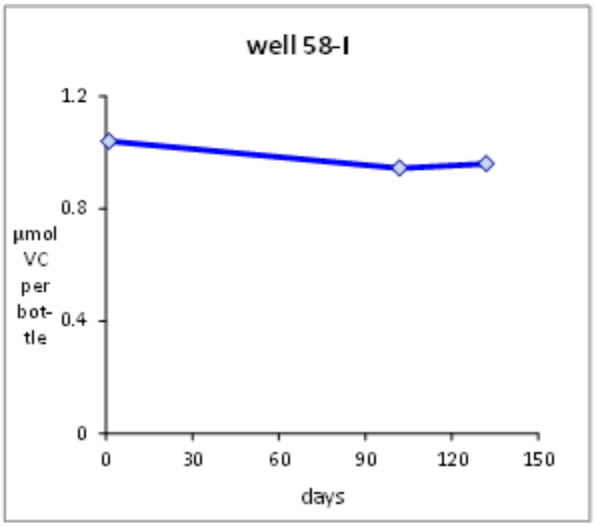
well 58-I
1.2
0.8
0.4
0
µmol VC per bot-tle
0
30
60
90
120
150
days

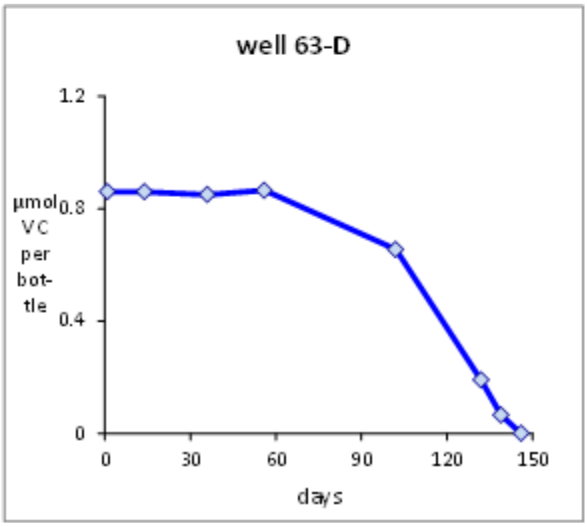
well 63-D
1.2
0.8
0.4
0
µmol VC per bot-tle
0
30
60
90
120
150
days

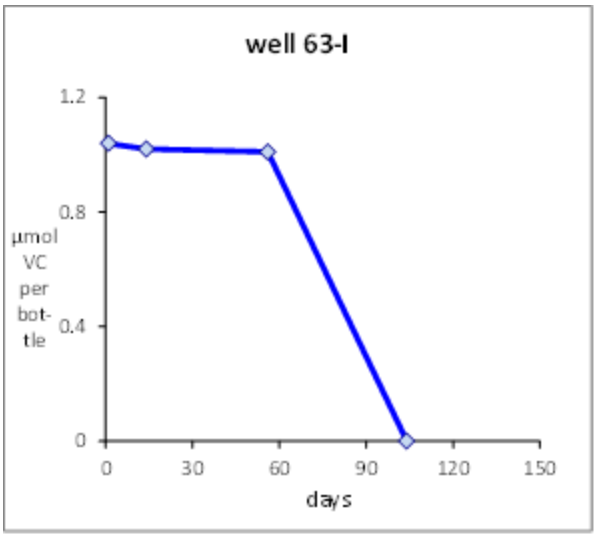
well 63-I
1.2
0.8
0.4
0
µmol VC per bot-tle
0
30
60
90
120
150
days

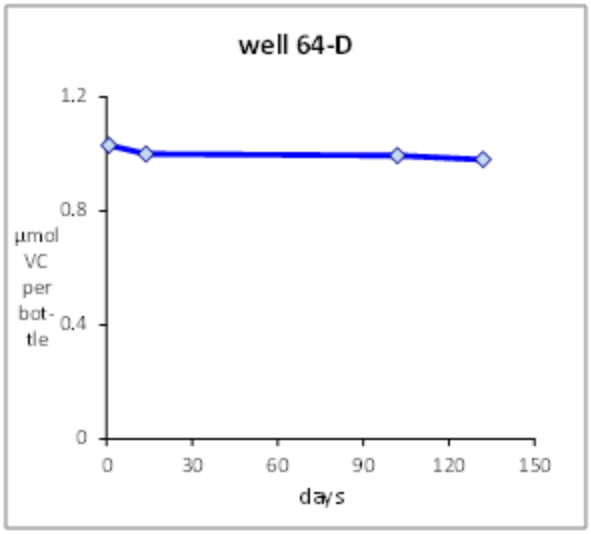
well 64-D
1.2
0.8
0.4
0
µmol VC per bot-tle
0
30
60
90
120
150
days

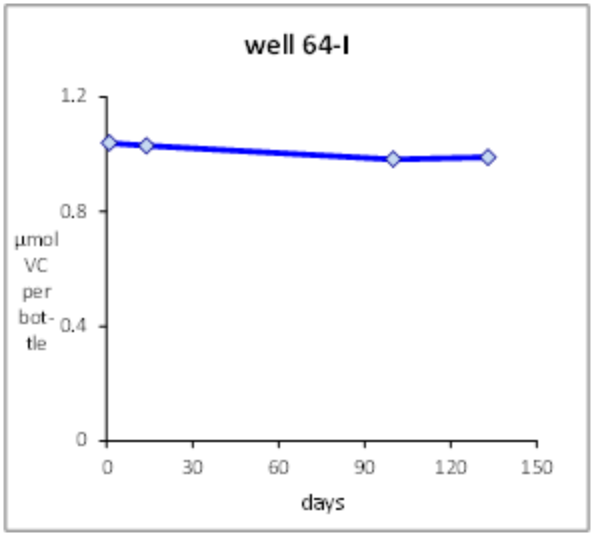
well 64-I
1.2
0.8
0.4
0
µmol VC per bot-tle
0
30
60
90
120
150
days

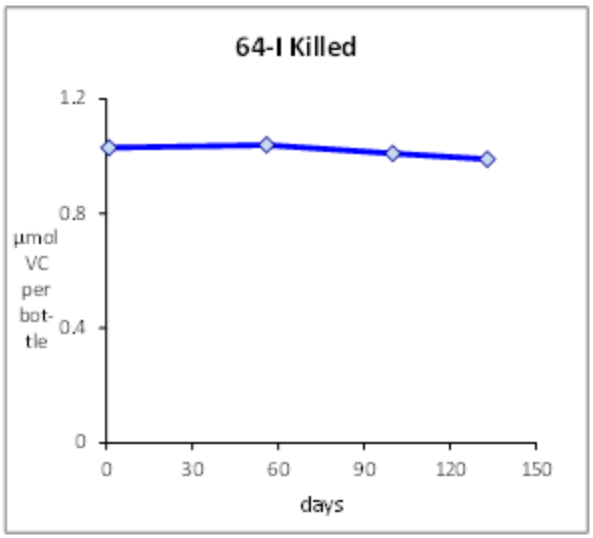
64-I Killed
1.2
0.8
0.4
0
µmol VC per bot-tle
0
30
60
90
120
150
days

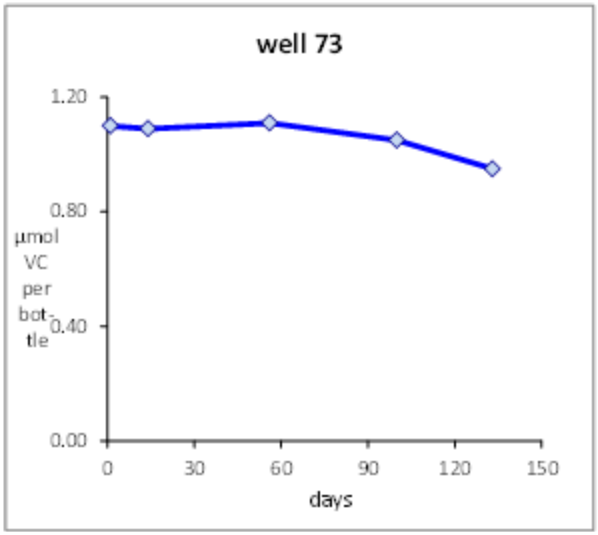
well 73
1.20
0.80
0.40
0.00
µmol VC per bot-tle
0
30
60
90
120
150
days

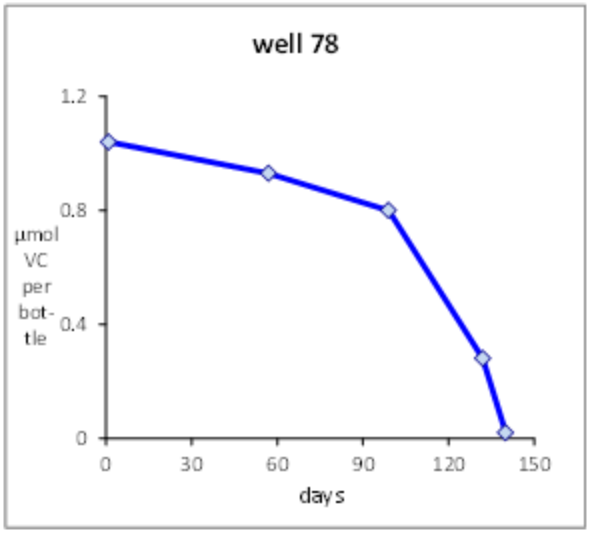
well 78
1.2
0.8
0.4
0
µmol VC per bot-tle
0
30
60
90
120
150
days

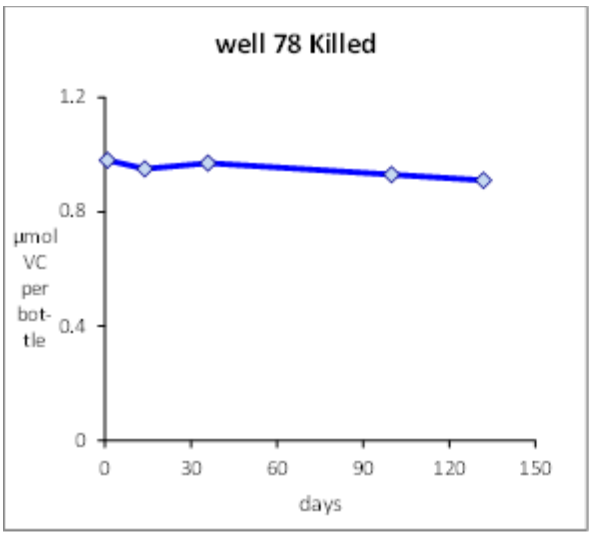
well 78 Killed
1.2
0.8
0.4
0
µmol VC per bot-tle
0
30
60
90
120
150
days

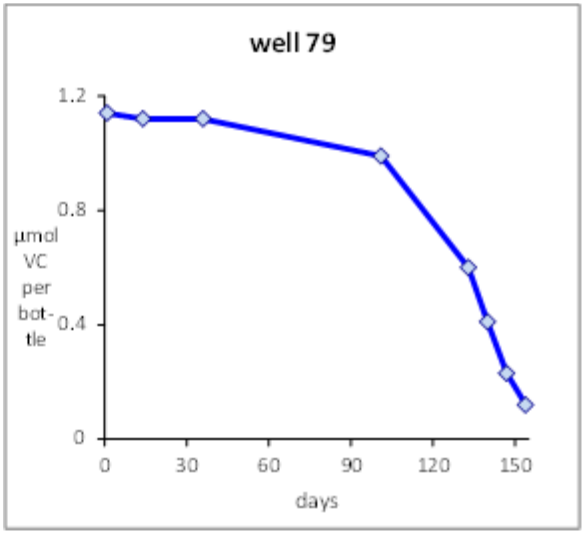
well 79
1.2
0.8
0.4
0
µmol VC per bot-tle
0
30
60
90
120
150
days

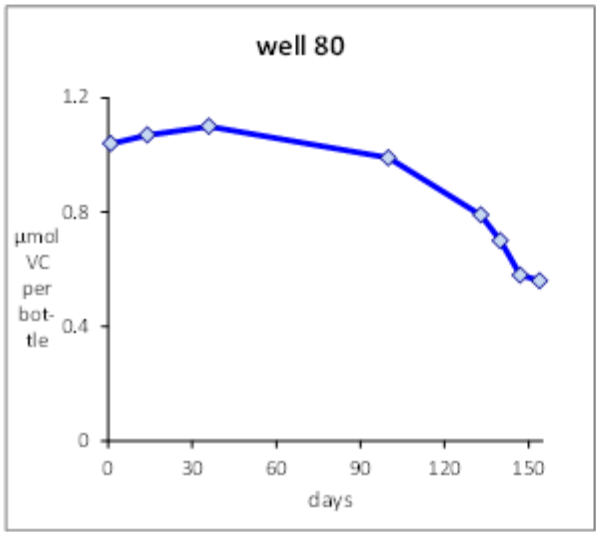
well 80
1.2
0.8
0.4
0
µmol VC per bot-tle
0
30
60
90
120
150
days

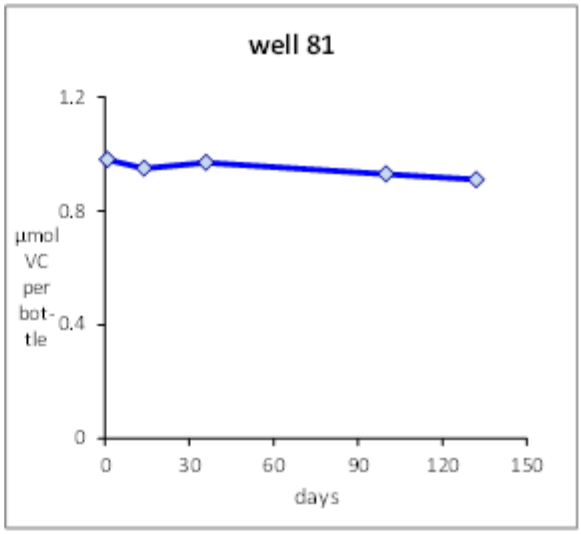
well 81
1.2
0.8
0.4
0
µmol VC per bot-tle
0
30
60
90
120
150
days

List of Scientific/Technical Publications

1. **Articles in peer-reviewed journals**
   a. Jin, Y.O. and **Mattes, T.E**., 2011. Assessment and modification of qPCR primers that amplify functional genes from etheneotroph and vinyl chloride-assimilators. *Letters in Applied Microbiology* (**53**:576-580).

   b. Jin, Y.O. and **Mattes, T.E.**, 2010. A Quantitative PCR Assay for Aerobic, Vinyl Chloride- and Ethene-Oxidizing Microorganisms in Groundwater. *Environmental Science and Technology* (**44**: 9036-9041).

2. **Conference abstracts**
   a. Jin, Y.O, Fogel, S. and **Mattes, T.E**. 2011. Quantifying the Presence and Activity of Aerobic, Vinyl Chloride-Degrading Microorganisms in Dilute Groundwater Plumes by Using Real-Time PCR. Partners in Environmental Technology Technical Symposium & Workshop, Washington, D.C.

   b. Jin, Y.O. and **Mattes, T.E**., 2011. A Quantitative PCR Assay for Aerobic, Vinyl Chloride- and Ethene-Assimilating Microorganisms in Groundwater. 20th Biocatalysis and Bioprocessing Conference, Iowa City, IA.

   c. Lee, M-C. and **Mattes, T.E**., 2011. VC Degradation by Methane-Oxidizing and Ethene-Oxidizing Bacteria in the Presence of Methane and Ethene Mixtures. 20th Biocatalysis and Bioprocessing Conference, Iowa City, IA.

   d. Jin, Y.O. and **Mattes, T.E**., 2011. Advanced Technique for Monitoring Bioremediation of Vinyl Chloride in Groundwater, oral presentation at the 2011 AEESP Research and Education conference by Y.O. Jin. Tampa, FL.

   e. Jin, Y.O. and **Mattes, T.E**., 2011. Development of a Reverse-Transcriptase Real-Time PCR Method for Aerobic, Vinyl Chloride- and Ethene-Assimilating Microorganisms in Groundwater. 111th General Meeting of the American Society for Microbiology, New Orleans, LA.

   f. Jin, Y.O. and **Mattes, T.E**., 2010.A Quantitative PCR Assay for Aerobic, Vinyl Chloride- and Ethene-Assimilating Microorganisms in Groundwater. 19h Biocatalysis and Bioprocessing Conference, Iowa City, IA.

   g. Jin, Y.O, Fogel, S. and **Mattes, T.E**. 2010. Development of real-time PCR primers for quantifying aerobic, vinyl chloride and ethene-oxidizing bacteria in groundwater. The 7th International Conference on the Remediation of Chlorinated and Recalcitrant Compounds. Monterey, CA.

   h. Jin, Y.O, Fogel, S. and **Mattes, T.E**. 2009. Quantifying the Presence and Activity of Aerobic, Vinyl Chloride-Degrading Microorganisms in Dilute Groundwater Plumes by

Using Real-Time PCR. Partners in Environmental Technology Technical Symposium & Workshop, Washington, D.C.